Upgrading the Benchmark Simulation Model Framework with emerging challenges - A study of N2O emissions and the fate of pharmaceuticals in urban wastewater systems

Snip, Laura

Publication date:
2015

Document Version
Publisher's PDF, also known as Version of record

Upgrading the Benchmark Simulation Model framework with emerging challenges

A study of N_2O emissions and the fate of pharmaceuticals in urban wastewater systems

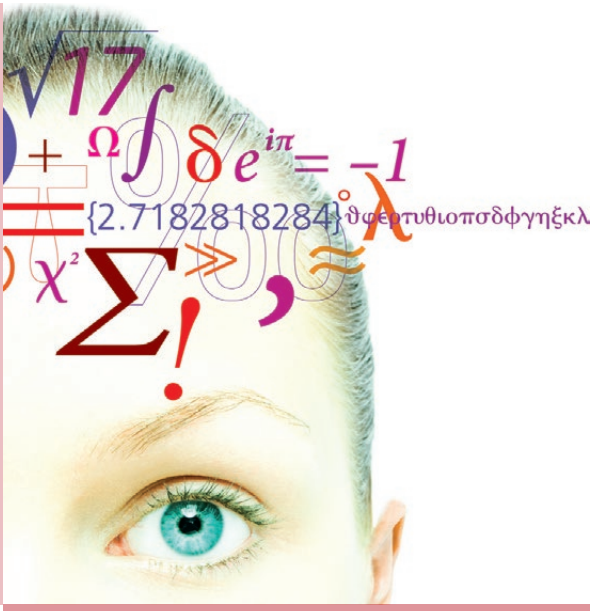

Laura Snip
Ph.D thesis
April, 2015

DTU Chemical Engineering
Department of Chemical and Biochemical Engineering

Upgrading the Benchmark Simulation Model Framework with emerging challenges

A study of N_2O emissions and the fate of pharmaceuticals in urban wastewater systems

PhD Thesis

Laura Snip

April, 2015

CAPEC-PROCESS Research Center

Department of Chemical & Biochemical Engineering
Technical University of Denmark

Preface

This thesis is submitted in partial fulfilment of the requirements for acquiring a PhD degree at the Technical University of Denmark (DTU). The research has been carried out from May 2012 to April 2015 and has received funding from the People Program (Marie Curie Actions) of the European Union's Seventh Framework Programme FP7/2007-2013 under REA agreement 289193. This thesis was prepared at the Center for Process Engineering and Technology (PROCESS) at the Department of Chemical and Biochemical Engineering under the main supervision of Professor Krist V. Gernaey and co-supervision of Associate Professor Ulf Jeppsson at the Division of Industrial Electrical Engineering and Automation (IEA) at Lund University, Marie Curie Research Fellow Xavier Flores-Alsina (PROCESS), Associate Professor Benedek Plósz at the Department of Environmental Engineering and Associate Professor Ulrich Krühne (PROCESS). In addition, there has been one research stay at Aquafin, Aartselaar, Belgium and another at Catalan Institute for Water Research (ICRA), Girona, Spain.

This work could not have been possible and as pleasant as it was without my supervisors: Krist, thanks for the trust in me and all the freedom it came with. I enjoyed our meetings with jokes in Dutch/English/Danish; Ulf, thank you for the fruitful discussions, code checking, reference checking and hosting of dinners; Xavi, thank you a million times for not only getting me this PhD job and helping me with everything related to it whenever I needed it, but also for the nice apartment and the fun!; Benedek, thank you for sharing your knowledge on micropollutants and the fresh view; Ulli, thanks for wanting to be on the supervisor list. In addition, I want to thank everyone at Aquafin and ICRA for making my stay enjoyable. Lluís and Ignasi (2), it was a pleasure working with you! Riccardo, thanks for being a smart and hardworking Msc student. I would also like to thank Erik for helping me in stressful times.

Of course, I didn't only work during the past three years; I managed to make me some friends! A big hug for my SANITAS family, making conferences and training weeks not feel as work but a lot of fun! A special thanks for Marina and Antonia as well as for my Benchmark buddies, Kim and Ramesh. I'm happy I could share it all with you, ups and downs. I also felt at home in DK due to the nice CAPEC-PROCESS people. Beginning your PhD with the country seminar coming up is a really good start, even if you get called a direct person! Of course, I cannot forget my family and friends back in the Netherlands (or Switzerland) for their support and visits with paprika ribbels chips. Both the visit and the chips were highly appreciated ;). Last but not least, thanks to Kees for all his support and encouragement, as well as the cooking, to make the most out of these three years, even if it meant spending time apart, then and now.

Laura van Duijvendijk-Snip

Copenhagen, April 2015

This thesis reflects only the author's views and the European Union is not liable for any use that may be made of the information contained therein.

"Did you ever stop to think,
and forget to start again?"

A.A. Milne

Abstract

Nowadays a wastewater treatment plant (WWTP) is not only expected to remove traditional pollutants from the wastewater; other emerging challenges have arisen as well. A WWTP is now, among other things, expected to also minimise its carbon footprint and deal with micropollutants. Optimising the performance of a WWTP can be done with mathematical models that can be used in simulation studies. The Benchmark Simulation Model (BSM) framework was developed to compare objectively different operational/control strategies. As different operational strategies of a WWTP will most likely have an effect on the greenhouse gas (GHG) emissions and the removal rate of micropollutants (MPs), modelling these processes for dynamic simulations and evaluation seems to be a promising tool for optimisation of a WWTP.

Therefore, in this thesis the BSM is upgraded with processes describing GHG emissions and MPs removal. Regarding GHGs emissions, the focus is placed on the production of nitrous oxide (N_2O). As micropollutants comprise a wide range of chemicals, pharmaceuticals are selected here as specific examples to be studied.

Different nitrification models containing N_2O producing processes are tested and used for an extension of the BSM. Various challenges were encountered regarding the mathematical structure and the parameter values when expanding the BSM. The N_2O models produced different results due to the assumptions on which they are based. In addition, pH and inorganic carbon concentrations have been demonstrated to significantly influence the nitrification. Therefore a physicochemical model in combination with a N_2O model is calibrated with data from a full-scale sequencing batch reactor (SBR) to gain insight into the N_2O production pathways. Most likely the pathways of nitrifier denitrification and hydroxylamine oxidation alternated during the nitrification phase in the SBR.

The BSM framework is also extended with the occurrence, transport and fate of pharmaceuticals. The occurrence is modelled with a phenomenological approach for pharmaceuticals, including a daily pattern and a stochastic approach for pharmaceuticals with a more random occurrence. Different sewer conditions demonstrated effects on the occurrence of the pharmaceuticals as influent patterns at the inlet of the WWTP were smoothed or delayed. The fate in the WWTP showed that operational conditions can influence the biotransformation, retransformation and sorption rates. In addition, inhibition and co-metabolic effects can have opposite effects on the removal rates. A phenomenological influent generator has been successfully calibrated with high frequency data for traditional variables and data on the occurrence of pharmaceuticals and metabolites. The excretion pathways as well as in-sewer transformation processes proved to be of importance when calibrating the daily patterns.

Upgrading the BSM framework with these calibrated models can help to optimise the performance of a WWTP by not only taking operational costs and effluent quality into account, but also by including the GHG emissions and removal rates of pharmaceuticals.

Resumé på dansk

I dag forventes der at et spildevandsrensningsanlæg ikke kun fjerner de almindelige forurenende stoffer fra spildevandet. Indenfor de seneste årtier er mange nye udfordringer opstået, hvilket har markant øget kravene til rensningsanlæggene. For eksempel forventes et rensningsanlæg nu til dags også at minimere sit CO_2-aftryk (carbon footprint) og fjerne mikroforureninger fra spildevandet. Optimering af driften af et rensningsanlæg kan undersøges og forbedres ved brug af matematiske modeller, der kan anvendes i simuleringsstudier. Benchmark Simulation Model (BSM) blev specielt udviklet til objektiv sammenligning af forskellige drifts- og reguleringsstrategier gennem simuleringer. Forskellige driftsstrategier på et rensningsanlæg vil sandsynligvis have en effekt på både udledningen af drivhusgasser og fjernelsen af mikroforureninger. Derfor var det oplagt at udvikle og bruge matematiske modeller af disse processer i dynamiske simuleringsstudier, med formålet at optimere driften af et rensningsanlæg. Det vil sige at mindske udledning af drivhusgasser og optimere fjernelse af mikroforureninger.

Derfor er BSM platformen i denne afhandling blevet opgraderet med processer der beskriver dannelse og udledning af drivhusgasser, samt fjernelse af mikroforureninger. Vedrørende udledning af drivhusgas har afhandlingen fokus på produktion af lattergas (N_2O). Mikroforureninger omfatter en lang række kemikalier, og her er lægemidler blevet udvalgt som specifikke eksempler til at blive undersøgt nærmere.

Flere nitrifikationsmodeller indeholder processer til dannelse af N_2O og kan derfor anvendes til en udvidelse af BSM platformen. I forbindelse med denne udvidelse opstod flere udfordringer relateret til strukturen af den matematiske model til at beskrive N_2O dannelse, samt til parameterværdierne der skal bruges når BSM platformen udvides. De kendte N_2O-modeller producerer forskellige resultater på grund af forskel i de forudsætninger, som modellerne er baseret på. Desuden har pH og uorganisk kulstof vist sig at have en betydelig indflydelse på nitrifikationsprocesserne. Derfor blev en fysisk-kemisk model kombineret med en N_2O nitrifikationsmodel kalibreret på basis af et datasæt, fra en fuldskala sekventielt batch reaktor (SBR), til at få bedre indsigt i N_2O produktionsmekanismerne. Konklusionen er at det er sandsynligt at nitrificerendebakterier skifter mellem denitrifikation og hydroxylamin oxidation til N_2O dannelse under nitrifikationsfasen i SBR eksemplet.

BSM platformen blev også udvidet med modeller til at beskrive forekomsten, transport og skæbnen af lægemidler i spildevand. Forekomsten er blevet modelleret med en fænomenologiskmodel der er specielt udviklet til farmaceutiske produkter. Forekomsten beskrives på basis af et dagligt mønster, eller en stokastisk tilgang specifikt for lægemidler med en mere uregelmæssig forekomst. Ændringer i betingelserne i kloaksystemet har vist sig at have en indflydelse på forekomsten af lægemidler, ved enten at forsinke eller udligne forekomsten af lægemidler i indløbet til rensningsanlægget. I rensningsanlægget kan de

operationelle forhold påvirke balancen mellem biotransformation, re-transformation og sorption af lægemidler. Desuden kan hæmning og co-metabolisme have den modsatte effekt på mængden af lægemidler der fjernes i anlægget. En fænomenologiskmodel til beskrivelse af lægemidler i indløbet er blevet kalibreret med højfrekvente data for de traditionelle variable og specifikke data om forekomsten af lægemidler og metabolitter. Hvordan lægemidler udskilles samt transformationsprocesser i kloakken viste sig at være af stor betydning ved kalibrering af de daglige mønstre.

Opgradering af BSM platformen med disse kalibrerede modeller kan hjælpe med at optimere ydeevnen for et rensningsanlæg ved ikke blot at tage driftsomkostninger og spildevandskvalitet i betragtning, men også ved at inddrage udledningen af drivhusgas og fjernelse af lægemidler som kriterier til at beskrive effektiviteten af rensningsprocesserne.

Nomenclature

Abbreviations

ADM1	Anaerobic Digestion Model No.1
AER	Aerobic tank in the activated sludge unit of the BSM1
ANOX	Anoxic tank in the activated sludge unit of the BSM1
AOB	Ammonia oxidising bacteria
AS	Activated sludge
ASMs	Activated Sludge Models
ASM1	Activated Sludge Model No. 1
ASM2	Activated Sludge Model No. 2
ASM2d	Activated Sludge Model No. 2d
ASM3	Activated Sludge Model No. 3
ASMN	Activated Sludge Model for Nitrogen
ASM-X	Activated Sludge Modelling Framework for Xenobiotic Trace Chemicals
BCM	Biochemical model
BOD_5	Biochemical oxygen demand [g O_2/m^3]
BSM1	Benchmark Simulation Model No.1
BSM2	Benchmark Simulation Model No.2
CH_4	Methane
CIP	Ciprofloxacin, antibiotic drug
CMZ	Carbamazepine, anti-epileptic drug
CMZ-2OH	Metabolite of carbamazepine, 2-Hydroxy Carbamazepine
CO_2	Carbon dioxide
CO_2e	CO_2 equivalent
COD	Chemical Oxygen Demand [g COD/m^3]
CSTR	Continuously stirred tank reactor
DCF	Diclofenac, non-steroidal anti-inflammatory drug
GHG	Greenhouse gas
GWP	Global Warming Potential [kg CO_2e/100 years]
HH	Households block in influent generator
HRT	Hydraulic retention time [h]
IBU	Ibuprofen, non-steroidal anti-inflammatory compound
IBU-2OH	Metabolite of ibuprofen, 2-Hydroxyibuprofen
IC	Inorganic carbon
IndS	Industry block in influent generator
IoAd	Index of Agreement (Quantitative evaluation criteria)
IWA	International Water Association
MAE	Mean absolute error (Quantitative absolute evaluation criteria)

MARE	Mean absolute relative error (Quantitative relative evaluation criteria)
ME	Mean error (Quantitative absolute evaluation criteria)
MLSS	Mixed Liquor Suspended Solids [g/m^3]
MLVSS	Mixed Liquor Volatile Suspended Solids [g/m^3]
MP	Micropollutant
MPE	Mean percentage error (Quantitative peak evaluation criteria)
MSDE	Mean squared derivative error (Quantitative peak evaluation criteria)
MSRE	Mean squared relative error (Quantitative relative evaluation criteria)
N_2	Dinitrogen gas
NH_2OH	Hydroxylamine
NO_2^-	Nitrite
NO_3^-	Nitrate
NOB	Nitrite oxidising bacteria
O_2	Oxygen
OCI	Operational cost index [cost unit/d]
OHO	Ordinary heterotrophic organisms
PCM	Physicochemical model
PDIFF	Peak difference (Quantitative peak evaluation criteria)
PE	Person equivalent ('Households' and 'Micropollutants' model block) [-]
PEC	Predicted environmental concentration [g/L]
PEP	Peak error percentage (Quantitative peak evaluation criteria)
PNEC	Predicted no effect concentration [g/L]
QQ plot	Quantile-quantile plot (Qualitative evaluation criteria)
RMSE	Root mean square error (Quantitative absolute evaluation criteria)
RWQM1	River Water Quality Model No.1
SBR	Sequencing batch reactor
SMX	Sulfamethoxazole, antibiotic drug
SMX-N4	Metabolite of sulfamethoxazole, N4-acetyl-sulfamethoxazole
SRT	Sludge retention time [d]
STD Boots	Standard deviation of the Bootstrap calibration
T	Temperature [°C]
TCY	Tetracycline, antibiotic drug
TN	Total nitrogen [g N/m^3]
TP	Total phosphorus [g P/m^3]
TSS	Total suspended solids concentration [g S_S/m^3]
WFD	EU Water Framework Directive
WWTP	Wastewater treatment plant

Symbols

A	Surface area of the variable volume tank, soil model block [m^2]
a	Activity of a species or component in the PCM
aH	Parameter determining the direct contribution of rainfall falling on impermeable surfaces in the catchment area to the flow rate in the sewer ('Rain generator' model block) [%]
b_{AOB}	Decay rate of ammonia oxidising bacteria [1/d]
BI	Evaluation criteria concerning fate of micropollutants: biotransformation index [%]
C	Concentration [g/m^3]
C_{CJ}	Concentration of total retransformable parent chemical (micropollutant) [g/m^3]
$CIP_{gperPEperd}$	Total average daily load of CIP ('Micropollutants' model block) [g CIP/(day.1000 PE)]
C_{LI}	Concentration of parent form of micropollutant [g/m^3]
$CMZ_{gperPEperd}$	Total average daily load of CMZ ('Micropollutants' model block) [g CMZ/(day.1000 PE)]
$CODpart$	Particulate Chemical Oxygen Demand [g COD/m^3]
$CODpart_{gperPEperd}$	Total average daily load of COD particulates per day per PE [g COD/(day.PE)]
C_{SL}	Concentration of the sorbed form of micropollutant [g/m^3]
$C_{SL,I}$	Concentration of the sequestered form of micropollutant [g/m^3]
$DCF_{gperPEperd}$	Total average daily load of DCF ('Micropollutants' model block) [g DCF/(day.1000 PE)]
DCF_S	Transition probability matrix of different states of occurrence of DCF ('Micropollutants' model block) [-]
$DS1$	Long term dataset
$DS2$	Short term dataset
Eff	Overflow of the secondary settler
$FFfraction$	Fraction of suspended solids that can settle in the sewer, first flush effect model block [-]
G_{N2O}	Quantity of generated nitrous oxide emissions per day [kg N_2O-N/d]
G_{rain_Temp}	Proportional gain to adjust the temperature after a rain event, temperature model block [-]
ΔH^o	Enthalpy change of the reaction [kJ/mole]
$IBU_{gperPEperd}$	Total average daily load of IBU per day per 1000 PE [g IBU/(day.1000PE)]
$IBU\text{-}2OH_{gperPEperd}$	Total average daily load of IBU-2OH per day per 1000 PE [g IBU-2OH/(day.1000PE)]

K_i	Equilibrium constant
k	Time instance in the calculation of the transition probability to describe the occurrence of the micropollutant with a Markov Chain ('Micropollutants' model block)
k_{Bio}	Biotransformation kinetic parameter [mg/(L.h)]
k'_{Bio}	Biotransformation kinetic parameter [1/h]
$k_{Bio,Ax}$	Parameter in ASM-X: anoxic biotransformation rate coefficient for SMX, TCY and CIP as C_{LI} [m^3/(g X_{SS}.day)]
$k_{Bio,Ox}$	Parameter in ASM-X: aerobic biotransformation rate coefficient for SMX, TCY and CIP as C_{LI} [m^3/(g X_{SS}.day)]
$k_{Bio,Ax,Ss}$	Parameter in ASM-X: anoxic biotransformation rate coefficient under growth substrate limiting conditions for DCF and CMZ as C_{LI} [m^3/(g X_{SS}.day)]
$k_{Bio,Ox,Ss}$	Parameter in ASM-X: aerobic biotransformation rate coefficient under growth substrate limiting conditions for DCF and CMZ as C_{LI} [m^3/(g X_{SS}.day)]
K_D	Solid-water distribution coefficient [L/g S_S]
$K_{D,Ax}$	Parameter in ASM-X: anoxic solids-liquid sorption coefficient [m^3/(g X_{SS})]
K_{down}	Gain for adjusting the flow rate to downstream aquifers, soil model block [m^2/d]
$K_{D,Ox}$	Parameter in ASM-X: aerobic solids-liquid sorption coefficient [m^3/(g X_{SS})]
k_{Dec}	Rate constant of retransformation of C_{CJ} to C_{LI} [m^3/(g X_{SS}.day)]
$k_{Dec,Ax}$	Parameter in ASM-X: anoxic retransformation rate coefficient for C_{CJ} to C_{LI} [m^3/(g X_{SS}.day)]
$k_{Dec,Ox}$	Parameter in ASM-X: aerobic retransformation rate coefficient for C_{CJ} to C_{LI} [m^3/(g X_{SS}.day)]
k_{Des}	Parameter in ASM-X: Desorption rate coefficient for C_{SL} [1/day]
K_{FA}	Half-saturation coefficient for S_{FA} [g N/m^3]
K_{FNA}	Half-saturation coefficient for S_{FNA} [g N/m^3]
K'_H	Henry coefficient
K_i	Equilibrium constant of physicochemical model [-]
K_{I9FA}	Free ammonia inhibition coefficient for ASMN process no. 9 [g N/m^3]
K_{I9FNA}	Free nitrous acid inhibition coefficient for ASMN process no. 9 [g N/m^3]
K_{inf}	Infiltration gain, soil model block [$m^{2.5}$/d]
K_La	Volumetric oxygen transfer coefficient [1/d]
$k_La_{CO_2}$	Volumetric oxygen transfer coefficient of CO_2 [1/d]

$K_{NH2OH,AOB}$	S_{NH2OH} affinity constant for AOB [g N/m^3]
$K_{NH4,AOB}$	S_{NH4} affinity constant for AOB [g N/m^3]
K_{NH4}	Half-saturation coefficient for S_{NH4} [g N/m^3]
$K_{NO2,AOB}$	S_{NO2} affinity constant for AOB [g N/m^3]
$K_{NO,AOB}$	S_{NO} affinity constant for AOB [g N/m^3]
K_{NOH}	Half-saturation coefficient for S_{NOH} [g N/m^3]
$K_{NOH,AOB}$	S_{NOH} affinity constant for AOB [g N/m^3]
K_{O2}	Parameter in ASM: Half-saturation coefficient for S_{O2} [g/m^3]
K_{OA1}	Half-saturation coefficient for S_{O2} [g COD/m^3]
K_S	Parameter in ASM: Half-saturation coefficient for S_S [g/m^3]
$K_{S1,O2}$	Model A: S_{O2} affinity constant for S_{NH4} oxidation [g COD/m^3] Model C: S_{O2} affinity constant for process *C-1* [g COD/m^3]
$K_{S2,O2}$	Model A: S_{O2} affinity constant for S_{NH2OH} oxidation [g COD/m^3] Model C: S_{O2} affinity constant for process *C-2* [g COD/m^3]
$K_{S3,O2}$	Model C: S_{O2} affinity constant for process *C-3* [g COD/m^3]
$i_{Charge,NH4}$	Charge of NH_4^+ [charge/g N]
$i_{Charge,NO2}$	Charge of NO_2^- [charge/g N]
$i_{N,AOB}$	Nitrogen content in ammonia oxidising bacteria [g N/g COD]
inf	Influent
M	Mass flow (Evaluation criteria) [g/d]
M_{max}	Maximum mass of stored sediment in the sewer system, first flush effect model block [kg]
MW_N	Molar weight of nitrogen [g/mole]
MW_O	Molar weight of oxygen [g/mole]
N_2O	Nitrous oxide
N_C	Number of components in PCM
NH_4^+	Ammonium concentration [g N/m^3]
$NH4_{gperPEperd}$	Total average daily load of ammonium per day per PE [g NH_4-N/(day.PE)]
NO	Nitric oxide
NOH	Nitroxyl
N_{sp}	Number of species in PCM
P	Transition probability used to describe the occurrence of the micropollutant with a Markov Chain ('Micropollutants' model block) [-]
Q	Flow [m^3/d]
$q_{AOB,1,max}$	Specific maximum rate of R1 in model C (1/d)
$q_{AOB,2,max}$	Specific maximum rate of R2 in model C (1/d)
$q_{AOB,3,max}$	Specific maximum rate of R3 in model C (1/d)

$q_{AOB,4,max}$	Specific maximum rate of R4 in model C ($1/d^-$)
$q_{c,Ax}$	Parameter in ASM-X: Anoxic maximum specific co-metabolic substrate biotransformation rate in the presence of growth substrates for DCF and CMZ as C_{LI} [m^3/(g.day)]
$q_{c,Ox}$	Parameter in ASM-X: Aerobic maximum specific co-metabolic substrate biotransformation rate in the presence of growth substrates for DCF and CMZ as C_{LI} [m^3/(g.day)]
Q_{intr}	Internal recycle flow rate in the BSM1 [m^3/d]
Q_{lim}	Flow rate limit triggering a first flush effect, first flush effect model block [m^3/d]
Qpermm	Flow rate per mm rain [m^3/mm]
QperPE	Wastewater flow rate per person equivalent ('Households' model block) [m^3/d]
Q_R	Return sludge flow rate in the BSM1 [m^3/d]
Q_W	Sludge wastage flow rate in the BSM1 [m^3/d]
R	Universal gas constant [J/(mole.K)]
rTI	Evaluation criteria concerning fate of micropollutants: retransformation index [%]
$S_{Al^{3+}}$	Aluminium concentration [mole/L]
$S_{Al_2(OH)_2CO_3{}^{2+}}$	Aluminium concentration [mole/L]
s_1	State representing low level of occurrence used to describe the occurrence of the micropollutant with a Markov Chain ('Micropollutants' model block) [-]
s_2	State representing medium level of occurrence used to describe the occurrence of the micropollutant with a Markov Chain ('Micropollutants' model block) [-]
s_3	State representing high level of occurrence used to describe the occurrence of the micropollutant with a Markov Chain ('Micropollutants' model block) [-]
S_{ac^-}	Acetate concentration [mole/L]
S_{ALK}	Alkalinity [mole HCO_3^-/m^3]
S_{an}	Total equivalent concentrations of anions [mole/L]
$SC1_{trans}$	Scenario 1 in transport with different dissolved oxygen concentrations
$SC2_{trans}$	Scenario 2 in transport with different sewer lengths
$SC3_{trans}$	Scenario 3 in transport with different TSS loadings
$SC1_{fate}$	Scenario 1 in fate under default conditions
$SC2_{fate}$	Scenario 2 in fate with addition of extra carbon
$SC3_{fate}$	Scenario 3 in fate with a step-feed configuration
$SC4_{fate}$	Scenario 4 in fate with a longer SRT

$S_{Ca^{2+}}$	Calcium concentration [mole/L]
S_{cat}	Total equivalent concentrations of cations [mole/L]
S_{CO2} *	Saturation concentration of CO_2 [g C/m^3]
$S_{\mathrm{CO_3^{2-}}}$	Carbonate (CO_3^{2-}) concentration [mole/L]
$S_{\mathrm{Cl^-}}$	Chloride concentration [mole/L]
S_{FA}	Free ammonia [g N/m^3]
$S_{\mathrm{Fe^{2+}}}$	Iron (II) concentration [mole/L]
S_{FNA}	Free nitrous acid [g N/m^3]
s_{i}	State *i* in the Markov Chain representation used to describe the occurrence of the micropollutant ('Micropollutants' model block) [-]
SI	Evaluation criteria concerning the fate of micropollutants: sorption index [%]
S_{i}	Species i [mole/L] in PCM
S_{IC}	Inorganic carbon [mole/L]
S_{IN}	Inorganic nitrogen [mole/L]
S_{IP}	Inorganic phosphorus [mole/L]
S_{j}	Components j [mole/L] in PCM
$S_{\mathrm{K^+}}$	Potassium concentration [mole/L]
$S_{Mg^{2+}}$	Magnesium concentration [mole/L]
$SMX_{\mathrm{gperPEperd}}$	Total average daily load of SMX ('Micropollutants' model block) [g SMX/(day.1000 PE)]
$SMX\text{-}N4_{\mathrm{gperPEperd}}$	Total average daily load of SMX-N4 ('Micropollutants' model block) [g SMX-N4 /(day.1000 PE)]
S_{O2}	Dissolved oxygen [g (-COD)/m^3]
S_{N2O}	Dissolved nitrous oxide [g N/m^3]
S_{N2}	Dissolved dinitrogen [g N/m^3]
$S_{\mathrm{Na^+}}$	Sodium concentration [mole/L]
S_{NH2OH}	Dissolved hydroxylamine [g N/m^3]
S_{NH4}	Dissolved ammonium [g N/m^3] in BCM or [mole/L] in PCM
S_{NO}	Dissolved nitric oxide [g N/m^3]
S_{NO2}	Dissolved nitrite [g N/m^3] in BCM or [mole/L] in PCM
S_{NO3}	Dissolved nitrate [g N/m^3] in BCM or [mole/L] in PCM
S_{NOH}	Dissolved nitroxyl radical [g N/m^3]
$S_{\mathrm{PO_4^{3-}}}$	Phosphate [mole/L]
S_{S}	Readily biodegradable COD [g COD/m^3]
Subarea	A parameter that forms a measure of the size of the catchment area. It will determine the number of variable volume tanks in series that will be used for describing the sewer system, sewer model block [-]
T_{Bias}	Seasonal temperature variation, average, temperature model block

	[°C]
T_{dAmp}	Daily temperature variation, amplitude, temperature model block [°C]
TRI	Evaluation criteria concerning the fate of micropollutants: total removal index [%]
was	Waste activated sludge flow from the settler
X_{AOB}	Ammonia oxidising biomass [g COD/m^3]
X_{NOB}	Nitrite oxidising biomass [g COD/m^3]
X_{OHO}	Heterotrophic biomass [g COD/m^3]
X_P	Inert products from biomass decay [g COD/m^3]
X_{SS}	Concentration of suspended solids [g COD/m^3]
ΔH^0	Enthalpy change of reaction [kJ/mole]
$\eta_{\mu AOB,Ax}$	Anoxic reduction factor [-]
η_{Bio}	Parameter in ASM-X: Correction factor for S_S inhibition on C_{LI} biotransformation [-]
η_{Dec}	Parameter in ASM-X: Correction factor for S_S inhibition on C_{LI} transformation [-]
Y_{AOB}	Yield of ammonia oxidising bacteria [g cell COD formed/g N oxidised]
μ_{A1}	Maximum specific growth rate of AOB [1/d]
$\mu_{AOB,AMO}$	Maximum ammonia mediated oxidising reaction rate [1/d]
$\mu_{AOB,HAO}$	Maximum hydroxylamine oxidoreductase mediated oxidising reaction rate [1/d]
γ	Activity coefficient

Table of contents

Part I

Introduction & Background

In this part an introduction to the emerging challenges of a wastewater treatment plant is given. Based on these emerging challenges the aim of the PhD study is formulated along with the challenges addressed and the important research contributions of the PhD study. In Chapter 2 more background on the emerging challenges – the greenhouse gas emissions and the micropollutant removal – is described.

1. Introduction

Wastewater treatment has initially mainly focused on carbon and nitrogen removal, and later also on phosphorus removal. However, nowadays wastewater treatment is facing a number of relatively new challenges, and as a result the design and operation of a treatment plant become increasingly complicated and complex.

A first challenge results from the growing awareness of climate change, where a wastewater treatment plant (WWTP) is challenged to minimise its carbon footprint, while also producing an effluent quality that is respecting the effluent criteria and minimising the costs of operation. Thus, as a consequence of this new challenge, instead of the two traditional performance criteria regarding effluent quality and costs, another WWTP performance criterion considering its greenhouse gas (GHG) emissions should be taken into account as well (Keller and Hartley, 2003).

Another emerging challenge for a WWTP is the occurrence of so-called micropollutants (MPs) (Ternes and Joss, 2006). The term “micropollutants” covers trace organic chemicals such as pharmaceuticals, chemicals from personal care products and biocides, which are found in low concentrations (micro- or nanogram per litre) in the influent and effluent of most WWTPs. In many cases, these pollutants can pose a significant risk to the aquatic environment and human health (Daughton and Ternes, 1999). Besides being one of the major disposal pathways of micropollutants, a WWTP can also be regarded as an obstacle for MPS.

The usage of models can help to understand the processes influencing GHGs and MPs, and can therefore help develop strategies to minimise the GHG emissions and/or remove MPs from the wastewater. Also, the use of models allows for testing different control and operational strategies without interfering with the operation of a real WWTP. The Benchmark Simulation Model (BSM) tools have been developed with the aim of having a platform to objectively compare different WWTP control strategies (Gernaey et al., 2014). The main objective of the Benchmark Simulation Model No. 1 (BSM1) was to create a platform for benchmarking carbon and nitrogen removal strategies in activated sludge systems (Copp, 2002). In order to evaluate the GHG emissions and the fate of MPs, the platform should be upgraded with mechanistic models for the GHGs and MPs.

When modelling a WWTP and evaluating its performance, it is important to consider the dynamics of the operation. The influent of a WWTP is highly dynamic and these dynamics will propagate through the entire plant (Butler et al., 1995). This can result in peaks of GHG emissions that should be taken into account when calculating the carbon footprint and could easily be missed when only looking at steady state performance (Kampschreur et al., 2008). Also, in order to minimise the emissions, it is important to know

during which times/conditions the highest emissions occur. The same applies to micropollutants, as the dynamics of the influent can be reflected in the effluent as well (Nelson et al., 2011). These peaks in the effluent might result in acute toxicity if the levels are high enough. In addition, the micropollutant concentrations influence the rate of the removal processes in the activated sludge units (Plósz et al., 2010a).

The objective of this thesis is to model processes describing the GHG emissions and fate of micropollutants in order to compare different operational/control strategies. Therefore, the BSM framework will be upgraded to include these processes as it is developed to compare different control strategies. Specific evaluation criteria concerning GHGs and MPs will also be developed to be able to perform an analysis of the different scenarios.

With respect to the GHGs, the focus of the thesis is on the extension of models for the prediction of nitrous oxide (N_2O) emissions, one of the three different GHGs emitted at a WWTP (Foley et al., 2010a). The focus on N_2O can be explained as N_2O is the strongest GHG emitted at a WWTP, and moreover the processes responsible for the N_2O production are not completely clear (Kampschreur et al., 2009).

As MPs comprise a wide range of chemicals, not all can be covered in this thesis. The focus has therefore been placed on pharmaceuticals, as these chemicals are often used on a world-wide scale and have been shown to affect the aquatic environment (Coe et al., 2008) and even bio-accumulate in fish (Zenker et al., 2014). The occurrence of antibiotics in the wastewater is also a major point of concern since it can cause microbial resistance in bacteria which can become dangerous for humans (Schwartz et al., 2003). Pharmaceuticals are therefore an important group of MPs to focus on.

1.1 Challenges

Certain challenges are encountered during the study, which are described in this Section. Most of these challenges will be mentioned in the thesis; however some are out of the scope of the PhD study or could not be solved. These challenges will be addressed in the discussion in Chapter 7. The challenges are divided between challenges related to modelling, to N_2O and to pharmaceuticals.

1.1.1 Modelling

When modelling processes, the challenge is to make the model as simple as possible while still demonstrating realistic behaviour. This applies also to the modelling of wastewater treatment processes. It is important to take the intended use and purpose of the model into account when deciding upon how detailed it should be. In this thesis the purpose of the model development is to obtain a model that should

give realistic predictions of emissions from the activated sludge units and describe the fate of MPs in the same units. It is not necessary to know what is happening at the cellular level in the WWTP as the focus is on the general reactor behaviour. The model should furthermore be able to explain the behaviour of different WWTPs, not only one specific WWTP, and therefore be general.

The model should also include complete mass balances and the continuity should be ensured, which can be checked with the methods proposed by Hauduc et al. (2010).

It is also a challenge when modelling processes, to create a parsimonious model. When calibrating a model, eventually all behaviour can be described by increasing the number of parameters, however without any physical/biological meaning attached to these additional parameters. Therefore, the number of parameters should be limited and preferably all parameters should have a physical/biological interpretation.

The calibration of the model should be done with good quality data. However, in a situation where one is dependent on others for experimental data, it is difficult to check the quality and to ensure that all required data is available. Many calibrations of WWTP models are done manually based on trial and error approaches, nevertheless an automatic calibration procedure is preferable (Sin et al., 2008b). This is because of the possibility to apply quantitative evaluation methods to assess the accuracy of the calibration and thereby objectively assess the quality of the fit of the model.

1.1.2 N_2O

Certain challenges arise when trying to model the processes related to GHGs. As mentioned before, there is no consensus on the processes responsible for the emissions of N_2O in a WWTP. There are three different mechanisms capable of producing N_2O; heterotrophic denitrification, nitrifier denitrification and chemical breakdown of hydroxylamine. Modelling of heterotrophic denitrification has been done during the past years (Sin et al., 2008a), however the modelling of N_2O production by ammonia oxidising bacteria (AOB) is less well-known (Ni et al., 2013). How to model this production is therefore a challenge as it is not exactly known which process is the responsible one for the emissions.

Another challenge is that the N_2O has a relatively low solubility in water (Henry constant of 0.024 M/atm at 25°C (Kampschreur et al., 2009)) and therefore will be stripped to the gas phase. However, the solubility is not low enough for the N_2O to be immediately stripped. The N_2O produced during the anoxic phase thus stays in the liquid phase before being stripped during the subsequent aerobic phase. This makes it more difficult to know whether the measured N_2O emission is due to the biological activity in the aerobic or the anoxic phase. Measuring the N_2O in the liquid phase is difficult as the concentrations are low and not many sensors are capable of performing such measurements. This furthermore indicates that the transfer of the

dissolved N_2O to the gas phase needs to be modelled, since N_2O dynamics are typically measured in the gas phase.

1.1.3 Pharmaceuticals and their metabolites

Different challenges can be encountered when modelling the fate of pharmaceuticals in wastewater systems. As there are many different chemicals present which all have diverse characteristics, various processes and/or parameters are needed to describe the fate of such chemicals. These parameters need to be estimated for each chemical and its metabolites. The conditions of the operation of the WWTP such as anoxic or aerobic conditions, also have an effect on the processes describing pharmaceuticals and might lead to another set of parameters (Helbling et al., 2012). Studies have shown that the composition of the sludge of the WWTP might have an effect on the fate of the micropollutants through different sorption rates, which makes it difficult to benchmark (Barret et al., 2010). When trying to model various pharmaceuticals simultaneously, the computational time can increase as many state variables have to be calculated.

As the concentrations of the pharmaceuticals and their metabolites are extremely low, the chemical analysis of the samples is expensive and data is not easily available for modelling. Performing a quality check of the data is also complex as there can be differences in the results due to the use of different methods of sampling (Coes et al., 2014) or analysis (Johnson et al., 2008).

Regarding the evaluation of the WWTP performance with respect to the removal of pharmaceuticals, challenges arise as well. If only the removal of the pharmaceutical consumed (parent compound) is taken into account, a significant underestimation of the removal can be made when the metabolites are retransforming back into the parent compound in the WWTP (Plósz et al., 2010b, 2012). In addition, the toxicity can be underestimated as metabolites can exhibit the same toxic effects as the parent compound (Escher and Fenner, 2011). Therefore, the metabolites of the pharmaceuticals should be taken into account as well through model-based risk assessment. Assessing the impacts of the pharmaceuticals and their metabolites on the aquatic environment is challenging as they depend on the receiving waters as well as on the mixtures of MPs (Vasquez et al., 2014). Predicted effect concentration (PEC) and predicted no effect concentration (PNEC) values can often be found in the literature for different MPs (Ellis, 2006). However, one has to interpret such data carefully, since long term influences might not be included in those studies. Also the PEC and PNEC are assessed for one typical organism, which might not apply to the organisms in the receiving waters. Therefore, including the toxicity effects of the MPs is a challenge for the evaluation of the WWTP performance (Clouzot et al., 2013).

1.2 Objectives

The main objective of this study is to:

"Extend mathematical models of WWTPs with processes describing GHG emissions and the removal of micropollutants."

The main objective of this study can be translated into different research objectives:

1. Test different models for the production of N_2O by AOB in a WWTP;
2. Test the combination of an N_2O producing model with a physicochemical model;
3. Develop different models to describe the occurrence, transport and fate of pharmaceuticals in a WWTP;
4. Simulate the occurrence, transport and fate of pharmaceuticals in urban wastewater systems;
5. Propose additional evaluation criteria related to the removal efficiency of pharmaceuticals;
6. Evaluate the performance of the WWTP on pharmaceutical removal with different scenario analyses;
7. Calibrate the extended models with automatic calibration methods.

1.3 Contributions to research

The following contributions to research are made in this thesis:

- Benchmarking of N_2O producing models. Different N_2O models are evaluated and corrected in order to be compatible with the ASM framework. These extensions to the ASM1 and ASM2d are implemented in the Benchmark Simulation Model framework. The implementations are carried out by two independent users to ensure good quality.
- Benchmarking of the pharmaceutical influent generator. The BSM2 influent generator is extended with the occurrence of pharmaceuticals originating from households. Two different approaches are used; a phenomenological approach for pharmaceuticals with a daily pattern in their occurrence and a stochastic approach for pharmaceuticals with a more random behaviour. Transport conditions in the sewer are shown to have an effect on the occurrence of the soluble and particulate compounds which is important when back calculating the consumption of pharmaceuticals/illicit drugs.
- Benchmarking the fate of pharmaceuticals in the WWTP. The BSM framework is upgraded with the Activated Sludge Model for Xenobiotic trace organics (ASM-X) predicting the fate of pharmaceuticals. Different parameters for different operational conditions are included in order to

take the effect of the operation of the WWTP into account. In addition, co-metabolic and inhibitory effects of other wastewater compounds on the removal rates of pharmaceuticals are included. This work has furthermore resulted in a software tool that is freely distributed to the interested users.

- Combination of N_2O producing model with a physicochemical model. The coupled models are capable of describing the trend of pH and the inorganic carbon concentration, which both have an influence on the N_2O emissions.
- Calibration of the pharmaceutical influent generator. The extended BSM2 influent generator is calibrated using pharmaceutical data with a sampling frequency of two hours during high flow rates and four hours during low flow rates. The influent generator was capable of describing the occurrence of both traditional variables and pharmaceuticals and its metabolites. The excretion pathway of the pharmaceutical and the metabolites was of influence to the occurrence pattern. The tool was also capable of effectively interpolating and extrapolating the time series. The activation of in-sewer biotransformation was demonstrated when estimating consumption rates of drugs.
- Different quantitative and qualitative evaluation criteria were used to assess the predictive accuracy of the extended models. The evaluation criteria pointed out the strong points of the calibration and the points that could be improved.
- Evaluation criteria considering pharmaceutical removal percentages are proposed in order to assess the performance of the different scenarios objectively.

The different extended models can be used combined or as stand-alone models and will provide additional information when defining and selecting the best operational strategies of a WWTP.

1.4 Structure of the thesis

The thesis consists of four different parts (**Figure 1.1**), where each part first discusses the N_2O and then the pharmaceuticals. The first part consists of the introduction and background on the topics of the thesis. The second part contains information on model development of N_2O and pharmaceuticals in wastewater. Both of these Chapters have been published. The calibration and use of the models described in part 2 is detailed in part 3. Lastly, a general discussion of the thesis results and recommendations for future work are provided in part 4. The Sections in the thesis on pharmaceuticals are more elaborate than the Sections on N_2O because the sewer network is considered as well for the pharmaceutical compounds in addition to the WWTP. Furthermore, the pharmaceuticals comprise more substances than N_2O and also additional processes, which requires more explanation.

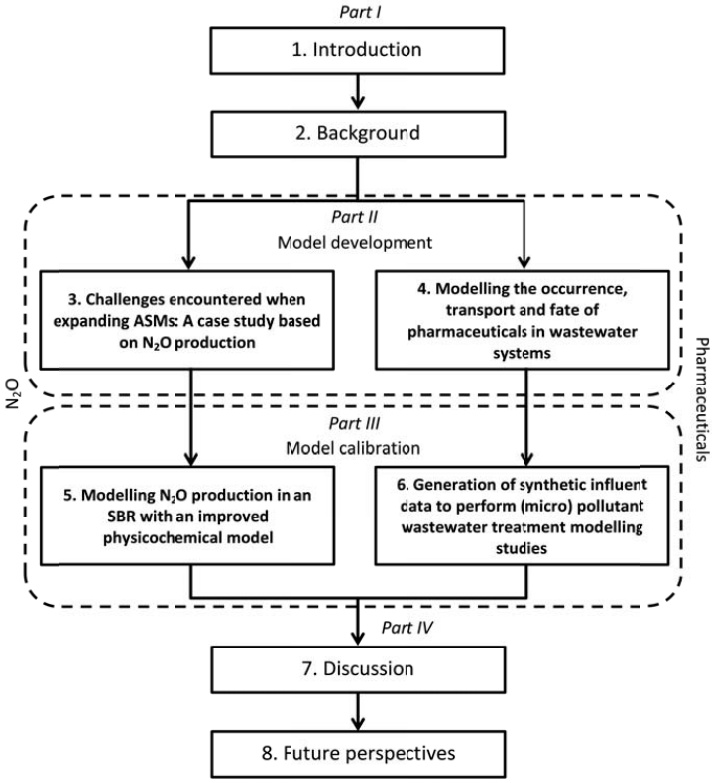

Figure 1.1. Flow diagram of the structure of the thesis

1.5 Dissemination of the PhD results

Publications

Flores-Alsina, X., Arnell, M., Amerlinck, Y., Corominas, L., Gernaey, K.V., Guo, L., Lindblom, E., Nopens, I., Porro, J., Shaw, A., **Snip, L.**, Vanrolleghem, P.A., Jeppsson, U., 2014. Balancing effluent quality, economic cost and greenhouse gas emissions during the evaluation of (plant-wide) control/operational strategies in WWTPs. Sci. Total Environ. 466-467, 616–624.

Snip, L.J.P., Flores-Alsina, X., Plósz, B.G., Jeppsson, U., Gernaey, K.V., 2014. Modelling the occurrence, transport and fate of pharmaceuticals in wastewater Systems. Environ. Model. Softw. 62, 112–127.

Snip, L.J.P., Boiocchi, R., Flores-Alsina, X., Jeppsson, U., Gernaey, K.V., 2014. Challenges encountered when expanding activated sludge models: a case study based on N_2O production. Water Sci. Technol. 70 (7), 1251–60.

Snip, L.J.P., Flores-Alsina, X., Aymerich, I., Rodríguez-Mozaz, S., Plósz, B.G., Corominas, L., Barceló, D., Rodríguez-Roda, I., Jeppsson, U., Gernaey, K.V., 2015. Generation of synthetic influent data to perform (micro)pollutant wastewater treatment modelling studies. Sci. Total Environ. Submitted.

Conferences (peer review)

Snip, L.J.P., Boiocchi, R., Flores-Alsina, X., Jeppsson, U., Gernaey, K.V., 2013. Expanding activated sludge models with additional processes: A case study based on nitrous oxide production by autotrophic ammonia-oxidizing bacteria. 11th IWA Conference on Instrumentation, Control and Automation (ICA 2013), 18-20 September 2013, Narbonne, France. Oral presentation.

Flores-Alsina, X., Ort, C., Martin, C., Benedetti, L., Belia, E., **Snip, L.**, Saagi, R., Talebizadeh, M., Vanrolleghem, P.A., Jeppsson, U., Gernaey, K.V., 2014. Generation of (synthetic) influent data for performing wastewater treatment modelling studies. 4th IWA/WEF Wastewater Treatment Modelling Seminar (WWTmod2014), 30 March – 2 April 2014, Spa, Belgium. Poster presentation.

Snip, L.J.P., Aymerich, I., Flores-Alsina, X., Jeppsson, U., Plósz, B.G., García-Galán, M.J., Rodríguez-Mozaz, S., Barceló, D., Corominas, Ll., Gernaey K.V., 2015. Generation of synthetic influent data for performing (micro)pollutant wastewater treatment modeling studies. 2nd New Developments in IT & Water Conference, 8-10 February 2015, Rotterdam, the Netherlands. Oral presentation.

Snip, L.J.P., Aymerich, I., Flores-Alsina, X., Jeppsson, U., Plósz, B.G., García-Galán, M.J., Rodríguez-Mozaz, S., Barceló, D., Corominas, Ll., Gernaey K.V., 2015. Calibration and evaluation of predictive accuracy of a (micro)pollutant influent generator. 9th IWA Symposium on Systems Analysis and Integrated Assessment (Watermatex 2015), 14-17 June 2015, Gold Coast, Queensland, Australia. Oral presentation.

2. Background

2.1 Greenhouse gas emissions at a WWTP

Greenhouse gases are gases that absorb and emit thermal infrared radiation in the atmosphere. This causes a trapping of the heat within the atmosphere and is called the greenhouse effect. Due to the greenhouse effect the temperature of the earth is increasing. There are three different types of GHGs that can be emitted during wastewater treatment: carbon dioxide (CO_2), nitrous oxide (N_2O) and methane (CH_4) (**Figure 2.1**). These gases all contribute to global warming but in different degrees. The contribution of a gas to the global warming is typically normalised to the contribution of CO_2 and is called the global warming potential (GWP). The GWP is expressed in kg CO_2 equivalent over a certain time horizon (CO_2e). One kg of CH_4 has a GWP of 34 kg CO_2e over 100 years, while 1 kg of N_2O has a GWP of 298 kg CO_2e, i.e. 1 kg of CH_4 has the same effect on global warming as 34 kg of CO_2 (IPCC, 2013). This indicates that N_2O is the strongest greenhouse gas emitted by a WWTP as it is 298 times more potent than CO_2. Besides having the largest GWP, N_2O is also the primary source of NO_2^- and NO in the atmosphere. These nitrogen oxides are ozone depleting substances, meaning they react with the ozone in the atmosphere (Ravishankara et al., 2009). This results in a thinner layer of ozone. The latter is not good since the ozone protects us from harmful UV radiation of the sun.

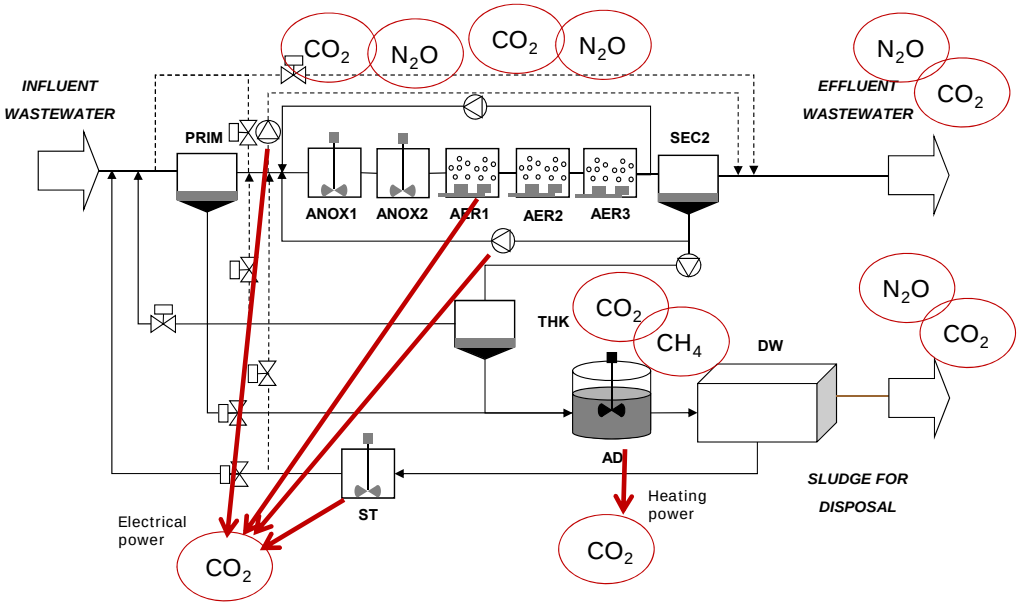

Figure 2.1. The different GHGs emitted from the different units of a WWTP.

The processes responsible for the CO_2 and CH_4 emissions are known and have been incorporated into mathematical models of the WWTP (Corominas et al., 2012), unlike all the N_2O emissions (Ni et al., 2013). There are three different processes in a WWTP that can occur and produce N_2O (Chandran et al., 2011). The most well-known is the denitrification by heterotrophic biomass (Zumft, 1997). Denitrification is one of the pathways used in a WWTP to remove nitrogen. It occurs when there is a lack of oxygen to use as electron acceptor. Heterotrophs can in that case use nitrogen oxides as electron acceptor instead of oxygen and this leads to a four step process of the reduction of nitrate (NO_3^-) to finally N_2. N_2O is an intermediate of this process as can be seen in **Figure 2.2**.

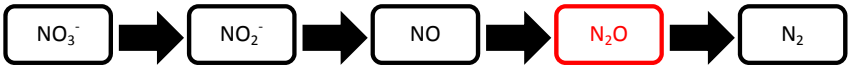

Figure 2.2. The different steps in the denitrification by heterotrophic biomass.

The most commonly used model for the inclusion of N_2O production by heterotrophic biomass is the Activated Sludge Model for Nitrogen (ASMN) (Hiatt and Grady, 2008). This model extends the Activated Sludge Model No. 1 (ASM1) (Henze et al., 2000) with a four step denitrification process and two step nitrification process besides including other nitrogen related processes. The four step denitrification and two step nitrification processes were implemented in BSM1 and successfully calibrated with the results of the original ASM1 (Flores-Alsina et al., 2011; Corominas et al., 2012). Recently, another approach has been modelled based on electron competition instead of chemical oxygen demand (COD) (Pan et al., 2013). However, as this model is not compatible with the ASMs it is not considered in this thesis.

The nitrogen oxides that are present in the wastewater are formed during nitrification, a process which is performed by ammonia oxidising bacteria (AOB) and nitrite oxidising bacteria (NOB) (**Figure 2.3**). Nitrification is the other process responsible for the removal of nitrogen, and is extensively used in traditional WWTPs in combination with denitrification to achieve biological N removal. The autotrophic bacteria – AOB and NOB – need oxygen to oxidise the ammonia and nitrite. However, during periods with low oxygen concentrations, AOB are also capable of performing denitrification, which is called nitrifier denitrification (Kampschreur et al., 2009). AOB lack the enzyme to perform the final step of denitrification from N_2O to N_2 and therefore the production of N_2O is the final step of the denitrification by AOB (Kampschreur et al., 2008).

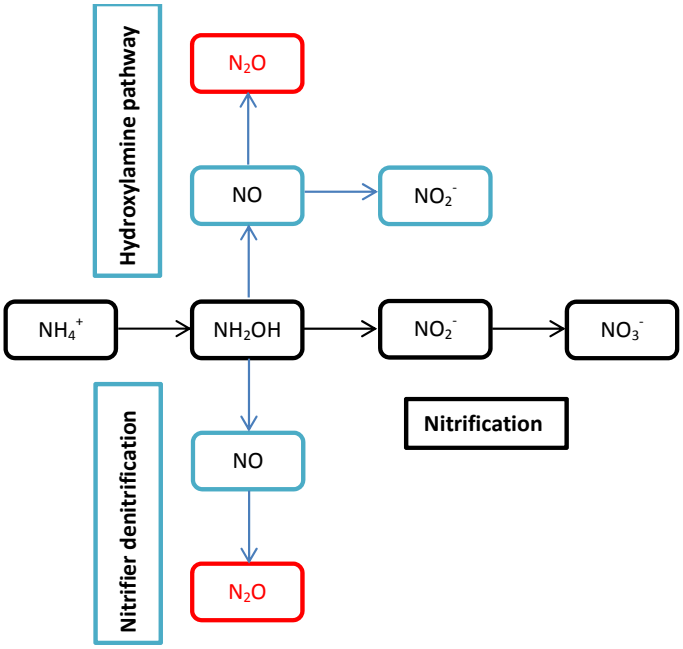

Figure 2.3. The different steps of the nitrification pathway by autotrophic biomass (black) and the possible N_2O producing pathways (blue).

The other mechanism is a chemical reaction of the intermediate hydroxylamine of the first step of the nitrification process (**Figure 2.3**). Hydroxylamine is oxidised to NO which further reacts to form N_2O. This pathway can occur when there are higher oxygen concentrations, in contrast to the nitrifier denitrification pathway (Porro et al., 2014). Law et al. (2012a) also developed another model with an additional intermediate in the nitrification. The radical NOH is formed after the NH_2OH formation and this radical decomposes into N_2O; however it was also stated that these processes are occurring at a low rate as a low consumption of electrons is involved and biomass cannot grow on it. Therefore it would be unlikely that this process is the major process responsible for the N_2O emissions in a WWTP.

It is important to realise that the transfer of dissolved nitrogen oxides to the gas phase also needs to be modelled. In order to predict the emissions, stripping equations need to be added to the model. These equations are required for N_2O, NO and N_2 and can be modelled as demonstrated by Foley et al. (2010a). The volumetric mass transfer coefficients are calculated from the aeration intensity, represented as the volumetric oxygen transfer coefficient (k_La) combined with an empirical correlation between the molecular diffusivity of O_2 and N_2O in water.

2.2 Micropollutants in wastewater

As mentioned in the introduction MPs are present in water bodies at low concentrations and can be harmful for the aquatic environment (Baquero et al., 2008; Lange et al., 2009). As WWTPs are still one of the major disposal pathways for many micropollutants, they can also be considered as one of the possibilities to remove MPs from the wastewater. Different operational strategies of the WWTP could have an impact on the removal of MPs (Clara et al., 2005). Therefore, comparing different operation strategies of a WWTP can be a promising approach to evaluate the removal of MPs. In order to test these strategies, models of the WWTP can be used; however these require that reliable processes of the fate of MPs are included in the WWTP models.

In a WWTP, different processes can remove the micropollutants from the wastewater. Even though each MP has different characteristics, the removal in the WWTP will occur by the same mechanisms. Depending on the micropollutant, it can be volatilised into the atmosphere, be sorbed onto the sludge, biotransformed into another chemical or even mineralised (**Figure 2.4**).

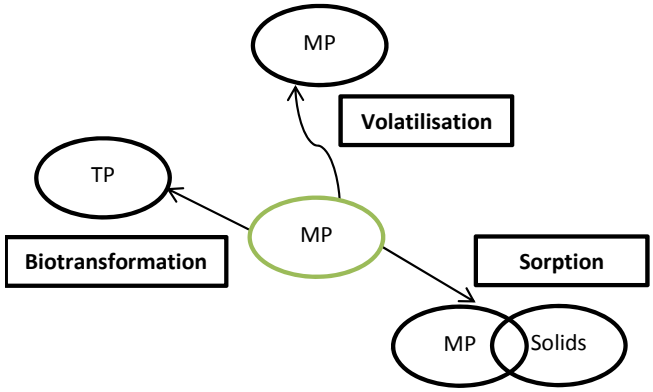

Figure 2.4. The different removal processes of micropollutants in a WWTP (MP is micropollutant, TP is transformation product).

2.2.1 Volatilisation

Volatilisation happens when the micropollutant transfers from the liquid phase to the gas phase. This can be done by surface volatilisation or by stripping when the wastewater is aerated which enhances the transfer between liquid and gas phase. It can be assumed that more musks are transferred from the dissolved phase to the gas phase during aerobic treatment due to the characteristics of these compounds. The Henry constant of the micropollutant can give an indication of the likelihood of stripping (Lee et al., 1998) and a Henry constant higher than a threshold of $3 \cdot 10^{-3}$ is needed to observe volatilisation (Ternes and

Joss, 2006). Due to this threshold, volatilisation can often be neglected for micropollutants (Pomiès et al., 2013). This is especially the case for pharmaceuticals as these substances are required to stay in the blood and therefore usually have a Henry constant lower than 10^{-5} (Ternes and Joss, 2006).

2.2.2 Biotransformation

As each chemical is different, the biotransformation rate is different as well. As mentioned before, also the activated sludge could have an influence on the biotransformation. Studies have shown that an increase in sludge retention time (SRT) can lead to a higher biotransformation rate of micropollutants (Clara et al., 2005). This is most likely due to a more diverse microbial community which has a higher chance to contain microorganisms capable of biotransforming the micropollutant (Ahmed et al., 2007) or the microorganisms are more efficient in removing the micropollutant at higher SRTs (Petrie et al., 2014).

There is no consensus on the fractions in which biotransformation takes place, i.e. if it occurs with dissolved or sorbed micropollutants or both fractions. Justifications for the inclusion or exclusion of the fractions are hardly given (Pomiès et al., 2013).

To model the biotransformation of a micropollutant, first order kinetic expressions as well as pseudo first order are typically used (Pomiès et al., 2013). Compared to first-order kinetics, pseudo first-order equations include the biomass concentration:

First order kinetics: $$\frac{dC_{\mathrm{LI}}}{dt} = -k_{\mathrm{Bio}} C_{\mathrm{LI}}$$ **Eq. 2.1**

Pseudo first order kinetics: $$\frac{dC_{\mathrm{LI}}}{dt} = -k'_{\mathrm{Bio}} C_{\mathrm{LI}} X_{\mathrm{Active}}$$ **Eq. 2.2**

where C_{LI} is the dissolved micropollutant concentration (mg/L), k_{Bio} is the biotransformation kinetic parameter (1/h), k'_{Bio} is the biotransformation kinetic parameter (L/(mg.h)) and X_{Active} is the active biomass concentration (mg/L). However, the active biomass cannot be measured and therefore usually mixed liquor suspended solids (MLSS) or mixed liquor volatile suspended solids (MLVSS) is chosen as the variable to represent the biomass concentration (Byrns, 2001).

Nevertheless, these (pseudo) first order kinetics will not take operational conditions into consideration. For example, oxygen concentration can have an influence on the transformation and therefore also Monod kinetics of oxygen have been used (Lindblom et al., 2006; Plósz et al., 2012). These Monod kinetic parameters are estimated for each specific micropollutant under different operational conditions. Therefore extrapolating parameters to other units of the WWTP and other conditions is not wise to do. Moreover different inhibition kinetics might be needed, such as substrate inhibition or co-metabolic effects

which need to be accounted for at a micro-gram and milligram per litre micropollutant concentration range (Criddle, 1993; Plósz et al., 2010b). Considering that the concentrations of micropollutants are relatively low, it is unlikely that biomass can grow solely on this substrate and their impact on microbial growth is therefore negligible.

It is also important to take the metabolites or transformation products into account as these can occur in higher concentrations than the parent compound (Zhang et al., 2008) and can even be more toxic (Magdeburg et al., 2014). Some of these metabolites/transformation products can also biotransform back into their parent form in the WWTP. This has been reported in different studies on sulfamethoxazole (*SMX*) (Göbel et al., 2005; Plósz et al., 2010a). A challenge is that usually there are multiple chemicals (human metabolites, commercial derivatives of the parent chemical, etc.) that can retransform to the parent compound in the WWTP, and it would be difficult to assess the biokinetics for all different chemicals. The biotransformation of chemicals using a catchall state variable - accounting for the total retransformable chemical concentration - can be modelled as a first order kinetic as demonstrated by Plósz et al. (2010b, 2012).

Retransformation of conjugate $$\frac{dC_{\mathrm{CJ}}}{dt} = -k_{\mathrm{Dec}} C_{\mathrm{CJ}} X_{\mathrm{SS}}$$ **Eq. 2.3**

C_{cj} is the concentration of the total retransformable chemical concentration (mg/L), k_{Dec} is the rate constant (L/(mg X_{SS}·d)), X_{SS} is the concentration of suspended solids (mg/L).

2.2.3 Sorption

A micropollutant can also have the ability to sorb to the particles in a WWTP depending on its properties. There are two different kinds of sorption, namely adsorption and absorption. Adsorption is the process in which the chemical binds to the surface of the particle, absorption is the process of the chemical entering the particle and thus the volume of the particle is involved, not the surface (Ternes et al., 2004a). The likelihood of sorption processes depends on the properties of the chemical as well as on the properties of the particles in the wastewater (Barret et al., 2011).

An indication of the sorption capacity of the chemical can be given by the parameter K_{ow}, the octanol-water partition coefficient describing the partitioning of the chemical in water-octanol mixtures. However, the charge of the chemical is also important when estimating the sorption capacity (Hyland et al., 2012; Sathyamoorthy and Ramsburg, 2013). These characteristics lead to different ways of binding to the particles. There can be van der Waals interactions, which happen mainly with organic non-ionic compounds, but also ion exchanges or charge-charge interactions when positively charged compounds are

involved (Hyland et al., 2012). Pharmaceuticals are developed to be excreted once metabolised and therefore sorption usually plays a minor role for the transformation products (Plósz et al., 2010b).

As mentioned before, also the properties of the particles in the activated sludge can have an effect on the sorption capacity of the chemicals (Holbrook et al., 2004; Barret et al., 2011). As the particles in primary sludge are different from secondary sludge, the sorption rate could also differ when comparing these units, even though the chemical is still the same (Yamamoto et al., 2003; Holbrook et al., 2004). In the secondary sludge, microorganisms represent the greater portion of the suspended solids, while the primary sludge essentially contains fewer microorganisms and has a large lipid fraction (Ternes et al., 2004a). Barret et al. (2011) examined among others the effect of the protein content in the sludge on the sorption rate of micropollutants and found a positive correlation. As the sludge from one WWTP can differ from another due to differences in the circumstances in which the sludge grows (Lu et al., 2014) this should be taken into account when examining sorption of micropollutants. Barret et al. (2010) even suggested that the characteristics of sludge have a higher influence on the sorption than the characteristics of the micropollutant. However, Hyland et al. (2012) tested sorption of micropollutants on sludge from different WWTPs and found little variation among the sludges. As the characteristics of the sludge have only recently been considered when examining sorption there are no models available in the literature that have been developed with the aim of including these characteristics for the sorption of pharmaceuticals.

There is also a part of the sorbed fraction that can become sequestered. This means that the compound is bound to the particle and the process is irreversible. Barret et al. (2011) showed that for polycyclic aromatic hydrocarbons (PAHs) the aging did not affect the sorption and desorption kinetics as the processes were rapid and in equilibrium. The only process active over time was the sequestering of the sorbed fraction of PAH. This sequestered fraction should be excluded from the calculations of the solid-water equilibrium as otherwise an overestimation of the sorbed concentration could be made (Barret et al., 2011; Plósz et al., 2012). However, it should be taken into account when calculating the total concentration of the pharmaceutical in the wastewater.

In order to mathematically model the sorption of micropollutants, different types of sorption isotherms can be used, including the Freundlich isotherm, the Langmuir isotherm and the BET isotherm (Gevaert, 2010). The most commonly used isotherm is the Freundlich isotherm which is based on an equilibrium between the sorbed and dissolved fraction of the micropollutant, and including the concentration of suspended solids as a variable as well (Wang and Grady Jr., 1995; Ternes et al., 2004a; Carballa et al., 2008):

$$\frac{C_{\mathrm{Tot}} - C_{\mathrm{LI}}}{C_{\mathrm{m}}} = K {C_{\mathrm{LI}}}^{n} \qquad \textbf{Eq. 2.4}$$

C_{Tot} is the total concentration of the micropollutant (mg/L) while C_{LI} is the dissolved concentration (mg/L). C_m is the carrier biomass concentration (mg/L) and K and n are Freundlich isotherms. As the constant n is usually approximated to 1, the equation can be rewritten as:

$$C_{SL} = C_{LI} \cdot C_m \cdot K_D \qquad \textbf{Eq. 2.5}$$

where C_{SL} is the sorbed concentration of micropollutant (mg/L) and K_D is the sorption coefficient (L/mg X_{SS}). The X_{SS} corresponds to the suspended solids concentration in the wastewater treatment plant. According to Ternes et al. (2004), these suspended solids should be the newly generated sludge. The recycled sludge can be assumed to be in equilibrium with the wastewater and therefore will not sorb more micropollutant. However, many models use the mixed liquor suspended solids concentration to calculate the K_D (Stasinakis et al., 2010; Plósz et al., 2012).

The mathematical model can include a sorption and desorption rate separately. Including desorption makes the sorption process reversible which is needed when dilution occurs (Barret et al., 2011). The process is also mostly modelled as instantaneously and being in an equilibrium.

Part II

Model development

In this part the Benchmark Simulation Model framework is extended with mathematical models describing nitrous oxide production by ammonia oxidising bacteria (Chapter 3) and by the occurrence, transport and fate of pharmaceuticals in wastewater (Chapter 4). Chapter 3 addresses the objective of testing different N_2O production models. The objectives of modelling the occurrence, transport and fate of pharmaceuticals, developing additional evaluation criteria for removal of pharmaceuticals and comparing different operational strategies are addressed in Chapter 4.

Chapter 3 has been published as:

Snip, L.J.P., Boiocchi, R., Flores-Alsina, X., Jeppsson, U., Gernaey, K.V., 2014. Challenges encountered when expanding activated sludge models: a case study based on N_2O production. Water Sci. Technol. 70 (7), 1251–60.

Chapter 4 has been published as:

Snip, L.J.P., Flores-Alsina, X., Plósz, B.G., Jeppsson, U., Gernaey, K.V., 2014. Modelling the occurrence, transport and fate of pharmaceuticals in wastewater Systems. Environ. Model. Softw. 62, 112–127.

3. Challenges encountered when expanding ASMs: A case study based on N_2O production

Abstract

It is common practice in wastewater engineering to extend standard ASMs with extra process equations derived from batch experiments. However, such experiments have often been performed under conditions different from the ones normally found in WWTPs. As a consequence, these experiments might not be representative for full-scale performance and unexpected behaviour may be observed when simulating WWTP models using the derived process equations. In this Chapter the problems encountered are highlighted using a simplified case study: a modified version of the ASM1 is upgraded with N_2O formation by AOB. Four different model structures have been implemented in the BSM1. The results of the investigations revealed two typical difficulties: problems related to the overall mathematical model structure and problems related to the published set of parameter values. The Chapter describes the model implementation incompatibilities, the variability in parameter values and the difficulties to reach similar conditions when simulating a full-scale activated sludge plant. Finally, the simulation results show large differences in oxygen uptake rates, nitritation rates and consequently the predicted quantity of N_2O emission (G_{N2O}) using the different models.

3.1 Introduction

The ASM1 (Henze et al., 2000) describes organic carbon and nitrogen removal processes in activated sludge systems and has been successfully applied to simulate a large number of WWTPs. The realistic results obtained in the early years promoted intensive research to improve and further expand the scope and phenomena included in ASM1, e.g. by including the description of bacterial storage, two-step nitrification, four-step denitrification and biological phosphorus removal. In this way, ASM1 evolved into ASM2, ASM2d and finally ASM3 as well as many other versions (Henze et al., 2000). This trend led to an increased number of state variables, biochemical processes and model parameters in the models. These extensions improved the level of detail, the realism and predictive capabilities of the developed models. However, they also increased the difficulties regarding model selection, simulation, parameter identification and validation (Vanrolleghem et al., 2003).

Extending standard activated sludge models (ASMs) with additional processes is not always a straightforward task. Engineers may encounter multiple problems when trying to incorporate additional model equations that are normally generated from batch experiments. Most of the time, these batch

experiments were performed under well-controlled conditions and their performance has been evaluated for short periods of time. Different conditions can lead to different microbial communities in activated sludge (Lu et al., 2014). The resulting model equations focus on the phenomena of interest, and therefore only describe part of the existing processes of the system under investigation.

The objective of this Chapter is to illustrate with a simple case study the difficulties encountered when upgrading an ASM with additional processes. The starting point for the case study is a modified version of the ASM1 (Henze et al., 2000) with two-step nitrification and four-step denitrification (Hiatt and Grady, 2008), that is upgraded with nitrous oxide (S_{N2O}) formation during nitritation performed by ammonia oxidising bacteria (X_{AOB}). Four different model structures – based on either formation of S_{N2O} as the final product of nitrifier denitrification with nitrite (S_{NO2}) as the terminal electron acceptor or on generation of S_{N2O} as a by-product of oxidation of hydroxylamine (S_{NH2OH}) to S_{NO2} (Ni et al., 2013) – have been implemented in the BSM1 (Copp, 2002). The Chapter details the general issues that need to be considered for model extension and also provides specific examples.

3.2 Methods

3.2.1 WWTP under study

The BSM1 is the WWTP under study and the plant layout is a modified Ludzack-Ettinger configuration. Tanks 1 and 2 are anoxic, while tanks 3, 4 and 5 are aerobic. An internal recycle sends part of the effluent of tank 5 back to tank 1. The activated sludge unit is followed by a secondary settler. A part of the sludge separated in the settler is returned to the first anoxic reactor to ensure a reasonable sludge age. The remaining part leaves the plant through the sludge line. The standard BSM1 input is used with additional influent concentration of 13.3 g N_2/m^3.

The ASM1 (Henze et al., 2000) extended with a two-step nitrification and four-step denitrification according to the Activated Sludge Model for Nitrogen (ASMN) of Hiatt and Grady (2008) and adjusted as explained in Corominas et al. (2012) is selected as the biochemical model for the activated sludge units. This model already includes N_2O production by ordinary heterotrophic bacteria (OHO). The 10-layer Takács model (Takács et al., 1991) based on the double exponential settling velocity function is used to represent the settling process. Further details about the different BSMs can be found in Gernaey et al. (2014).

3.2.2 Investigated mathematical models

Four different models describing S_{N2O} formation by X_{AOB} (Ni et al., 2013) were incorporated in the ASM framework that was implemented in BSM1. It is important to note that these models expanded the first nitrification step, nitritation, in which ammonium (S_{NH4}) is converted into nitrite (S_{NO2}) by AOB (X_{AOB}),

resulting in a more detailed nitritation model. The four models are shown in **Figure 3.1** with the component N_2O depicted in red, as the focus is on that nitrogen component.

- Models A & B: Nitrous oxide (S_{N2O}) is produced by X_{AOB} as a result of the nitrifier denitrification pathway. In model A, nitrifier denitrification with nitrite (S_{NO2}) as the terminal electron acceptor produces nitric oxide (S_{NO}) and subsequently S_{N2O} by consuming hydroxylamine (S_{NH2OH}) as the electron donor (Ni et al., 2013). In model B, the same nitrifier denitrification pathway is followed as in model A except that the electron donor used is S_{NH4} and not S_{NH2OH} (Mampaey et al., 2013). Another important difference between the two models is the consumption of oxygen during nitrifier denitrification in model B, while model A assumes no consumption of oxygen and even incorporates an inhibitory effect of oxygen. Furthermore, model A takes no biomass growth into account during nitrifier denitrification, while model B assumes growth of AOB for the same process.
- Models C & D: S_{N2O} is produced as a product of incomplete oxidation of S_{NH2OH} to S_{NO2}. In model C the S_{N2O} production is due to the chemical decomposition of the unstable radical S_{NOH}, an intermediate of S_{NH2OH} oxidation (Law et al., 2012b). In this model, nitritation is split up into a three-step process with S_{NH2OH} and S_{NOH} as intermediates. All three of these steps consume oxygen. During the nitrification and the chemical decomposition of S_{NOH}, no biomass growth is modelled as it is assumed that too few electrons are released during the processes (Law et al., 2012b). Contrarily, model D assumes that S_{N2O} is produced from the reduction of S_{NO}, an intermediate of the aerobic oxidation of S_{NH2OH} (Ni et al., 2013). This model assumes biomass growth during nitrification but not during the biological reduction of S_{NO}. Oxygen is needed for all processes except the biological reduction from S_{NO} to S_{N2O}.

Stripping equations are implemented for S_{N2O}, S_{NO} and S_{N2} as given by Foley et al. (2010b) to estimate the quantity of N_2O (generated by both AOB and ordinary heterotrophic organisms (OHO) activities) emitted per day (G_{N2O}). Nitrous oxide volumetric mass transfer coefficients are calculated from aeration intensity, represented as the volumetric oxygen transfer coefficient (K_La) combined with an empirical correlation between the molecular diffusivity of O_2 and N_2O in water. The volumetric mass transfer coefficients of S_{NO} and S_{N2} are calculated by the same approach as used for S_{N2O}.

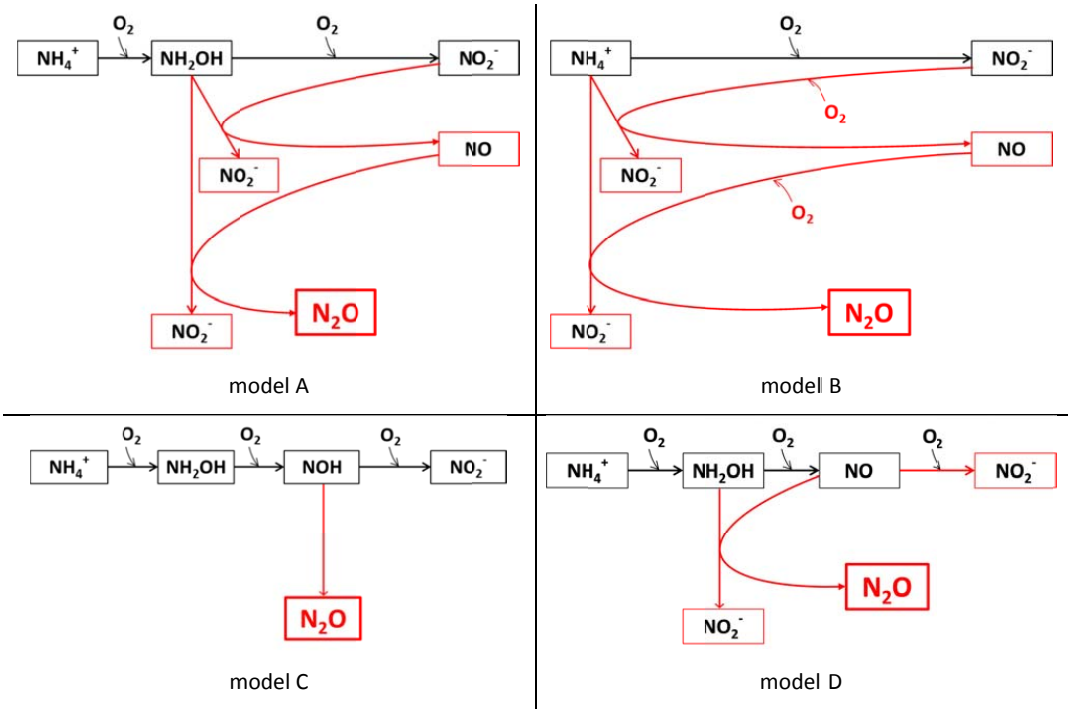

Figure 3.1. Overview of the four different models that predict N_2O production by AOB. Model A is based on the nitrifier denitrification pathway using hydroxylamine as an intermediate of the first step of nitrification. Model B is also based on the nitrifier denitrification pathway; however it excludes hydroxylamine as an intermediate. Model C describes the chemical breakdown of radical NOH and model D expresses the biological reduction of NO.

3.3 Results and Discussion

Note that the corrected model matrices for models A and C are included in the Chapter (**Tables 3.1** and **3.2**, respectively), whereas models B and D are included in Appendix A.1 (**Tables A.1.1** and **A.1.2**, respectively).

3.3.1 Mathematical model structure

Before implementing the four models presented above into the BSM1, the continuity of the stoichiometry and the consistency of the kinetic expressions were verified. The continuity check was carried out numerically by multiplying the stoichiometric matrix with the composition matrix (COD, nitrogen and charge). The resulting matrix should contain only zeros, or values near zero in case of rounding approximations (Hauduc et al., 2010). Kinetic expressions were checked carefully ensuring: 1) reactant limitation; 2) coherence in the switching functions; and, 3) consistency in the rates (Hauduc et al., 2010). The results of these two analyses revealed four different types of problems: 1) *inconsistencies*; 2) *gaps*; 3) *typing errors*; and, 4) *coupling problems*.

Table 3.1. The corrected process matrix for autotrophic N_2O formation according to model A within the ASM context (full description of the process parameters can be found in (Ni et al., 2013)).

Process	S_{O2}	S_{NH4}	S_{NH2OH}	S_{NO2}	S_{NO}	S_{N2O}	X_{AOB}	S_{ALK}	*rate*
A-1	-1.14	*-1*	*1*					$-1 * i_{Charge,NH4}$	$\mu_{AOB,AMO} \frac{S_{O2}}{K_{S1,O2\_AOB} + S_{O2}} \frac{S_{NH4}}{K_{NH4,AOB} + S_{NH4}} X_{AOB}$
A-2	$-\frac{2.29 - Y_{AOB}}{Y_{AOB}}$	$-i_{N_{AOB}}$	$-\frac{1}{Y_{AOB}}$	$\frac{1}{Y_{AOB}}$			*1*	$-i_{N_{AOB}} * i_{Charge,NH4} + \frac{1}{Y_{AOB}} * i_{Charge,NO2}$	$\mu_{AOB,HAO} \frac{S_{O2}}{K_{S2,O2\_AOB} + S_{O2}} \frac{S_{NH2OH}}{K_{NH2OH,AOB} + S_{NH2OH}} \frac{S_{NH4}}{K_{NH4} + S_{NH4}} X_{AOB}$
A-3			*-1*	*-3*	*4*			$-3 * i_{Charge,NO2}$	$\mu_{AOB,HAO} \eta_{\mu,AOB,Ax} \frac{K_{I,O2\_AOB}}{K_{I,O2\_AOB} + S_{O2}} \frac{S_{NO2}}{K_{NO2,AOB} + S_{NO2}} \frac{S_{NH2OH}}{K_{NH2OH,AOB} + S_{NH2OH}} X_{AOB}$
A-4			*-1*	*1*	*-4*	*4*		$1 * i_{Charge,NO2}$	$\mu_{AOB,HAO} \eta_{\mu,AOB,Ax} \frac{K_{I,O2\_AOB}}{K_{I,O2\_AOB} + S_{O2}} \frac{S_{NO2}}{K_{NO2,AOB} + S_{NO2}} \frac{S_{NH2OH}}{K_{NH2OH,AOB} + S_{NH2OH}} X_{AOB}$
ASMN-12							***-1***		$\boldsymbol{b_{AOB} X_{AOB}}$

Table 3.2. The corrected process matrix for autotrophic N_2O formation according to model C within the ASM context (full description of the process parameters can be found in (Ni et al., 2013)).

Process	S_{O2}	S_{NH4}	S_{NH2OH}	S_{NOH}	S_{NO2}	S_{N2O}	X_{AOB}	S_{ALK}	*rate*
C-1	$-\frac{1}{2}*2*\frac{MW_O}{MW_N}$	*-1*	*1*					$-1*i_{Charge,NH4}$	$q_{AOB,1,max}\frac{S_{O2}}{K_{S1,O2\_AOB}+S_{O2}}\frac{S_{NH4}}{K_{NH4,AOB}+S_{NH4}}X_{AOB}$
C-2	$-\frac{1}{2}*2*\frac{MW_O}{MW_N}$		*-1*	*1*					$q_{AOB,2,max}\frac{S_{O2}}{K_{S2,O2\_AOB}+S_{O2}}\frac{S_{NH2OH}}{K_{NH2OH,AOB}+S_{NH2OH}}X_{AOB}$
C-3	$-\frac{1}{2}*2*\frac{MW_O}{MW_N}$			*-1*	*1*			$1*i_{Charge,NO2}$	$q_{AOB,3,max}\frac{S_{O2}}{K_{S3,O2\_AOB}+S_{O2}}\frac{S_{NOH}}{K_{NOH,AOB}+S_{NOH}}X_{AOB}$
C-4				*-1*		*1*			$q_{AOB,4,max}\frac{S_{NOH}}{K_{NOH}+S_{NOH}}$
ASMN-9	$-\frac{3.43-Y_{AOB}}{Y_{AOB}}$	$-i_{N_{AOB}}-\frac{1}{Y_{AOB}}$			$\frac{1}{Y_{AOB}}$		***1***	$\left(-i_{N_{AOB}}-\frac{1}{Y_{AOB}}\right)*i_{Charge,NH4}+\frac{1}{Y_{AOB}}*i_{Charge,NH4}$	$\hat{\mu}_{A1}X_{AOB}\frac{S_{FA}}{K_{FA}+S_{FA}+S_{FA}^2/K_{I9FA}}\frac{S_{O2}}{K_{OA1}+S_{O2}}\frac{K_{I9FNA}}{K_{I9FNA}+S_{FNA}}$
ASMN-12							***-1***		$b_{AOB}X_{AOB}$

3.3.1.1 Inconsistencies

The first problem was related to the kinetic rate expression of nutrient (ammonium) limitation in the autotrophic growth process. This term was missing in models A, C and D, which could induce negative ammonium concentration values, especially during long term simulations. The kinetic rates were modified in models A, C and D to include switching functions. **Table 3.1** shows an example of the corrected kinetics of rate *A-2* (grey shaded) of model A.

Another inconsistency is how AOB growth is (mathematically) represented in the different models. For example, model A has growth included in only one process, namely the reduction of S_{NH2OH}, while model B has included AOB growth in all three processes (**Tables 3.1** and **A.1.1**). Thermodynamically speaking, it is difficult to assess in which process the energy is used for growth and thus in which process the growth should be modelled. This can be done by choosing one process as is done in model A, or by dividing the growth accordingly over the different processes as is shown in model B. In model D the growth was modelled in two processes which lead to an overestimation of the growth of AOB as the growth was not equally divided. Therefore the matrix was adjusted to remove the growth of AOB in process *D-3* by dividing the $\mu_{AOB,HAO,1}$ by the yield of AOB (see **Table A.1.2**).

3.3.1.2 Gaps

The second problem concerned the correct descriptions of alkalinity (S_{ALK}) to guarantee the continuity in ionic charge of the biological processes and thereby the possibility to predict potential pH changes. The effect of the different charged compounds on S_{ALK} was taken into account in models A, B, C and D. No alkalinity limitations were assumed in the models. **Table 3.1** shows the calculated stoichiometric coefficients for S_{ALK} to balance charges for model A in the dashed box.

3.3.1.3 Typing errors

Typing errors were found in models A and D in the publication of Ni et al. (2013). In the stoichiometry matrices of these models, S_{NH4} was modelled as being produced instead of consumed as nutrient during growth of X_{AOB}. In **Table 3.1**, the correct sign is included to describe growth-related uptake of S_{NH4} by X_{AOB} (in the box).

3.3.1.4 Coupling challenges

There were three different challenges encountered with the models when trying to couple them with the ASMN. The first challenge is related to process omission, the second to the units used and the last to the structure of the model.

Models A, B and D describe the first step of nitrification and the corresponding growth of X_{AOB}. However, the models do not include the decay of these bacteria. In the work of Ni et al. (2013) the models were used to describe batch experiments and therefore absence of decay rates was indeed not an issue due to the limited duration of the experiments (hours). However, when extending the simulation time to weeks, which is required when simulating an activated sludge plant, this assumption could lead to unrealistic concentration values. In order to correct this situation, the ASMN (Hiatt and Grady, 2008) decay rates were used. **Table 3.1** shows an example for model A, which includes the decay of AOB (*ASMN-12*) and its rate (shown in bold). In addition, the whole ASM is assumed to be based on the death-regeneration principle (not shown in the table). Thus, one fraction of the decayed biomass is transformed to inert products (X_P) and the other part becomes biodegradable organic material (X_S) that may potentially be hydrolysed.

Model C had no biomass growth associated with nitritation due to a low consumption of electrons (Law et al., 2012b). Therefore the nitritation process of ASMN could not be replaced by the nitritation of model C as was done for the other three models. An option to include AOB growth may be to use the X_{AOB} growth of ASMN (Hiatt and Grady, 2008). This can be seen in **Table 3.2** where the X_{AOB} growth (ASMN-9) and X_{AOB} decay (ASMN-12) are added to the model (bold). However, such an addition could lead to an unrealistic high consumption of S_{NH4} as this consumption is included twice. Another possibility to overcome the exclusion of biomass growth could be to include growth of AOB in the process equations of model C. There is a possibility to add biomass growth to *C-2* and/or *C-3* (**Table 3.2**). If this inclusion would be done, the stoichiometric matrix should be adjusted in those processes to include the yield of the AOB and also the rates (q_{AOB}) should be divided by the yield of AOB in order to represent maximum growth rates. However, the yield of AOB was not used for the estimation of parameters as model C has no biomass growth included. Also it is uncertain if *C-2* and *C-3* or only one of those processes should have biomass growth modelled. Due to these uncertainties and in order to stay as close to the original model as possible, it was decided to use the processes of ASMN for the X_{AOB} growth even though the S_{NH4} consumption could be unrealistically high.

The second challenge was related to the units used in the different models and appeared in model C. The state variables of model C were defined in mmole/L units, while the ASM is based on g COD/m^3 and g N/m^3. To be able to implement model C in an ASM context, the units have to be identical, and thus the model had to be rewritten and stoichiometry and parameter values needed to be converted. This was done by calculating the amount of COD or N in the components per mole (**Table 3.2**, boxes).

The last challenge was encountered in the model structure and also found in model C. The structure of model C was based on the different steps occurring within the AOB cells and with a last process (*C-5*) closing the electron balance by only taking reduction of oxygen into account. When implementing this

model in the ASM framework, the continuity of the processes could not be verified with process *C-5* standing alone. Therefore this process was divided over the processes *C-1*, *C-2* and *C-3* in order to close the mass balance of each process (boxes). The implemented model can be seen in **Table 3.2**.

3.3.2 Parameter values

3.3.2.1 Parameter variability

The presented parameter sets for models A-D show high variability (Ni et al., 2013). For example, in model A the maximum hydroxylamine oxidoreductase mediated reaction rate ($\mu_{AOB,HAO}$) shows 50% variation (from 0.092 to 0.183 1/h). Another example, and even more extreme, is the anoxic reduction factor ($\eta_{\mu,AOB,AX}$) in model B, which changes from 0.0006 to 0.72 (a factor of 1200). One should of course be aware that those parameters were estimated under different conditions of temperature, sludge retention time and feeding composition, and therefore correction factors must be adjusted by e.g. Arrhenius equations. Thus, Ni et al. (2013) fitted the parameter values to describe the data. However, in some cases the values could not fully represent the real situation. Furthermore, the parameters could also have been lumped, meaning they represent multiple parameters, which could explain the large variation of the estimated values.

3.3.2.2 Parameter compatibility

As mentioned at the beginning of this Chapter, some of the models describing the added phenomena are developed based on quite exceptional experimental situations (control, duration). It has been a concern for some years if batch experiments can provide parameter values that are applicable to continuous long-term processes (Vanrolleghem and Keesman, 1996; Checchi and Marsili-Libelli, 2005). Another issue is linking a partial nitration model with its subsequent processes such as decay of AOB and growth of NOB for which no parameter values have been obtained during the batch experiments. Inadequate decay rates for AOB or growth rates and affinity constants for NOB may produce undesirable results and will require an extra calibration effort. An example of the effect of different parameter values is given in **Figure 3.2**. The decay rates were based on the minimum, default and maximum value mentioned by Hiatt and Grady (2008). The maximum growth rates are based on the smallest and the largest value found in Ni et al. (2013). With these values, the largest variation in the results can be found.

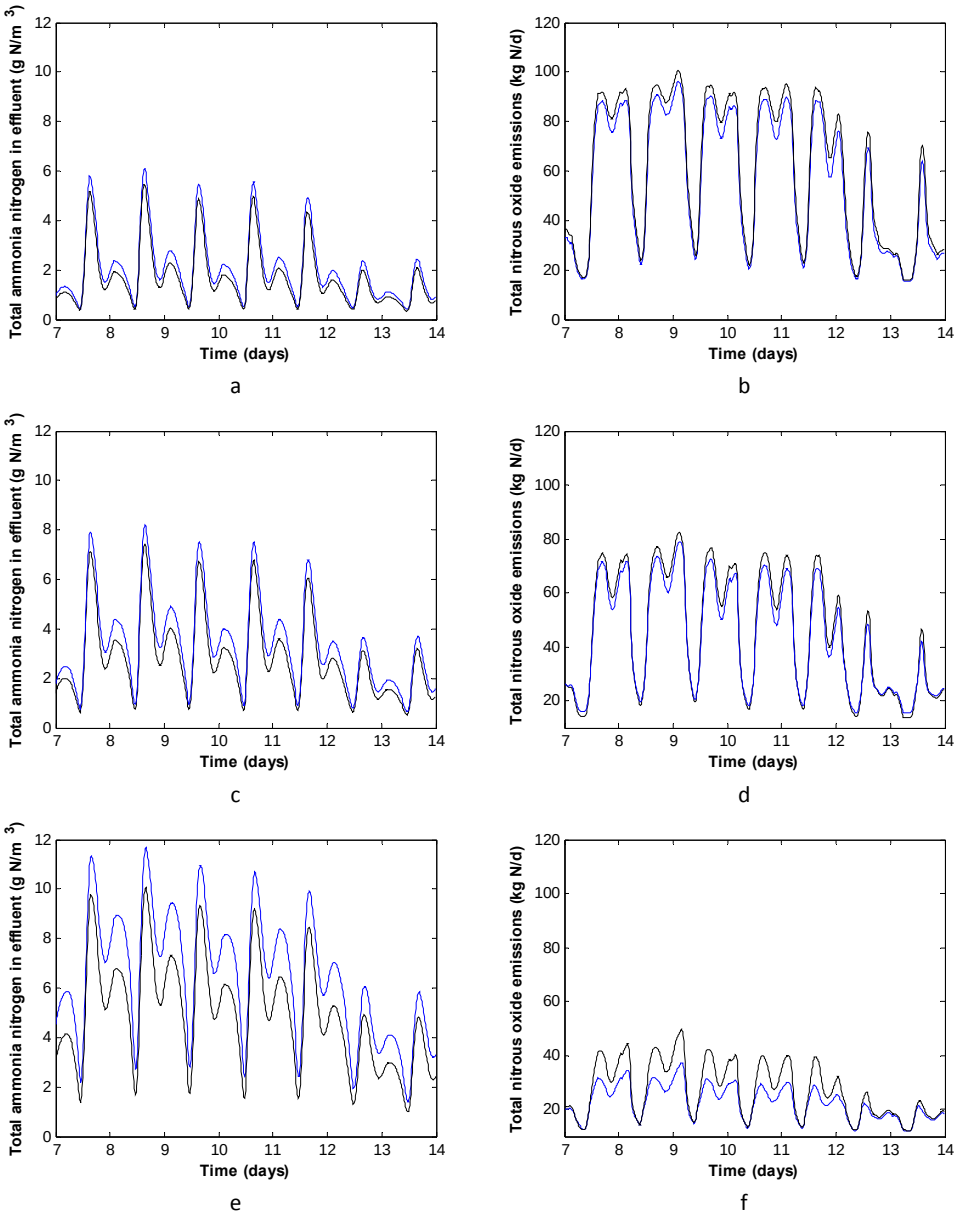

Figure 3.2. The effluent concentration of total ammonia nitrogen and the total N_2O emissions of model A with a maximum growth rate for AOB of 2.928 1/d (black) and 2.760 1/d (blue) in combination with different decay rates for AOB of 0.05 1/d (a, b), 0.096 1/d (c, d) and 0.15 1/d (e, f).

Figure 3.2 shows how the S_{NH4} concentration will change when different maximum growth rates and decay rates of the X_{AOB} are used. The effect of these different parameter values is even larger on the N_2O

emissions. From **Figure 3.2** it can be concluded that according to model A the more AOB are present, the lower the ammonium concentration in the effluent will be and the higher the N_2O emissions.

3.3.3 Simulation results

The default parameter values of ASM1 (Henze et al., 2000) and ASMN (Hiatt and Grady, 2008; Corominas et al., 2012) were used to simulate models A, B, C & D when possible, and were complemented with the estimated parameters from the experiments performed by Yang et al. (2009) and estimated by Ni et al. (2013). Dynamic simulation results of the (open loop) BSM1 plant are summarised in **Table 3.3**. Results show very different oxygen uptake rates, nitritation, nitratation and consequently N_2O formation rates (from 21.32 to 175.20 kg N_2O-N per day, equivalent to 2.1% and 17.5% of the total influent nitrogen load per day), although the models in the literature show similar behaviour when fitting the data from the batch experiments. The difference in the N_2O production between model A and model B is due to the different roles of oxygen in the AOB denitrification pathway. Model C predicts the lowest concentration of X_{AOB} as there are two processes consuming S_{NH4} while only one of those has AOB growth associated. Thus a fraction of substrate is being consumed without growth of X_{AOB} (see Section 3.3.1.4). The lower total N_2O emissions of model C compared to ASMN can be due to the lower S_{NO} concentrations and due to the additional nitrogen components S_{NH2OH} and S_{NOH}. Model D has the lowest emissions of the four models due to a more complete heterotrophic denitrification, as a result of higher NO consumption, which has an inhibitory effect on OHOs.

The discrepancies among the predictions of the different models are the result of both different parameter values and mathematical structures used to express the kinetic rates. It must be noted that processes related to NOB and OHO all have the same model structure and use identical parameter sets in all four models. Also, note that model parameters have not been calibrated for the BSM1 system, which can contribute to the relatively high N_2O emissions seen in **Table 3.3** compared to Aboobakar et al. (2013) who reported only 0.036 % N_2O emissions of the total nitrogen influent. However, emission levels are still comparable with those reported by Kampschreur et al. (2009) for full-scale systems. The reader should also be aware that the focus of this Chapter is not to discuss how realistic these model predictions are, but rather to demonstrate the challenges encountered when extending ASMs with additional processes and reactions.

Table 3.3. Dynamic results of the AOB description of models A, B, C & D into the ASMN context simulated using BSM1 (parameter values can be found in Appendix A.1).

Effluent conc.	ASMN (Corominas et al., 2012)	AOB denitrification		Incomplete oxidation of hydroxylamine (NH_2OH)		Units
		Model A	Model B	Model C	Model D	
S_{O2}	2.38	2.51	3.96	5.42	2.52	**g O_2/m^3**
S_{NH4}	5.74	2.86	0.042	2.31	3.35	**g N/m^3**
S_{NO3}	16.71	14.34	2.99	23.82	13.96	**g N/m^3**
S_{NO2}	0.45	1.81	1.98	0.0030	1.10	**g N/m^3**
S_{NO}	0.015	0.019	0.33	0.0010	0.0020	**g N/m^3**
S_{N2O}	0.11	0.026	0.098	0.069	0.046	**g N/m^3**
X_{AOB}*	83.53	102.72	95.16	48.53	81.25	**g COD/m^3**
X_{NOB}*	32.22	30.38	13.20	29.22	30.52	**g COD/m^3**
X_{OHO}*	2148.96	2145.04	2097.12	2213.11	2144.61	**g COD/m^3**
G_{N2O}	**21.32**	**68.42**	**175.20**	**70.13**	**56.70**	**kg N_2O-N/d**
	2.1%	**6.8%**	**17.5%**	**7.0%**	**5.7%**	**mass % N_2O-N of N-influent**

*Concentrations of X_{AOB}, X_{NOB} and X_{OHO} are taken from the last reactor.

Regarding the production of N_2O by AOB it is still unclear which pathway is the dominant pathway in full-scale WWTPs. A possibility can be that more than one of the mentioned pathways are active, which has been tested by Ni et al. (2014) by modelling oxidation and reduction processes separately. Also, Wunderlin et al. (2012) mention that heterotrophic denitrification, nitrifier denitrification as well as hydroxylamine oxidation should be considered when studying strategies to avoid N_2O emissions.

Another possibility could be that in different WWTPs different pathways are responsible for the N_2O production. Another question that should be answered is how much detail is needed in the models to predict the N_2O production, for example is the intermediate S_{NH2OH} needed? Another important note is that the four models describe nitritation using different parameter values and with different stoichiometry and kinetics. Also this last issue contributes to the variation of the predicted N_2O emissions.

3.4 Conclusion

This case study demonstrates the problems that typically arise when expanding an ASM with additional processes. These problems were both related to the mathematical structure and the parameter values. The mathematical structure of the additional model equations should be checked for: 1) *inconsistencies*; 2) *gaps*; 3) *typing errors*; and, 4) *coupling problems*. Regarding the parameter values, care must be taken when coupling different processes. The parameter values estimated during batch experiments may not be adequate for the continuous process and may not be compatible with the values of other parameters. Also, a large variation can be found in parameter values when fitting them to data from batch experiments. The different N_2O producing models mentioned in the case study demonstrate different behaviour as they are based on different assumptions regarding both nitritation and the autotrophic N_2O production.

Finally, one should keep in mind that models are approximations, and therefore one should also have realistic expectations about their predictive capabilities and be aware of their inherent uncertainty.

4. Modelling the occurrence, transport and fate of pharmaceuticals in wastewater systems

Abstract

This Chapter demonstrates how occurrence, transport and fate of pharmaceuticals at trace levels can be assessed when modelling wastewater treatment systems using two case studies. Firstly, two approaches based on: 1) phenomenology; and, 2) Markov Chains, are developed to describe the dynamics of pharmaceuticals with or without clear administration patterns. Additional simulations also show that sewer conditions might have an important effect on the behaviour of the generated compounds and their metabolites. The results demonstrate that different operating conditions in wastewater treatment plants can have opposite effects on the studied pharmaceuticals, especially when they present co-metabolic or inhibitory behaviour in the presence of biodegradable substrate. Finally, the Chapter ends with: 1) a critical discussion of the presented results; 2) a thorough analysis of the limitations of the proposed approach; and, 3) future pathways to improve the overall modelling of micropollutants.

4.1 Introduction

The term “micropollutants” covers trace organic chemicals such as pharmaceuticals, personal care products and biocides. These compounds are found in low concentrations in some water bodies despite the fact that they are not expected to be present in the environment. In many cases, these substances are found within an organism but they are normally not naturally produced by or expected to be present within that organism. This is the consequence of the increasing number of chemicals (from 50,000 up to 100,000) which are being commercially manufactured by industry, subsequently used in households and finally released to the environment through wastewater (Mackay et al., 2006). The potential adverse effects of micropollutants in aquatic environments have been an object of intensive research during the last years (e.g. Ferrari et al., 2003). In many cases, these pollutants can pose a significant risk on the environment and human health (Ternes et al., 2004b). On aquatic life, such adverse effects can be characterised as spread and maintenance of antibacterial resistance (Baquero et al., 2008), sex reversal and/or intersexuality (Lange et al., 2009) or reduction of the reproductive behaviour (Coe et al., 2008).

WWTPs are still one of the major disposal pathways for many micropollutants as they are not designed to remove these compounds (Ternes et al., 2004b). However, there are different investigations that demonstrate that a change in operating conditions such as sludge retention time (Clara et al., 2005) can effectively improve the elimination of micropollutants from the liquid phase by sorption, transformation or

biodegradation (Joss et al., 2008). Therefore, comparison of operational/control strategies in WWTPs is a promising tool to test the relative removal effectiveness of these compounds.

The BSM tools have been developed with the aim of having a platform to objectively compare different control strategies of WWTPs. The main objective of BSM1 was creating a platform for benchmarking carbon and nitrogen removal strategies in activated sludge systems (Copp, 2002). The initial platform evolved into BSM1-P (Gernaey and Jørgensen, 2004), BSM1_LT (Rosen et al., 2004) and finally into BSM2 (Jeppsson et al., 2007; Nopens et al., 2010), which allowed the evaluation of: 1) nitrogen and phosphorus removal strategies; 2) monitoring algorithms; and, 3) plant-wide control strategies. In addition, researchers working within the International Water Association (IWA) Task Group on Benchmarking of Control Strategies for Wastewater Treatment Plants developed other BSM related spin-off products such as the dynamic influent generator (Gernaey et al., 2011), sensor/actuators/fault models (Rosen et al., 2008) and the different computationally efficient implementations (Rosen et al., 2006) of the Anaerobic Digestion Model No. 1 (ADM1) (Batstone et al., 2002), which have been widely used as stand-alone applications in both industry and academia. Over 400 publications, dealing with BSM platforms (or related material), clearly show the interest for the BSM related models within the scientific community (Gernaey et al., 2014). Nevertheless, these tools have not been developed to include one of the emerging challenges that wastewater engineering is facing nowadays: micropollutants.

Literature offers a wide range of studies with extensive measuring campaigns analysing the occurrence of these compounds at the inlet of WWTPs (Göbel et al., 2005; Ratola et al., 2012; Verlicchi et al., 2012). At this moment there are only a few published studies which are trying to describe mathematically how these compounds appear at the inlet of the WWTP. For example, De Keyser et al. (2010), within the framework of the European Research Project Score-PP, developed a stand-alone application that generates time series according to specific (phenomenological/stochastic) release patterns. Influent generators have in general demonstrated to be useful tools for modelling studies since they: 1) significantly reduce the cost and workload related to measuring campaigns; 2) fill gaps due to missing data in the influent flow-rate/pollution/temperature profiles; and, 3) create additional disturbance scenarios following the same catchment principles (Gernaey et al., 2011). Regarding micropollutants, modelling the influent dynamics is of the utmost importance as the occurrence at the WWTP inlet shows a high variability (Ort and Gujer, 2006). This variability is also – at least to some extent – present in the effluent of the WWTP, and the peak concentrations can easily exceed the PNEC of a compound while the average concentration can be below this limit (Nelson et al., 2011).

Another important factor to consider when modelling micropollutants is the transport within the sewer. Ort et al. (2005) stated that the micropollutant load fluctuations are strongly affected by the sewer system topology and properties. In addition, Plósz et al. (2013a) demonstrated the importance of considering in-sewer biotransformation when back-calculating illicit drug consumption rates using end-of-pipe (i.e. WWTP influent) trace organics concentrations and flow data. To our knowledge, there have not been many (modelling) studies assessing the potential of biotransformation or sorption processes within the sewer system. Such processes in the sewer have an important effect on the load of the traditional pollutants arriving at a WWTP (Hvitved-Jacobsen et al., 1998; Ashley et al., 2005). For this reason, it can be expected that this effect will also be visible on the micropollutants load. The latter factor might have important implications when back-calculating drug consumption values based on measured WWTP influent micropollutant data.

Finally, it is important to mention fate models as well, when discussing modelling of micropollutants. Most dynamic models describing the fate of micropollutants in a WWTP include pseudo-first order kinetics for biotransformation and sorption/desorption equations (Melcer et al., 1994; Joss et al., 2005; Collado et al., 2012; Lust et al., 2012; Vezzaro et al., 2014). Parameter estimation and calibration/validation of these models are usually performed using batch experiments spiked with the commercially available micropollutant (Ternes et al., 2004a; Joss et al., 2005). These conventional models can be limited in describing the behaviour in full-scale systems due to several reasons. First of all, the presence of substances that facilitate/inhibit removal and/or transformation of these compounds might not be present in these model systems (Grady, 1998). Secondly, the electron dependency (anaerobic, anoxic or aerobic conditions) on the different removal/retransformation rates should be taken into account (Plósz et al., 2010b; Suarez et al., 2010). Thirdly, the retransformation of parent chemicals from e.g., human metabolites and sequestration of parent chemicals in solids can significantly influence the observed removal rate and sorption, respectively (Plósz et al., 2010b, 2012). Fourthly, the total concentration of microorganisms with the metabolic activity to biotransform xenobiotics should be explicitly represented in models (Lindblom et al., 2009).

In view of the different above-mentioned issues, an extension of the current benchmark simulation framework with an additional module dealing with micropollutants is proposed. Specifically, the study presented herein will focus on a particular type of micropollutants: pharmaceutical compounds. This additional module is based on the ASM-X framework (Plósz et al., 2010b, 2012), as it includes guidelines on: 1) characterization of the pharmaceutical loading and variability in the loading; 2) assessment of the pharmaceutical fractions in aqueous, solid, retransformable, and sequestered state variables; 3) model

identification and calibration using batch experiments; and, 4) model evaluation and validation using full-scale WWTP data. The ASM-X is compatible with the BSM tools as it uses the same modelling approach (see methods Section). Also, the model has been published by Plósz et al. (2010b, 2012, 2013a), clearly stating the processes (and equations) as well as the parameter values, making it a transparent model.

The extension of the benchmark simulation framework with pharmaceuticals will result in a set of generic model blocks (influent generation, sewer systems, wastewater treatment plant and controllers) that are upgraded with specific features to realistically describe the behaviour of pharmaceuticals in urban water systems.

The objective of this Chapter is to demonstrate how occurrence, transport and fate of pharmaceuticals can be assessed when modelling wastewater treatment systems (i.e. catchment, sewer network and wastewater treatment plants). As a result of this combined BSM-ASM-X approach, it is possible to generate pharmaceutical loads based on different information sources (lab experiments, literature data) and different mathematical principles (phenomenological/stochastic). In addition, the proposed approach accounts for some of the physico-chemical processes taking place in the sewer system. Finally, our approach enables a simulation-based investigation of the effect of specific control strategies/operational procedures on the biotransformation, retransformation and sorption rates of the different pharmaceuticals. The Chapter details the development of the BSM-ASM-X extension and then illustrates the performance of this approach with a number of case studies. These case studies investigate the overall WWTP performance for: 1) compounds with different release patterns (three antibiotics (sulfamethoxazole (*SMX*), ciprofloxacin (*CIP*), tetracycline (*TCY*)), one non-steroidal anti-inflammatory drug (diclofenac (*DCF*)) and one anti-epileptic drug (carbamazepine (*CMZ*)); 2) different transport conditions; and, 3) different modes of operation of the WWTP.

This Chapter describes the development of a set of tools that: 1) use the same modelling approach as the well-known ASMs; 2) take into account many of the interactions between traditional and emerging pollutants when mathematically describing both transport and fate; 3) integrate all the different mathematical models in one single software platform which can be easily coupled with traditional ASMs (Henze et al., 2000); and, finally, 4) propose a set of simplified evaluation criteria to objectively assess the fate of the pharmaceuticals. This Chapter thus contributes to the field of wastewater engineering filling some of the gaps left behind by previous work through, for example, model compatibility, simulation input-output transferability, in-sewer compound transformation, WWTP and control strategy/operational procedure performance assessment.

4.2 Methods

4.2.1 Influent generation model

The modelling approach proposed by Gernaey et al. (2011), which generates influent pollutant disturbance scenarios, is used as a starting point (see **Figure 4.1**). The first model block contains the flow rate generation model. The generation of the influent flow rate is achieved by combining the contributions from households, industry, rainfall and infiltration (see **Figure 4.1** top). Rainfall contributes to the total flow rate in two ways: the largest part (*aH*) of the rainfall contribution originates from run-off from impermeable surfaces, and is thus transported directly to the sewer. Rainfall on permeable surfaces (fraction *100 - aH* of the rainfall) will influence the groundwater level, and thus the contribution of infiltration to the influent flow rate. Similarly to the flow rate generation model, it is assumed (see **Figure 4.1** middle) that there are two pollutant sources, households and industry, which is an acceptable simplification.

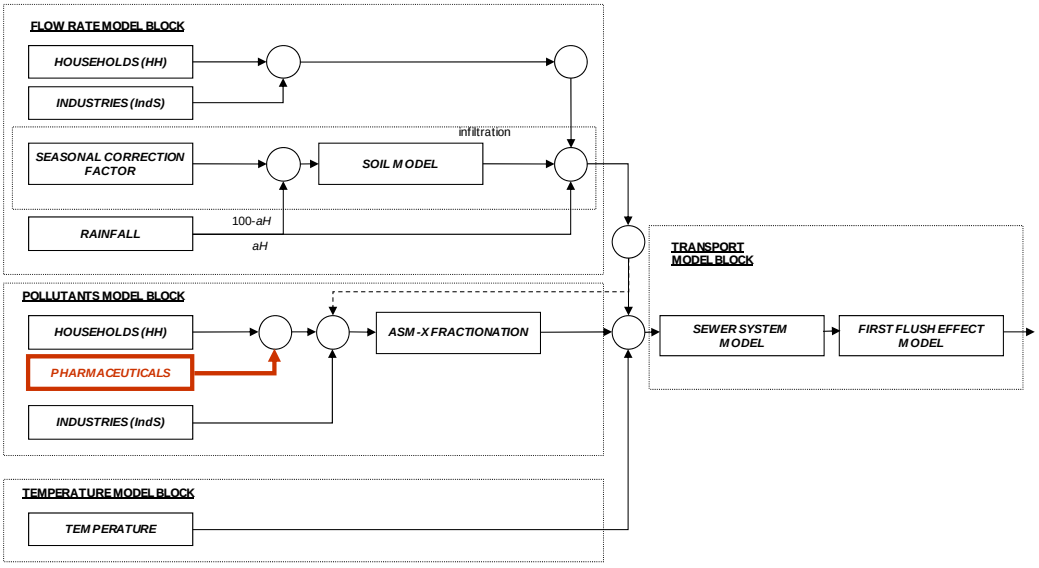

Figure 4.1. Schematic representation of the influent pollutant disturbance scenario modelling approach with the addition of pharmaceuticals.

Pollutants from both sources are combined and converted to ASM1, ASM2d or ASM3 variables. The temperature of the wastewater is added as an additional state variable in the influent model (see **Figure 4.1** bottom). The temperature profile includes a seasonal variation, i.e. there is a warm and a cold season, and also a daily variation. The size of the sewer system can be incorporated in the influent dynamics as well: the larger the sewer system, the smoother the simulated diurnal flow rate and concentration variations (see **Figure 4.1** right). Finally, the particulate pollutants of each model are passed through the

'First Flush Effect' model block, where first flush effects are mimicked as a function of flow rate, occurring for example during severe rain events following dry periods.

Besides describing the occurrence of traditional pollutants (TSS, COD, BOD_5, TN and TP), the models have been upgraded to describe the behaviour of selected pharmaceuticals. Daily, weekly and seasonal influent dynamics of pharmaceuticals are generated based on two different principles: 1) a phenomenological approach based on predefined pollutant profiles; and, 2) a stochastic approach based on Markov Chains.

The first approach (phenomenological) is particularly suited to describe the occurrence of compounds that have a clear daily, weekly and/or seasonal variation (Teerlink et al., 2012). The predefined profiles are stored in input files, and are constructed based on available knowledge on: 1) administration patterns; 2) bioavailability; 3) half-time; and, 4) total annual consumption rates (Göbel et al., 2005; Plósz et al., 2010a). These profiles are sampled cyclically at different time scales and the resulting signal is obtained by multiplication. The resulting signal is the pollutant flux of the pharmaceutical.

The second approach (stochastic) is used to describe the occurrence of compounds with a more random behaviour. In this case, a Markov Chain approach is used to describe the source pattern characteristics (Hastings, 1970; Barber, 1978). The Markov Chain contains a number of different states (s_i) between which the system switches according to certain transition probabilities. The transition probability (P) to switch from s_i to s_j at time instance, k, is:

$$P_{i,j} = \left[P(s_j(k)|s_i(k-1)\right] \qquad \textbf{Eq. 4.1}$$

In the simplest form, the occurrence of a pharmaceutical X is modelled by two states. The two states (s_1 and s_2) represent the presence or absence of the pharmaceutical and the transition probability (P) describes the probability of switching between the states. In the transition matrix information can be introduced about the frequency, intensity and duration of the events by defining: 1) the set of probabilities; and, 2) the number of states. The profile obtained by the Markov Chain approach can also be combined with a more deterministic weekly and seasonal variation by multiplication. The resulting signal is the pollutant flux.

The pollutant fluxes are transformed into g/PE (Person Equivalent), by multiplying the values in the input files – containing normalised information on the dynamics – with their loads (normally given in mg/(day.1000 PE)) and with PE, the number of person equivalents in the catchment area. Zero-mean white noise can be added to give more realism to the generated series using the noise variance as a tuning parameter. A schematic representation of the whole calculation procedure is presented in **Figure 4.2**. The

concentrations of the different forms of the pharmaceutical are calculated by dividing the results of the pollutant model block (**Figure 4.1** middle) by the result of the flow rate model block (**Figure 4.1** top).

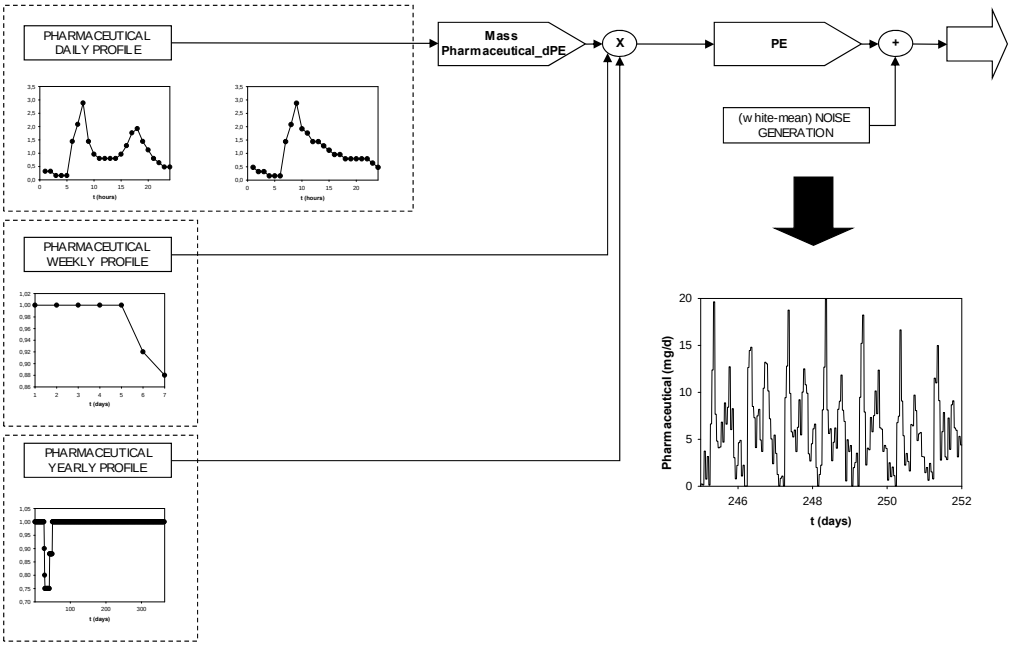

Figure 4.2. Model blocks to create the different pharmaceutical loading profiles.

4.2.2 BSM1 plant layout and default biological models

The influent generated by the influent generator is passed through a primary clarifier before connecting to the WWTP. The primary clarifier model is based on the Otterpohl/Freund model (Otterpohl and Freund, 1992). The WWTP model used in this study is the BSM1. The BSM1 plant layout is a modified Ludzack-Ettinger configuration (Copp, 2002) (see schematic representation of the plant layout in **Figure 4.3**).

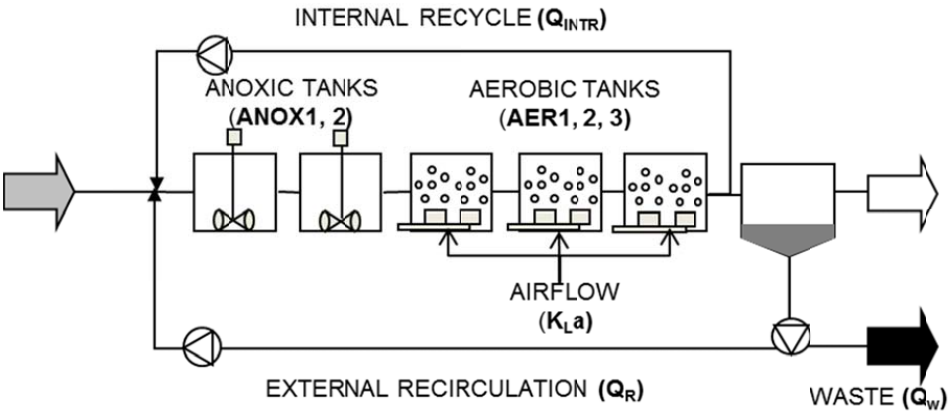

Figure 4.3. Schematic layout of the Benchmark Simulation Model No. 1 physical plant.

Tanks 1 and 2 are anoxic (ANOX1 and 2), while tanks 3, 4 and 5 (AER1, 2 and 3) are aerobic. An internal recycle (Q_{intr}) sends part of the effluent of tank 5 back to tank 1. The activated sludge (AS) unit is followed by a secondary settler. A part of the effluent (Q_R) of the secondary settler is sent back to the activated sludge unit to ensure that enough biomass is present. The other part of the effluent (Q_W) leaves the plant and is wasted. The ASM1 (Henze et al., 2000) is selected as the biochemical model for the activated sludge Section and is extended with the ASM-X framework (Plósz et al., 2010b, 2012) to describe the fate of selected pharmaceuticals. A 10-layer Takács model (Takács et al., 1991) based on the double exponential settling velocity function is used to represent the settling process. Further details can be found in Gernaey et al. (2014).

4.2.3 Pharmaceuticals under study

In this Chapter the occurrence, transport and fate of five different pharmaceuticals are studied. These pharmaceuticals are three antibiotics; sulfamethoxazole (*SMX*), ciprofloxacin (*CIP*) and tetracycline (*TCY*), one non-steroidal anti-inflammatory compound; diclofenac (*DCF*) and one psychoactive drug; carbamazepine (*CMZ*). Antibiotics are used to treat infections, *DCF* is used to reduce inflammation and as an analgesic reducing pain in certain conditions and *CMZ* is used primarily in the treatment of epilepsy and bipolar disorder, as well as trigeminal neuralgia. The selection of these compounds is based on accounting for different patterns, bioavailability, half-life and administration pattern values. Also, their differences in chemical structure (aromatic rings), metabolism (co-metabolism/inhibition) and properties (hydrophobicity, biodegradability) will influence their behaviour when evaluating transport and fate.

4.2.4 Pharmaceutical modelling using the ASM-X framework

The fate of pharmaceuticals is described using the principles of ASM-X and can be seen in **Table 4.1** (Plósz et al., 2010b, 2012). This modelling framework considers several processes, namely sorption-desorption, biotransformation and parent compound retransformation with different kinetics. Each pharmaceutical under investigation is decomposed into four different state variables. One of the two state variables in the liquid phase is the parent chemical concentration (C_{Ll}). The other is the total retransformable chemical concentration (C_{Cl}) that accounts for: 1) human metabolites, e.g., glucoronide, acetyl, sulphate; 2) other commercially available pharmaceuticals biotransformed via the parent compound; and, 3) parent compounds sequestered in hydrolysable particulate material. The other two state variables are in the solid phase; the sorbed concentration (C_{SL}) and the sequestered form ($C_{SL,I}$) – the latter state variable only being used for DCF and CMZ. The sorbed and sequestered fractions of the pharmaceutical are not available for biotransformation. Also the retransformable fraction is not (further) biotransformed; it can only retransform into the parent chemical. As the concentrations of the pharmaceutical, secondary and possibly co-metabolic substrates are in the range of µg/L or ng/L, it is assumed that the biomass growth is negligible during the consumption of the pharmaceuticals and therefore no biomass formation is modelled in the ASM-X framework related to the micropollutant transformations. Also, potential effects of the pharmaceuticals on the actual biomass activity are not taken into account.

All processes are modelled under aerobic and anoxic conditions with different parameters that are also compound specific. Finally, besides compound specific parameters also the model structures are compound specific, and account for the impact (e.g. competitive inhibition for antibiotics) of growth substrates (chemicals present in wastewater) as well as for the co-metabolic substrate (xenobiotics) biotransformation. For example, as mentioned in Section 4.2.3, the biotransformation of *SMX* is inhibited by readily biodegradable substrates which influence the biotransformation rate of the compound in the wastewater. On the contrary, the biotransformation rate of *CMZ* is enhanced by readily biodegradable substrates and therefore the process of biotransformation of this compound is different from that of *SMX*. **Table 4.1** shows the Gujer matrix of ASM-X identified for the micropollutants *SMX*, *TCY*, *CIP*, *DCF* and *CMZ* (Plósz et al., 2010b, 2012). The lower part of the table shows the parts of the model structure, which are compound specific. These processes are only activated in the sewer system model during the investigation of different conditions in the transport Section. The processes are also added to the ASM1 in the BSM1, as mentioned before, to examine the fate of the different pharmaceuticals.

Table 4.1. Stoichiometric (Gujer) matrix of the ASM-X fate model. Special structures (f) are necessary to describe competitive inhibition (*SMX*, *TCY*, *CIP*) and co-metabolism (*DCF*, *CMZ*) with soluble biodegradable organic matter (S_S) of retransformation/ biotransformation processes.

(i) Component → i (j)Processes ↓	C_{LI}	C_{CJ}	C_{SL}	$C_{SL,I}$	Process rate
De-sorption	1		-1		$k_{Des}C_{SL}$
AEROBIC PROCESSES					
Sorption	-1		1		$k_{Des}K_{D,Ox}C_{LI}\frac{S_O}{K_O+S_O}X_{SS}$
Parent compound retransformation	1	-1			$f(k_{Dec})C_{CJ}\frac{S_O}{K_O+S_O}X_{SS}$
Biotransformation	-1				$f(k_{Bio})C_{LI}\frac{S_O}{K_O+S_O}X_{SS}$
ANOXIC PROCESSES					
Sorption	-1		1		$k_{Des}K_{D,Ax}C_{LI}\frac{K_O}{K_O+S_O}X_{SS}$
Parent compound retransformation	1	-1			$f(k_{Dec})C_{CJ}\frac{K_O}{K_O+S_O}X_{SS}$
Biotransformation	-1				$f(k_{Bio})C_{LI}\frac{K_O}{S_O+K_O}X_{SS}$

SMX, TCY, CIP		***DCF, CMZ***	
Impact of parent compound retransformation $f(k_{Dec})$			
Parent compound retransformation (*aerobic*)	$k_{Dec,Ox}\frac{K_S\eta_{Dec}}{K_S\eta_{Dec}+S_S}$	Parent compound retransformation (*aerobic*)	$k_{Dec,Ox}$
Parent compound retransformation (*anoxic*)	$k_{Dec,Ax}\frac{K_S\eta_{Dec}}{K_S\eta_{Dec}+S_S}$	Parent compound retransformation (*anoxic*)	$k_{Dec,Ax}$
Impact of biotransformation kinetics $f(k_{Bio})$			
Biotransformation (*aerobic*)	$k_{Bio,Ox}\frac{K_S\eta_{Bio}}{K_S\eta_{Bio}+S_S}$	Biotransformation (*aerobic*)	$q_{c,Ox}\frac{S_S}{K_S+S_S}+k_{Bio,Ox,Ss}$
Biotransformation (*anoxic*)	$k_{Bio,Ax}\frac{K_S\eta_{Bio}}{K_S\eta_{Bio}+S_S}$	Biotransformation (*anoxic*)	$q_{c,Ax}\frac{S_S}{K_S+S_S}+k_{Bio,Ax,Ss}$

4.2.5 Evaluation criteria

A new set of evaluation criteria is used to compare the fate of the different pharmaceuticals in the extended BSM1. The overall pollution removal of the plant is obtained by calculating the total removal index (TRI) (**Equation 4.2**), which is expressed in units of %. Three additional criteria, biotransformation

index (BI) (**Equation 4.3**), retransformation index (rTI) (**Equation 4.4**) and sorption index (SI) (**Equation 4.5**), provide more information about the fate of the different state variables, which are used to describe the behaviour of the studied compounds. As discussed in Gernaey et al. (2014) all influent dynamic simulations comprise 728 days, of which the last 609 days are used to create the influent file. The dynamic simulations of the BSM1 are preceded by a steady state simulation (200 days) to eliminate the bias in the initial conditions and only the data generated during the final 364 days (t) (influent from day 245 to 609) are used for plant performance evaluation as is shown in **Equations 4.2**, **4.3**, **4.4** and **4.5**.

$$TRI = \int_{t_1=245}^{t_2=609} \frac{(M_{LI,\text{inf}} + M_{CJ,\text{inf}} + M_{SL,\text{inf}} + M_{SL,I,\text{inf}}) - (M_{LI,eff} + M_{CJ,eff} + M_{SL,eff} + M_{SL,I,eff})}{(M_{LI,\text{inf}} + M_{CJ,\text{inf}} + M_{SL,\text{inf}} + M_{SL,I,\text{inf}})} dt * 100\% \quad \textbf{Eq. 4.2}$$

$$BI = \int_{t_1=245}^{t_2=609} \frac{(M_{LI,\text{inf}} + M_{CJ,\text{inf}} + M_{SL,\text{inf}} + M_{SL,I,\text{inf}}) - \left[(M_{LI,eff} + M_{CJ,eff} + M_{SL,eff} + M_{SL,I,eff}) + (M_{LI,was} + M_{CJ,was} + M_{SL,was} + M_{SL,I,was})\right]}{(M_{LI,\text{inf}} + M_{CJ,\text{inf}} + M_{SL,\text{inf}} + M_{SL,I,\text{inf}})} dt * 100\% \quad \textbf{Eq. 4.3}$$

$$rTI = \int_{t_1=245}^{t_2=609} \frac{M_{CJ,\text{inf}} - M_{CJ,eff}}{M_{CJ,\text{inf}}} dt * 100\% \quad \textbf{Eq. 4.4}$$

$$SI = 1 - \int_{t_1=245}^{t_2=609} \frac{(M_{LI,\text{inf}} + M_{CJ,\text{inf}}) - \left[M_{SL,eff} + M_{SL,was}\right]}{(M_{LI,\text{inf}} + M_{CJ,\text{inf}})} dt * 100\% \quad \textbf{Eq. 4.5}$$

M is the mass flow (*C***Q*) and the sub-indices *inf*, *eff* and *was* represent respectively, influent of the BSM1, overflow of the secondary settler and waste activated sludge flow taken from the underflow of the settler for the different ASM-X state variables.

4.3 Results

4.3.1 Results of occurrence of pharmaceuticals

This Section summarises the results of generating dynamic influent pollutant disturbance scenarios using the two different approaches, the phenomenological one and the stochastic one.

4.3.1.1 Phenomenological modelling of pharmaceuticals

The selected compounds represent the original parent form of the chemical (C_{LI}). For *SMX* and *CIP* a total average load of 78 ($SMX_{\text{gperPEperd}}$) and 621 ($CIP_{\text{gperPEperd}}$) mg/(day.1000 PE) respectively is assumed (Plósz et al., 2010b). In all cases, *PE* equals 80,000 which results in a daily load of 6.24 g *SMX*/day and 49.68 g *CIP*/day. In this particular case predefined profiles are created based on observations which are derived

from expert knowledge, full-scale measurements or literature data (Göbel et al., 2005; Plósz et al., 2010a). **Figure 4.4** shows an example of the occurrence of *SMX* and *CIP* which have different characteristics.

The load of *SMX* (body residence time/half-time = 10 h, prescription time = every 8 hours) is assumed to be strongly correlated to the hydraulic profile and the ammonium profile (**Figure 4.4a**). Thus, the occurrence of *SMX* presents a rather regular behaviour with one morning peak, one evening peak, and with late night and mid-day minima. The predefined profiles are normalised (average = 1). When the weekly pattern is included, there is an 8% load reduction on Saturdays and a 12% reduction on Sundays, as it is assumed people leave the city during the weekend (**Figure 4.4c**). Finally, the seasonal variation shows a decrease in the summer period corresponding to the summer holidays (**Figure4.4e**). The daily profile of *CIP*, which is administrated every 12 hours and has a body residence time of 4 hours, shows only one daily peak value in the morning (presumably after accumulating during the night and new intake) while gradually decreasing during the afternoon and evening (**Figure 4.4b)**. Again, the same weekly pattern is assumed with the same reduction factors on Saturdays and Sundays (**Figure 4.4d**). Finally, the seasonal variation was modified with an increase of 25% during winter time, which correlates to a higher antibiotic consumption during that period (**Figure 4.4f**).

It is important to highlight that literature is not conclusive as to determining weekly and seasonal variations for *SMX* and *CIP*. Nevertheless, the purpose of the simulations has been to demonstrate the flexibility of the tool assuming hypothetical weekly and seasonal variations based on well-educated guesses. Numerous studies showed clear weekly patterns when monitoring the occurrence of other compounds such as illicit drugs (Plósz et al., 2013a). Also, macrolides, which are primarily used against respiratory tract infections, show higher loads during winter time (McArdell et al., 2003). These types of variations can be easily described with the proposed mathematical approach.

Zero-mean white noise can be added to the occurrence signals. Noise is included by adding a random signal to a time series, e.g. the pharmaceutical loads. The noise variance is a tuneable model parameter and depends on: 1) the nature of the temporal series (type of compound and load); and, 2) the temporal resolution. In our particular case, noise variance is calculated by multiplying a “noise factor” with the assumed daily load of the compound (for example, $SMX_{\mathrm{gperPEperd}}$) and the total number of *PE* in the catchment. The main purpose of adding noise is to avoid generating exactly the same profile for subsequent days (see **Figure 4.5**), which would represent an unrealistic situation.

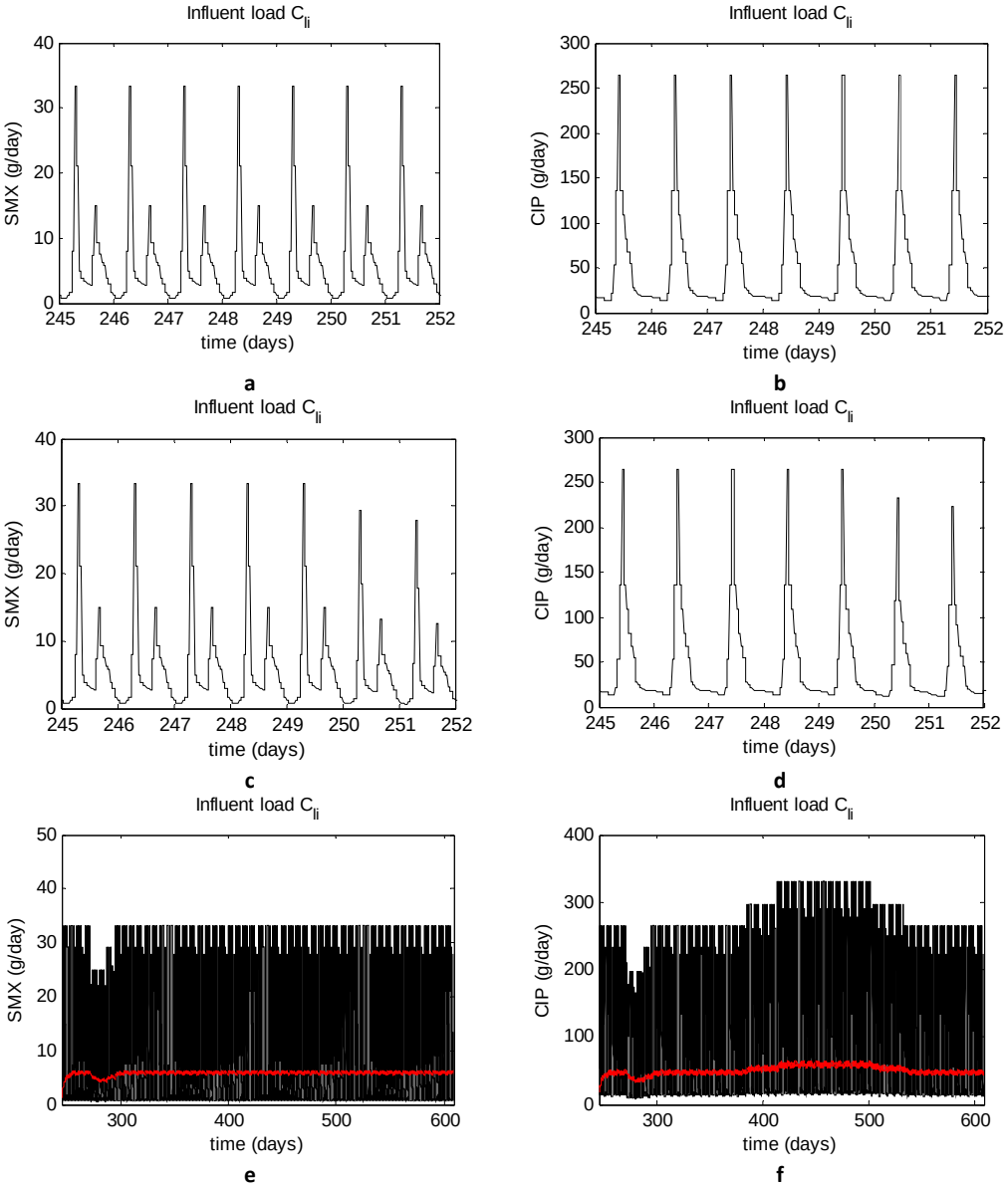

Figure 4.4. Model-based generation of dynamic occurrence of *SMX* (a, c, e) and *CIP* (b, d, f) parent chemical loads (C_{LI}) showing: only diurnal effect (a, b), weekend effects (c, d) and diurnal, weekend and holiday effects (e, f). One year of data is shown in figures e and f, starting on July 1st. An exponential smoothing filter (time constant = 1 day) is used in e and f to improve visualization of the data (in red).

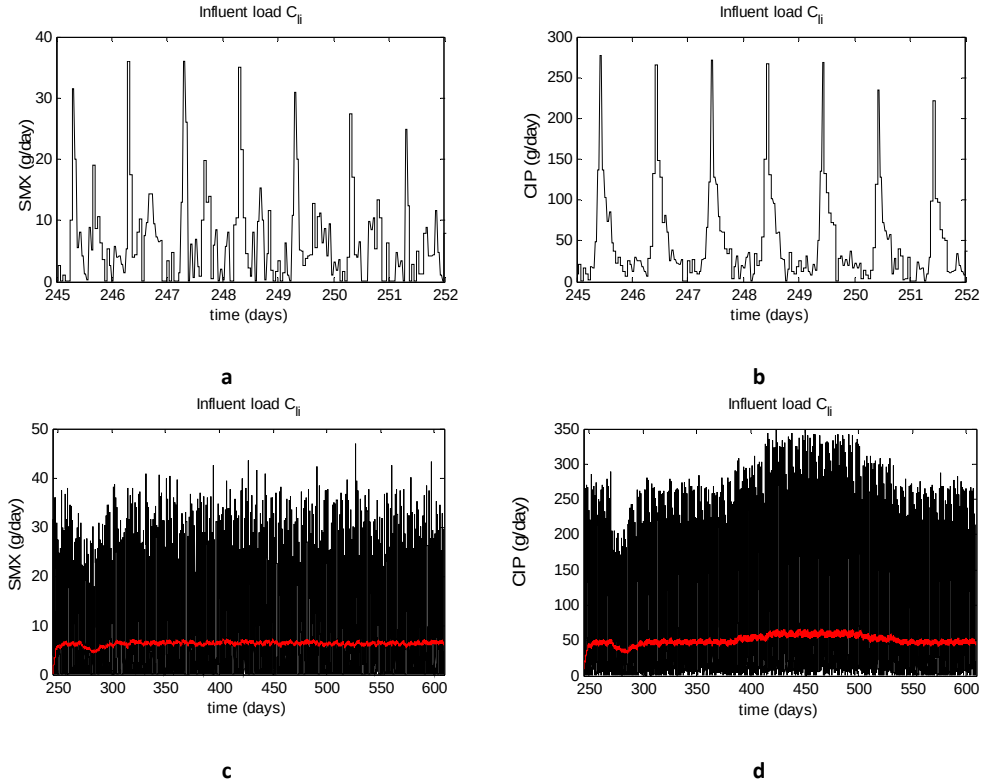

Figure 4.5. Model-based generation of dynamic occurrence of *SMX* (a, c) and *CIP* (b, d) parent chemical loads (C_{LI}) after including the effect of white noise: diurnal and weekend effects (a, b) and diurnal, weekend and holiday effects (c, d). One year of data is shown in **4.5 c** and **d**, starting on July 1st. An exponential smoothing filter (time constant = 1 day) is used in c and d to improve visualization of the data (in red).

When the results of the generated time series are further processed in three evaluation periods: night (0.00 – 8.00), morning-afternoon (8.00 – 16.00), evening (16.00 – 24.00), one can observe different behaviours depending on the studied compound (see the values in **Table 4.2**). As can be seen, the antibiotic *SMX* is basically distributed between the morning/afternoon and evening evaluation periods. On the other hand, the antibiotic *CIP* shows a different behaviour having a peak during the morning-afternoon fraction and a dramatic decrease during evening and night time. An important fact to consider is that *SMX* correlates well with the ammonium load and flow rate, while *CIP* has a more independent behaviour. These results are also in agreement with: 1) the expected distribution patterns according to different body residence times; and, 2) the results of experimental campaigns that can be found in literature (Göbel et al., 2005; Plósz et al., 2010a). **Table 4.2** also shows the effect of different noise levels on the different compounds. As expected the correlation between the profiles of ammonium and *SMX* is almost one if random noise is not included.

This is evident since the predefined profiles for both compounds are based on similar principles. However, when the noise level is increased, the degree of correlation decreases, without changing the total load in each evaluation interval. Depending on what correlation with ammonium is desirable, the noise level can be adjusted.

In the measurement campaign performed by Coutu et al. (2013), the diurnal pattern of *CIP* shows an extra peak in the evening at the inlet of the WWTP. This low peak is due to the consumption around dinner time and the subsequent excretion about 4 hours later. In this study the second evening peak is not added, as it was assumed that the consumers go to sleep before excretion and accumulate the drug in the night. Thus the only excretion of *CIP* takes place in the morning, after waking up and consuming again the antibiotic during breakfast. However, if preferred, a second peak in the evening can be included by adjusting the input file containing the daily profile. Finally, it must be mentioned that input files could of course reflect different catchment characteristics. For example, as the distribution and usage of products that contain micropollutants is different per country, the pollutant flux is also geographically dependent (Johnson et al., 2008). A spatial difference in occurrence between urban and rural areas is also noticeable for illicit drugs (Zuccato et al., 2008; Banta-Green et al., 2009). The presence of hospitals will also influence the pollutant flux (Heberer and Feldmann, 2005) as will the age groups of the inhabitants in a catchment (van Nuijs et al., 2011). These differences are in fact not only visible in the occurrences of the micropollutants, but also in the occurrences and dynamic profiles of the 'traditional' pollutants.

Table 4.2. Daily load distribution/correlation with ammonium for flow rate, ammonium, *SMX* and *CIP* at different noise levels. Noise variance =NL*$X_{gperPEperd}$, where $X = Q_{in}$, NH_4^+, *SMX* and *CIP*.

Noise level (NL)	0-8 (AM) %	8-4 (PM) %	4-12 (PM) %	Correlation with NH_4^+
		Flow rate		
0	26.01	37.04	36.95	0.35
2	26.66	36.64	36.70	0.24
		NH_4^+		
0	31.37	33.78	34.85	1
2	31.75	33.51	34.73	1
		SMX		
0	31.89	33.12	35.00	0.99
0.01	31.87	33.13	35.00	0.89
0.5	32.59	32.76	34.65	0.80
2	33.50	32.50	34.00	0.65
		CIP		
0	10.66	75.31	14.03	-0.16
0.01	10.66	75.31	14.03	-0.02
0.5	10.64	75.30	14.07	-0.02
2	10.79	75.07	14.14	-0.02

4.3.1.2 Stochastic modelling of pharmaceuticals

Since the medical uses of *DCF* are quite diverse, i.e., the intake of this compound is quite random compared to the intake of antibiotics, it is difficult to characterise a daily occurrence pattern at the WWTP inlet using a phenomenological approach (except for a reduced load during night time). For this reason, it was decided to describe the occurrence of *DCF* during daytime mathematically using a Markov Chain approach. Three different states are defined representing a low (s_1), medium (s_2) and high (s_3) level of occurrence. The total simulation time is 728 days (17,472 hours) and the probability for transition from the first state, s_1, to the two other states is equal to (5,824/17,472), and is identical to the probability to stay in the current state. The duration of the events of medium and high occurrence is around 3 hours, and this effect is obtained by including a high probability that the system will stay in either state s_2 or s_3 (11,648/17,472). There is again an equal probability to move from state s_2 or s_3 to the two other states (2,912/17,472). These theoretical probabilities can of course be adjusted according to the needs of the users. The resulting output from the

Markov Chain is normalised (average = 1). The transition probability matrix for the Markov Chain representing the three different states for *DCF* is summarised in **Equation 4.6**, where each element represents the probability of a transition from state *i* to state *j* (row number = *i* and column number = *j*) and consequently the diagonal elements represent the probabilities to remain in the same state. A graphical display of the states and probabilities can be found in the Appendix A.2, **Figure A.2.1**.

$$DCF_S = \begin{bmatrix} 5824/17472 & 5824/17472 & 5824/17472 \\ 2912/17472 & 11648/17472 & 2912/17472 \\ 2912/17472 & 2912/17472 & 11648/17472 \end{bmatrix} \quad \textbf{Eq. 4.6}$$

As presented in the previous approach, the time series are adapted to the different catchment characteristics using two parameters. The first parameter is related to the consumption of the compound by the inhabitants ($DCF_{gperPEperd}$ = 58 mg/(day.1000 PE) (Plósz et al., 2012). The second parameter is the total number of inhabitants in the catchment (*PE* = 80,000). Night time, weekend and seasonal effect are included using predefined profiles which are stored in data files. The time series generated using **Equation 4.6** are multiplied by a cyclic signal which drastically reduces the influent load from 10 PM to 7 AM, to simulate night time with low consumption of *DCF*. Again, the average value resulting from the multiplication of these two signals is scaled to 1. Zero-mean white noise can be added to the influent signals as well, if desired by the user. However, in this example it was preferred not to activate the optional noise since the resulting profile already demonstrated a high degree of randomness. **Figure 4.6** shows the dynamics of the generated time series. On this occasion it can be seen that the distribution of *DCF* during daytime is quite random, i.e. changing substantially from day to day. The only observable pattern is a substantial – and intentionally introduced – reduction during night time. The weekly and seasonal variation of *DCF* is described assuming the same profiles as used for *SMX*. Nevertheless, this variation can be modified on the basis of different available sources of information, thus customising the pollutant behaviour to each individual catchment. Further information about seasonal variation in the occurrence of micropollutants can be found in Carballa et al. (2004), Jelic et al. (2012), Joss et al. (2005), Spongberg and Witter (2008), Verlicchi et al. (2012) and Yu et al. (2013).

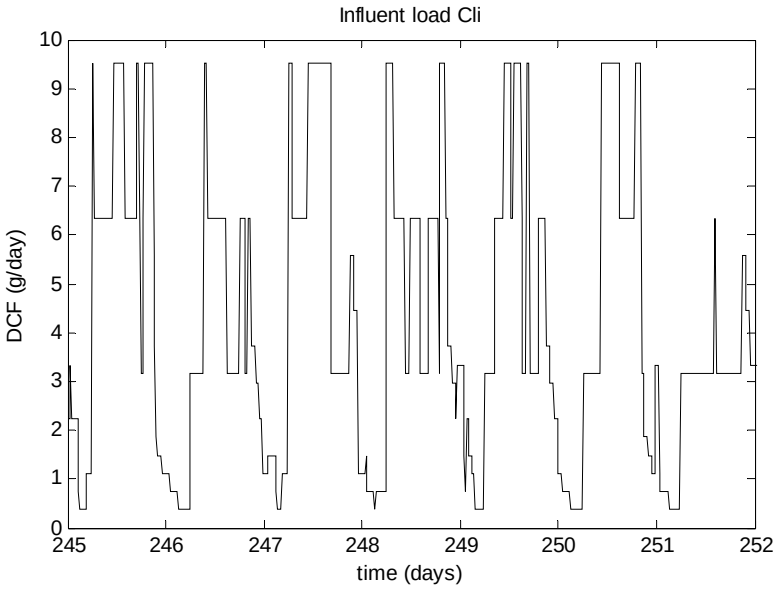

Figure 4.6. The dynamic influent load of parent *DCF* chemical (C_{LI}) created with the Markov Chain approach combined with a daily profile to prevent *DCF* peaks during the night.

4.3.2 Results of transport of pharmaceuticals

The different pharmaceuticals presented in the previous Section are subsequently passed through the transport model block (see **Figure 4.1**). In that transport model block, the first model block is the sewer system, which is constructed as a set of continuously stirred tank reactors (CSTR) with changing volumes. The size of the sewer system can be incorporated in the influent dynamics by increasing or decreasing the number of CSTRs: the basic assumption behind this is that the larger the sewer system, the smoother the simulated diurnal flow rate and concentration variations should be. Furthermore, the sewer model also takes into account the ASM-X (bio)chemical reactions as summarised in **Table 4.1.** Again, the size of the sewer will play an important role in the accounted reaction rates. The second model block in the transport model block is the first flush model (see **Figure 4.1**), where the accumulation and release of particulates in the sewer during dry and rain weather conditions is mimicked. As a result of the presence of this model block, there will be a substantial increase of the total load of particulates in the influent wastewater following a severe rain event. More information on the transport model blocks can be found in Gernaey et al. (2011) and a figure of the sewer model can be found in the Appendix A.2, **Figure A.2.2**.

4.3.2.1 Transport of soluble compounds

Different scenarios were simulated for testing the effect of several transport conditions on the state variables used to describe the occurrence of *SMX* (**Figure 4.7**). Scenario 1 ($SC1_{trans}$) tests different dissolved oxygen concentrations in the sewer (0, 1 and 2 g(-COD)/m^3), scenario 2 ($SC2_{trans}$) evaluates the effect of considering different sewer lengths (6, 12, 18 and 24 CSTRs in series), and scenario 3 ($SC3_{trans}$) tests different TSS loadings (190, 380 and 570 mg SS/L).

The different oxygen concentrations ($SC1_{trans}$) show the largest effect on the concentration of C_{SL} (**Figure 4.7c**). Anaerobic conditions show higher concentrations of C_{SL} (black line) compared to aerobic conditions (blue and red line). This is mainly due to a lower solids-liquid sorption coefficient under aerobic conditions than under anaerobic conditions (0.31 vs. 0.55 L/g X_{SS}) and thus more *SMX* is attached to the particulate fraction. The slight reduction of C_{LI} is because of its sorption onto solids i.e. $C_{LI} \rightarrow C_{SL}$ (process details are explained in **Table 4.1**). No substantial reduction is observed in the biotransformation and retransformation rates. This is mainly because the parameters related to retransformation ($k_{Dec,Ox}$ = 6.80*10^{-3} and $k_{Dec,Ax}$ = 7.85*10^{-3} m^3/(g X_{SS}.day)) and biotransformation ($k_{Bio,Ox}$= 0.41*10^{-3} and $k_{Bio,Ax}$ = 0.41*10^{-3} m^3/(g X_{SS}.day)) are rather similar under aerobic and anoxic conditions. Also the inhibition term of S_S for the biotransformation and retransformation is high, leaving sorption as the predominant removal mechanism from the aqueous phase in the sewer (K_S = 10 mg/L, S_S in the sewer = 58 mg/L, making the inhibition term 10/68). This corresponds to the observations of Plósz et al. (2010b) where the biotransformation and retransformation processes of SMX and TCY show a high degree of inhibition in the sewer. It is important to highlight that the behaviour of these compounds under aerobic/anaerobic conditions is somewhat uncertain. A recent investigation carried out by Polesel et al. (2014) showed that the sorption in WWTPs is highly affected by pH and the chemical speciation. For this reason the parameter values for $k_{Dec,Ox}$ and $k_{Dec,Ax}$ adjusted in the WWTP might be different in the sewer and sorption rates can be under- or over-estimated as a consequence.

$SC2_{trans}$ shows that the largest impact of the retention time in the sewer can be found in the sorbed fraction of *SMX*. The longer the sewer and consequently the hydraulic retention times (HRT_6 = 2.76 hours, HRT_{12} = 6.84 hours, HRT_{18} = 11.71 hours, HRT_{24} = 17.13 hours), the higher the concentration of C_{SL} (**Figure 4.7f**). This phenomenon is in close agreement with the experimental observations of Plósz et al. (2010a) where variations in the hydraulic retention time lead to different ratios between the parent compound and the retransformable compound at the inlet of the WWTP. A longer sewer allows a longer time for the C_{LI} and C_{CJ} to react and form C_{SL}. It is important to notice that the sewer length also has a smoothing effect on the peaks of the C_{LI} and C_{CJ} concentration profiles (**Figures 4.7d** and **e**), as expected.

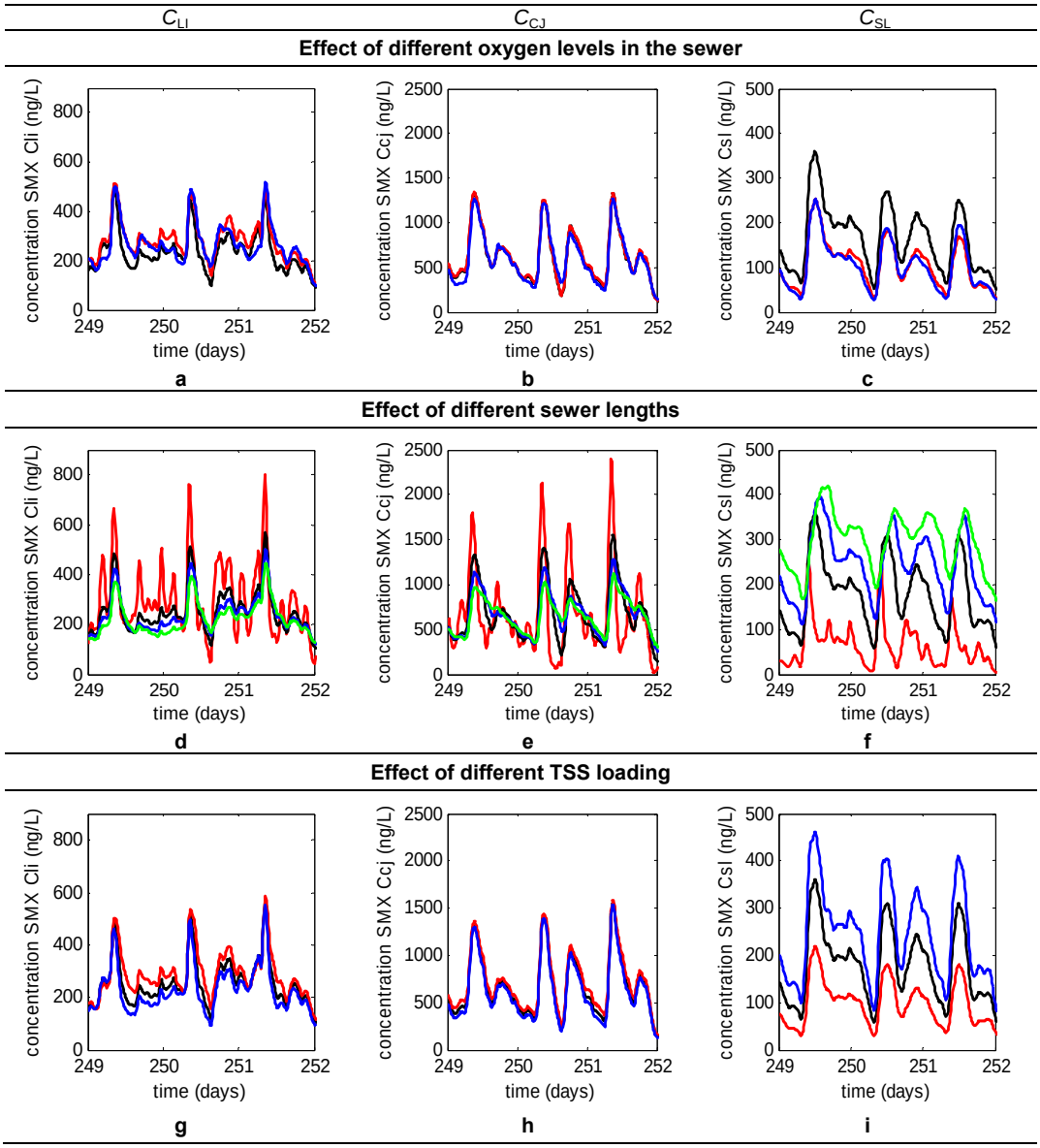

Figure 4.7. Effect of sewer transport conditions on the different *SMX* related variables: C_{LI} (a, d, g), C_{CJ} (b, e, h), C_{SL} (c, f, i) for three different scenarios: oxygen concentration (black: 0 g(-COD)/m^3, red: 1 g(-COD)/m^3, blue: 2 g(-COD)/m^3), sewer length: (red: 6 CSTRs in series, black: 12 s CSTRs in series, blue: 18 CSTRs in series, green: 24 CSTRs in series), different TSS loading (red: 190, black: 380, blue: 570 mg SS/L).

The last scenario shows the effect of the TSS loading on the different compounds. Again, the largest effect can be seen in the concentration of C_{SL}, where the higher TSS loading results in an increased sorbed concentration (**Figure 4.7i**). Only a small effect can be seen for C_{LI} (**Figure 4.7g**) where a higher TSS loading leads to a lower C_{LI} concentration, and this effect is even smaller for the component C_{CJ} (**Figure 4.7h**). When there is more TSS present, more *SMX* can be sorbed, thus leaving less *SMX* present as C_{LI} and C_{CJ}.

4.3.2.2 Transport of particulate compounds

The first flush model presented in Gernaey et al. (2011) is used to describe the physical behaviour of particulate compounds in the sewer system. The model is constructed using a set of differential equations (see **Equation A1**) and it is based on the following assumptions: 1) only a part of the particulates settle in the sewer system; 2) particulates are accumulated under dry weather conditions; and finally, 3) there is a threshold flow rate that, when exceeded, results in the first flush, i.e. all the accumulated particulate material is suddenly pushed out of the sewer system. The paper by Gernaey et al. (2011) should be consulted for further information on the mathematical model structure and the parameter values.

Figure 4.8 shows the effect of the first flush on *TCY* in the form of C_{SL}. This compound has the highest sorption parameters ($K_{D,Ox}$ is $1.1*10^{-3}$ and $K_{D,Ax}$ is $1.6*10^{-3}$ m^3/g X_{SS}) and therefore a large *TCY* fraction will be retained in the solid fraction and behave as a particulate. The effect of the first flush can be observed by the additional peaks of C_{SL} that are generated in the concentration time series. These peaks are created due to the sudden washout of the accumulated material in the sewer, and will strongly affect the dynamics of the particulate compounds in the inlet of the WWTP. This flushing is associated with heavy rain events. The inclusion of this first flush model block introduces an additional degree of realism in the concentration profiles, and full-scale results have also demonstrated the need to calibrate/validate this module to correctly describe the dynamics of particulates in the influent to the treatment plant (Flores-Alsina et al., 2014b).

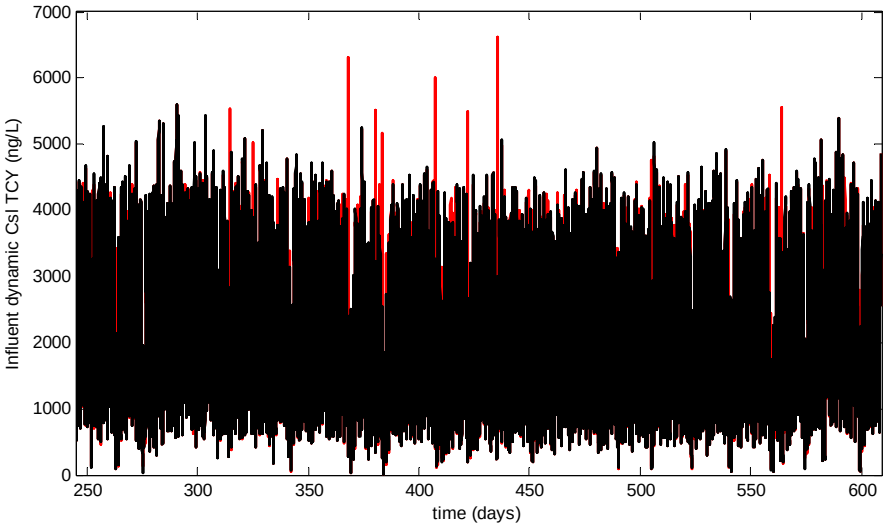

Figure 4.8. The concentration of C_{SL} of *TCY* without the first flush effect (black) and with (red).

4.3.3 Results of fate of pharmaceuticals

In this Section the fate of *SMX*, *CIP*, *TCY*, *DCF* and *CMZ* is analysed and evaluated. The influent profiles for *SMX*, *CIP* and *TCY* are generated following the principles stated in Section 4.3.1.1, i.e. these compounds have a well-defined administration pattern. However, since *DCF* and *CMZ* have an irregular administration pattern, a stochastic approach based on Markov Chains is used to reproduce their dynamics. In both cases, the parameters reported in (Plósz et al., 2010b, 2012) and Gernaey et al. (2011) were used to create different WWTP pollution disturbance scenarios.

The WWTP described in Section 4.2.2 is simulated under different operating conditions. First of all, a base case ($SC1_{fate}$) is defined with constant dissolved oxygen concentration in *AER*1, *AER*2 and *AER*3 (S_O = 1 g/m^3) and constant TSS concentration in *AER*3 (TSS = 4,500 g/m^3). Internal (Q_{intr} = 55,338 m^3/day) and external recirculation (18,446 m^3/day) flow rates are set to their default values. Further information can be found in Copp (2002). Additionally, three extra scenarios ($SC2_{fate}$, $SC3_{fate}$ & $SC4_{fate}$) are simulated by changing the operational conditions. In $SC2_{fate}$, the quantity of (readily) biodegradable organic matter is increased using an external carbon source (Q_{carb} = 5 m^3/day). In $SC3_{fate}$, a step feed strategy is adopted by distributing the influent flow rate into the five tanks (50% in ANOX1, 25% ANOX2, 25% in AER1, 12.5% in AER2 and 12.5% in AER3). In the last scenario the sludge retention time (SRT) is increased from 15 days to 23 days by increasing the TSS concentration in the recycle from 4,500 to 5,000 g MLSS/m^3. This scenario is only

simulated for *DCF* and *CMZ*, as the biotransformation rates of those two compounds were the only ones reported for higher SRTs (Plósz et al., 2012).

Using the default operating conditions the calculated average percentages of TRI are 33, 28, 34, 28 and 24% for *SMX*, *CIP*, *TCY*, *DCF* and *CMZ*, respectively (**Equation 4.2**). On the one hand, *CMZ* has the lowest TRI (and also BI) (**Equation 4.3**) mainly due to its chemical structure consisting of a tricyclic ring (one azepine ring with two benzene moieties). Indeed, in the literature *CMZ* is identified as a persistent pollutant (Clara et al., 2004; Castiglioni et al., 2006) and proposed as a possible anthropogenic marker of contamination by pharmaceuticals (Clara et al., 2004). Some authors reported negative removal rates for *CMZ*, indicating a higher measured concentration of *CMZ* in the WWTP effluent compared to the influent of the WWTP. An explanation can be the exclusion of metabolites in the calculation of the removal rate (Vieno et al., 2007). In the WWTP the metabolites retransform into their parent compound, which results in a higher effluent concentration of *CMZ*. As in this study the retransformation of metabolites into their parent compound is included, no negative removal rates are observed. On the other hand, *SMX* and *TCY* have the highest TRI (and also BI) (**Equation 4.3**) rates. The high removal rate of *SMX* is attributed to biotransformation i.e. $k_{Bio,Ax}$= $k_{Bio,Ox}$= 0.41*10^{-3} m^3/(g.day) in both aerobic and anoxic phases. For *TCY*, the main mechanism is sorption. The sorption coefficient for *TCY* is the highest amongst the five compounds studied with $K_{D,Ox}$ = 1.1*10^{-3} m^3/(g X_{SS}). *DCF* has comparably low k_{Bio} under growth substrate limitation and for an SRT<20 days (0.14*10^{-3} and 0.1*10^{-3} m^3/(g X_{SS}.day)), and its K_D value is also very low, increasing the probability of the parent compound to remain in its original form.

All studied compounds show high rTI (**Equation 4.4**) (> 90%) except *CIP* (around 80%). This is attributed to the low $k_{Dec,Ax}$ for *CIP* compared to the other compounds and to the highest ratio C_{LI}:C_{CJ} in the influent amongst the five compounds. With respect to sorption, the *CIP* data show the highest SI rates (**Equation 4.5**). This was not expected as the sorption coefficients of *TCY* are higher than the sorption coefficients ($K_{D,Ox}$ & $K_{D,Ax}$) of CIP (1.1*10^{-3} and 1.6*10^{-3} vs. 0.42*10^{-3} and 1.1*10^{-3} m^3/(g X_{SS}), respectively). An explanation for these results can be the higher TRI of *TCY* compared to *CIP*, which would lead to lower concentrations of C_{LI} for *TCY* which are available for sorption. Finally, it is also important to highlight the low *DCF* and *CMZ* sorption rate (≈ 0%). Note, however, that the literature suggests that a significant fraction of the *CMZ* concentration associated to the solids phase can originate from processes other than the sorption-desorption equilibrium (Radjenović et al., 2009). For this reason it is necessary to account for this fraction in the solids phase as sequestered ($C_{SL,I}$) in order to describe the correct behaviour (Plósz et al., 2012).

The scenario analyses show variations in the concentrations of the different ASM-X state-variables: 1) when the operating conditions are modified; and, 2) for the different studied compounds (see **Table 4.3**).

Table 4.3. Influent and effluent concentrations showing the effect of different operating conditions on *SMX*, *CIP*, *TCY*, *DCF* and *CMZ* (DO set point in AER1,2 and 3 is 2 g/m^3 in $SC1_{fate}$, $SC2_{fate}$, $SC3_{fate}$ and $SC4_{fate}$, MLSS is 4,500 g/m^3 in $SC1_{fate}$, $SC2_{fate}$ and $SC3_{fate}$ and 5,000 g/m^3 in $SC4_{fate}$). C_{LI} and C_{CI} behave like soluble compounds (same concentration in over and underflow) while C_{SL} and $C_{SL,I}$ behave like particulate compounds (different concentration in overflow and underflow).

	C_{LI}(ng/L)	C_{CI}(ng/L)	C_{SL}(ng/L)	$C_{SL,I}$(ng/L)
			Over/Underflow	
		SMX		
Influent	321	690	0	-
$SC1_{fate}$	632	46	2/1,187	-
$SC2_{fate}$ **(Increase OM)**	652	60	2/1,075	-
$SC3_{fate}$**(Step feed)**	601	67	2/1,197	-
		CIP		
Influent	2,346	24,070	0	-
$SC1_{fate}$	15,364	3,868	89/45,781	-
$SC2_{fate}$ **(Increase OM)**	15,547	3,932	80/41,049	-
$SC3_{fate}$**(Step feed)**	14,746	4,246	94/49,165	-
		TCY		
Influent	2,709	3,974	0	-
$SC1_{fate}$	4,204	272	15/7,930	-
$SC2_{fate}$ **(Increase OM)**	4,343	352	14/7,199	-
$SC3_{fate}$**(Step feed)**	4,013	392	15/7,985	-
		DCF		
Influent	234	262	0	5
$SC1_{fate}$	340	24	0/30	1/369
$SC2_{fate}$ **(Increase OM)**	290	24	0/22	1/286
$SC3_{fate}$**(Step feed)**	334	32	0/31	1/376
$SC4_{fate}$**(Increase SRT)**	169	21	0/18	2/424
		CMZ		
Influent	777	311	0	7
$SC1_{fate}$	817	28	0/4	1/558
$SC2_{fate}$ **(Increase OM)**	661	28	0/3	1/432
$SC3_{fate}$**(Step feed)**	819	38	0/4	1/568
$SC4_{fate}$ **(Increase SRT)**	838	24	0/5	1/461

Two different effects can be observed in $SC2_{fate}$. On the one hand, *SMX*, *CIP* and *TCY* show a lower TRI (30% for *SMX*, 27% for *CIP* and 31% for *TCY*). The same type of behaviour can be observed for the rTI values (**Equation 4.4**). This phenomenon is mainly because organic matter has an inhibitory effect in the case of

SMX, *CIP* and *TCY*, exhibited by growth substrates in ASM-X (see **Table 4.1**). On the other hand, *DCF* and *CMZ* conversions are enhanced when the influent organic matter content is increased (from 28 and 24%, respectively, to 38% for both when extra carbon source is dosed in the WWTP). In this case, co-metabolic biotransformation of *DCF* and *CMZ*, which is enhanced by increased availability of readily biodegradable (growth) substrates (see equations in **Table 4.1**), is responsible for these results. No effect on rTI can be observed for *DCF* and *CMZ* (see **Table 4.1**).

In $SC3_{fate}$, a step feed strategy is evaluated. The introduction of step feed leads to a slight increase of the TRI for *SMX*, *CIP* and *TCY* (35%, 29% and 35%). This is mainly due to a lower inhibitory effect by organic matter in the first reactors (see the pseudo first-order kinetic equations in **Table 4.1**), since part of the organic matter is now dosed in the last reactors through the step-feeding strategy. For the compounds *DCF* and *CMZ* this situation is not favourable as it results in a slightly lower or similar TRI of 28 and 23%, respectively. On this occasion, this is attributed to a reduction of the organic matter gradient and a better distribution of substrate all along the plug flow reactor.

Finally, in $SC4_{fate}$ the effect of a longer SRT on the fate of *DCF* and *CMZ* is examined. The parameters $k_{Bio,Ox}$ and $k_{Bio,Ax}$ for *DCF* are increased from $0.14*10^{-3}$ and $0.1*10^{-3}$ $m^3/(g\ X_{SS}.day)$ to $1.04*10^{-3}$ $m^3/(g\ X_{SS}.day)$. The biotransformation increases as the biomass becomes more diverse at a higher SRT and has more and different enzymes to break down different compounds (Leu et al., 2012). There is no variation in the process rates for *CMZ* when increasing the SRT and therefore the parameters remain constant. The increase of k_{Bio} for *DCF* leads to an increase in the TRI, which is 62% instead of the 28% in the default scenario. Clara et al. (2005) reported contradicting results on the removal of *DCF* when increasing the SRT: both increased removal and no increased removal were reported. They furthermore stated that *CMZ* was not removed and an increase in the SRT had no effect on the removal, which corresponds to our results as TRI is not affected by a longer SRT (24%). As no retransformation rates for *DCF* and *CMZ* were included by Clara et al. (2005), this can explain the higher removal rates obtained in this study.

4.4 Discussion

This study has demonstrated that the presented set of models is promising as a toolbox to improve model-based simulation/evaluation studies of pharmaceutical occurrence, transport and fate in wastewater transport and treatment. A first major advantage is the generation of dynamic influent pollutant disturbance scenarios because this approach can significantly reduce the cost and workload of measuring campaigns by creating synthetic data based on administration patterns of pharmaceuticals, while also enabling to fill gaps due to missing data in the pharmaceutical profiles. Finally, the user can also create

additional disturbance scenarios following the same catchment modelling principles. A second advantage of the proposed approach is that the proposed models can reproduce some of the biochemical and physical processes that these compounds are subjected to during the transport from the households to the wastewater treatment facilities. Finally, it is also possible to study the impact of certain treatment plant operational strategies on the total removal, biotransformation, retransformation and sorption rates of the compounds of interest. Even though the set of advantages derived from using these tools is extensive, they also open the door to several discussion points, which are analysed below.

4.4.1 General applicability of the software tool

Although the results reported here might seem very specific, the presented set of models (influent generator, BSM platform, ASM-X framework) is rather generic. The influent characteristics (Gernaey et al., 2011) can be easily adjusted to different catchments (Flores-Alsina et al., 2014b). The same can be said for the WWTP design (Nopens et al., 2010), which has for example been adapted to a Swedish facility (Arnell et al., 2013). The original treatment plant, Bekkelaget WWTP, Oslo, Norway where the ASM-X framework was developed had indeed a very similar configuration as the BSM1 (Plósz et al., 2010b). In case of simulating another catchment and another treatment plant, it would be necessary to correctly describe the occurrence (pattern, consumption rates) and transport (sewer length, aeration conditions, TSS conditions) of the compounds under investigation, phenomena which are rather specific (antibiotics, hormones, anti-inflammatory drugs) and require sufficient data. Also, future users will have to update the different processes within the ASM-X framework with parameter values corresponding to the studied compounds, for example when new compounds are to be studied, as well as including possible co-metabolism or inhibition processes. As in some cases the transformation products can be more toxic than the parent compounds, these should also be taken into account when evaluating the performance of the WWTP. The newly developed models should be evaluated properly, which can be done according to the methods mentioned in Bennett et al. (2013).

The different parts of the tool can be used as standalone models as well. When one is more interested in for example the occurrence, the focus should be on the influent generator, while the transport model and BSM platform can be neglected. Taking these factors into account, the presented set of models can be used as a decision support tool for process managers, water authorities and regulators for the evaluation of the effect and suitability (when dealing with pharmaceuticals) of different engineering applications such as: 1) design; 2) process optimisation; and, 3) evaluation of alternatives for plant upgrading/expansion when dealing with pharmaceuticals.

4.4.2 Assessment of consumption rates from wastewater analysis

The estimation of consumption rates at community level is carried out by means of wastewater analysis. The common approach used in wastewater engineering is to back calculate the daily consumption of a micropollutant normalised per 1000 inhabitants in a given catchment from the measurements taken at the inlet of the WWTP ($XXX_{gperPEday}$). Depending on the analysed data several corrections can be included to consider weekly or seasonal variation. The set of models presented here can be helpful in improving those estimates by accounting for some of the drainage phenomena occurring at a catchment level. Plósz et al. (2013a) demonstrated (experimentally) that metabolism and biotransformation processes are not exclusively taking place in the human body and in WWTPs but may occur in the sewer network as well. In addition, the simulation results included in Section 4.3.2 clearly demonstrated that sewer length and concentration of total suspended solids can have an impact on biotransformation and sorption kinetics. Neglecting those processes may lead to underestimation or overestimation of consumption rates in the studied catchments.

4.4.3 Design of sampling campaigns

Influent generators can be helpful when designing sampling campaigns. Ort and Gujer (2006) demonstrated that errors in the order of 40% (standard deviation) are possible for 24-h composites when the micropollutant is not sampled at a sufficiently high frequency. Such a high error level mainly occurs when there is a high variability in the occurrence of the micropollutant. A high variability of occurrence can be due to a consumption of the micropollutant by a small number of people. Another possible explanation is related to the sewer system, which is subjected to high dynamics because of intermittently operated pumping stations in the catchment. The tool presented herein can be used to for example calculate the relative error of different composites (2h, 4h, 8h and 24h) at different sampling intervals (1 – 30 min) for different generation patterns (phenomenological and stochastic). The results will provide an idea of the representativeness of the average loads of the composite samples.

4.4.4 Analysis, propagation and interpretation of uncertainties

An important point to consider when modelling micropollutants is uncertainty (Neumann et al., 2007). The presented set of tools also allows considering different sources of uncertainties and how those are propagated through the different models. As an example, **Figure 4.9** shows the simulation results obtained by considering different types of model parameter uncertainty when describing occurrence, transport and fate of *CMZ*. These uncertainties are categorised in two types: low (assuming 5% of variation with respect to the default value) and medium (assuming 25% of variation with respect to the default value) uncertainty. They are mapped into (uniform) probability distribution functions. Type 1 uncertainty, the lowest level of

uncertainty, includes the number of *PE*, the pollution load ($CMZ_{gperPEday}$) and the flow rate generated by each person equivalent (*QperPE).* Type 2 uncertainty includes the length of the sewer (subarea, which is the number of CSTRs in series the sewer consists of) and the (bio)-kinetic parameters of the ASM-X model. In this study, 500 Monte Carlo simulations were generated, and the results of these simulations are displayed according to the evaluation criteria mentioned in Section 4.2.5. This exercise has furthermore been repeated for all the different scenarios of Section 4.3.3 ($SC1_{fate}$, $SC2_{fate}$, $SC3_{fate}$ and $SC4_{fate}$).

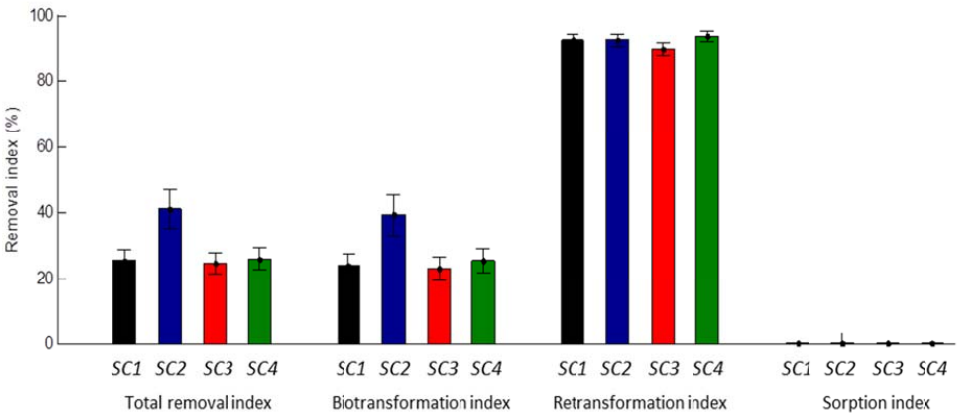

Figure 4.9. The removal indices for CMZ resulting from the different scenarios ($SC1_{fate}$: black; $SC2_{fate}$: blue; $SC3_{fate}$: red; $SC4_{fate}$: green) including standard deviations.

The average values of the Monte Carlo simulations show the same type of behaviour as the deterministic analysis, i.e. it is clear that organic matter plays an important role in the overall process performance. TRI and BI values and their associated uncertainties are increased when adding a carbon source. This is related to the fact that addition of carbon has a major effect on the overall output uncertainty (Flores-Alsina et al., 2008). On the other hand, step-feeding the influent does not seem to affect the TRI and BI values and output uncertainty, but it does play a small role in the decrease of rTI.

It is important to highlight that the interpretation of these results should be done with care. Even though the results of the generated scenarios might seem different from a model point of view ($SC1_{fate}$, $SC3_{fate}$), from a practical point of view (when including uncertainty) they can be considered (almost) identical. The inclusion of other uncertainties like sampling, calculating flow rate and the analytical method can have a paramount impact on the results (Lai et al., 2011; Mathieu et al., 2011; Vezzaro et al., 2012). Indeed, as the effects of some operational conditions for certain compounds are relatively low, the observed differences might also be due to the above-mentioned uncertainties instead of differences in operational conditions.

4.4.5 Challenges and limitations

The reader must be aware that, unavoidably, some simplifications have been made during the construction of the simulation models presented here. For this reason, the analysis of the results must be done with care. For example, the sewer system model is a rather simplified representation, and some of the processes occurring (e.g. biofilm formation) are not accounted for. In order to consider the effect of the biofilm on pharmaceuticals without having a proper biofilm model, the fraction of (heterotrophic) biomass (X_{OHO}) in the total COD was increased. However, mass transfer limitations are not taken into account either. For this reason, there might be errors in the estimation of the conversion rates taking place during the transport. Currently, research is undertaken to improve the sewer model by differentiating both bulk and biofilm. Hence, a one-dimensional layered model (Huisman and Gujer, 2002) is currently under development and implemented in the same platform. Biofilm thickness is a function of microbial growth and decay and it is controlled using attachment and detachment terms. The biofilm model will also include diffusion equations and the full set of ASM1 plus ASM-X reactions.

The processes considered in the ASM-X framework are basically suitable to describe the behaviour of different pharmaceutical compounds. If additional micropollutants like solvents should be modelled, additional fate processes such as stripping and surface volatilisation should be included. These are not included for most pharmaceuticals as the volatilisation is negligible due to the chemical structure of the compounds (large molecules).

Another important extension will be the addition of tertiary treatment. The TRI of some of these compounds is quite small (e.g. *CMZ*), and there will be a need for extra treatment if they must be totally removed, for example as a result of strict effluent regulations for these compounds. The addition of new units like ozone chambers would give a better idea of: 1) the real cost of treating micropollutants; and, 2) the effectiveness of combined AS/tertiary strategies to enhance their removal (Joss et al., 2008). There are some good/reliable ozonation models available already (Hollender et al., 2009). Nevertheless, a major limitation is that these models are very compound specific and reliable data must be found for the parameters. There are also problems about how to deal with the other compounds in the wastewater that are ozone demanding, the so-called ozone scavengers. COD and TN are examples of such compounds, and it is necessary to determine the energy requirements and the cost models of the ozonation process to include them in a realistic way in the operational cost index (OCI) of the simulated treatment plant with tertiary treatment.

The EU Water Framework Directive (WFD) has introduced a crucial change in European policy on protection of water resources, shifting the focus from the control of point sources of pollution (emission-based

regulations) to integrated pollution prevention and control at river basin level by setting quality objectives for the receiving waters (immission-based regulations), which form the basis for setting the upstream emission limits. This new approach results in more freedom in basin management – due to the expansion of the boundaries of the managed system, increasing the number of subsystems to be considered as well as the interactions between them – which can lead on the one hand to a better allocation of economic resources in pollution abatement, but on the other hand introduces increased complexity in the analysis of different options, due to the synergies emerging from the implementation of different measures to different components of the river basin system (Benedetti et al., 2006). The WWTP effluent should be linked to receiving media models such the IWA River Water Quality Model (RWQM1) (Reichert et al., 2001). The main advantage of RWQM1 is its compatibility with other ASM models, since RWQM1 is also COD based. The model considers aerobic/anoxic growth and decay of heterotrophs/nitrifiers/algae/consumers. It also includes hydrolysis, chemical equilibrium and sorption/desorption. Therefore, it would be possible to calculate the PEC of the micropollutant. In combination with the PNEC of the micropollutant a risk assessment can be made by dividing PEC with PNEC. If this ratio is smaller than 1, no risk for the aquatic environment can be assumed. However, if the ratio is higher than 1, a risk for the aquatic environment is assumed (EMEA, 2006). For these risk assessments, dynamic models are important as the average concentration might not exceed the PNEC, whereas the peaks can easily do so.

The EU WFD (2008/105/EC) has also included criteria for 33 priority substances and more are likely to follow in the future. There has been a proposal (COM(2011)876) for a second list of priority substances and a watch-list including compounds of possible concern. The criteria mentioned in the WFD can also be included in the evaluation criteria of the models. The pharmaceuticals under study are not included in the list of priority substances and therefore there are no criteria from the WFD taken into account in this evaluation. However, *DCF* has been put on the watch-list of 2011 and there are maximum allowable annual average concentrations for inland and other surface waters mentioned (COM(2011)876). These concentrations could be included in the evaluation criteria if the treatment plant model was connected with a receiving media model as mentioned above.

Natural extensions of the proposed approach will include considering effects of compounds discharged from WWTP effluents on individual aquatic organisms, as well as whole ecosystem responses that occur through ecological interactions, such as feeding and competition (Clouzot et al., 2013). In this way it should be possible to get a better picture of the effects of micropollutants on the receiving water bodies.

4.5 Conclusion

The key findings of this Chapter can be summarised in the following points:

- A dynamic influent pollutant disturbance scenario generator has been extended with the purpose of generating pharmaceutical data. This set of models describes the occurrence of pharmaceuticals based on different principles (administration patterns, bioavailability, body residence, transition probabilities).
- The potential effect that the transport conditions might have on the dynamics, loads and partitioning of the generated pharmaceutical concentration profiles is demonstrated.
- Different operational conditions might have an important effect on biotransformation, retransformation and sorption rates.
- The set of models can be used by process engineers, water utilities and environmental scientists as a decision support tool when analysing occurrence, transport and fate of pharmaceuticals.
- Special care must be taken to address the inherent uncertainties of the systems when analysing the different simulation results.

Even though one might have the impression that the results are quite specific, the presented set of tools is quite generic and can be easily customised to represent different systems, on condition that sufficient data are available.

Part III

Calibration of extended BSM framework

The extended Benchmark Simulation Models are calibrated in this part. In Chapter 5, data from a full-scale sequencing batch reactor is used to calibrate an N_2O production model in combination with a pH model in order to gain insights into the N_2O production pathways. An extended phenomenological influent generator is developed and calibrated with influent data on pharmaceuticals in Chapter 6. Chapter 5 focuses on the objective of testing a physicochemical model in combination with a N_2O producing model and both Chapters address the objective of calibrating the extended BSM framework.

Chapter 6 has partly been published as:

Snip, L.J.P., Flores-Alsina, X., Aymerich, I., Rodríguez-Mozaz, S., Plósz, B.G., Corominas, L., Barceló, D., Rodríguez-Roda, I., Jeppsson, U., Gernaey, K.V., 2015. Generation of synthetic influent data to perform (micro)pollutant wastewater treatment modelling studies. Sci. Total Environ. Submitted.

&

Snip, L.J.P., Aymerich, I., Flores-Alsina, X., Jeppsson, U., Plósz, B.G., García-Galán, M.J., Rodríguez-Mozaz, S., Barceló, D., Corominas, Ll., Gernaey K.V., 2015. Calibration and evaluation of predictive accuracy of a (micro)pollutant influent generator. 9th IWA Symposium on Systems Analysis and Integrated Assessment (Watermatex 2015), 14-17 June 2015, Gold Coast, Queensland, Australia.

5. Modelling N_2O production in an SBR with an improved physicochemical model

Abstract

Recent investigations reveal that most of the nitrous oxide (N_2O) emissions in wastewater treatment systems are released in the aeration tanks. These emissions could originate from denitrification or be produced by ammonia oxidising bacteria (AOB) during nitrifier denitrification or through hydroxylamine oxidation. It is widely acknowledged that pH and inorganic carbon concentration of the wastewater are influencing the nitrification process since free ammonia and free nitrous acid are the real substrates. Nevertheless, pH and inorganic carbon are not included in most of the N_2O production models due to the additional (numerical) complexity of incorporating a weak acid-base chemical model. In this study, a biochemical model (BCM) describing N_2O production by both AOB and ordinary heterotrophic organisms is combined with a physicochemical model (PCM). Numerical problems are overcome by solving the PCM algebraically using a special Newton-Raphson sub-routine. The proposed model is capable of predicting cationic and anionic behaviour in the aqueous phase simultaneously with predicting pH dynamics. The coupled model is successfully calibrated using full-scale data originating from a sequencing batch reactor (SBR) treating anaerobic digester supernatants. Additionally, results show a positive linear correlation between the N_2O production rate and the inorganic carbon in the last part of the nitrification phase. Finally, it was hypothesised, by means of a risk index, that as a result of the conditions in the SBR during the nitrification phase, the nitrifier denitrification pathway and hydroxylamine oxidation (not described by the model) alternate and thus are both responsible for the N_2O emissions during the aerobic phase.

5.1 Introduction

Mathematical mechanistic models, such as the Activated Sludge Model No. 1 (ASM1), have been used frequently in recent years in simulation studies to optimise the performance of wastewater treatment plants (WWTPs) (Rivas et al., 2008). Such optimisation has mainly been focussed on operational costs and effluent quality regarding nitrogen and chemical oxygen demand concentrations (Gernaey et al., 2014). However, due to the climate change awareness, the carbon footprint of wastewater treatment is becoming an important factor that should be considered during the optimisation (Flores-Alsina et al., 2011, 2014a). As nitrous oxide (N_2O) is the most powerful greenhouse gas (GHG) emitted by a WWTP, it is an essential compound to take into account (IPCC, 2013). However, there is no consensus on the main responsible pathway for N_2O production as there are multiple pathways possible, namely 1) heterotrophic

denitrification, 2) nitrifier denitrification, and 3) hydroxylamine oxidation (Kampschreur et al., 2009). The last two pathways are performed by ammonia oxidising bacteria (AOB) during nitrification. In order to understand the processes responsible for the N_2O production at the WWTP, different mathematical models have been developed describing the various pathways (Hiatt and Grady, 2008; Law et al., 2012a; Mampaey et al., 2013; Ni et al., 2013; Pan et al., 2013).

pH is among the factors influencing the N_2O production (Kampschreur et al., 2009; Law et al., 2011), however it is not taken into account in most of the current N_2O models. This is mainly due to the fact that traditional physicochemical models (PCMs) are described as ordinary differential equations (Stumm and Morgan, 1996; Musvoto et al., 2000; Hauduc et al., 2015a) which should be tackled simultaneously with the ASM/ADM processes, where time constants differ significantly. As a consequence, model stiffness strongly limits the (practical) application of some of the existing physicochemical models.

The bacteria responsible for nitrification (AOB) and nitrite oxidising bacteria (NOB), use the substrates free ammonia and free nitrous acid whose concentrations depend on pH (Anthonisen et al., 1976; Hiatt and Grady, 2008). Therefore, fluctuations in the pH could lead to different concentrations of substrate. In addition, these pH fluctuations can also lead to differences in the inorganic carbon (IC) concentration as the IC consists (amongst others) of bicarbonate and carbon dioxide (Stumm and Morgan, 1996). The IC concentration has been demonstrated as a factor influencing the nitrification (Guisasola et al., 2007; Torà et al., 2010) and also to be linearly correlated to the N_2O production rate (Peng et al., 2015). Due to the effects of the pH and the IC concentration on nitrification, the importance of including a dynamic physicochemical model in N_2O models of AOB is underlined.

In line with this thinking, a physicochemical model is coupled with an ASM1 extended with a N_2O production model in this study. The denitrification processes are adapted from the Activated Sludge Model for Nitrogen (ASMN) (Hiatt and Grady, 2008; Corominas et al., 2012) and the nitrification processes are derived from Mampaey et al. (2013). The PCM consists of a weak-acid base chemistry module which includes ionic strength corrections and ion pairing (Flores-Alsina et al., 2015). A special solving routine is used to handle numerical problems and solve simultaneously both the biochemical model and PCM without any significant loss of simulation speed. The calculation of pH is based on the charge balance approach, as shown in the Anaerobic Digester Model No. 1 (ADM1) (Batstone et al., 2002). The combined models are calibrated using data from a full-scale sequencing batch reactor (SBR).

The objective of the study is to gain insights into the active N_2O production pathways by using the additional information on pH and IC provided by the combined models. Therefore the correlation between

the simulated IC concentration and the N_2O production rate is examined (Peng et al., 2015) as well as the risk model of Porro et al. (2014). In addition, the study is concluded with a discussion on the modelling assumptions made.

5.2 Methods

5.2.1 Case study

The data set used for the calibration originates from an SBR process at Slottshagen WWTP (Norrköping, Sweden) where Stenström et al. (2014) performed an intensive measurement campaign of two days. The campaign includes N_2O measurements in the off-gas as well as in the liquid phase besides the measurements of traditional variables. In addition, the pH of the SBR is measured on-line. Alkalinity is analysed with grab samples of the SBR operation. Also, composite samples to analyse alkalinity are taken during each cycle in both the influent and effluent of the SBR. More information on the measuring campaign can be found in Stenström et al. (2014).

Each cycle of the SBR lasts for 8 hours and starts with a denitrification phase of 3.5 hours followed by a 3.5 hour nitrification phase (**Figure 5.1**). During the last hour of the cycle, sedimentation takes place and part of the volume of the SBR is decanted. Each cycle starts with the filling of the SBR which lasts for two hours. To ensure enough carbon to complete denitrification, ethanol is dosed for 1 hour, starting 1.5 hours after the start of each denitrification phase.

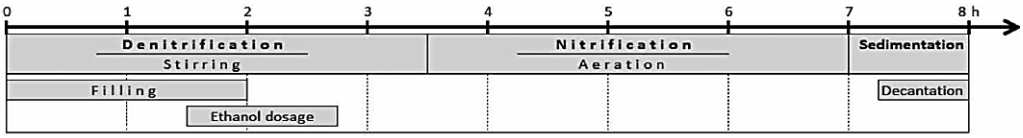

Figure 5.1. The different phases of the SBR cycle operation (Stenström et al., 2014).

5.2.2 Hydraulic model of SBR

The SBR model is based on the reactive settler model (Flores-Alsina et al., 2012). The double exponential velocity function suggested by Takács et al. (1991) using a ten layer pattern is implemented as fair representation of the settling process. During the filling and decanting phase, the volume of the SBR is variable as well as the heights of each layer in the settler model. However, the layers are mixed during the denitrification and the nitrification phase, due to stirring and aeration respectively. A constant influent is used for the filling phases of the SBR as there is little variation in the influent.

5.2.3 Biochemical model

The biochemical model (BCM) used in this study is based on the ASMN (Hiatt and Grady, 2008; Corominas et al., 2012) and is extended with N_2O production by AOB during nitrifier denitrification (Mampaey et al., 2013). This BCM has been calibrated for the SBR case study (Lindblom et al., 2015), and is used as a starting point for this study.

In the calibrated model the dosed ethanol has been added as a state variable with additional denitrification processes. This was necessary to explain the rapid changes of the dissolved N_2O concentration after ethanol dosage (Lindblom et al., 2015). The denitrification processes contain different affinity constants compared to the standard ASMN in order to describe the data. Additional adjustments have been made to couple the BCM with the PCM, which are discussed in the next Section.

5.2.4 Physicochemical model

5.2.4.1 General description of the PCM

The activated sludge aqueous phase composition is represented as a set of chemical entities called species S_i (mole/L) and components S_j (mole/L). A species is defined as every chemical entity to be considered for the aqueous phase. For the set of species, a set of components is selected which completely accounts for the molar content of the aqueous phase (that is, all species concentrations can be fully determined from an independent linear combination of component concentrations) (Stumm and Morgan, 1996). In this study only 9 of the 19 components are considered to decrease the complexity: acetate (S_{ac^-}), ammonium ($S_{\mathrm{NH_4}^+}$), carbonate ($S_{\mathrm{CO_3}^{2-}}$), chloride (S_{Cl^-}), nitrate ($S_{\mathrm{NO_3}^-}$), nitrite ($S_{\mathrm{NO_2}^-}$), phosphate ($S_{\mathrm{PO_4}^{3-}}$), potassium (S_{K^+}) and sodium (S_{Na^+}). Note that these component concentrations are different to the total concentrations which in turn are the output of the BCM. In **Table 5.1,** for exemplary purposes, a representation of the considered species (rows) and how each species can be represented by a linear molar balance combination is shown for the inorganic carbon system (S_{IC}) (see Flores-Alsina et al. (2015) for further details).

The equilibrium equations are formulated as a set of non-linear algebraic equations including one law of mass-action for each species (i) (**Equation 5.1**) and one mass balance for each component (j) (**Equation 5.2**) to guarantee the component conservation principle. Species (i) are expressed in a way that can be written as the product of components (j) and the equilibrium constant. In **Equation 5.1** and **Equation 5.2**, ${}^{a_i}/_{S_i}$ represents the activity/concentration of the i^{th} species, ${}^{a_j}/_{S_j}$ is the activity/concentration of the j^{th} component, $v_{i,j}$ is the stoichiometric coefficient of the j^{th} component in the i^{th} species (see **Table 5.1**), γ is

the activity coefficient, K_i is the equilibrium constant, N_{sp} corresponds to the number of species and N_C represents the number of components. Further information about how to include activity corrections in wastewater treatment models can be found in Solon et al. (2015).

Table 5.1. Stoichiometric matrix of the carbonate-component system (S_j) and the considered species (S_i)

i/j	formula	$S_{CO_3^{2-}}$	$S_{Al^{3+}}$	$S_{Ca^{2+}}$	$S_{Fe^{2+}}$	$S_{Mg^{2+}}$	$S_{Na^{+}}$	log K_i	ΔH^0
$S_{CO_3^{2-}}$	CO_3^{2-}	1						0	0
$S_{Al^{3+}}$	Al^{3+}		1					0	0
$S_{Ca^{2+}}$	Ca^{2+}			1				0	0
$S_{Fe^{2+}}$	Fe^{2+}				1			0	0
$S_{Mg^{2+}}$	Mg^{2+}					1		0	0
$S_{Na^{+}}$	Na^{+}						1	0	0
$S_{Al_2(OH)_2CO_3^{2+}}$	$Al_2(OH)_2CO_3^{2+}$	1	2					4.31	0
$S_{CaCO_3(aq)}$	$CaCO_3$ (aq)	1		1				3.22	16
$S_{CaHCO_3^{+}}$	$CaHCO_3^{+}$	1		1				11.434	0
$S_{FeHCO_3^{+}}$	$FeHCO_3^{+}$	1			1			11.429	0
$S_{H_2CO_3^{*}}$	$H_2CO_3^{*}$	1						16.681	-32
$S_{HCO_3^{-}}$	HCO_3^{-}	1						10.329	-14.6
$S_{Mg_2CO_3^{2+}}$	$Mg_2CO_3^{2+}$	1				2		3.59	0
$S_{MgCO_3(aq)}$	$MgCO_3$ (aq)	1				1		2.92	10
$S_{MgHCO_3^{+}}$	$MgHCO_3^{+}$	1				1		11.34	-9.6
$S_{NaCO_3^{-}}$	$NaCO_3^{-}$	1					1	1.27	-20.35
$S_{NaHCO_3(aq)}$	$NaHCO_3$ (aq)	1					1	10.029	-28.33

$$a_i = K_i \prod_{j=1}^{Nc} a_j^{v_{i,j}} \qquad i = 1, 2, \ldots, N_{sp} \qquad \textbf{Eq. 5.1}$$

$$S_{j,tot} = S_j + \sum_{i=1}^{N_{sp}} v_{i,j} S_i = \frac{a_j}{\gamma} + \sum_{i=1}^{N_{sp}} v_{i,j} \frac{a_i}{\gamma} \qquad \begin{matrix} j = 1, 2, \ldots, N_C \\ i = 1, 2, \ldots, N_{sp} \end{matrix} \qquad \textbf{Eq. 5.2}$$

The effect of temperature on K_i is corrected for by the constant enthalpy form of the van ´t Hoff equation (Stumm and Morgan, 1996). In **Equation 5.3**, K_1 and K_2 are the equilibrium constants at temperatures T_1 and T_2 (in K), respectively, ΔH^o is the enthalpy change of the reaction and R is the universal gas constant.

$$\ln \frac{K_2}{K_1} = \frac{\Delta H^o}{R} \left(\frac{1}{T_1} - \frac{1}{T_2} \right) \qquad \textbf{Eq. 5.3}$$

Full specification of the algebraic equation set requires an additional equation, which can be resolved by the charge balance (Batstone et al., 2002), as shown in **Equation 5.4:**

$$\sum S_{\mathrm{cat}} - \sum S_{\mathrm{an}} = 0 \qquad \textbf{Eq. 5.4}$$

where S_{cat} and S_{an} represent the total equivalent concentrations of cations and anions, respectively, which are the concentrations of respective ions multiplied by their valence. An alternative is to use a proton balance (Morel and Hering, 1993), which generates the same equation set but with a different structure (see for example Harding et al., 2011 and Ikumi et al., 2011), and gives near identical model results (Solon et al., 2015).

5.2.4.2 Interfacing BCM and PCM

In order to combine the PCM with the BCM, some adjustments had to be made. The main modifications are:

- The ASM alkalinity state (S_{ALK}) is removed and inorganic carbon (S_{IC}) is used instead. The S_{IC} is modelled as a source-sink compound to close the mass balances (inorganic carbon pool). Hence, the C, N, P, O and H contents of all state variables in all models are assumed known in order to calculate the mass of each element per mass of COD. Composition for the different ASMs is taken from Reichert et al. (2001).
- Phosphorus (P) is introduced in the same way (non-reactive).
- Carbon dioxide stripping needs to be included. The specific CO_2 volumetric mass transfer rate constant ($k_{\mathrm{L}}a_{\mathrm{CO_2}}$) is calculated from the oxygen volumetric mass transfer rate constant ($k_{\mathrm{L}}a$) multiplied by the square root of the ratio between O_2 and CO_2 diffusivities. K_{H} (Henry coefficient) is corrected for temperature via the van't Hoff equation to correctly estimate the saturation concentration ($S_{\mathrm{CO2}}*$) (Wett and Rauch, 2003). This method is similar to the one used for defining the stripping equations of N_2, N_2O and NO (Foley et al., 2010b).

The outputs of the adjusted BCM at each integration step are used as inputs for the aqueous-phase module to estimate pH from inorganic carbon (S_{IC}), inorganic nitrogen (S_{IN}), inorganic phosphorus (S_{IP}), acetate (S_{ac}), potassium ($S_{\mathrm{K^+}}$) and nitrate ($S_{\mathrm{NO_3^-}}$). Additional cations (S_{cat}) and anions (S_{an}) are also included as tracked soluble/non-reactive states. Therefore, S_{cat} is defined in this study as sodium (S_{Na}). S_{an} is represented by chloride ($S_{\mathrm{Cl^-}}$) and nitrite ($S_{\mathrm{NO_2^-}}$). These ions will have future use for describing precipitation, other model formulations (ADM1), additional biochemical model extensions (sulphate

reducing bacteria, iron reducing bacteria) or simply to adjust pH/ionic strength. The estimated pH is used as an input for the BCM to assess the effect on the substrates of nitrification.

5.2.5 Evaluation of calibration pH

In order to assess the fitness of the model objectively, different evaluation techniques are used, which consist of quantitative and qualitative evaluation methods. Moreover, using objective evaluation methods could provide additional insights into the model and the calibration. The quantitative evaluation methods are comprised of peak evaluation, absolute criteria for residuals and overall criteria. Plotting the sequence of the residuals as well as the distribution is used for the qualitative evaluation.

5.2.5.1 Quantitative evaluation methods

The quantitative evaluation methods used in this study are criteria related to the dynamics as well as criteria related to the average of the residuals. Additionally, criteria concerning overall performance are examined. The equations used for the analysis can be found in Appendix A.3 (**Table A.3.1**).

The first type of criteria described is related to the dynamics of the calibration. The fitness of the magnitude of the peaks, the differences between the maximum in the data and the maximum in the simulation (*PDIFF*), is calculated as well as the percentage in error of peak (*PEP*) (Dawson et al., 2007; Hauduc et al., 2015b). However, these criteria do not take the timing of the peak into account. For the timing of the peak, the mean square derivative error of the time steps is evaluated (*MSDE*) as it examines the differences between the observed and predicted variations between two time steps (Hauduc et al., 2015b).

The second set of criteria evaluates the average errors between the simulations and the data. The mean error (*ME*) is calculated which tests for systematic bias between the data and the simulations. However, the negative and positive residuals can cancel each other out and therefore also the mean absolute error (*MAE*) is calculated. The bias can be assessed with this criterion, however it will not indicate whether the bias is positive or negative. Another possibility to assess bias is to analyse the root mean square error (*RMSE*). This criterion also emphasises the larger errors and therefore focuses on the outliers. By taking the root of the squared error, the value is still comparable with the value of the variable and is therefore easier to interpret than the mean square error. These absolute criteria should always be compared with the value of the same variable and can therefore not be used for absolute comparisons among different variables. However, they can be used in automatic calibration techniques (Sin et al., 2005).

Finally, also overall criteria are analysed. The modified index of agreement (*IoAd*) focuses on the average residuals as well as the peak performance (Dawson et al., 2007). Calculating the correlation between the

data and the simulation is also a good method to assess if the same pattern is shown. In this case, the correlation is calculated with the Pearson index.

5.2.5.2 Qualitative evaluation methods

Besides using quantitative evaluation methods, also qualitative evaluation methods can be explored. The first qualitative method involves plotting the sequence of the normalised residuals over the time span of the calibration. This method helps to identify specific parts during the simulation in which the model is not representing the data. Additionally, it could also indicate a systematic over- or underestimation of the model. The second evaluation method is plotting the distribution of the normalised residuals. An over- or underestimation could become even clearer in this distribution plot. In addition, the plot should show a normal distribution centred around 0 as it is assumed that the model represents the 'true' model along with noise, which should have a mean of 0 and is distributed normally (Neumann and Gujer, 2008). If the distribution is not centred around 0, a bias is identified. If the distribution is not normal, the model might not represent the 'true' model as the residuals contain more than the noise. With the information in the different plots an assessment can be made of the performance of the model.

5.3 Results

5.3.1 pH calibration

The simulation results of the pH can be seen in **Figure 5.2** where the first two cycles of the measurement data are modelled. The other calibrated variables can be seen in **Figure 5.3**. The influent concentration of S_{IC} to the BCM was calculated from the alkalinity grab samples and assumed to be 1082 g C/m^3. The $S_{\mathrm{Cl^-}}$, $S_{\mathrm{K^+}}$ and $S_{\mathrm{Na^+}}$ for the physicochemical model are adjusted to 265, 290 and 300 g/m^3, respectively. These concentrations might be higher than normally expected in wastewater; however they are used as generic ions and a pool to calibrate the pH. Therefore they represent the concentration of all ions present in the wastewater.

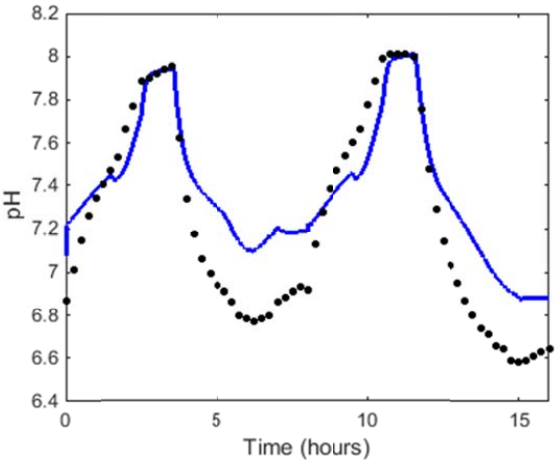

Figure 5.2. The calibrated pH (blue line) with the measured pH (black dots) during two cycles of the SBR operation.

During the filling phase the pH increases as the ammonia concentration increases. The addition of ethanol at 1.5 hours leads first to a small decrease before a steeper increase in pH is shown as the $S_{NO_3^-}$ concentration decreases more rapidly due to higher denitrification rates. Once the filling stops, the $S_{NH_4^+}$ concentration is not increasing steeply anymore and therefore the pH increase is minimal. As soon as the aeration is turned on, the pH decreases. The aeration leads to CO_2 stripping which results in an increase in the H^+ concentration as can be seen in **Equation 5.5**.

$$CO_2 + H_2O \leftrightarrow H_2CO_3 \leftrightarrow HCO_3^- + H^+ \leftrightarrow CO_3^{2-} + H^+ \qquad \textbf{Eq. 5.5}$$

The stripping of CO_2 moves the balance from right to left and thus a consumption of H^+ is taking place. However, the pH is not increasing during the aeration phase. The decrease in concentration of $S_{NH_4^+}$ and the increases in $S_{NO_3^-}$ and $S_{NO_2^-}$ are more influential on the pH than the stripping of CO_2 (the IC is relatively low compared to the nitrogen, the latter being the main pH driver).

Comparing the calibrated pH with the pH data, some differences stand out. The lower pH values of 6.8 and 6.6 during the aeration and sedimentation phases are not reached by the model, which would indicate that there is a higher buffering capacity than shown in the data. As the IC can react as a buffer for the system, this could be a reason for the mismatch. **Figure 5.4** shows the differences between the simulated values and the experimental values (calculated from alkalinity measurements).

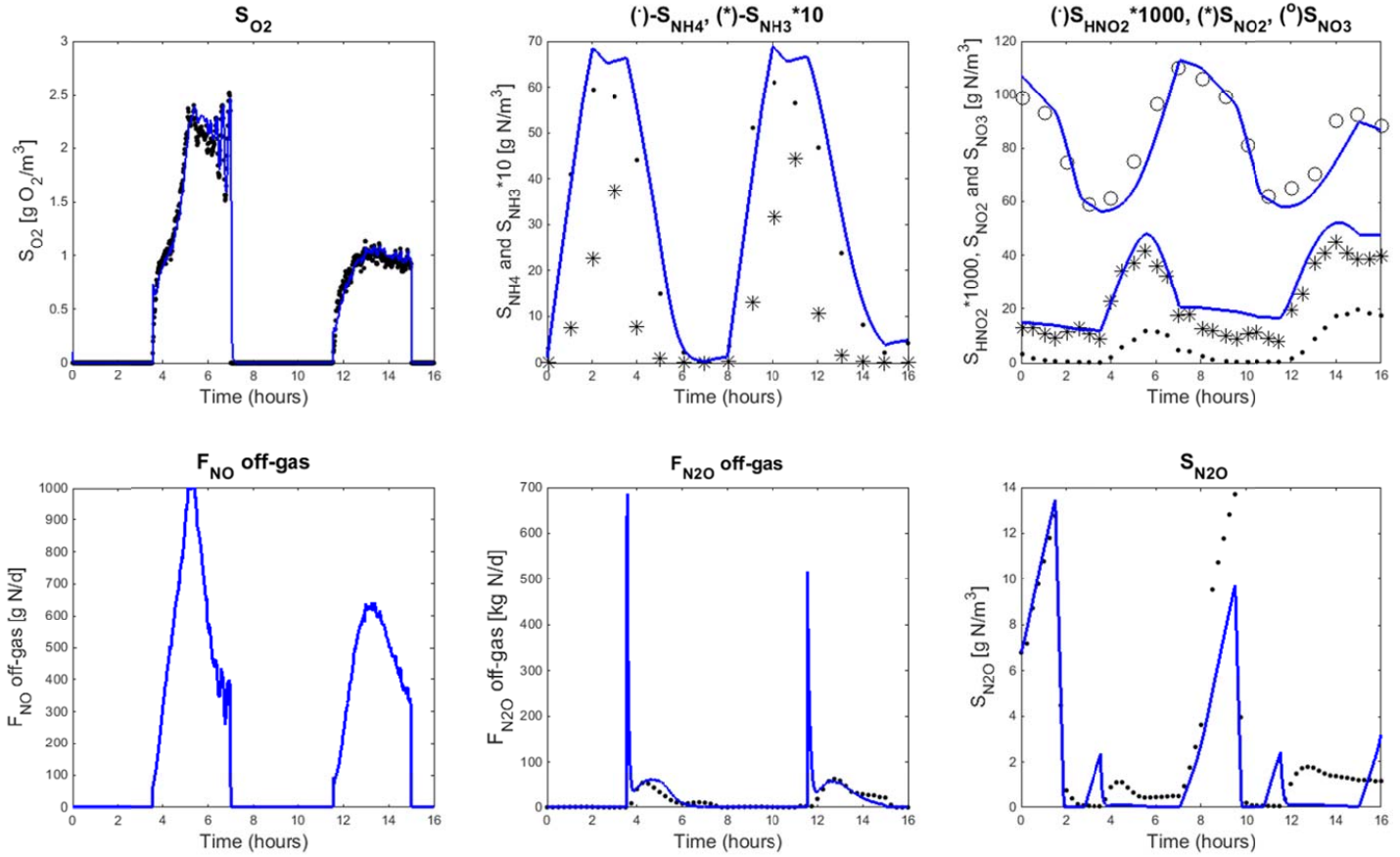

Figure 5.3. Measured (markers) and simulated (solid lines) concentrations and mass flows for the nitrification/denitrification SBR process for two cycles calibrated by Lindblom et al. (2015).

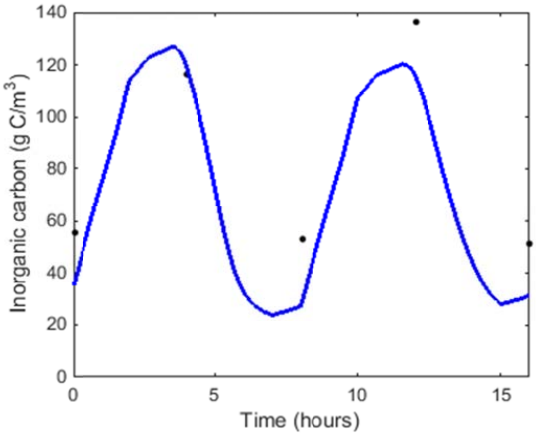

Figure 5.4. The calibrated inorganic carbon concentration (blue line) with the measured inorganic carbon (black dots) during two cycles of the SBR.

The S_{IC} concentration follows the same pattern as the pH, it increases during the filling/denitrification phase and decreases during the nitrification phase. Nevertheless, when comparing the absolute values of the experimental data versus the model predictions it can be seen that the simulated S_{IC} concentration is lower than the measured S_{IC} concentration in grab samples, which would indicate that there is less buffering capacity in the simulations than in the measurements. This is the opposite of what is shown in **Figure 5.2**. Increasing the initial conditions of S_{IC} or the influent concentration in order to match the grab samples will lead to even higher buffering capacity of the model and the pH calibration will deteriorate as a consequence. Therefore, it is hypothesised that the model overestimates the system´s buffer capacity because of two main factors. Firstly, there is a high uncertainty in the S_{IC} and $S_{PO_4^{3-}}$ concentrations of the grab samples used to define initial and influent conditions. The other factor is the effect of ion pairing with the ions used to calibrate the pH (S_{Cl^-}, S_{K^+}, S_{Na^+}). In this study, the quantity (and valence) of cations used to adjust pH might have been underestimated. Indeed, a higher cationic load would make the carbonate ions less available since they will be paired and would thereby reduce the buffering capacity of the system. Nevertheless, no information whatsoever was available about the quantity and type of cations present in the wastewater. These two factors have led to adjustments in the mass transfer phenomena in the reactor. Indeed, the incorrect estimation of the inorganic carbon in the system resulted in the need to adjust the stripping equations by using reduction factors (see Section 5.4.3).

5.3.2 Evaluation of pH calibration

The predictive accuracy of the calibration is evaluated by quantitative and qualitative methods. Different concentrations of S_{Cl^-} are compared to demonstrate their influence on the performance of quantitative criteria. **Table 5.2** shows how the different calibrations score in terms of the quantitative evaluation criteria.

Table 5.2. The scores of the different pH calibrations for the quantitative evaluation criteria.

Quantitative method	Peak evaluation			Absolute criteria			*IoAd*	*Corr*
Compound evaluated	*PDIFF*	*PEP*	*MSDE*	*ME*	*MAE*	*RMSE*		
pH (S_{Cl^-} 255)	-0.050	-0.63	0.0033	0.17	0.22	0.25	0.90	0.96
pH (S_{Cl^-} 260)	0.0058	0.073	0.0030	0.14	0.20	0.23	0.91	0.95
pH (S_{Cl^-} 265)	0.063	0.79	0.0032	0.10	0.20	0.23	0.91	0.95

The peak evaluation criteria demonstrate that the heights of the peaks as well as the timing are captured by all calibrations, as the values for these criteria are small. The calibration with a S_{Cl^-} concentration of 260 mole/L scores best on the combination of the height of the peak and the timing. Increasing or decreasing the S_{Cl^-} concentration increases the error in the magnitude of the peaks and in the timing.

The highest concentration of S_{Cl^-} scored the best on the absolute criteria, while the lowest concentration scored worst. The *ME* indicates that there is a small bias towards overestimating the pH with the model and the *MAE* demonstrates that there is some cancelling out of the errors. This indicates that the model is not always overestimating the pH.

All concentrations of S_{Cl^-} give a successful fit of the pH data, as the *IoAd* and *Corr* are above 0.9. A higher *IoAd* does not automatically lead to a higher *Corr*. A high correlation indicates that the trend of the data is captured successfully; however the values of the calibration can differ from the data. A high *IoAd* indicates low mean residuals and good peak performance, yet the trend of the data can be missed.

The qualitative evaluation methods can assist in pinpointing the part of the calibration that is not captured by the model and demonstrate a bias as can be seen in **Figure 5.5**. When looking at the different plots of the qualitative evaluation methods, the calibration seems less successful. The sequence of the normalised residuals demonstrates that the peaks of the pH are underestimated by the model, while the lower pH is overestimated. This corresponds to the higher buffering capacity of the model compared to the data as is mentioned in Chapter 5.3.1. The distribution of the normalised residuals indicates that the residuals are not normally distributed. The right tail of the distribution is not divided normally. In addition, the distribution is not centred

around 0, indicating a small bias. This was also shown by the quantitative absolute evaluation criteria. In addition, Even though the distribution is not normal, the calibration can be deemed successful taken into account the difference due to the buffering capacity

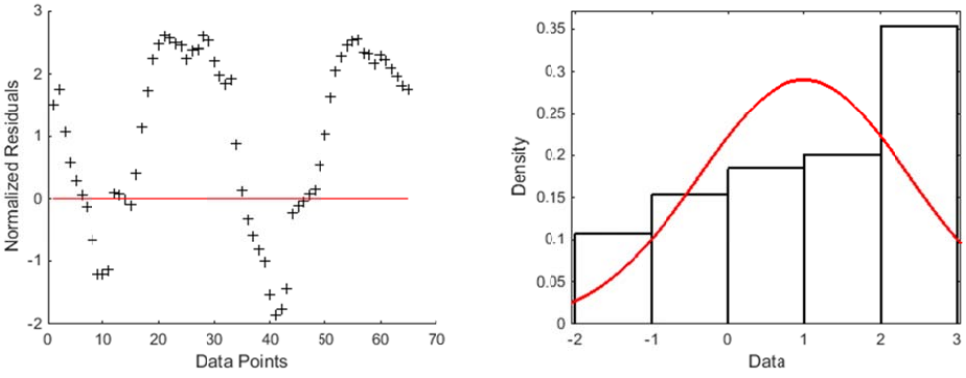

a b

Figure 5.5. The qualitative plots of the pH calibration with the sequence of the normalised residuals (a), and the distribution of the residuals (b).

5.3.3 IC correlation to N_2O emissions

A linear correlation between the N_2O production rate and the IC concentration has been demonstrated by Peng et al. (2015) in a nitrifying system and this correlation is also studied in this Section. The N_2O production rate is calculated by taking the measured N_2O in the off-gas or the simulated N_2O flux. These are plotted against the simulated S_{IC} concentration provided by the combined BCM and PCM. As the system of Peng et al. (2015) was only nitrifying, the aerated period of both cycles is used to compare the linear correlation. The correlation between the N_2O production rate and the S_{IC} concentration during the aerated period can be seen in **Figure 5.6**.

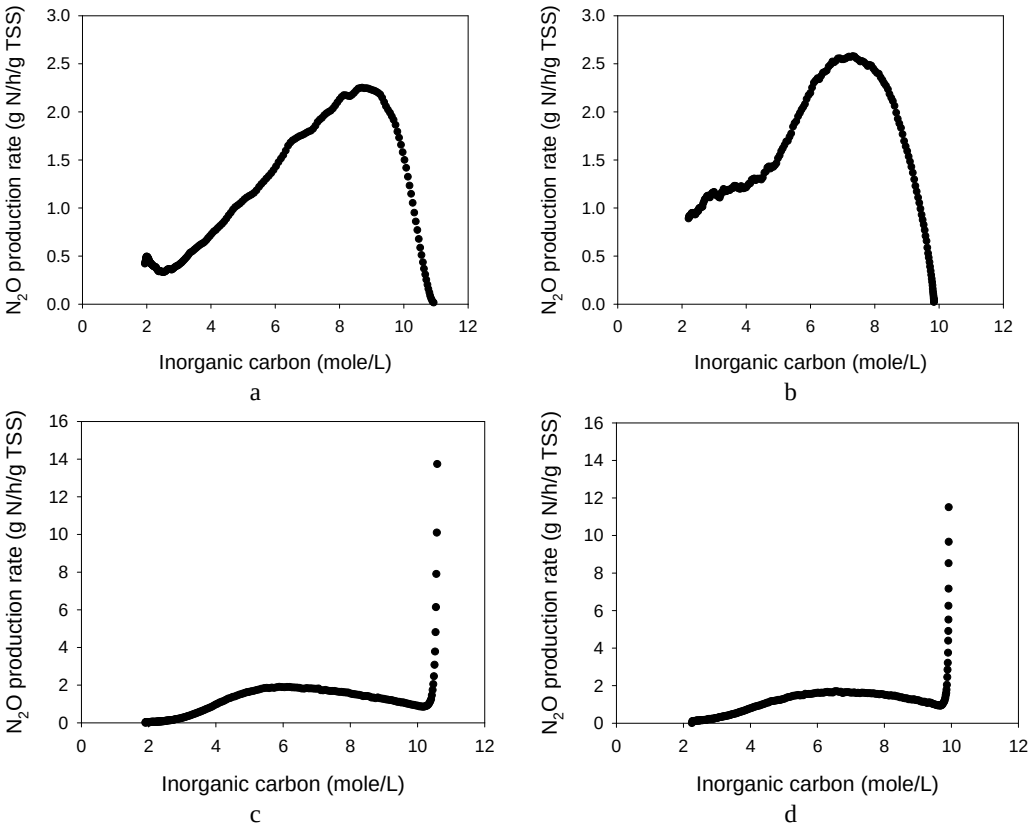

Figure 5.6. The linear correlation between the measured N_2O production rate and the IC concentration in cycle 1 (a) and cycle 2 (b) during the whole aerated period and the correlation between the simulated N_2O production rate and the IC concentration for cycle 1 (c) and cycle 2 (d).

The correlation between the N_2O production rate and the S_{IC} concentration during the entire aeration period shows only a positive linear correlation for the lower S_{IC} concentrations (up to 9 mole/L). At higher concentrations of S_{IC}, the N_2O production rate decreases. In addition, a high peak in the N_2O production rate at the highest S_{IC} concentrations is observed for the simulated N_2O production rate. This is most likely due to a release of N_2O produced during denitrification. The SBR model has no stripping activated during the denitrification phase and therefore all the N_2O produced during denitrification is stripped as soon as aeration is turned on. The range of S_{IC} concentrations found in the SBR is similar to the range tested by Peng et al. (2015)

and therefore inhibition of IC is not an explanation for the decrease in the N_2O production rate at higher concentrations.

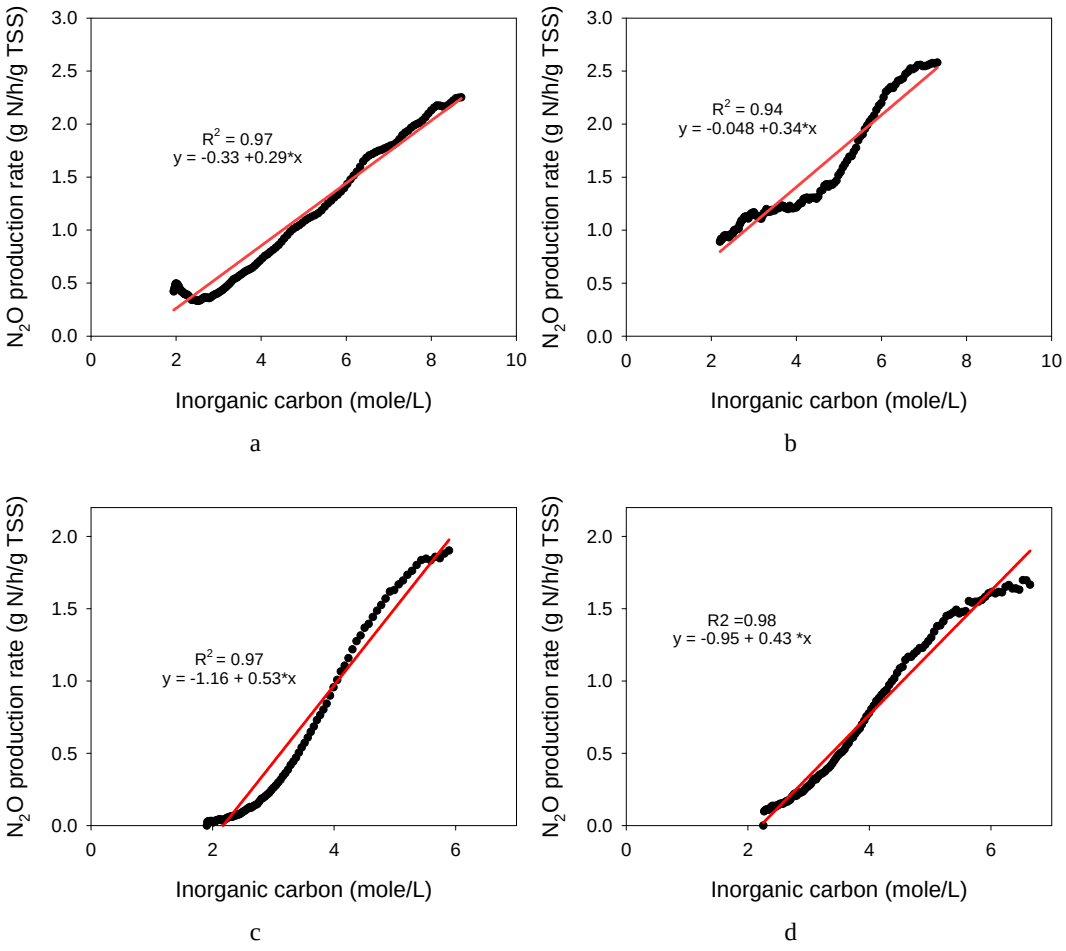

Figure 5.7. The linear correlation between the N_2O production rate and the IC concentration of the measurements in cycle 1 (a) and cycle 2 (b) during the last half of the aerated period and the correlation between the simulated N_2O production rate and the IC concentration for cycle 1 (c) and cycle 2 (d) during the last half of the aerated period.

In order to examine the linear correlation at lower S_{IC} concentrations, the aerated phase is divided into two different parts. The results of the lower S_{IC} concentration correlations with the N_2O production rate can be found in **Figure 5.7**. The calculated correlations are similar to the one found in Peng et al. (2015), where an increase in the S_{IC} concentration corresponds to an increase in the N_2O production rate. The R^2 of the simulated N_2O production rate is higher than the R^2 of the measured N_2O. This is due to a small increase in the N_2O production rate found in the data in the last hour of the nitrification phase, which is not modelled.

In addition, the higher S_{IC} concentrations also demonstrate a correlation with the N_2O production rate. It is important to note that this is a negative correlation, where higher S_{IC} concentrations lead to lower N_2O production rates. An explanation for this could be the oxygen concentration in the system as well as the mechanisms responsible for the N_2O production. When aeration is turned on, the N_2O produced during denitrification is stripped and can therefore influence the linear correlation at high S_{IC} concentrations. In addition, the shift from anoxic to aerobic conditions when an excess of NH_4^+ is available, has been shown to lead to N_2O production by the nitrifier denitrification pathway as well as hydroxylamine oxidation (Chandran et al., 2011). However, if both pathways are active, this would lead to an even higher N_2O production rate at the beginning of the aeration phase and therefore a positive linear correlation should be present.

5.3.4 Risk of different N_2O production pathways

To test the likelihoods of the different AOB N_2O pathways occurring during the operation of the SBR, the risk model proposed by Porro et al. (2014) is used. This risk model is based on expert knowledge and indicates a medium (1) or high (2) risk for N_2O emissions. The risks accounting for the two different mechanisms for N_2O production by AOB are shown in **Figure 5.8** together with the simulated and measured N_2O in the off-gas.

As can be seen in **Figure 5.8**, during the denitrification period a higher risk for AOB denitrification exists, which lowers to a medium risk when aeration is turned on and nitrification starts. During the nitrification phase in the first cycle, the oxygen concentration increases to 2 g O_2/m^3 and results in a low risk of AOB denitrification while high and medium risks of AOB hydroxylamine oxidation occur. This is the same pathway as the most likely active pathway in the study of Peng et al. (2015) and the part of the nitrification for which the same linear correlation is found. The oxygen concentration in the system of Peng et al. (2015) is controlled between 2.5 and 3.0 mg O_2/L and an excess of NH_4^+ is present. However, during the second cycle there is no risk of the hydroxylamine pathway, while the linear correlation is found. It could be that the linear correlation is found for

both pathways as the dependence of nitrification on IC concentration has been demonstrated in various studies (Wett and Rauch, 2003; Guisasola et al., 2007; Torà et al., 2010).

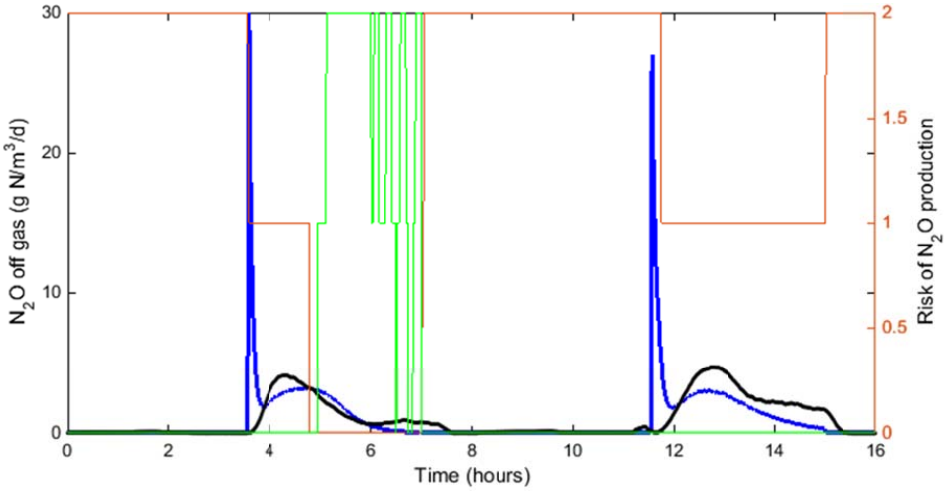

Figure 5.8. The measured N_2O off-gas (black) and simulated N_2O off-gas (blue) combined with the risk (medium risk is 1, high risk is 2) for N_2O production due to AOB denitrification (red) and hydroxylamine oxidation (green).

At time equal to 6 hours, there is a small increase in the measured N_2O production while there is a high risk of hydroxylamine oxidation. However, the $S_{NH_4^+}$ concentration is decreased during the nitrification to around 1 mg/L and an excess of NH_4^+ is needed for the hydroxylamine pathway. Nevertheless, it is not mentioned how high the concentration should be and depending on the type of AOB the threshold concentration differs (Chandran et al., 2011). Therefore it is possible that the concentration of 1 mg/L is still high enough for the hydroxylamine pathway to be active. In the second cycle at time 13, also a plateau in the N_2O off-gas can be seen. Yet no risk of the hydroxylamine pathway is detected, while the $S_{NH_4^+}$ concentration is around 9 mg/L. More research is needed to be able to establish the responsible pathways of N_2O production during the SBR operation.

5.4 Discussion

5.4.1 N_2O model selected

The denitrification process is modelled according to Hiatt and Grady (2008) which includes the denitrification as a four step process based on COD balances. Pan et al. (2014) compared this COD based model with an approach focussed on electron competition. As the carbon is often the limiting factor during denitrification,

there will be a competition for electrons between the different denitrification steps. The electron model seems to be better at predicting the concentrations of the nitrogen intermediates under carbon limiting conditions. At COD/N ratios of 3.5 or lower (Itokawa et al., 2001) denitrification is incomplete and N_2O emissions are increased due to this incomplete denitrification (Kampschreur et al., 2009). Stenström et al. (2014) reported a COD/N ratio of 2.3 in the SBR and an inhibition of denitrification before carbon dosing. Therefore, it is possible that the ASMN is not capable of describing denitrification under carbon limiting conditions. Nevertheless, it is still not clear how the model of Pan et al. (2014) can be coupled with standard ASM models. Indeed, in Chapter 3 of this manuscript it was demonstrated how complex it is to adapt these models. Therefore, this possible way of modelling denitrification was not included.

The N_2O model developed by Mampaey et al. (2013) was used for the simulation of N_2O production by AOB. This model was selected as it represents the nitrifier denitrification pathway which was mentioned by Stenström et al. (2014) as the most likely responsible pathway for the N_2O production during nitrification. However, there are other N_2O models available in literature that predict the nitrifier denitrification pathway (Ni et al., 2013; Guo and Vanrolleghem, 2014). One of the main differences between these models is the influence of oxygen. Mampaey et al. (2013) modelled a consumption of oxygen during nitrification and the nitrifier denitrification steps. Ni et al. (2013) modelled an inhibition of oxygen by using Monod kinetics while Guo and Vanrolleghem (2014) used Haldane kinetics for the oxygen inhibition. As the aim was to test the combination of the physicochemical model with the biochemical model, the other nitrifier denitrification models are not examined. In addition, it would be interesting to analyse the nitrifier denitrification pathway in combination with the hydroxylamine pathway as the risk model demonstrated the possibility that both pathways alternate during the aerated phase.

5.4.2 Calibration technique

Both the SBR model and the physicochemical model are sensitive to the selection of initial values. This makes the calibration more difficult as it increases the number of parameters that need to be adjusted to fit the model. In addition, using an automatic calibration technique is complicated as the physicochemical model crashes when the initial values are too far off. This is a common problem with systems that are solved using the Newton-Raphson approach. Indeed, the solver is able to converge in a few iteration steps, but the initial values must be relatively close to the "true solution". Therefore no automatic calibration could be performed in this study. However, by including quantitative and qualitative evaluation methods a more objective assessment of the fitness of the model is made.

5.4.3 Effect of stripping

The stripping equations implemented in the BCM are based on adjusting the k_{L}a coefficients of oxygen to other specific compounds by using their diffusivity coefficients (CO_2, N_2, N_2O, NO) (Foley et al., 2010b). During the denitrification phase, the k_{L}a of oxygen is assumed to be 0, which indicates that there is no stripping. However, due to mixing and wind, some stripping can take place, which is also indicated by the measured N_2O in the off-gas during the denitrification phases in both cycles. In addition, the high peaks of N_2O emissions when aeration is turned on are not visible in the data. If some of the dissolved N_2O would be stripped during the denitrification phase, there will not be a large build-up leading to such a high peak in emissions when the aeration is turned on. Therefore, including a small k_{L}a value during the denitrification phase due to mixing would be preferable.

In addition, the stripping of CO_2 in the SBR has been calibrated by using a factor to reduce the stripping of the model layers below the top layer. As mentioned in Section 5.3.1 the stripping leads to an increase in pH and with the stripping in all layers activated, the predicted decrease in pH differed significantly in shape from the measurements. The effect can be seen in **Figure 5.9** where different factors are used for the stripping in the layers below the top layer.

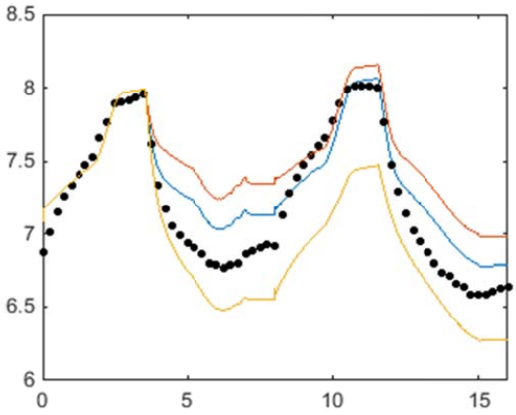

Figure 5.9. The simulated pH when assuming a stripping factor of 0.25 (blue), of 0.5 (red) or only considering stripping in the top layer (yellow).

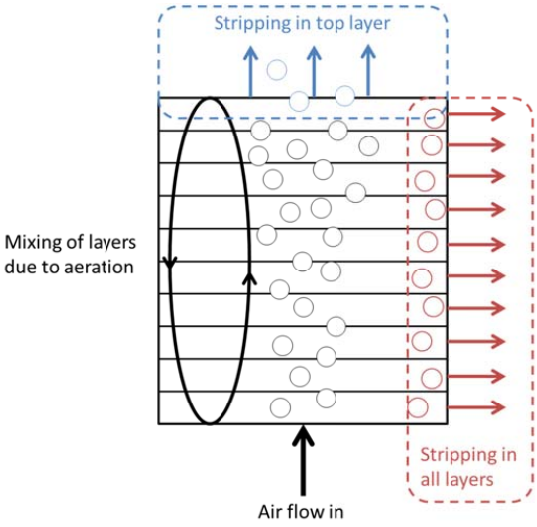

Figure 5.10. A schematic overview of the modelling of stripping in the top layer only (blue) and in all layers (red).

The shape of the decrease in the pH is more similar when using only stripping in the top layer. However, the pH of the second cycle is too low in that case. This level is reached when using stripping in all layers, but the decrease in pH has a different shape. This would indicate that the real contribution of stripping is situated in between the case with stripping in all layers and the case with stripping only in the top layer. By stripping in the top layer only, an underestimation of the contribution of stripping is made, as the air bubbles are moving from the bottom to the top and therefore pass through all the layers (**Figure 5.10**). This would result in an exchange between the liquid and gas phase in all layers. Nevertheless, when including stripping in all layers, an overestimation is made as the CO_2 that is formed is leaving the system from that layer instead of moving up towards the next layer (**Figure 5.10**). By including a factor for the stripping in the layers below the top layer, this overestimation can be avoided. Still, this factor is empirical and modelling the CO_2 transfer from bottom layers to the layers on top is the preferable approach.

5.5 Conclusion

The key findings of this study can be summarised as follows:

- The physicochemical model is capable of describing the pH variation measured in the SBR system.
- The difference in buffering capacity (measured versus simulated) may be a result of the uncertainty in the grab samples and/or the ion pairing of the monovalent ions.
- A positive linear correlation between the N_2O production rate and the IC concentration is found during the last part of the nitrification phase.
- The risk model indicates that both N_2O pathways are most likely alternating during the nitrification phase.

6. Generation of synthetic influent data to perform (micro) pollutant wastewater treatment modelling studies

Abstract

The use of process models to simulate the fate of micropollutants in wastewater treatment plants is constantly growing. However, due to the high workload and cost of measuring campaigns, many simulation studies lack sufficiently long time series representing realistic wastewater influent dynamics. In this Chapter, the feasibility of the Benchmark Simulation Model No. 2 (BSM2) influent generator is tested to create realistic dynamic influent (micro)pollutant disturbance scenarios. The presented set of models is adjusted to describe the occurrence of three pharmaceutical compounds and one of each of its metabolites with samples taken every 2-4 hours: the anti-inflammatory drug ibuprofen (*IBU*), the antibiotic sulfamethoxazole (*SMX*) and the psychoactive carbamazepine (*CMZ*). Information about type of excretion and total consumption rates form the basis for creating the data-defined profiles used to generate the dynamic time series. In addition, the traditional influent characteristics such as flow rate, ammonium, particulate chemical oxygen demand and temperature are also modelled using the same framework with high frequency data. The calibration is performed pseudo-automatically with two different methods depending on data availability. The 'traditional' variables are calibrated with the Bootstrap method while the pharmaceutical loads are estimated with a least squares approach. The simulation results demonstrate that the BSM2 influent generator can describe the dynamics of both traditional variables and pharmaceuticals. By using different quantitative and qualitative evaluation methods, the accuracy of the calibration is shown. Lastly, the study is complemented with: 1) the generation of longer time series for *IBU* following the same catchment principles; 2) the impact of in-sewer *SMX* biotransformation when estimating the average daily load; and, 3) a critical discussion of the results, chances and opportunities of the presented approach balancing model structure/calibration procedure complexity versus predictive capabilities.

6.1 Introduction

It has been more than 25 years since the publication of the Activated Sludge Model No. 1 (ASM1) (Henze et al., 1987). The ASM1 describes organic carbon and nitrogen removal processes in activated sludge systems and has been successfully applied to a large number of wastewater treatment plants (WWTPs). The successful results obtained in the early years have resulted in the further expansion of the number of phenomena included in

activated sludge models (ASMs), e.g. by including the description of bacterial storage, 2-step nitrification, 4-step denitrification and phosphorus removal. In this way, ASM1 evolved to ASM2, ASM2d and finally ASM3 as well as many other versions of ASM inspired models. As a consequence, the use of ASMs (Henze et al., 2000) is constantly growing and practitioners in both industry and academia are increasingly applying these tools when performing WWTP engineering studies. Numerous publications demonstrate the usefulness of ASMs for benchmarking (Copp, 2002; Jeppsson et al., 2007; Gernaey et al., 2014), diagnosis (Rodriguez-Roda et al., 2002; Olsson, 2012), design (Flores et al., 2007; Rieger et al., 2012), teaching (Hug et al., 2009) and optimisation (Rivas et al., 2008) of WWTPs.

The potential adverse effects of xenobiotics in aquatic environments (e.g. Ternes, 1998) have promoted a substantial amount of research regarding the extension of ASMs to describe micropollutants (Clouzot et al., 2013; Plósz et al., 2013b). The term micropollutants includes compounds such as pharmaceuticals, personal care products, and biocides which are released into the environment in low concentrations (µg/L or ng/L). In many cases, these pollutants can pose a significant risk to the environment and human health. On aquatic life, such adverse effects can be characterised as spread and maintenance of antibacterial resistance (Baquero et al., 2008), sex reversal and/or intersexuality (Lange et al., 2009) or reduction of the reproductive behaviour (Coe et al., 2008).

Most models describing the fate of micropollutants in a WWTP include among others: volatilisation (Lee et al., 1998), sorption/desorption (Joss et al., 2006; Lindblom et al., 2009), and biotransformation (Plósz et al., 2010b; Suarez et al., 2010; Delgadillo-Mirquez et al., 2011). These models are used as decision support tools to help understand the underlying mechanisms of micropollutant fate in the WWTP, and thus they provide a prediction of the efficiency of different treatment technologies (Lindblom et al., 2006; Snip et al., 2014; Vezzaro et al., 2014).

In essence, the performance of WWTP modelling studies depends heavily on availability of the influent time series as these form the main disturbance of a typical WWTP (Rieger et al., 2012). These influent time series should represent the inherent natural variability of the traditional and/or micropollutant dynamics as accurately as possible (Ráduly et al., 2007). However, obtaining sufficiently long and qualitatively adequate time series for micropollutant modelling projects is costly and requires a high workload. This is because micropollutant analysis requires expensive analytical equipment, complex analytical procedures with costly consumable supplies and analysis methods requiring significant knowledge about the matrix effects in order to

be successful (Richardson, 2012). Along this line of thinking, it is believed that synthetic data generation is a promising tool since it can: 1) significantly reduce the cost and workload of measuring campaigns by inter- and extrapolating the obtained data; 2) fill gaps due to missing data in influent flow rate/pollution/temperature profiles; and, 3) create additional disturbance time series for scenario analysis following the same catchment principles.

There are several published studies that try to describe mathematically how these compounds appear at the inlet of the WWTP (Martin and Vanrolleghem, 2014). For example, Ort et al. (2005) developed a stochastic model, describing short-term variations of benzotriazole concentrations (a chemical contained in dishwasher detergents). On the other hand, De Keyser et al. (2010) developed within the framework of the European Research Project Score-PP, a model that generates time series of micropollutant occurrences according to specific (phenomenological/stochastic) release patterns. Gernaey et al. (2011) presented a phenomenological influent model capable to reproduce daily, weekly, and seasonal influent variation as well as dry and wet weather episodes for the Benchmark Simulation Model No. 2 (BSM2) platform. This influent model was later calibrated and validated using data from two large Scandinavian WWTPs for a period of 2 years (Flores-Alsina et al., 2014b). The same framework was upgraded with toxic/inhibitory compounds (Rosen et al., 2008) and more recently with pharmaceuticals (Snip et al., 2014). However, most of the previous studies were focused on model development rather than on practical applications. In addition, on the basis of the literature that has been collected in the frame of this PhD thesis, it can be concluded that there is no (validated) tool described in the literature that is capable of describing the dynamics of traditional and non-traditional pollutants simultaneously using the same framework.

The objective of this Chapter is to test the feasibility of the BSM2 influent generator model, upgraded according to the principles stated in Chapter 4, for creating realistic dynamic influent (micro) pollutant disturbance scenarios using data from an intensive measuring campaign. The occurrence of three pharmaceutical compounds (one anti-inflammatory, one antibiotic and one psychoactive drug) and one of each of its metabolites together with traditional influent characteristics (flow rate, ammonium, particulate chemical oxygen demand and temperature) will be (synthetically) modelled. Information about excretion pathways and total consumption rates form the basis for generating the diurnal profiles of pharmaceuticals in wastewater at the discharge point of a real urban catchment. Automatic calibration is performed using: 1) a least-squares approach for the calibration of the pharmaceutical loads; and, 2) the Bootstrap method (Efron, 1979; Joshi et al., 2006) for the calibration of the traditional variables. The predictive accuracy of the BSM2 influent generator

is assessed by using different quantitative and qualitative evaluation techniques. These quantitative evaluation techniques concern the peak performance, relative and absolute error as well as the overall performance. Qualitative evaluation is performed by visualization of the distribution of the errors. Finally, the study includes a scenario analysis and a critical discussion of the results.

6.2 Methods

6.2.1 WWTP and catchment under study

The WWTP under study is located in the North-East of Spain in Puigcerdà (**Figure 6.1**). It serves around 16.000 PE (person equivalent) from both Spain and France and has a high seasonal load variation with fluctuating average flows of 8300 and 4100 m^3/day, and fluctuating organic/nitrogen load 595 and 1785 kg BOD/day and 123-349 kg N/day, respectively. This seasonal load variation is due to the touristic activities in the area during the winter time. There is also a significant increase in population during the weekends as many people living in larger cities have their second house located in the catchment area. The catchment is sparsely populated while covering a large area (approximately 100 km^2) and contains urban and agricultural areas. The WWTP is located close to the largest town in the area (Puigcerdà). Therefore, the majority of the flow and pollutant loads received by the WWTP (60%) are expected to originate from nearby (distance <1.5 km).

Figure 6.1. The catchment under study with the location of the WWTP and the different towns.

6.2.2 Compounds under study

The occurrence of a specific type of micropollutant, namely pharmaceuticals, will be described in this study. These pharmaceuticals are one non-steroidal anti-inflammatory compound - ibuprofen (*IBU*), one antibiotic - sulfamethoxazole (*SMX*), and one mood stabilising drug - carbamazepine (*CMZ*). These three compounds are selected because their occurrence and removal in wastewater have been extensively studied during the past years (e.g., *IBU*: Buser et al., 1999; Collado et al., 2012, *SMX*: Göbel et al., 2005; Carballa et al., 2008, *CMZ*: Clara et al., 2004; Leclercq et al., 2009). For each pharmaceutical, a human metabolite is additionally included since these chemicals can occur in comparable or even higher concentrations than their parent chemicals (Zhang et al., 2008). For *IBU*, the metabolite chosen was 2-hydroxyibuprofen (*IBU-2OH*); for *SMX*, N4-acetyl-sulfamethoxazole (*SMX-N4*), and for *CMZ*, 2-hydroxyl-carbamazepine (*CMZ-2OH*). In addition, the wastewater stream was characterised by means of traditional pollutants, including flow rate, a soluble pollutant (NH_4^+), a particulate pollutant (*CODpart*), and the temperature (*T*) at the inlet of the WWTP.

6.2.3 Measuring campaign

A data set comprising two measuring campaigns (long: *DS1*/short: *DS2*) is used for the calibration of the BSM2 influent generator. The long term (*DS1*) on-line data was collected using S::CAN sensors (Scan Messtechnik GmbH, Vienna, Austria) for organic matter (spectrolyzer) and nitrogen (ammolyzer) at 2 minute intervals (from 02/10/2012 at 6:00 to 31/10/2012 at 14:00). The flow rate was measured with an electromagnetic meter (ABB Kent-Taylor: MagMaster 400T Series) (data frequency: 1 min). Grab samples, taken at the influent of the WWTP, were used to compare with the on-line data. Rainfall data was retrieved from a weather station, which had a rain gauge in Queixans (4.1 aerial km from WWTP).

The short term data set (*DS2*) comprises an intensive three day measuring campaign (from Monday 08/10/2012 at 10:00 to Thursday 11/10/2012 at 8:00). The sampling interval was four hours during periods with low flow rates and two hours during periods with high flow rates. Grab samples were collected after the pumping station and the grids and just before the biological treatment (there is no primary treatment). All samples were transferred into amber glass bottles and filtered with 0.7/0.45/0.22 µm Nylon filters (Whatman, Maidstone, UK), and were afterwards kept at 4°C in darkness until analysis. All the analyses were carried out in triplicates. More information on the measuring campaign and the WWTP can be found in Corominas et al. (2015).

6.2.4 Analytical methods

Analysis of pharmaceuticals was performed following the fully automated on-line methodology by (García-Galán et al., 2015). Briefly, 1 mL of wastewater is loaded on the on-line chromatographic system (Thermo Scientific EQuanTM166 , Franklin, MA, US) consisting of 2 quaternary pumps and 2 LC columns, one for pre-concentration of the sample and the second one for chromatographic separation. The sample will be further eluted by means of the mobile phase into the coupled mass spectrometer (TSQ Vantage triple quadrupole; Thermo Scientific, Franklin, MA, US). Chromatographic separation was achieved using a Thermo Scientific Hypersil GoldTM (50 x 2.1 mm, 1.9 µm particle size) column. Target compounds were analysed under dual negative/positive electro-spray ionization in multiple reaction monitoring (MRM) mode, monitoring two transitions between the precursor ion and the most abundant fragment ions for each compound. Recoveries of the compounds ranged between 51% and 139% (*CMZ-2OH* and *IBU*, respectively), whereas limits of detection ranged from 0.5 ng/L to 150 ng/L for *CBZ* and *IBU-2OH*, respectively.

6.2.5 Model-based influent generator

The modelling approach described in Chapter 4 is used to simulate the influent dynamic time series of the catchment. The compounds studied, exhibited a daily pattern in their occurrence and therefore the phenomenological approach is applied which makes use of data-defined profiles. The data-defined profiles are taken from the BSM2 influent generator (Gernaey et al., 2011), and are case specific. The length of the sewer system can be incorporated in the influent dynamics: the larger the simulated sewer network, the smoother the simulated diurnal flow rate and concentration profiles. In addition, as *DS1* comprises dry weather as well as wet weather episodes, the ''first-flush'' effect from the sewer network and the influent dilution phenomena are included in the calibration. Zero-mean white noise is added to the time series to provide more realism using the variance of the noise as a tuning parameter. A schematic representation of the whole calculation procedure is presented in **Figure 6.2**.

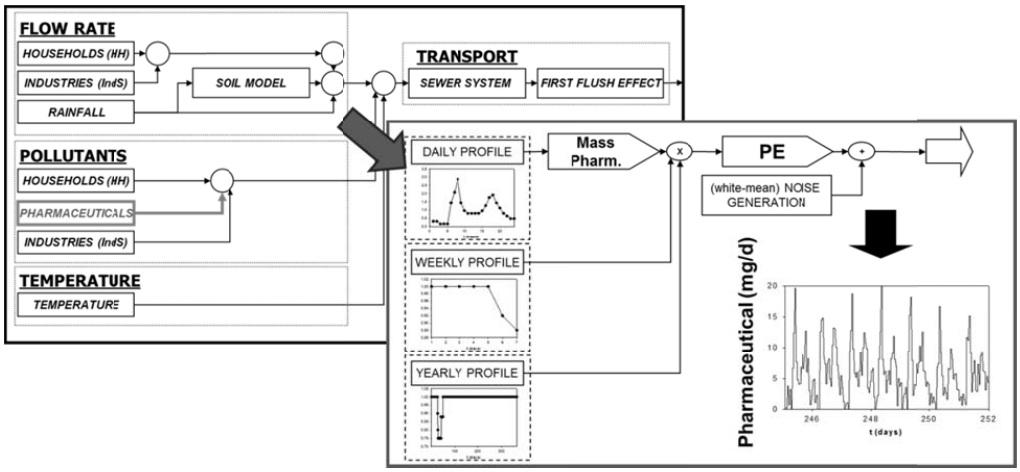

Figure 6.2. Model blocks used to create the different pharmaceutical loading profiles.

6.2.6 Calibration technique

The calibration is performed using first a manual approach followed by automatic methods. The catchment characteristics and some of the features in the *soil model* are manually adjusted based on the information available using a step-wise procedure (Flores-Alsina et al., 2014b). The previous study identified at different time scales and for different weather conditions the model´s parameters to which the outputs are most sensitive. Therefore, those parameters are adjusted under dry weather conditions before modifying the parameters concerning wet weather conditions. This is mainly due to the fact that *DS1* comprises both dry weather and wet weather episodes which need to be treated differently. For *DS2* this distinction is not necessary as there are only dry weather conditions in the data set.

Secondly, the model parameters such as the average daily loads are estimated with automatic calibration techniques. The parameter estimation is carried out using a least squares approach, minimising the errors between the model prediction and the measurement data. These optimisations are performed in MatLab R2014b with the lsqnonlin function, which uses the sum of squares of relative errors as objective function. The use of this function has the advantage that it allows a definition of lower and upper bounds of the parameters to be estimated, and therefore negative parameter values can be avoided. The automatic calibration of the flow rate, temperature, particulate COD and ammonium also included the Bootstrap method (Efron, 1979; Joshi et al., 2006). This method uses the initial set of data to replicate additional data sets (100 additional data

sets in this study). For all these additional data sets the parameters are estimated again, resulting in a range of different parameter estimates. Therefore, additionally a confidence interval of the parameters can be obtained. To create the additional data sets, a comparably high number of data points are needed. As this high number of data points is not available for the pharmaceuticals (*DS2* has only 24 data points), no additional data sets are created for pharmaceuticals and the parameter estimation is only performed once.

6.2.7 Evaluation methods

In order to assess the predictive accuracy of the influent generator, different quantitative and qualitative evaluation methods are used, which are described in this Section.

6.2.7.1 Quantitative evaluation methods

In the case of the influent generator, it is important that the generated time series capture besides the averages of the data also the trend/peaks. In order to assess the performance of the influent generator, different types of quantitative evaluation methods are used, such as the ones mentioned in Chapter 5.2.5. These methods include criteria related to the dynamics as well as absolute and relative criteria related to the average of the residuals. Additionally, criteria concerning overall performance are examined. In order to avoid a bias in the results, the data points with values of 0 are removed before the analysis. Therefore the number of data points involved in this comparison is different for the different variables. The equations used for the analysis can be found in Appendix A.3 and A.4 (**Tables A.3.1** and **A.4.1**).

The criteria related to the dynamics are taken from Chapter 5.2.5 as well as the absolute criteria concerning the averages of the residuals. In addition, relative criteria are calculated to compare the performance of the influent generator among the variables. The mean percentage error (*MPE*) is calculated for the bias of the calibration, however similar to the *ME*, the negative and positive residuals/errors can cancel each other out. In order to avoid the cancelling out, the mean absolute relative error (*MARE*) is calculated. Lastly, the mean squared relative error (*MSRE*) is evaluated, which also emphasises the larger errors.

Finally, besides the overall criteria mentioned in Chapter 5.2, also the standard deviation of the Bootstrapping method is compared (*STD Boots*). If this standard deviation is small compared to the value of the estimate, this also indicates a precise fit. To be able to compare the *STD Boots* between the different variables, the percentage of the standard deviation is calculated.

6.2.7.2 Qualitative evaluation methods

The qualitative evaluation methods described in Chapter 5.2 are also used in this study. The distribution of the residuals is shown in distribution plots for the traditional variables; however these plots also include the density of the residuals. As the number of data points for the pharmaceuticals is relatively low, the distribution plot can be unclear. Therefore quantile-quantile plots will be used for the pharmaceuticals as these also contain information on the distribution of the residuals. By combining the plots, an assessment can be made on the points of interest where the model is not representing the data.

6.3 Results

6.3.1 Dynamic modelling of traditional influent characteristics

In this Section, the BSM2 influent generator is used to describe the dataset comprised in *DS1*. Parameters concerning the traditional variables (*QperPE, Qpermm, CODpartgperdperPE, SNHgperdperPE,* T_{Bias}, T_{dAmp} and G_{rain_Temp}) are estimated using the Bootstrap method (Efron, 1979; Joshi et al., 2006). Other parameters are adjusted using a manual procedure (see Section 6.3.2.6) based on the information available.

6.3.1.1 Influent flow rate, pollution loads and temperature

In dry weather conditions 28% of the influent flow rate is assumed to originate from *HH*. The *IndS* contribution to the flow rate is assumed to be negligible. The remaining 72% of the influent flow rate (dry weather conditions) originates from groundwater infiltration, which could be due to the large catchment compared to the number of inhabitants. Additionally, there is an irrigation channel connected to the sewer network, resulting in a higher flow rate and a high percentage of 'clean' water in the influent. The dynamic (dry weather) flow rate pattern is obtained by repeating the default (daily, weekly and seasonal) data profiles in a cyclic manner (see Gernaey et al., 2011). The generated signal is then multiplied with two gains corresponding to the flow rate per person equivalent (*QperPE* = 110 m^3/PE.day, **Table 6.1**) and the number of person equivalents in the catchment area (*PE* = 16,000). Finally, a continuous groundwater contribution due to infiltration processes is assumed. Thus, soil parameter values (K_{down} = 400 m^2/d, K_{inf} = 4400 and A = 27,916 m^2) are adjusted to reach the pre-established flow rate due to infiltration. Wet-weather conditions are modelled by converting rainfall intensities into flow rate values using an empirical factor (*Qpermm* = 824 m^3/mm, **Table 6.1**). Finally, the sewer length is calibrated by adjusting the parameter subarea, which here corresponds to a HRT of 3 hours. A description of the rest of the FLOW RATE and TRANSPORT (sewer) model block parameters can be found in Gernaey et al. (2011).

In this study, one soluble (NH_4^+) and one particulate compound (*CODpart*) were selected to describe different types of traditional pollution dynamics. In dry weather conditions, the predefined data profiles are also sampled cyclically and multiplied by the pollution load and the number of person equivalents in the catchment (*PE* =16,000). Accordingly, the daily average ammonium and total *CODpart* loads in the *HH* block are 5.53 g N/(day.PE) ($NH4_{gperPEperd}$) and 57.11 g *CODpart*/(day.PE) ($CODpart_{gperPEperd}$), respectively (**Table 6.1**). The same assumptions as made in the previous paragraph apply here as well (industrial contribution is negligible). During wet weather conditions, the parameters of the first-flush model should be adjusted (**Figure 6.2**). Hence, the flow rate at which the particles will be flushed out of the sewer system (Q_{lim}) is set to 10,000 m^3/d. The maximum total mass of particles that can settle in the sewer (M_{Max}) is 700 kg SS, and the fraction (*FFfraction)* of particles capable of settling in the sewer network is 0.40. The same sewer length is assumed (HRT = 3 h). A description of the rest of the POLLUTANTS and TRANSPORT (first flush) model block parameters can be found in Gernaey et al. (2011).

Table 6.1. The inputs for the automatic calibration are given as an initial parameter estimate with lower and upper parameter value bounds, as well as the outputs of the Bootstrap method, i.e. the calibrated parameter and its standard deviation.

Parameter	First estimate	Lower bound	Upper bound	Calibrated parameter	Standard deviation
Flow rate					
QperPE	150	50	500	*101.91*	3.89
Qpermm	1250	500	3000	*819.20*	31.07
Ammonium					
SNHgperdperPE	6	1	25	*5.53*	0.020
COD particulates					
CODpartgperdperPE	80	0	200	*57.11*	0.472
Temperature					
T_{Bias}	18	10	30	*17.67*	0.0049
T_{dAmp}	0.4	0	1	*0.378*	0.0071
G_{rain_Temp}	0.4	0	1	*0.141*	0.0040

Lastly, the wastewater temperature (*T*) is calibrated following the same dry/wet weather procedure. Dry weather temperature is modelled based on two sine functions; one for the daily variation and another one for the seasonal variation. The daily variation is calibrated by adjusting the amplitude of the daily variation (T_{dAmp} = 0.38°C, **Table 6.1**). The seasonal variation can be obtained by shifting the sine wave into the correct season and adjusting the average temperature (T_{Bias} = 17.7°C, **Table 6.1**). In order to describe how temperature decreases due to wet weather events, rain data is added to the influent generators as an additional input. Thus, rainfall data is multiplied with a gain (G_{rain_Temp} = 0.14, **Table 6.1**) before subtracting it from the temperature. In order to correctly simulate the slow increase in the wastewater temperature following a rain event, a first-order transfer function is added. The rest of the TEMPERATURE model block parameters can be found in Gernaey et al. (2011). The result of the calibration using the Bootstrap method is shown in **Table 6.1**. It is important to highlight that the estimations performed with the Bootstrap method are complemented with standard deviations of the calibrated parameters. These standard deviations are within the range of 0.03% to 3.8% of the calibrated value, indicating low variability on the assumed values. The standard deviations are the highest for the parameters related to the flow rate, which is due to the fact that these can compensate for each other to some extent (identifiability problem). The standard deviations can also be used as inputs for an uncertainty analysis, but this was not pursued here.

6.3.1.2 Simulation results

Simulation results show that the four model blocks can successfully reproduce daily and weekly dry weather variations. **Figures 6.3** and **6.4** describe the daily flow rate and pollutant (NH_4^+, *CODpart*) profiles which represent a general behaviour, namely one morning peak, one evening peak, and late night and midday minima. The morning and evening peaks represent the increased activity of the residents just before going to work or after returning from work. The daily minimum flow rate corresponds to the night hours with reduced water consumption. The daytime flow rate shows a small decrease corresponding to the residents' working hours. When it comes to the daily variation of the wastewater influent temperature, the model successfully describes the dynamics reflecting the differences between night and day (**Figure 6.5**).

Figures 6.3, **6.4** and **6.5** also demonstrate that the previously presented model blocks can predict reasonably well the wet-weather episodes. It is important to highlight that the flow rate model block was not able to reproduce all the peaks found in the measurements (**Figure 6.3**, grey line). This is due to the fact that some wet weather episodes within the catchment were not entirely captured by the rain gauge in Queixans (see **Figure**

6.1, Section 6.2.3). It is furthermore hypothesised that it is necessary to have additional data from rain gauges covering the entire geographical area in order to improve the description of the rain contribution to the influent flow rate, but such data are not available. It is assumed that the rainfall might come from a part of the catchment where data was not available (or not registered). Therefore, in order to represent all rainfall events a synthetic (rainfall) dataset had to be generated by subtracting the simulated dry weather flow from the measurements. Sewer HRT had to be accounted for to correctly describe the dynamics.

When it comes to the concentration dynamics of particulates, **Figure 6.4** shows that the influent model can describe re-suspension of particulates (see days 12, 19 and 26) following a rain event (**Figure 6.3**). The increase of the *CODpart* load is mainly caused by the flush out of the particulate fraction that has settled in the sewer system during the preceding period with dry weather conditions. However, there are also increases in *CODpart* loads when there is no increase of flow rate (see days 7, 27 and 28). This could be due to the placement of the sensors, which are located in a tank into which the influent is pumped. The pumping of the influent could have an impact on the re-suspension of the solids. Unfortunately, it was not possible to place the sensor before this pump and therefore no conclusions could be drawn about the potential re-suspension.

Finally, **Figure 6.5** demonstrates that temperature drops due to rain events (see day 15). The additional rain events that had to be included in order to correctly describe wet-weather flow rate in **Figure 6.2** do not seem to have an effect on temperature dynamics (**Figure 6.4**). This strengthens the hypothesis of a geographically separated rain episode not captured by the rain gauge situated close to the WWTP as the effect of cold rain water on the influent temperature is reduced during transport of the water through the sewer network.

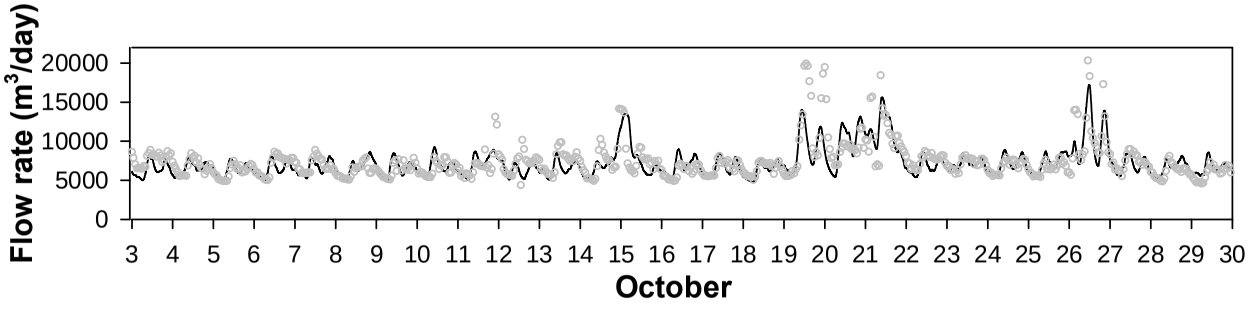

Figure 6.3. Calibration (grey line) of the influent flow rate data (grey dots) at the inlet of the WWTP. Synthetic rainfall data created to fill the missing rain events (black line) are shown as well.

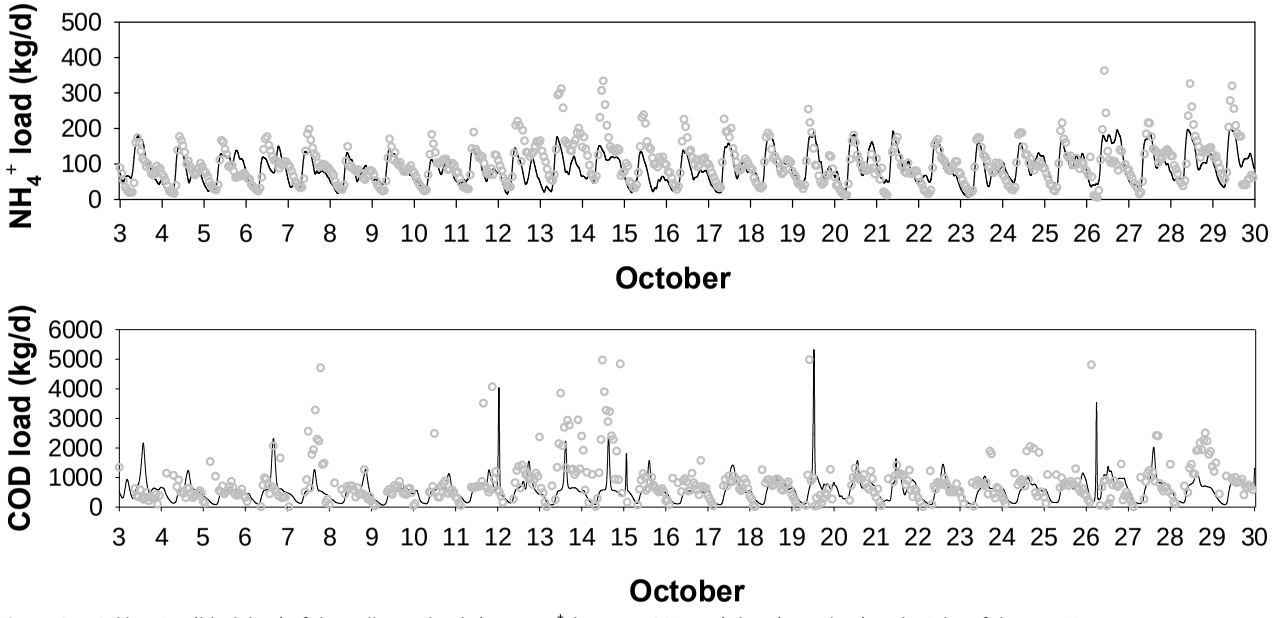

Figure 6.4. Calibration (black line) of the pollutant loads (top: NH_4^+, bottom: *CODpart*) data (grey dots) at the inlet of the WWTP.

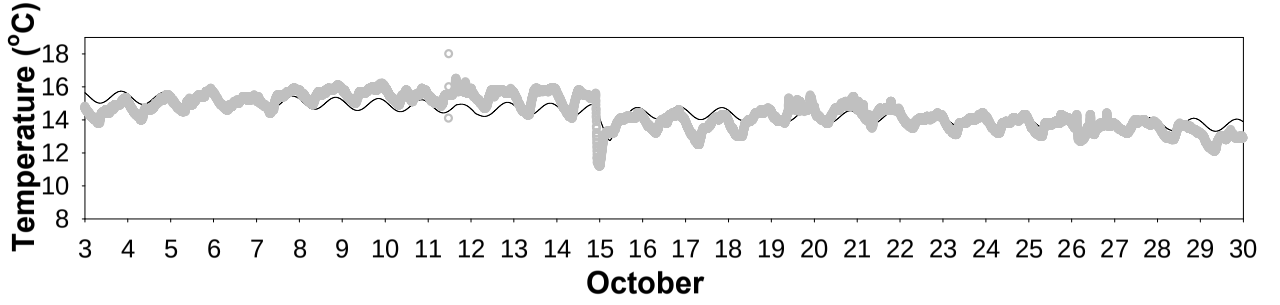

Figure 6.5. Simulation (black line) of the wastewater temperature data (grey dots) at the inlet of the WWTP.

6.3.2 Dynamic modelling of pharmaceutical compounds

The second part of the results details how the BSM2 influent generator describes the occurrence of a selected set of pharmaceuticals (*DS2*). For the calibration of the pharmaceuticals too few data points are available (24 data points) to use the Bootstrap method. Therefore, the automatic parameter estimation is only performed on the available data and no standard deviation of the estimate is given.

Table 6.2. The inputs for the automatic calibration are given as an initial estimate with lower and upper parameter bounds, as well as the resulting calibrated parameter value.

Parameter	First estimate	Lower bound	Upper bound	Calibrated parameter
Pharmaceuticals load				
IBUgperdperPE	1	0	5	*3.71*
IBU-2OHgperdperPE	1	0	5	*2.22*
SMXgperdperPE	0.01	0	1	*0.1227*
SMX-4NgperdperPE	0.01	0	1	*0.08*
CMZgperdperPE	0.01	0	1	*0.0886*
CMZ-2OHgperdperPE	0.01	0	1	*0.1538*

6.3.2.1 Ibuprofen (*IBU*) and 2-hydroxyibuprofen (*IBU-2OH*)

Measurement data reveal a high correlation of both *IBU* and *IBU-2OH* with NH_4^+ (R^2 of 0.69 and 0.79, respectively). These results are in agreement with Weigel et al. (2004), which state that *IBU* is mainly excreted in the urine. For this reason it was decided to use the same pre-defined data profile that was selected to describe NH_4^+ (morning peak, one evening peak, and late night and midday minima). The estimation of the load was performed automatically (**Table 6.2**). Similarly to the traditional pollutants, the generated signal (sampled cyclically) is multiplied by a gain that assumes the total *IBU* ($IBU_{gperPEperd}$ = 3.71 g/(day.1000PE)) and *IBU-2OH* ($IBU\text{-}2OH_{gperPEperd}$ = 2.22 g/(day.1000PE)) loads within the catchment (*PE* = 16,000). The average predicted loads of *IBU* and *IBU-2OH* are 59 and 35 g/day, respectively, which corresponds to concentrations at the inlet of the WWTP of 9.1 and 5.4 µg/L respectively. The estimated hydraulic retention time was 3 hours (the same as in Section 6.3.1).

6.3.2.2 Sulfamethoxazole (*SMX*) and N4-acetyl-sulfamethoxazole (*SMX-N4*)

A correlation – similar to that of *IBU* – was found between *SMX* and its metabolite *SMX-N4* with NH_4^+ (R^2 of 0.63 and 0.58, respectively), which indicates again that these compounds are mainly excreted via urine. This correlation corresponds well with the theoretically expected distribution pattern, assuming a half-life of 10 h in the human body and a typically prescribed oral administration of twice a day (morning/evening). A similar observation was made by Göbel et al. (2005) and Plósz et al. 2010b). Therefore, the ammonium data profile is also used to describe *SMX* and *SMX-N4* influent dynamics, even though the correlation is lower than that of *IBU* and *IBU-2OH*. The generation of the time series follows the same mechanisms as describe in Section 6.3.2.1. The estimated total pollution load for *SMX* ($SMX_{gperPEperd}$) and *SMX-N4* ($SMX\text{-}N4_{gperPEperd}$) is 0.123 and 0.08 g/(day.1000PE), respectively (**Table 6.2**). As a result, the quantity of compound arriving to the plant is 0.991 and 0.627 g/day (in terms of load) or 304 and 192 ng/L (in in terms of concentrations) for *SMX* and *SMX-N4* respectively**.** It is important to highlight here that to describe the influent dynamics and the corresponding sharp pulses, the in-sewer HRT is reduced to an average of 1 hour by modifying the parameter *subarea* (see Section 6.3.2.4 for further discussion details).

6.3.2.3 Carbamazepine (*CMZ*) and 2-hydroxy carbamazepine (*CMZ-2OH*)

In this particular case, the occurrence of *CMZ* is highly correlated with the occurrence of *CODpart* (R^2=0.82). On the other hand, the occurrence of *CMZ-2OH* is correlated with NH_4^+ (R^2=0.63), similar to the previous compounds. This is attributed to the fact that *CMZ* is excreted 28% in the faeces (Zhang et al., 2008), while *CMZ-2OH* is only present in urine. This is expected as one way human metabolism would reject drugs is by making them more water soluble through modifying the molecular structure (addition of e.g., glucuronide, OH moieties). Consequently, a particulate data profile was used to describe the dynamics of *CMZ*, while the NH_4^+ data profile was selected for *CMZ-2OH*. The main difference between the NH_4^+ and *CODpart* data pollution profiles is that particulate load dynamics lag slightly behind the soluble pollutant fluxes. This is mainly to introduce the delay in time in the influent model (see **Figure 6.2**) (further information can be found in Gernaey et al. (2011)). The loads of $CMZ_{gperPEperd}$ and $CMZ\text{-}2OH_{gperPEperd}$ loads are 0.0886 and 0.1538 g/(day.1000PE), respectively. The total quantity of *CMZ* and *CZM-2OH* arriving at the WWTP is 1.43 and 2.41 g/d, which in concentration terms equals 219 ng/L and 370 µg/L, respectively. The estimated HRT was 3 h (the same as used in Section 6.3.1).

6.3.2.4 Simulation results

Figure 6.6 shows the influent data and the model simulation results for *IBU* (**Figure 6.6a**) and *IBU-2OH* (**Figure 6.6b**). These show that the set of models presented herein can describe the general (daily) variation of both compounds (parent/metabolite). For the two cases, a substantial increase in the pollutant load can be observed during the morning/evening combined with night minima. Even though *IBU* has an irregular administration pattern, a dynamic correlation with NH_4^+ is found (**Figures 6.4** and **6.6a, b**) which depicts the impact of human urine. The ratio between the parent compound (*IBU*) and the metabolite (*IBU-2OH*) at the inlet of the WWTP was lower (1:0.6) than a typical human excretion ratio (1:1.7) (Weigel et al., 2004). The ratio between these compounds varies from study to study (Ferrando-Climent et al., 2012; Verlicchi et al., 2012). It is well known that different *IBU* administrations (i.e. oral and topical) might introduce active, unmetabolised compounds to the sewer (Daughton and Ruhoy, 2009). The lower *IBU* ratio could also indicate a waste of ibuprofen pills (these could have been flushed). Another influencing factor in the *IBU-OH/IBU-2OH* ratio could be biotransformation within the sewer. However, there are experimental evidences that state the contrary (Jelic et al., 2015). In addition, it cannot be excluded that there is a bias in the data. The concentrations reported in this study are within the ranges summarised in the review by Verlicchi et al. (2012).

The comparison of the predicted behaviour with the experimental data of *SMX* and *SMX-N4* is shown in **Figures 6.6c, d**. Again, the modified BSM2 influent model was capable of reproducing the behaviour of both compounds using the calibrated NH_4^+ profiles. The ratio between the parent compound (*SMX*) and its metabolite (*SMX-N4*) is 1:0.65 although the excretion ratio is 1:3 (Vree et al., 1995). This indicates a possible in-sewer re-transformation of *SMX-N4* to S*MX* as reported by numerous studies (Göbel et al., 2005; Plósz et al., 2010b; Jelic et al., 2015) (this aspect will be further analysed in Section 6.4.2). It is important to highlight that the parameter *subarea*, which characterises the length of the sewer and thus influences the HRT, had to be modified. Two possible explanations for this situation are hypothesised. Firstly, one must notice that *SMX* is several orders of magnitude lower in load than *IBU* and consequently more sensitive to errors related to the sampling method (Ort and Gujer, 2006). This could lead to missing toilet flushes that contain *SMX* when sampling, which would also explain the different times of the occurrence of peaks during the day. Secondly, due to the sparsely distributed catchment (Section 6.2.1), it is assumed that most of the detected compound is consumed and excreted in an urban area close to the sampling point. Hence, the shorter HRT prevents complete mixing of *SMX* and therefore the concentrations remain above detection limits. Indeed, the sources of NH_4^+ and *IBU* are higher and seem to point more plausibly towards a wide geographical distribution.

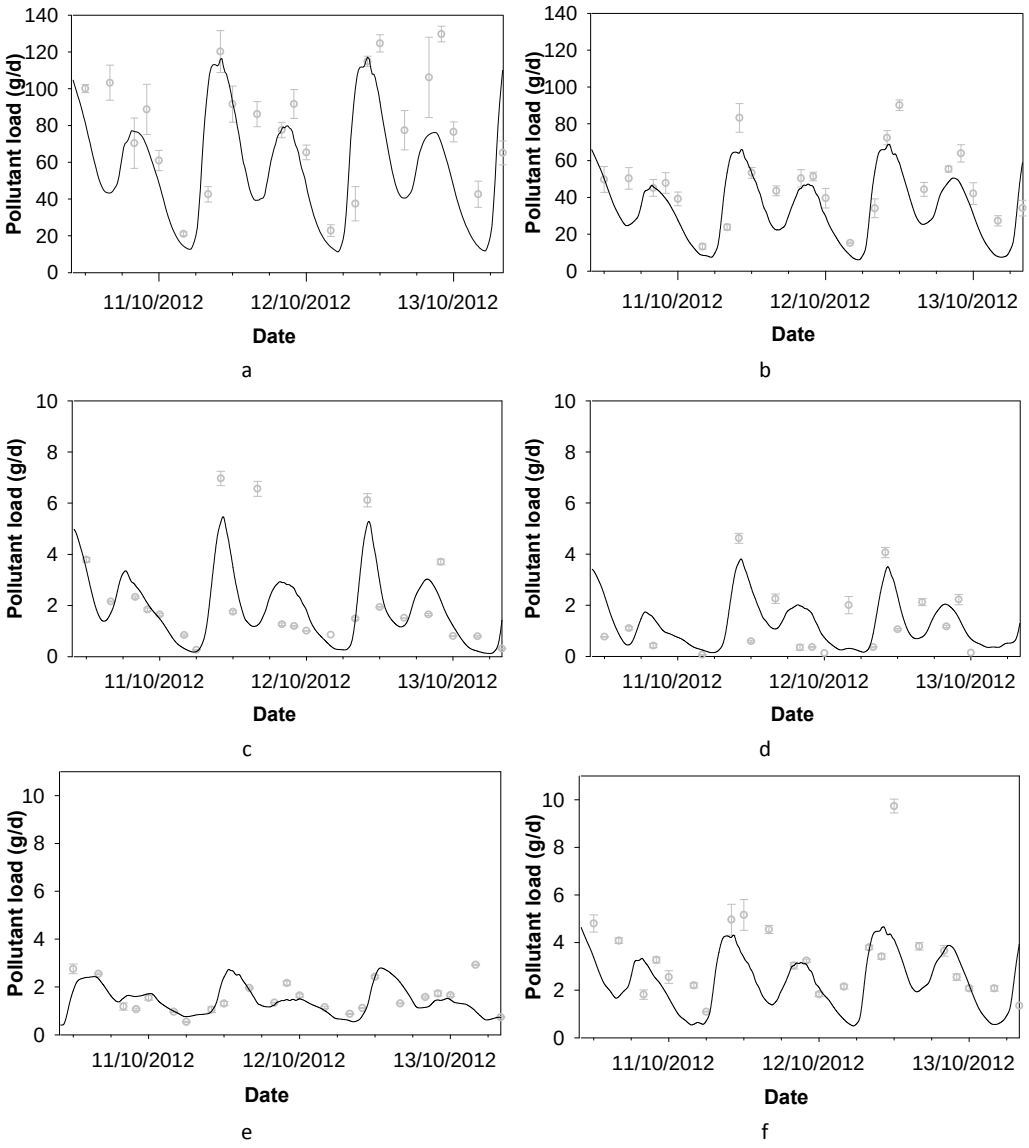

Figure 6.6. Simulations (black line) of the influent loads of *IBU* (a), *SMX* (c), *CMZ* (e) and the metabolites *IBU-2OH* (b), *SMX-N4* (d), *CMZ-2OH* (f) are compared to the measurements. Measurements are shown together with their standard deviations resulting from the chemical analysis (grey dots with error bars).

Again, when calculating the concentrations of *SMX* and *SMX-N4* at the inlet of the WWTP, they are within the ranges summarised by Verlicchi et al. (2012).

Figures 6.6e, f show a good prediction of the pollutant occurrence achieved by the modified BSM2 influent generator. Simulation and experimental results demonstrate the time difference in the different *CMZ* and *CMZ-2OH* peaks and the need to use different input data profiles to correctly describe their dynamics. The close link between *CMZ* and *CODpart* dynamics could be associated to desorption during filtering. The ratio between parent compound (*CMZ*) and metabolite (*CMZ-2OH*) in the wastewater is 1:2.9, which is similar to the one estimated by Plósz et al. (2012) in wastewater. However, these ratios differ from the theoretical excretion rate of 1:4 (Zhang et al., 2008). As *CMZ* is reported to be persistent and even suggested as an anthropogenic marker (Clara et al., 2004), biotransformation in the sewer seems unlikely to occur. However, the retransformation of metabolites of *CMZ* back into its parent compound has been reported (Vieno et al., 2007). Nevertheless, the possibility of desorption of excreted *CMZ* or the retransformation of metabolites should be further investigated. The ranges reported by Verlicchi et al. (2012) agree with the obtained concentrations in this study.

6.3.3 Evaluation of the calibration of traditional variables and pharmaceuticals

In this Section the results of the quantitative and qualitative evaluation methods for both traditional variables and the pharmaceutical calibration are demonstrated. By combining the results of the quantitative and qualitative evaluation methods in the discussion, more insights into the model's behaviour, the datasets and the calibration can be gained.

6.3.3.1 Quantitative evaluation of the calibration

The results of the quantitative evaluation can be found in **Table 6.3**, where the best and worst performances are presented in italics. It is important to note that the optimum for the peak evaluation, the absolute and relative criteria is 0, while the *IoAd* and correlation have an optimum of 1. The *STD Boots* should be as small as possible and therefore also has an optimum of 0.

Table 6.3. Quantitative evaluations of the BSM2 influent generator with high frequency data.

Quantitative method	Peak evaluation			Absolute criteria			Relative criteria			*IoAd*	*Corr*	*STD Boots*
Compound evaluated	*PDIFF*	*PEP*	*MSDE*	*ME*	*MAE*	*RMSE*	*MPE*	*MARE*	*MSRE*			
NH_4^+	1.27	*0.60*	3.40	**1.83**	4.40	5.59	**-2.31**	0.44	1.69	0.60	0.71	0.36
CODpart	103.16	15.76	$9.15 \cdot 10^{3}$	**-21.64**	59.20	101.60	***107.86***	*1.56*	*147.54*	*-0.15*	0.33	0.83
Flow rate	*623.34*	3.42	$1.46 \cdot 10^{6}$	*181.5*	$1.07 \cdot 10^{3}$	$1.66 \cdot 10^{3}$	*0.12*	0.13	0.03	0.82	0.70	3.81
Temperature	0.16	0.94	0.37	-0.0084	0.4707	0.60	-0.15	*0.033*	*0.0018*	0.78	*0.16*	1.58
IBU	$-7.76 \cdot 10^{-4}$	-9.02	$4.06 \cdot 10^{-5}$	$1.5 \cdot 10^{-3}$	$4.2 \cdot 10^{-3}$	$5.2 \cdot 10^{-3}$	7.41	0.40	0.30	0.71	0.50	x
IBU-2OH	$-6.34 \cdot 10^{-4}$	-11.85	$1.32 \cdot 10^{-5}$	$7.48 \cdot 10^{-4}$	$2.1 \cdot 10^{-3}$	$2.7 \cdot 10^{-3}$	9.47	0.35	0.23	0.77	0.62	x
SMX	$-2.27 \cdot 10^{-5}$	-6.43	$1.38 \cdot 10^{-7}$	$-5.27 \cdot 10^{-5}$	$1.57 \cdot 10^{-4}$	$2.24 \cdot 10^{-4}$	-71.58	0.91	2.96	0.84	*0.72*	x
SMX-N4	$2.23 \cdot 10^{-4}$	*-338.68*	$1.06 \cdot 10^{-7}$	$-1.03 \cdot 10^{-4}$	$1.89 \cdot 10^{-4}$	$2.91 \cdot 10^{-4}$	-78.16	1.43	3.84	*1.00*	*0.16*	x
CMZ	$-3.87 \cdot 10^{-4}$	-6.91	$1.31 \cdot 10^{-8}$	$\mathbf{-1.46 \cdot 10^{-5}}$	$6.39 \cdot 10^{-5}$	$9.06 \cdot 10^{-5}$	**0.63**	0.28	0.14	0.69	0.44	x
CMZ-2OH	$-3.50 \cdot 10^{-5}$	-8.38	$1.68 \cdot 10^{-7}$	$-7.04 \cdot 10^{-5}$	$2.17 \cdot 10^{-4}$	$2.84 \cdot 10^{-4}$	-3.17	0.52	0.63	0.51	0.26	x

For the peak evaluation, the highest value of the absolute criteria *PDIFF* and *MSDE* for flow rate is expected. Nevertheless, the *MSDE* of *CODpart* ($9.15 \cdot 10^3$) is high compared to the average value of *CODpart* (79 g/m^3) indicating that the difference in the timing of the peaks between the data and the simulations is large. Regarding the relative criterion *PEP*, the magnitude of the simulated *SMX-N4* peaks differs the most compared with the observed peaks. In order to describe the dynamics of *SMX* and *SMX-N4* the sewer hydraulic retention time was reduced from 3 hours to 1 hour. The *PEP* indicates that this decrease was still not enough for the influent generator to capture the sharp high peaks of *SMX-N4*. The best performance in the *PEP* can be found in NH_4^+. There are more peaks in this time series than in those of the pharmaceuticals, however the criterion indicates that the magnitude of most peaks is achieved with the influent generator.

When considering the evaluation of the residuals of the calibration and focussing on the absolute criteria, there seems to be little bias in the calibrations with respect to *ME*. However, it could be that negative and positive errors are cancelled out. Nevertheless, also *MAE* and *RMSE* show little bias. As the squared error was optimised during the automatic calibration, these absolute criteria should be low. Concerning the relative criteria, the calibrations of the flow rate and temperature are the best, while the *CODpart* has the worst performance. This is most likely related to the high value obtained for *MSDE* as it indicates that the timing of the peaks in the simulation is not entirely matching the peaks in the data leading to higher residuals.

It would be expected that the variables with low values of the relative criteria would also score well on the overall criteria. Nevertheless, the temperature has an *IoAd* of 0.78, while values of 0.8 or higher are assumed to demonstrate a good fit. Only the flow rate, *SMX* and *SMX-N4* show a fair fit as the values obtained for *IoAd* are 0.82, 0.84 and 1, respectively. The criterion is insensitive to low magnitude values, which would explain the high value for the *SMX* and *SMX-N4* even though they scored low on the other criteria (Bennett et al., 2013). This criterion might therefore not be the best assessment for the pharmaceuticals as these are represented in low concentrations. As these low concentrations are not found in the flow rate, the criterion indicates that the flow rate is predicted accurately. Remarkable, the *CODpart* was assessed with a negative *IoAd*, indicating that the model is not capable of capturing the behaviour shown in the data (Bennett et al., 2013). The highest correlation between data and simulation is found in *SMX*. It indicates that the trend of data was followed well, in spite of scoring low on the relative criteria. Even though the temperature scored well on the relative criteria, the correlation is only 0.16. This would indicate that the residuals might be small, but the trend is not followed well by the model. Nevertheless, the peak evaluation demonstrates a good fit, which could mean that there is another pattern present in the

temperature data which is not captured by the model. The standard deviations for the parameters estimated with the Bootstrap method show an accurate estimation as the percentages are below 5%.

One peculiarity (**Table 6.3, bold**) is the positive or negative value for *ME* for NH_4^+, *CODpart*, *SMX* and *CMZ* while its *MPE* has the opposite sign. The positive *ME* is due to large positive errors at peak values, while overall negative errors are found (negative *MPE*) or the other way around.

6.3.3.2 Qualitative evaluation of the calibration

As the aim of the qualitative evaluation methods is to objectively assess the predictive accuracy of the calibration, the plots in **Figure 6.2** to **Figure 6.6** are not taken into account for the evaluation.

In **Figure 6.7** the sequence of the residuals of the traditional variables is plotted against the data points. This shows for the calibration of NH_4^+ that there is a period between data points 500 and 750 where the model is underestimating the load of NH_4^+ (**Figure 6.7a**). Looking at the dates when this happened, it appeared to be during a holiday on Friday. Therefore, it could be that more tourists came to the area for a long weekend, and thus increasing the NH_4^+ load. During the same time period, there is also an increase in the *CODpart* load, however this increase is much higher than the increase in the NH_4^+, which can therefore not be explained by the same increase in number of tourists. Further, the time period of the increase in the load of NH_4^+ lasts longer than the Monday, which could also indicate that the sensor drifted during this period. Regarding the *CODpart* plot, more periods can be detected where the residuals are high. These periods were not preceded by increases of flow rate and can therefore not be explained by the first flush effect.

The flow rate shows a steady residual sequence with a few outliers concerning wet weather conditions. The values of the normalised residuals are between -30 and 30, while the values for the normalised residuals of the temperature are much higher (-400 to 400). This is due to the low mean value of the residuals, which are used for the normalisation. The plot shows that there is a time period when the temperature is overestimated, however there are also time periods when it is underestimated. This indicates there is a pattern in the temperature that is not captured by the model. Also, the rain fall event in the middle is not completely described by the model.

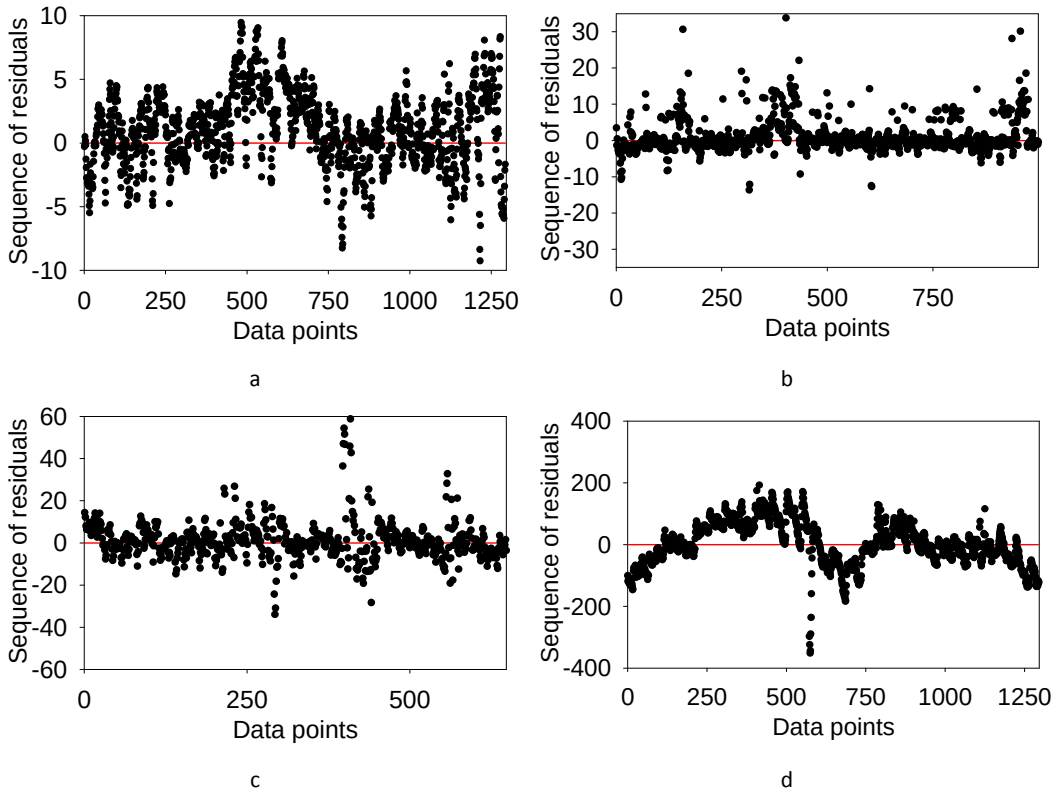

Figure 6.7. The sequence of the normalised residuals for NH_4^+ (a), *CODpart* (b), flow rate (c) and temperature (d).

Figure 6.8 shows the residual sequences of the different pharmaceuticals. For *IBU* it would seem that overall there is an underestimation of the model while there are a few points that are largely overestimated, due to the fact that most of the residuals are positive and a few are negative with a positive *ME*. As its metabolite *IBU-2OH* has a negative *ME*, the plots indicates an overestimation of the concentrations by the model except for a few points. This is also found for *SMX*, however not to the same extent as for its metabolite. *SMX-N4* has not been detected in all samples and therefore the number of data points is smaller than 24. This makes it more difficult to assess if the fit of the model is correct. The underestimation of *SMX* is most likely due to the low concentrations of it compared with the high peaks. The influent generator is not capable of describing these peaks without decreasing the hydraulic retention time. The automatic calibration technique then attempts to minimise the mean squared error, and if the peaks are not captured, the average is increased. The scatter of the residuals for *CMZ* and its metabolite seems to be more random and a systematic over- or underestimation can therefore not be detected.

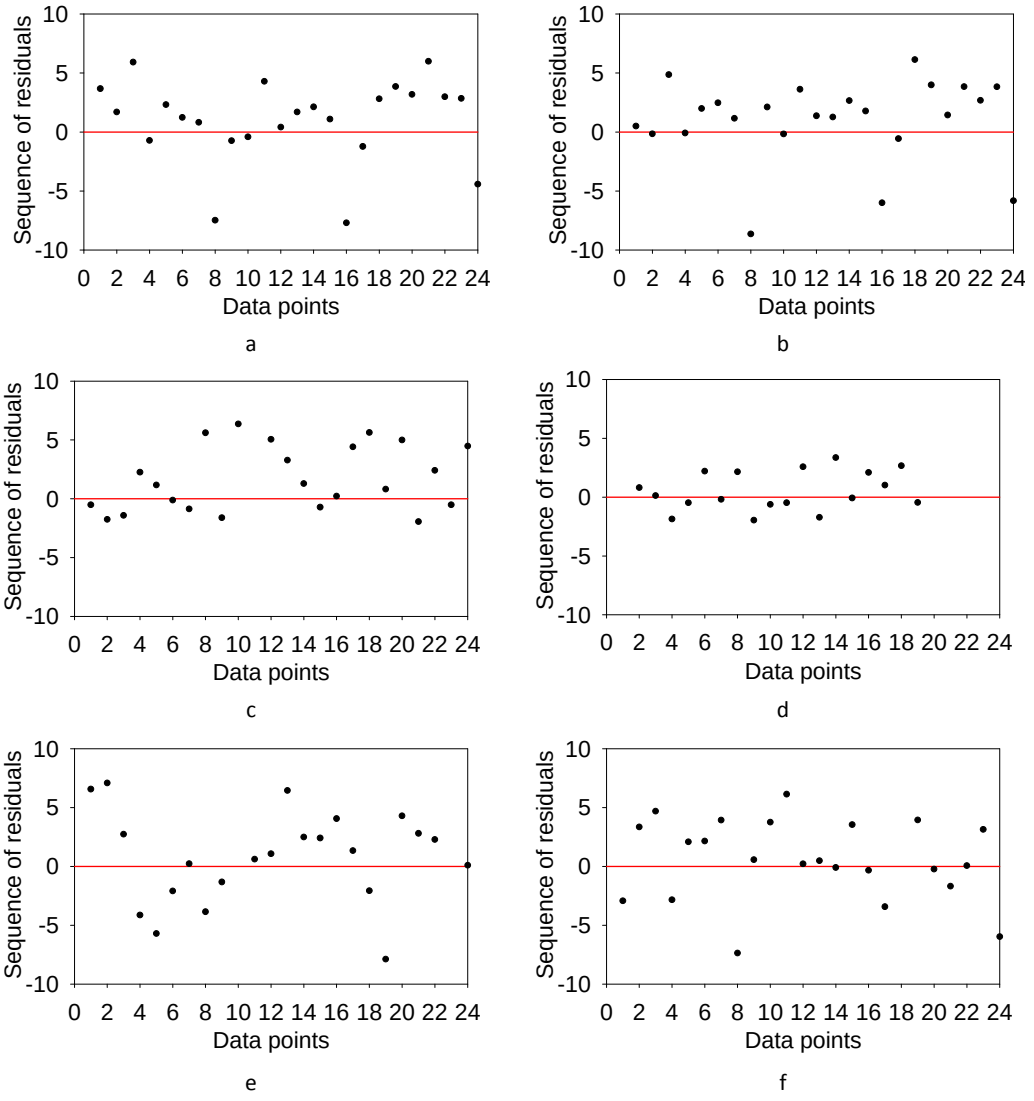

Figure 6.8. The sequence of the normalised residuals for *IBU* (a), *IBU-2OH* (b), *SMX* (c), *SMX-N4* (d), *CMZ* (e) and *CMZ-2OH* (f).

The second method of qualitative evaluation used examines the distribution of the normalised residuals (**Figure 6.9**). The distribution plot of the NH_4^+ demonstrates that the residuals are normally distributed, however they are not centred around 0, more around 1. There are no outliers present and therefore the centre of the distribution could indicate that there is an overestimation of the load of NH_4^+. The *CODpart* distribution of residuals is not normally distributed, it is positively skewed. The centre is around -2, while

the rest of the residuals seem to be positive. This indicates that there are data points that are overestimated as the centre is below 0, while the long tail towards the positive numbers indicates there is also underestimation of the model. Comparing it with the previous plot of the residuals of *CODpart*, it can be assumed that this long tail is due to increases in the load that are not captured by the model. The automatic calibration minimises the mean squared error and to compensate for the positive skewness other points are underestimated, giving a negative centre of the distribution. The distribution of the residuals of the flow rate shows a normal distribution and the centre is around 0. There are a few positive outliers that were also shown in **Figure 6.7a**, which are due to rain events. The same can be concluded for the temperature, where the distribution is also normal and the centre is around 0. Again a few outliers are present which are most likely due to the decrease in the temperature due to the heavy rain event as was shown in the previous plot.

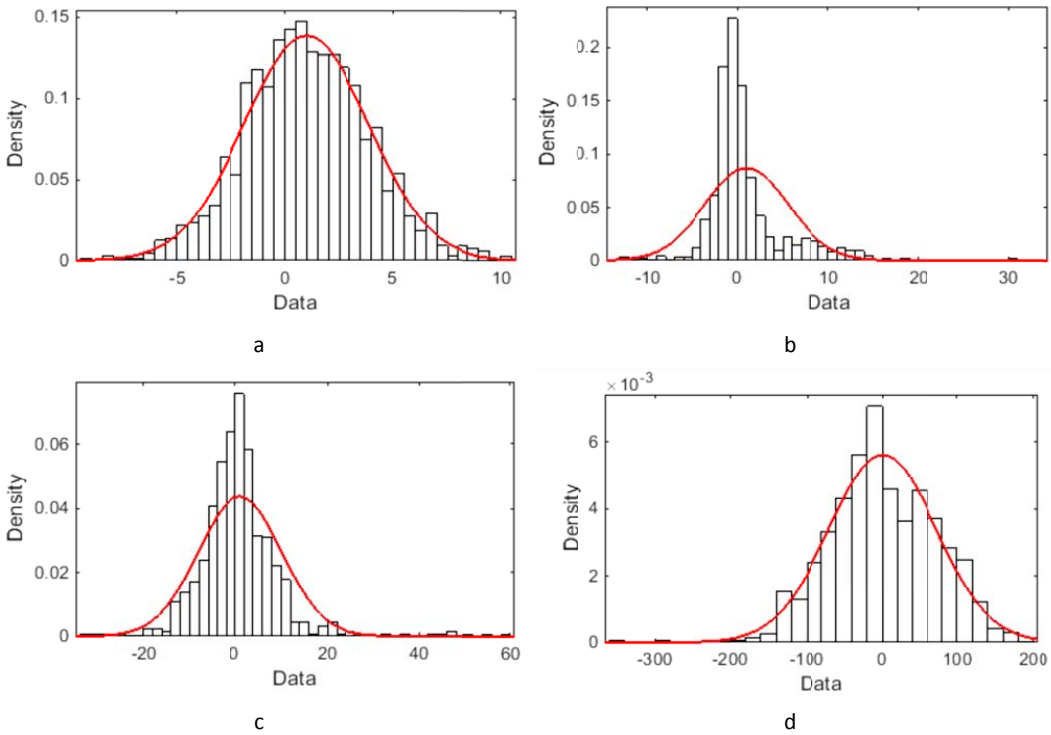

Figure 6.9. The distribution of the normalised residuals of NH_4^+ (a), *CODpart* (b), flow rate (c) and temperature (d) with the expected normal distribution (red line).

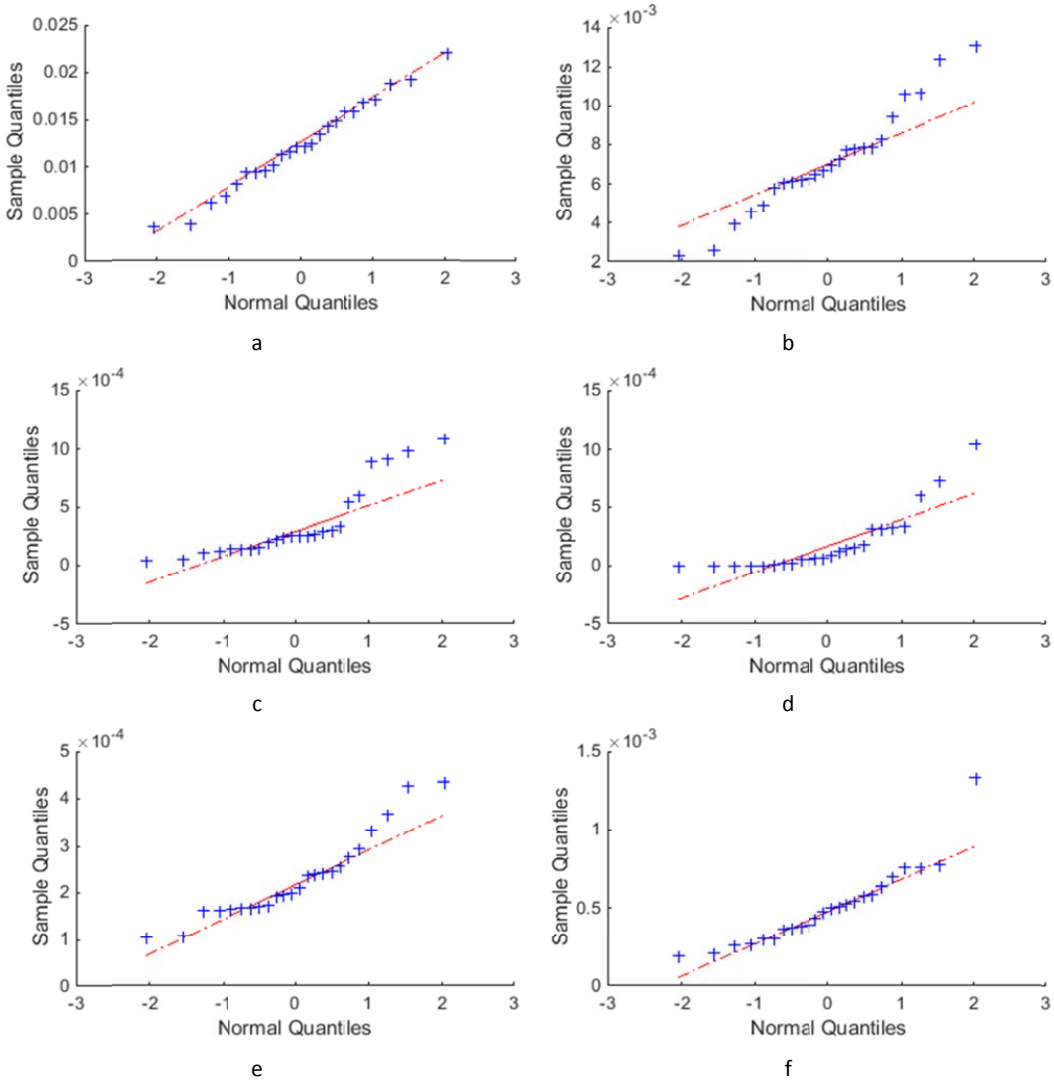

Figure 6.10. The QQ plots of the residuals of *IBU* (a), *IBU-2OH* (b), *SMX* (c), *SMX-N4* (d), *CMZ* (e) and *CMZ-2OH* (f).

The histograms of the pharmaceuticals are difficult to interpret due to the low number of data points (**Figure A3**) and therefore QQ plots are used. The *IBU* and *CMZ-2OH* show a normal distributions with a few outliers (**Figure 6.10a, f**). The profile of *IBU-2OH* starts below the line and finishes above the line, indicating significant tails of the distribution. Thus, the residuals show both large positive and negative errors that are larger than expected from a normal distribution. Lastly, *SMX*, *SMX-N4* and *CMZ* show the same pattern of a positive skewed distribution, indicating that there are more positive residuals and/or residuals with higher

positive values than for a normal distribution. When comparing this with the previous residuals plot, it can be seen that there is an underestimation of the time series by the model during the day and night minima.

6.3.3.3 Discussion of the quantitative and qualitative evaluation

Combining the results from the quantitative evaluation methods with the results from the qualitative evaluations helps to identify points of concern for the calibration. The NH_4^+ load prediction could be improved by addressing the period between data points 500 and 750 (Oct 12 – 17) where the increase of the data is not captured by the model. However, as it is not clear if this observed increase in the data is due to an increase in the *PE* or a result of a sensor drift, no measures to increase the fit of the model can be taken. Nevertheless, it can be concluded that the calibration of the NH_4^+ load succeeded as the quantitative criteria show a good fit (e.g. a correlation of 0.7). The *CODpart* also shows some underestimation of the model like the NH_4^+, however this leads to worse quantitative criteria values with even a negative *IoAd*. In this case, the dry weather data is not correctly described due to increases in the data that are not explainable by increases in the flow rate which was indicated by the *MSDE* and the plot of the residuals over the time span. The data seems to describe a pattern that is not explainable and therefore cannot be modelled. The flow rate demonstrates a good fit for both evaluation methods and thus it can be concluded that the model predicts the flow rate accurately. The temperature scores well on the absolute and relative criteria, however less good on the peak evaluation and the correlation. The residual plots also indicate that there is a pattern in the data that is not captured by the model. The increase in temperature at the beginning of the measuring campaign and the decrease at the end are not well explained. It could be that there is additional rain causing this decrease at the beginning of the time series. Nevertheless, the available data was showing a dry period before the measuring campaign.

The pharmaceuticals only have 24 or less data points to compare with the simulation and therefore the analysis should be done with care. There might be behaviour present between the data points that is not detected and that can therefore not be modelled. Regarding the parent compounds, both of the methods demonstrated an adequate fit. However, this was less convincing for *SMX*, which could be due to the sharp peaks present in the data while obtaining a low concentration. The hydraulic retention time of the sewer was decreased in order to achieve a higher peak, but proved to be inadequate. It can be seen that the average of the residuals is minimised at the cost of not capturing the peaks of the occurrences. In order to enhance the performance of the model, the description of the occurrence pattern could be improved. This can be done by adjusting the predefined daily profiles that describe the occurrence of the pollutant load. These were taken from the correlated 'traditional' pollutant and not adjusted during the calibration.

Another way could be to define the objective function during the automatic calibration as a peak performance criterion instead of the squared errors of all residuals.

An inaccurate fit of the model can indicate a model structure deficiency, a lack of good data or a combination of both. In the case of *CODpart*, the data quality is questionable as there is behaviour present that is unusual. The sensor was placed after a pumping station which could have caused a resuspension of solids. Moving the sensor before the pumping station was not possible, and therefore, placing it further away from the pumping station could be an option to find out if the pumping station was the cause of the unusual behaviour. Regarding the temperature calibration, there is behaviour present in the data that could not be explained by the model. In order to compensate for this behaviour the model can be adjusted to include an additional sine function which describes the increase in the beginning of the time series as well as the decrease at the end. However, there would be no physical explanation for the additional sine function. Just by increasing the number of parameters and making the model capable of describing any behaviour, the model could easily become an over-parameterised system (Brun et al., 2001). As there is no physical meaning for all parameters, this is not advisable. Additionally, the complexity of the model would increase making it less attractive to work with. Therefore, a trade-off should be made between the predictive accuracy and the complexity of the model.

6.4 Scenario analysis

The scenario analysis presented in this Section demonstrates some of the benefits of using the modified BSM2 influent generator when performing WWTP (micro) pollutant modelling studies. Therefore, for exemplary purposes, the calibrated model is used to study how the results are affected by changes in some settings in the two different scenarios investigated here. In *scenario 1* it is shown how the workload related to the measuring campaign can be reduced by synthetically generating additional high frequency data. In *scenario 2* the effect of including biotransformation when estimating *SMX* and its metabolite loadings at the influent of a WWTP is demonstrated.

6.4.1 Generation long-term (micropollutant) time series

Data frequency is critical in any dynamic modelling exercise (Rieger et al., 2012). This first scenario will demonstrate how the modified BSM2 influent generator can increase the length of the *IBU* time series on the basis of the available data. These extrapolated time series could replace expensive measuring campaigns based on: 1) the model predictions; and, 2) well-educated guesses obtained during the study. The extrapolation is achieved by combining calibrated outputs from the FLOW RATE model block (Section 3.1.1) and *IBU* (3.2.1). The generation of these extended time series for *IBU* (normalised) profiles is based

on assuming: 1) a weekly household flow pattern including the weekend effect; and, 2) a yearly pattern including the holiday effect. The weekly pattern supposes an additional 10-25% load on Friday, Saturday and Sunday, because the area is a touristic area. Finally, the holiday period (seasonal variation) leads to a higher consumption during winter time due to an increase in the number of tourists (25%) in that period of the year. In addition, it is also assumed that more people get sick during winter and this also increases the consumption of *IBU*. Moreover, also the influent flow rate time series have to be extended to calculate *IBU* concentrations (FLOW RATE model block). The latter involves the generation of a seasonal infiltration profile and yearly rainfall data based on four seasons (winter, spring, summer, autumn). Further information about the model blocks and how to create these profiles can be found in Gernaey et al. (2011). **Figure 6.11** depicts the extended dynamic *IBU* profile generated with the influent model. The assumed (increased) weekly variation and the effect on the total *IBU* concentration profile are shown in **Figure 6.11a**. There is also a higher concentration visible during the winter (beginning and end of the time series). During the generation of a yearly profile, the rainfall has an effect (dilution) on the *IBU* concentration especially during spring, when more rain is expected in the catchment compared to other seasons (**Figure 6.11b**).

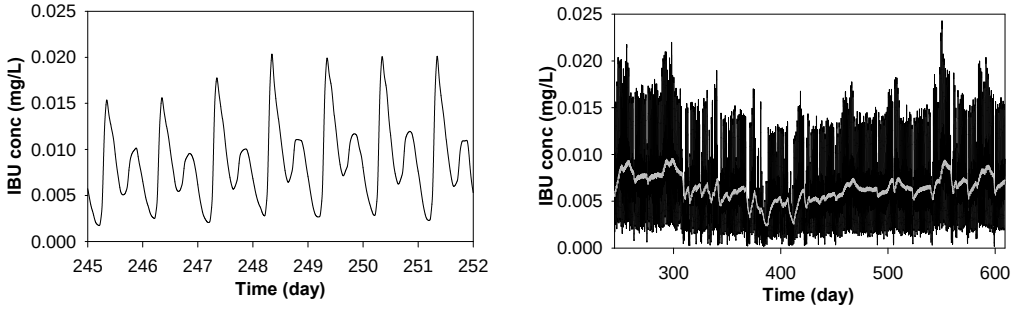

Figure 6.11. Simulations of influent *IBU* dynamics extended to a week (left) and a year (right) with a smoothed yearly profile of the *IBU* (grey).

6.4.2 Reactive sewer modelling

Previous simulation results showed that the size of the sewer system can be incorporated in the influent dynamics by increasing or decreasing the parameter s*ubarea* and consequently the HRT: The basic assumption behind this is that the larger the sewer system, the smoother the simulated diurnal flow rate and concentration variations should be. In addition, different reports have demonstrated the importance of considering biotransformation processes within the sewer systems (Hvitved-Jacobsen et al., 1998; Ashley et al., 2005). This has been shown for traditional pollutants (Sharma et al., 2008) but also for micropollutants (Jelic et al., 2015). The effect of such in-sewer reactions should especially be taken into account in the field

of sewage epidemiology where estimations of illicit drug consumptions are made (Zuccato et al., 2005; van Nuijs et al., 2012; Plósz et al., 2013a). To demonstrate the impact of sorption, desorption, biotransformation and biodegradation processes on the estimated average daily load, the sewer model is upgraded with the Activated Sludge Model for Xenobiotic trace chemical framework (ASM-X) (Plósz et al., 2010b, 2012). Further details about the ASM-X implementation in the sewer system are described in Chapter 4. The estimation of the loads is performed with the least squares approach mentioned in Section 6.2.6. The estimated loads without assuming any reactions are taken from the results in Section 6.3.2.2.

Table 6.4. Estimation results of *SMX* and *SMX-N4* loads with and without including in-sewer transformations.

	Estimated load without reactions (g/d.1000PE)	Estimated loads with reactions (g/d.1000PE)	Difference in estimation (%)	Estimated consumption no reactions (g/d)	Estimated consumption with reactions (g/d)
SMX	0.1227	0.1091	-11	14.02	12.47
SMX-N4	0.08	0.1281	+60		

Table 6.4 summarises the estimated loads for *SMX* and *SMX-N4* when reactions in the sewer are assumed. The estimated consumptions are calculated assuming an excretion ratio of 14% of *SMX* (Vree et al., 1995). Simulation results show that there are substantial differences in both *SMX* and *SMX-N4* (calculated) loads. Specifically, a lower load of *SMX* and a higher load of *SMX-N4* should be assumed at the beginning of the TRANSPORT model block in order to take into account re-transformation of *SMX-N4* (metabolite) to *SMX* (parent compound). The ratio of *SMX:SMX-N4* obtained with the in-sewer reactions activated (1:1.2) is closer to the excretion ratio of 1:3 (Vree et al., 1995) than the ratio without reactions (1:0.69). This indicates that it is likely that *SMX-N4* is retransformed into *SMX* in this study. The re-transformation of this metabolite to sulfamethoxazole was observed both during wastewater treatment (Göbel et al., 2005) and sewer transportation (Jelic et al., 2015). Even though some assumptions were made during this exercise (see Section 5.6), the aim has been to make the reader aware that accounting for reactions within the sewer system can have an important effect on the estimation of consumption rates (van Nuijs et al., 2012). The common approach used in wastewater engineering is to back-calculate the daily consumption of a micropollutant normalised per 1000 inhabitants in a given catchment from the measurements taken at the inlet of the WWTP. Depending on the analysed data, several corrections can be included to consider weekly or seasonal variations. The set of models presented here can be helpful in improving those estimates by accounting for some of the drainage phenomena occurring at the catchment level and the activation of reactions.

6.5 Discussion

This study has demonstrated that generation of synthetic influent data with the modified BSM2 influent generator is a promising tool to improve model-based (micro)pollutant simulation studies in WWTPs since they can: 1) significantly reduce the cost and workload of measuring campaigns; 2) fill gaps due to missing data in influent flow rate/pollution/temperature profiles; and, 3) create additional disturbance scenarios following the same catchment principles as the calibrated phenomenological influent model. Even though the set of advantages derived from using these tools is extensive, the use of these tools also opens the door to several discussion points, which are analysed below.

6.5.1 Sampling method

In this study, grab samples were taken at different time intervals to analyse the diurnal variation of the pharmaceuticals. There has been discussion on the best way of sampling for micropollutants. Ort et al. (2010) developed guidelines on the appropriate way of sampling. Depending on the objective of the study, different sampling frequencies can be used and even though grab samples can be accurate in some cases, composite samples should be preferred. Grab samples can miss increases or decreases in concentrations, which composite samples would capture. However, one should be aware of the fact that degradation of micropollutants can also occur in composite samples (Baker and Kasprzyk-Hordern, 2011). In this study, it was decided to use grab samples, partly to avoid degradation, and partly due to its simplicity compared to the use of flow-proportional sampling techniques in sewer systems.

6.5.2 Description of compounds with irregular pattern

It is important to highlight that the load dynamics of almost all pharmaceuticals presented in this case study display a high correlation with the NH_4^+ dynamics, which clearly shows the impact of human urine. However, there are other types of pharmaceuticals with different medical uses, consumption rates and excretion pathways that would be difficult to characterise with the presented set of (phenomenological) models. Likewise, micropollutants other than pharmaceuticals, could have a more random occurrence at the inlet of a WWTP and could therefore also not be described by the same phenomenological approach.

In order to cope with this type of compounds with random occurrence, a prototype module in the BSM2 influent generator based on Markov Chains has been implemented (Chapter 4.2.1). In the simplest form, the occurrence of a compound *X* is modelled by two states. The two states represent the presence or absence of the micropollutant and the transition probability matrix describes the probability of switching between these states. In the transition matrix information can be introduced about the frequency, intensity and duration of the events by defining: 1) the set of probabilities; and, 2) the number of states. The profile

obtained by the Markov Chain approach can also be combined with a more deterministic weekly and seasonal variation by multiplication. The resulting output is the pollutant flux. Further research in the practical use of the Markov chain based approach is on-going, but not presented in this study since the available data did not contain a pharmaceutical with random occurrence. A correlation with either NH_4^+ or *CODpart* was found for the pharmaceuticals considered in this study. In order to calibrate a Markov Chain, enough data has to be available to distinguish between the different states and to calculate the transition probabilities between these states (Madsen et al., 1985).

6.5.3 Calibration procedure

The Bootstrap method is used for the automatic calibration of the traditional variables. This method is based on the generation of additional sets of data which are subsets of the original data set, and subsequently generate estimations of additional sets of parameters based on the created data. As a result of these additional sets, no prior information on the parameter is needed and the result is an estimate of the parameter with confidence intervals (Efron, 1979; Joshi et al., 2006). A drawback of the Bootstrap method is that it needs many measured data points, which were not available for the pharmaceuticals. Also, the method is computationally intensive as the optimisation is repeated for the number of additional parameter sets that are estimated (Bootstrap samples). In order to decrease the computational effort, parameters that could be estimated manually were excluded from the procedure. As has been shown by Flores-Alsina et al. (2014a) the influent generator uses many non-identifiable parameters, which would increase the computational burden of an automatic calibration. Another possibility for the automatic calibration could be the Bayesian technique. Bayesian approaches are better choices for model predictions when there are poorly identifiable model parameters (Omlin and Reichert, 1999). However, the justification of the available knowledge that would be required to obtain the *a priori* distribution of the model parameters when using a Bayesian approach can be considered an entire study on its own (Lindblom et al., 2011; Rieckermann et al., 2011). In addition, the computational burden required in order to obtain "reasonable" results exponentially increases the required calibration time and effort.

The objective function used in the optimisation is focused on the minimization of the error between the data and the simulation results. However, this optimisation might overlook the magnitude or locations of the peaks. This was revealed when trying to use the automatic method for the *CODpart* calibration as the increases in *CODpart* after a rain event were not captured. In order to overcome this drawback, the objective function could be changed to focus on the timing or magnitude of the peaks.

6.5.4 Structural model deficiencies

The simulation results of the different variables (traditional and micropollutants) obtained by using the influent generator showed some deviations from the data. An important factor which could explain some of these deviations is structural model uncertainty, or in other words, that the current model is not describing all of the fundamental phenomena. For example, there are existing models that are more accurate in accounting for pollution run-off (Bertrand-Krajewski et al., 1993; Ashley et al., 2002), combined sewer overflows (Ashley et al., 2004), storm tanks (Schütze et al., 2002) and back-flow effects (Vanrolleghem et al., 2008) in the sewer system. Depending on the micropollutants of concern, e.g., pesticides, some of these phenomena could have a significant effect and should thus be considered as well when creating a model aiming at generating realistic influent concentration dynamics of such compounds (Loos et al., 2013).

Another simplification made in this work is in *scenario 2* (Section 6.4.2). For this reason, the analysis of those results must be done with care. For example, the sewer system model is a rather simplified representation, and some of the processes occurring (e.g. biofilm formation) are not accounted for. To consider the effect of the biofilm on pharmaceuticals without having a proper biofilm model, the fraction of (heterotrophic) biomass (X_{OHO}) in the total COD was increased. However, mass transfer limitations are not taken into account either. Additionally, the parameters estimated for an activated sludge unit are used for reactions in the sewer. For this reason, there might be errors in the estimation of the conversion rates taking place during the transport. Nevertheless, the increased calibration effort to adjust the additional parameter(s) would come with the drawback of making this tool less attractive for process engineers and water/wastewater designers (Flores-Alsina et al., 2014b).

6.5.5 Development of control strategies in WWTP

The generation of multiple influent profiles can be used to develop (model-based) control strategies in the WWTPs. It is important to highlight that WWTPs are still one of the major disposal path for micropollutants and they have not been designed to deal with those (Ternes et al., 2004b). Nevertheless, there are different investigations that demonstrate that a change in operational conditions such as sludge retention time (Clara et al., 2005) can effectively improve the elimination of trace chemicals from the liquid phase by sorption, transformation or biodegradation. Co-metabolic/inhibitory behaviour with other substances present in the influent might have an overall effect on their fate within the WWTP. The results of the investigations carried out in Chapter 4.3.3 demonstrate that different operating conditions can have opposite effects on the studied compounds, especially when they present co-metabolic or inhibitory behaviour with other substances present in the influent wastewater. The same has been shown for

compounds with higher biodegradability at high sludge retention times compared to compounds with high sorption capacity. As the sludge turnover is lower, less compounds can sorb onto the sludge (Petrie et al., 2014).

6.5.6 Use in sewer epidemiology

The set of models presented here may be potentially used in sewer epidemiology. In the same way as demonstrated here for the model-based description of the influent dynamics of one anti-inflammatory compound, one antibiotic and one psychoactive drug, the modified version of the BSM2 influent generator could be used to model illicit drugs. In addition, the proposed approach could help to back-calculate consumption rates taking into account a list of possible uncertainties (sampling, analytical method, stability of biomarkers, estimation of the number of *PE* (Castiglioni et al., 2013)). As demonstrated in Section 6.4.2, also reactions in the sewer can be taken into account. As the ratio between the parent compound and the metabolite was closer to the theoretical excretion ratio when reactions were activated, it is probable quite likely that (some of) these reactions are indeed occurring. Considering the back-calculation of the consumption of illicit drugs and specifically cocaine as a well-known example which has shown to be unstable in wastewater, these in-sewer transformations should be taken into account (van Nuijs et al., 2011).

6.6 Conclusions

The key points of the presented study can be summarised as follows:

- It can be concluded that the influent generator is capable of predicting the time series for flow rate and NH_4^+ as well as the parent compounds of *IBU* and *CMZ*.
- The calibration of *CODpart* is not precise due to increases in the *CODpart* during dry weather, which are not captured by the model. An explanation for this could be the data quality of the *CODpart* data used in this study.
- Additionally the calibration of the wastewater temperature is not precise enough as there is a pattern present which is not described by the influent generator. This could be due to missing rainfall data or a model structure deficiency or a combination of both.
- The prediction of *SMX* and *SMX-N4* is less successful because the sharp peaks found in the data cannot be described sufficiently well with the model. This is due to a model deficiency as the model is not capable of describing the measured increases with the same magnitude. An improvement could possibly be achieved by taking the predefined daily profile also into account during the calibration instead of copying it from the highest correlated 'traditional' variable, as was done in the study presented here.
- The other two metabolites, *IBU-2OH* and *CMZ-2OH* score lower on both types of evaluation methods than the parent compounds. Also here calibrating the predefined daily profile could help improving the prediction capabilities.
- The potential use of the tool when: 1) interpolating incomplete data series; and, 2) extrapolating additional dynamics following the same catchment principles are demonstrated using the ibuprofen case as an example.
- The effects of in-sewer biotransformations and their potential impact when estimating consumption rates were pointed out using the sulfamethoxazole case. The ratios between the parent compound and the metabolite were closer to the theoretical excretion rates when biochemical reactions were activated within the sewer network
- The presented set of models has potential use for engineers, managers and regulators to be used as a decision support tool in integrated (urban) water systems.

Part IV

Discussion and future perspectives

The aim of this PhD study was to "*Extend mathematical models of WWTPs with processes describing GHG emissions and the removal of micropollutants.*" The extensions to the BSM framework have been demonstrated in this thesis. However, some discussion points have arisen which will be addressed in Chapter 7. In addition, future perspectives will be mentioned in Chapter 8.

7. Discussion of PhD study

The discussion of the work performed in this PhD study is divided in a general Section concerning the mathematical modelling followed by a specific discussion on the N_2O part and finishing with a more detailed discussion on the work related to pharmaceuticals. The challenges mentioned in the introduction that have not been addressed in the previous Chapters will be discussed in this Chapter.

7.1 General discussion

7.1.1 Modelling – BSM framework

In order to keep the extended models as simple as possible, the BSM1 has been used as a base case model in this thesis in Chapters 3 and 4. The mathematical models available in the literature that describe the emissions of N_2O are focused on the activated sludge units, as denitrification and nitrification occur here, and these processes are responsible for the emissions. Using the BSM2, which includes a sludge line with a primary settler and anaerobic digester (Vrecko et al., 2006), would be beneficial when taking all GHGs into account, i.e. not just focussing only on the N_2O emissions (Flores-Alsina et al., 2011).

The same applies to the modelling of the fate of pharmaceuticals in a WWTP. The ASM-X framework predicts the processes of pharmaceuticals in the activated sludge units only. Therefore there is no benefit in using the BSM2. However, in the primary settler, secondary settler and anaerobic digester removal of MPs can also take place (Barret et al., 2010; Delgadillo-Mirquez et al., 2011). Yet, less research has been performed on the modelling of the removal mechanisms of pharmaceuticals in these different treatment units. Copying the processes from the ASM-X with the corresponding parameters would not provide realistic results for such units as the microbial communities and redox conditions are not the same as in the activated sludge units. For example, the particles in a primary settler vary from the particles in the activated sludge units as there is less biomass present, which would lead to different sorption rates.

If the extended models of Chapter 3 and 4 will be used for the BSM2, the number of state variables in the other models should be increased to match the number of state variables in the extended models. This would also require the adjustment of the interfaces of the BSM2 (Rosen et al., 2006). Using the BSM2 for the extended models would then only increase the computational burden without providing additional information on the N_2O emissions or the fate of pharmaceuticals. However, the demonstration of the capabilities of the BSM1 with the extension of pharmaceuticals shows the potential of the tools as different control strategies could be tested.

7.1.2 Data availability

Due to issues with data availability, N_2O measurements from a full-scale SBR system have been used instead of N_2O measurements of an activated sludge unit. An SBR system is operated under different conditions than an continuous-flow activated sludge system and therefore the N_2O emissions can vary (Kampschreur et al., 2009) as well as the biomass (Lu et al., 2014). Extrapolating the results and conclusions of the calibrated SBR model with its set of parameters to an activated sludge unit can be speculative. One might be able to correct for the temperature differences by including temperature dependencies on the growth and decay rates of the biomass; however, inhibition parameters might also be influenced. As the temperature of the SBR is stable, fluctuations of N_2O emissions during different seasons are not expected (Daelman et al., 2013). However, the different loads to the WWTP during the week might have an effect on the emissions in the SBR and therefore evaluating more cycles than those during two weekdays would have been interesting. However, the aim of the SBR model study was to test the capability of a physicochemical model in combination with the N_2O model and therefore the data was considered sufficient for this purpose. Nevertheless, the pH calibration showed that more information on the alkalinity and ions present in the system is needed than solely grab samples. In order to improve the pH calibration on-line alkalinity measurements and information on the composition of the wastewater is crucial.

The pharmaceuticals' model has only been tested for one catchment, in Puigcerdà (Spain), and this only concerned the influent generator, not the ASM-X. The ASM-X was not calibrated as this was done during the development of the model with full-scale data (Plósz et al., 2010b, 2012), which was one of the reasons for selecting the modelling framework for the extension of the BSM. Nevertheless, calibrating the influent generator also for another catchment in order to validate the extended model would have been preferable. Unfortunately, there was a general lack of measurements in the influent at a frequency higher than three times a day. Additionally, information on the catchment and 'traditional' variables should be provided as well, which was information that was not always available or accessible.

7.2 Extension of N_2O

7.2.1 Focus on N_2O

According to the study of IPCC in 2013 (IPCC, 2013), the anthropogenic N_2O emissions are due to application of nitrogenous fertilisers in agriculture, fossil fuel use and industrial processes, biomass burning and land emissions due to atmospheric nitrogen deposition. Wastewater treatment processes are not mentioned as a source of N_2O emissions in the report of 2013. However, it was mentioned in the IPCC report of 2006 that an N_2O emission factor could be used to calculate the N_2O emissions from a WWTP as 0.5% of the nitrogen content of the influent of a WWTP (IPCC, 2006). Nevertheless, due to variations of

measurements at different WWTPs (Daelman et al., 2013), the factor set by IPCC will give an unrealistic estimate of the real emissions. Even though the amount of N_2O emitted by WWTPs might be small compared to agricultural activities, it does not mean that nothing should be done about it. When regarding only the carbon footprint of a WWTP, the N_2O emissions can make up 80% of the total GHG emissions (Desloover et al., 2012a). In addition, changing operational strategies can have an impact on the emissions (Flores-Alsina et al., 2011).

7.2.2 Modelling of N_2O

For now only the possibility one pathway of AOB, namely AOB denitrification. However, it could be possible that there are several pathways active at the same time or that the use of different pathways switches depending on the specific environmental conditions (Ni et al., 2013; Wunderlin et al., 2013). The N_2O risk model of Porro et al. (2014) indicated that there was a high to medium risk of AOB denitrification at the start of the nitrification phase, which switched to no risk while a medium and high risk for hydroxylamine oxidation was obtained. Therefore, testing both pathways during nitrification would be interesting.

In addition, no inorganic carbon limiting conditions are included in the nitrification processes even though these effects have been demonstrated (Wett and Rauch, 2003; Guisasola et al., 2007; Torà et al., 2010). However, only Wett and Rauch (2003) tested their developed model in full-scale but no N_2O production processes were included. Therefore, no parameters of inorganic carbon limitations are available for the different N_2O production rates.

7.3 Pharmaceuticals

7.3.1 Focus on pharmaceuticals

The focus of the thesis has been on pharmaceuticals in order to diminish the broad spectrum that MPs represent. The choice of pharmaceuticals has been made due to the fact that the selected compounds are commonly used in the Western world and have been extensively studied recently. There have also been reported effects of these pharmaceuticals in the aquatic environment as was mentioned in the introduction. Nevertheless, Taylor and Senac (2014) mention a misplaced focus on pharmaceuticals in recent studies. According to them, pharmaceuticals should not be categorised into one group as they display different features, such as different removal rates and different toxicity effects. In addition, the majority of the pharmaceuticals do not affect the environment to the same extent as has been shown for ethinylestradiol. Therefore, the ecotoxicity of pharmaceuticals should be assessed case by case. In order to assist these case by case studies, models can be used to identify the potential effluent peaks of pharmaceuticals instead of solely performing expensive measuring campaigns.

The EU WFD (2008/105/EC) has composed a list of 33 priority substances and more are likely to follow in the future. There has been a proposal (COM(2011)876) for a second list of priority substances and a watch-list including compounds of possible concern. Among these compounds are many pesticides/herbicides/insecticides, heavy metals and PAHs. However, for these compounds the municipal WWTP is not one of the major disposal pathways as the main sources are agriculture and industry and therefore they were not selected to be studied in this thesis.

By focusing on pharmaceuticals, the number of phenomena that needed to be modelled could be decreased. This is especially visible with the influent generator. By selecting pharmaceuticals, the source of the pollutant was assumed to be only coming from households and the occurrence of the pharmaceuticals could be linked to 'traditional' pollutants such as NH_4^+ (Göbel et al., 2005). In addition, the same processes could be used and the volatilisation of pharmaceuticals could be neglected (Ternes and Joss, 2006). These simplifications were only possible by focusing on pharmaceuticals. As the long term effects of mixtures of pharmaceuticals on the aquatic environment have not been extensively studied yet, the study of pharmaceuticals could still prove to be important in the future.

7.3.2 Modelling of pharmaceuticals

The sorption of pharmaceuticals in ASM-X is modelled by a two-compartment system, an aqueous and a solid compartment. However, including more compartments could be a method to increase the effect of the composition of the sludge on the sorption process. Including the colloidal organic matter fraction as a third compartment has been demonstrated to increase the predictability of sorption of micropollutants (Warren et al., 2003). However, this impact has not been demonstrated for pharmaceuticals and therefore was not taken into account. The inclusion of a third compartment might have a larger impact when moving towards full-scale modelling as the sludge in a primary settler differs from the sludge in a secondary settler with different concentrations of colloidal organic matter (Ternes and Joss, 2006).

In addition to different particles in the sludge, also the biodiversity of the sludge will differ from one WWTP to another (Lu et al., 2014). The differences in biodiversity could lead to different removal rates of micropollutants (Johnson et al., 2015). This suggests that it would be difficult to benchmark the removal of micropollutants indicating that measurements at a WWTP are needed to assess the specific parameters of the processes. For diclofenac and carbamazepine, however, a simple re-calibration approach using ASM-X has been shown to effectively account for MP biotransformation under two distinctive operating SRT conditions, i.e. 6≤SRT≤16 days and SRT≥16 days (Plósz et al., 2012) in full-scale conventional activated sludge and membrane bioreactor systems. To assess the effect of biomass characteristics on the removal rates of MPs, more research is needed.

8. Future perspectives

In this Chapter different recommendations based on the findings in this study or on the developments in the field are given. Firstly, the N_2O and greenhouse gases will be discussed after which the pharmaceuticals and micropollutants will be addressed.

8.1 N_2O

8.1.1 Different N_2O models

The N_2O models have been tested for an SBR system, which indicates that the results are not directly applicable to the activated sludge units. Therefore, the same models should be tested for the activated sludge units in order to validate whether the same conclusions apply. The models can then be used to minimise the N_2O emissions as well as other GHG emissions. However, besides testing different AOB models, also the electron based denitrification model should be tested. Carbon limiting conditions during denitrification can occur and if these have an effect, the calibrated nitrification models might not be producing realistic results.

The data on N_2O in this thesis has only been tested with one AOB denitrification model. In order to gain more insight into the different N_2O pathways responsible for N_2O formation, the other models should also be tested in combination with the physicochemical model. As mentioned in Section 7.3, not only one pathway but also a combination of pathways should be explored.

8.1.2 Inorganic carbon concentration

The correlation between the N_2O production rate and the inorganic carbon concentration has now been made with the modelled inorganic carbon concentration. It would be preferable if data on the inorganic carbon concentration could be correlated with the N_2O production rate as it would exclude an extra uncertainty. In addition, the calibration of the physicochemical model could be improved by using on-line data on the alkalinity and including information on the ions present in the wastewater.

It would also be interesting to investigate the effect of pH and inorganic carbon on the N_2O production under different conditions. Peng et al. (2015) only studied the effect of inorganic carbon at high oxygen concentrations, therefore encouraging the pathway of hydroxylamine oxidation and not the AOB denitrification.

In addition, the IC concentration is demonstrated to be of influence on the nitrification rate (Wett and Rauch, 2003; Guisasola et al., 2007; Torà et al., 2010; Ma et al., 2015; Peng et al., 2015), however this is not

included in the process models of N_2O production. This inclusion might help improving the prediction capacities of N_2O production models by AOB.

8.1.3 Other GHGs

Besides the greenhouse gas N_2O, also CH_4 is emitted during the wastewater treatment (Czepiel et al., 1993; Wang et al., 2011; Daelman et al., 2012). In the BSM framework, CH_4 is only included in the anaerobic digester where it is used for describing biogas formation. Different leakages of CH_4 are included as well as CH_4 from the influent, and these effects are included as percentages based on the information accessible in the literature. In order to optimise the WWTP regarding the GHG emissions, dynamic models of CH_4 should be included in the activated sludge units. When considering the urban wastewater cycle, the formation of CH_4 in the sewer should be taken into account as well as the fate of CH_4 in the receiving waters.

8.1.4 Urban wastewater cycle modelling

The N_2O emissions are now focused on the processes occurring in the activated sludge units, however dissolved N_2O could also be stripped in other units in the WWTP, such as the secondary settlers (Mikola et al., 2014). In order to move towards a plant-wide model, these emissions should also be taken into account. The same applies to the effluent of the WWTP, as N_2O emissions in receiving waters have been measured. These emissions can be due to the dissolved N_2O or due to denitrification processes in the rivers (Beaulieu et al., 2011) and should be included when modelling the urban wastewater system.

8.1.5 Recovery of nitrogen

Instead of focusing on the removal of nitrogen and minimising the N_2O emissions, also techniques to recover nutrients and therefore nitrogen could be used. This has been demonstrated by Desloover et al. (2012b) by using electrolysis cells. As the focus of wastewater treatment is moving towards a resource recovery system, this is an interesting option to combine with the reduction of N_2O emissions (Verstraete et al., 2009).

8.2 Pharmaceuticals

8.2.1 Pollutants

In this study, the priority pollutants mentioned in the Water Framework Directive have not been included in the models. As the WFD marks them as a priority it would be wise to focus on those substances as well. This would indicate that the process parameters should be replaced by the ones describing these substances. The fate of heavy metals has been extensively studied and mainly sorption is responsible for their removal (Parker et al., 1994; Wang et al., 1999; Karvelas et al., 2003). As this process is included in the

ASM-X, the inclusion of heavy metals requires parameter values related to the sorption process. In addition, the heavy metals can occur in different forms and are capable of precipitating, and therefore these processes might need to be included in a model to be able to realistically predict the fate of heavy metals in a WWTP (Parker et al., 1994). As pH is also of importance to the precipitation of heavy metals, including the physicochemical model would be an option to improve the prediction (Wang et al., 1999). Possibly, also volatilisation should be added as a removal process to the ASM-X when musks are considered (Upadhyay et al., 2011). Additionally, the influent generator should be upgraded to predict the occurrence of chemicals from run-offs or industry (Payraudeau and Gregoire, 2012). Other studies have also included the combined sewer overflows as a source of micropollutants (Vezzaro et al., 2014). Considering that the control of a WWTP is extending to include the sewer system (Saagi et al., 2014), this might be an interesting option to pursue.

8.2.2 Plant-wide modelling

In order to model the fate of pharmaceuticals at the plant-wide level and in a BSM2 context, the processes in other units should be included and calibrated. To start this effort, different sorption models in the primary and secondary settler should be included as well as a fate model in the anaerobic digester. The plant-wide model can use the different units to optimise removal rates. For example, the removal of sorbed MPs in the two settlers in combination with a higher SRT in the activated sludge units for removal of biodegradable MPs could be tested. However, it is not likely that different operational/control strategies will be capable of removing all MPs completely from the wastewater. The work in this thesis demonstrates that operational strategies can have an opposite effect on pharmaceuticals as well as that more recalcitrant MPs will remain present. Therefore, it is important to focus on tertiary treatment of the wastewater.

8.2.3 Tertiary treatment

Modelling different tertiary treatment units will allow comparison of the removal efficiencies of MPs. Such a comparison can help the decision making about upgrading a WWTP. A model of a tertiary treatment unit can also be used to optimise the removal of MPs. Including a dynamic model of a tertiary treatment unit to the BSM would still require dynamic occurrence of the MPs as higher concentrations of MPs can lead to higher removal rates (Zimmermann et al., 2011). Another possibility would be to tackle the problem at the source. But it is not very feasible as nowadays everybody uses chemicals for different purposes, such as shampoo, dishwasher soaps and painkillers, which are disposed of in the wastewater at different locations in the houses (shower, sink, and toilet) (Joss et al., 2008).

Different tertiary treatment technologies have been demonstrated in the literature and range from ozonation to using enzymes for biodegradation. Abejón et al. (2015) tested a membrane reactor with the

enzyme laccase for its removal capacity of TCY while Popa et al. (2014) used *Streptomyces* bacteria for the removal of CMZ. This is a relatively novel treatment method and has not been tested in full-scale. Another novel technique is the use of electrolytic cells for the removal of oestrogens (Cong and Sakakibara, 2015). More established techniques are using granular and powdered activated carbon (Meinel et al., 2014), membranes (Camacho-Muñoz et al., 2012) or ozonation (Katsoyiannis et al., 2011).

There are different models available that describe ozonation of effluent wastewater (De Schepper et al., 2010; Zimmermann et al., 2011; Lee et al., 2013). The modelling of ozonation would include a gas transfer model of the ozone to the wastewater and a kinetic model of the oxidation of micropollutants. As the ozone added to the wastewater can also oxidise the organic matter present, the potential of the added ozone is difficult to assess. Modelling ozonation is therefore not a straightforward process. When modelling ozonation, it is important to take into account the transformation products as these can be more toxic than the MPs that were removed from the wastewater (Magdeburg et al., 2014). If the evaluation of the ozonation process would only include the removal efficiency of the MPs, an underestimation of the toxicity could be made. There could be chemicals present that are not analysed, but are highly toxic and only partly removed by sand filtration, as was shown by Magdeburg et al. (2014).

8.2.4 Urban wastewater system modelling

Besides modelling the fate of pharmaceuticals at the plant-wide level, the models could also be extended to the system-wide level and thereby include the entire urban wastewater system. In order to do this, a receiving water model should be included. This would allow for the inclusion of realistic PEC and PNEC values and provide more information about the toxicity. Also the transport and fate through the water body can be modelled and monitored in order to see the effect of for example pharmaceuticals on the aquatic environment (Chèvre et al., 2013). Ideally, the evaluation of operational/control strategies of the wastewater treatment plant would include the occurrence patterns of the pharmaceuticals in the receiving waters and take into account the effects that occur there.

8.2.5 Data quality

In order to continue the modelling of the MPs and ensure realistic models, the data should be of good quality. Due to the low concentrations and the large number of different chemicals, different analytical techniques are being used. These different techniques make it difficult to compare among studies as measured concentrations vary among laboratories and techniques (Johnson et al., 2008). As new detection techniques are still being developed (Gan et al., 2013; Oliveira et al., 2015), it is not possible to benchmark these analytical methods to be able to compare results. Another difficulty is the assessment of toxicity of mixtures of MPs and the long term effects (Vasquez et al., 2014; Zenker et al., 2014). For now PNEC and

PEC are used (Gros et al., 2010), however, the long term effects are not taken into account (Ellis, 2006; Musolff et al., 2010; Zenker et al., 2014). More research on these long term effects is needed; however it is important to realise that it takes time to obtain results.

8.2.6 QSARs/QPSRs

Alternatively, quantitative structure activity relationship (QSAR) or quantitative structure property relationship (QSPR) models could be used to assess the toxicity effects of pharmaceuticals and mixtures of pharmaceuticals (Cronin et al., 2003; Cai et al., 2008; Erdal et al., 2012). These models are based on correlations between a property of interest and a descriptor of the chemical. Based on these correlations an estimation of the unknown property of the chemical of interest can be made. The quality of a QSAR or QSPR depends on the database of chemicals with known properties and the chosen descriptor (Dearden et al., 2009). Besides using them to predict toxicity of chemicals, QSARs have also been used to predict the removal efficiency of MPs during ozonation (Lee and von Gunten, 2012) or the biodegradation in activated sludge units (Mansouri et al., 2013). The use of these models can be beneficial considering the large number of chemicals present in the wastewater and the cost related to estimating parameters for each of them. The costs for obtaining information about potential toxicity of a compound can be decreased if QSARs or QSPRs are used to estimate the toxicity of a micropollutant or its biodegradability.

Reference list

Abejón, R., De Cazes, M., Belleville, M.P., Sanchez-Marcano, J., 2015. Large-scale enzymatic membrane reactors for tetracycline degradation in WWTP effluents. Water Res. 73, 118–131.

Aboobakar, A., Cartmell, E., Stephenson, T., Jones, M., Vale, P., Dotro, G., 2013. Nitrous oxide emissions and dissolved oxygen profiling in a full-scale nitrifying activated sludge treatment plant. Water Res. 47 (2), 524–534.

Ahmed, Z., Cho, J., Lim, B.-R., Song, K.-G., Ahn, K.-H., 2007. Effects of sludge retention time on membrane fouling and microbial community structure in a membrane bioreactor. J. Memb. Sci. 287, 211–218.

Anthonisen, A.C., Loehr, R.C., Prakasam, T.B., Srinath, E.G., 1976. Inhibition of nitrification by ammonia and nitrous acid. J. Water Pollut. Control Fed. 48, 835–852.

Arnell, M., Sehlén, R., Jeppsson, U., 2013. Practical use of wastewater treatment modelling and simulation as a decision support tool for plant operators – case study on aeration control at Linköping wastewater treatment plant. 13th Nord. Wastewater Treat. Conf. (NORDIWA2013), 8-10 Oct. 2013, Malmö, Sweden.

Ashley, R.M., Dudley, J., Vollertsen, J., Saul, A.J., Jack, A., Blanksby, J.R., 2002. The effect of extended in-sewer storage on wastewater treatment plant performance. Water Sci. Technol. 45 (3), 239–246.

Ashley, R.M., Bertrand-Krajewski, J., Hvitved-Jacobsen, T., Verbanck, M., 2004. Solids in sewers. IWA Publishing, London, UK.

Ashley, R.M., Bertrand-Krajewski, J.L., Hvitved-Jacobsen, T., 2005. Sewer solids-20 years of investigation. Water Sci. Technol. 52 (3), 73–84.

Baker, D.R., Kasprzyk-Hordern, B., 2011. Critical evaluation of methodology commonly used in sample collection, storage and preparation for the analysis of pharmaceuticals and illicit drugs in surface water and wastewater by solid phase extraction and liquid chromatography-mass spectrometry. J. Chromatogr. A 1218, 8036–8059.

Banta-Green, C.J., Field, J.A., Chiaia, A.C., Sudakin, D.L., Power, L., De Montigny, L., 2009. The spatial epidemiology of cocaine, methamphetamine and 3,4-methylenedioxymethamphetamine (MDMA) use: a demonstration using a population measure of community drug load derived from municipal wastewater. Addiction 104, 1874–1880.

Baquero, F., Martínez, J.L., Cantón, R., 2008. Antibiotics and antibiotic resistance in water environments. Curr. Opin. Biotechnol. 19, 260–265.

Barber, M.C., 1978. A Markovian model for ecosystem flow analysis. Ecol. Modell. 5, 193–206.

Barret, M., Carrère, H., Latrille, E., Wisniewski, C., Patureau, D., 2010. Micropollutant and sludge characterization for modeling sorption equilibria. Environ. Sci. Technol. 44, 1100–1106.

Barret, M., Carrère, H., Patau, M., Patureau, D., 2011. Kinetics and reversibility of micropollutant sorption in sludge. J. Environ. Monit. 13, 2770–2774.

Batstone, D.J., Keller, J., Angelidaki, I., Kalyuzhnyi, S.V., Pavlostathis, S.G., Rozzi, A., Sanders, W.T., Siegrist, H., Vavilin, V.A., 2002. The IWA Anaerobic Digestion Model No 1 (ADM1). Water Sci. Technol. 45 (10), 65–73.

Beaulieu, J.J., Tank, J.L., Hamilton, S.K., Wollheim, W.M., Hall, R.O., Mulholland, P.J., Peterson, B.J., Ashkenas, L.R., Cooper, L.W., Dahm, C.N., Dodds, W.K., Grimm, N.B., Johnson, S.L., McDowell, W.H., Poole, G.C., Valett, H.M., Arango, C.P., Bernot, M.J., Burgin, A.J., Crenshaw, C.L., Helton, A.M., Johnson, L.T., O'Brien, J.M., Potter, J.D., Sheibley, R.W., Sobota, D.J., Thomas, S.M., 2011. Nitrous oxide emission from denitrification in stream and river networks. Proc. Natl. Acad. Sci. USA. 108, 214–219.

Benedetti, L., Dirckx, G., Bixio, D., Thoeye, C., Vanrolleghem, P.A., 2006. Substance flow analysis of the wastewater collection and treatment system. Urban Water J. 3, 33–42.

Bennett, N.D., Croke, B.F.W., Guariso, G., Guillaume, J.H.A., Hamilton, S.H., Jakeman, A.J., Marsili-Libelli, S., Newham, L.T.H., Norton, J.P., Perrin, C., Pierce, S.A., Robson, B., Seppelt, R., Voinov, A.A., Fath, B.D., Andreassian, V., 2013. Characterising performance of environmental models. Environ. Model. Softw. 40, 1–20.

Bertrand-Krajewski, J.L., Briat, P., Scrivener, O., 1993. Sewer sediment production and transport modelling: A literature review. J. Hydraul. Res. 31, 435–460.

Brun, R., Reichert, P., Künsch, H.R., 2001. Practical identifiability analysis of large environmental simulation models. Water Resour. Res. 37, 1015–1030.

Buser, H.-R., Poiger, T., Müller, M.D., 1999. Occurrence and environmental behavior of the chiral pharmaceutical drug ibuprofen in surface waters and in wastewater. Environ. Sci. Technol. 33, 2529–2535.

Butler, D., Friedler, E., Gatt, K., 1995. Characterising the quantity and quality of domestic wastewater inflows. Water Sci. Technol. 31 (7), 13–24.

Byrns, G., 2001. The fate of xenobiotic organic compounds in wastewater treatment plants. Water Res. 35 (10), 2523–2533.

Cai, B., Xie, L., Yang, D., Arcangeli, J.P., 2008. Application of QSARs model in toxicity evaluation of wastewater to bio-treatment system in WWTP. 2nd Int. Conf. Bioinforma. Biomed. Eng. 3027–3030.

Camacho-Muñoz, D., Martín, J., Santos, J.L., Alonso, E., Aparicio, I., De la Torre, T., Rodriguez, C., Malfeito, J.J., 2012. Effectiveness of three configurations of membrane bioreactors on the removal of priority and emergent organic compounds from wastewater: comparison with conventional wastewater treatments. J. Environ. Monit. 14, 1428–1436.

Carballa, M., Omil, F., Lema, J.M., Llompart, M., García-Jares, C., Rodríguez, I., Gómez, M., Ternes, T., 2004. Behavior of pharmaceuticals, cosmetics and hormones in a sewage treatment plant. Water Res. 38 (12), 2918–2926.

Carballa, M., Fink, G., Omil, F., Lema, J.M., Ternes, T., 2008. Determination of the solid-water distribution coefficient (Kd) for pharmaceuticals, estrogens and musk fragrances in digested sludge. Water Res. 42 (1-2), 287–295.

Castiglioni, S., Bagnati, R., Fanelli, R., Pomati, F., Calamari, D., Zuccato, E., 2006. Removal of pharmaceuticals in sewage treatment plants in Italy. Environ. Sci. Technol. 40, 357–363.

Castiglioni, S., Bijlsma, L., Covaci, A., Emke, E., Hernández, F., Reid, M., Ort, C., Thomas, K.V., van Nuijs, A.L.N., De Voogt, P., Zuccato, E., 2013. Evaluation of uncertainties associated with the determination of community drug use through the measurement of sewage drug biomarkers. Environ. Sci. Technol. 47, 1452–1460.

Chandran, K., Stein, L.Y., Klotz, M.G., van Loosdrecht, M.C.M., 2011. Nitrous oxide production by lithotrophic ammonia-oxidizing bacteria and implications for engineered nitrogen-removal systems. Biochem. Soc. Trans. 39, 1832–1837.

Checchi, N., Marsili-Libelli, S., 2005. Reliability of parameter estimation in respirometric models. Water Res. 39 (15), 3686–3696.

Chèvre, N., Coutu, S., Margot, J., Wynn, H.K., Bader, H.P., Scheidegger, R., Rossi, L., 2013. Substance flow analysis as a tool for mitigating the impact of pharmaceuticals on the aquatic system. Water Res. 47 (9), 2995–3005.

Clara, M., Strenn, B., Kreuzinger, N., 2004. Carbamazepine as a possible anthropogenic marker in the aquatic environment: Investigations on the behaviour of Carbamazepine in wastewater treatment and during groundwater infiltration. Water Res. 38 (4), 947–954.

Clara, M., Kreuzinger, N., Strenn, B., Gans, O., Kroiss, H., 2005. The solids retention time - A suitable design parameter to evaluate the capacity of wastewater treatment plants to remove micropollutants. Water Res. 39 (1), 97–106.

Clouzot, L., Choubert, J.M., Cloutier, F., Goel, R., Love, N.G., Melcer, H., Ort, C., Patureau, D., Plosz, B.G., Pomiès, M., Vanrolleghem, P.A., 2013. Perspectives on modelling micropollutants in wastewater treatment plants. Water Sci. Technol. 68 (2), 448–461.

Coe, T.S., Hamilton, P.B., Hodgson, D., Paull, G.C., Stevens, J.R., Sumner, K., Tyler, C.R., 2008. An environmental estrogen alters reproductive hierarchies, disrupting sexual selection in group-spawning fish. Environ. Sci. Technol. 42, 5020–5025.

Coes, A.L., Paretti, N.V., Foreman, W.T., Iverson, J.L., Alvarez, D.A., 2014. Sampling trace organic compounds in water: A comparison of a continuous active sampler to continuous passive and discrete sampling methods. Sci. Total Environ. 473-474, 731–741.

Collado, N., Buttiglieri, G., Ferrando-Climent, L., Rodriguez-Mozaz, S., Barceló, D., Comas, J., Rodriguez-Roda, I., 2012. Removal of ibuprofen and its transformation products: Experimental and simulation studies. Sci. Total Environ. 433, 296–301.

Cong, V.H., Sakakibara, Y., 2015. Continuous treatments of estrogens through polymerization and regeneration of electrolytic cells. J. Hazard. Mater. 285, 304–310.

Copp, J.B. (Ed.), 2002. The COST simulation benchmark: description and simulator manual. Office for Official Publications of the European Community, Luxembourg.

Corominas, L., Flores-Alsina, X., Snip, L., Vanrolleghem, P.A., 2012. Comparison of different modeling approaches to better evaluate greenhouse gas emissions from whole wastewater treatment plants. Biotechnol. Bioeng. 109, 2854–2863.

Coutu, S., Wyrsch, V., Wynn, H.K.K., Rossi, L., Barry, D.A.A., 2013. Temporal dynamics of antibiotics in wastewater treatment plant influent. Sci. Total Environ. 458–460, 20–26.

Criddle, C.S., 1993. The kinetics of cometabolism. Biotechnol. Bioeng. 41, 1048–1056.

Cronin, M.T.D., Walker, J.D., Jaworska, J.S., Comber, M.H.I., Watts, C.D., Worth, A.P., 2003. Use of QSARs in international decision-making frameworks to predict ecologic effects and environmental fate of chemical substances. Environ. Health Perspect. 111, 1376–1390.

Czepiel, P.M., Crill, P.M., Harriss, R.C., 1993. Methane emissions from municipal wastewater treatment processes. Environ. Sci. Technol. 27, 2472–2477.

Daelman, M.R.J., van Voorthuizen, E.M., van Dongen, U.G.J.M., Volcke, E.I.P., van Loosdrecht, M.C.M., 2012. Methane emission during municipal wastewater treatment. Water Res. 46 (11), 3657–3670.

Daelman, M.R.J., De Baets, B., van Loosdrecht, M.C.M., Volcke, E.I.P., 2013. Influence of sampling strategies on the estimated nitrous oxide emission from wastewater treatment plants. Water Res. 47 (9), 3120–3130.

Daughton, C.G., Ternes, T.A., 1999. Pharmaceuticals and personal care products in the environment: Agents of subtle change? Environ. Health Perspect. 107, 907–938.

Daughton, C.G., Ruhoy, I.S., 2009. Environmental footprint of pharmaceuticals: the significance of factors beyond direct excretion to sewers. Environ. Toxicol. Chem. 28, 2495–2521.

Dawson, C.W., Abrahart, R.J., See, L.M., 2007. HydroTest: A web-based toolbox of evaluation metrics for the standardised assessment of hydrological forecasts. Environ. Model. Softw. 22, 1034–1052.

De Keyser, W., Gevaert, V., Verdonck, F., Nopens, I., De Baets, B., Vanrolleghem, P.A., Mikkelsen, P.S., Benedetti, L., 2010. Combining multimedia models with integrated urban water system models for micropollutants. Water Sci. Technol. 62 (7), 1614–1622.

De Schepper, W., Dries, J., Geuens, L., Blust, R., 2010. A kinetic model for multicomponent wastewater substrate removal by partial ozonation and subsequent biodegradation. Water Res. 44 (18), 5488–5498.

Dearden, J.C., Cronin, M.T.D., Kaiser, K.L.E., 2009. How not to develop a quantitative structure-activity or structure-property relationship (QSAR/QSPR). SAR QSAR Environ. Res. 20, 241–266.

Delgadillo-Mirquez, L., Lardon, L., Steyer, J.-P., Patureau, D., 2011. A new dynamic model for bioavailability and cometabolism of micropollutants during anaerobic digestion. Water Res. 45 (15), 4511–4521.

Desloover, J., Vlaeminck, S.E., Clauwaert, P., Verstraete, W., Boon, N., 2012a. Strategies to mitigate N2O emissions from biological nitrogen removal systems. Curr. Opin. Biotechnol. 23, 474–482.

Desloover, J., Woldeyohannis, A.A., Verstraete, W., Boon, N., Rabaey, K., 2012b. Electrochemical resource recovery from digestate to prevent ammonia toxicity during anaerobic digestion. Environ. Sci. Technol. 46, 12209–12216.

Efron, B., 1979. Bootstrap methods: another look at the jackknife. Ann. Stat. 7, 1–26.

Ellis, J.B., 2006. Pharmaceutical and personal care products (PPCPs) in urban receiving waters. Environ. Pollut. 144, 184–189.

EMEA (European Medicines Agency), 2006. Guideline on the environmental risk assessment of medicinal products for human use. Pre-Authorisation Evaluation of Medicines for Human Use. London, UK.

Erdal, U.G., Daigger, G.T., Erdal, Z., Schimmoller, L., 2012. Incorporating quantitative structure activity relationship (QSAR) into an Excel tool to predict removal efficiencies of CECs during wastewater treatment. Proc. Water Environ. Fed. (WEFTEC2012), 29 Sept. - 3 Oct. 2012, New Orleans, USA. 7213–7223.

Escher, B.I., Fenner, K., 2011. Recent advances in environmental risk assessment of transformation products. Environ. Sci. Technol. 45, 3835–3847.

European Commission, 2008. Directive 2008/105/EC of the European Parliament and of the Council of 16 December 2008 on environmental quality standards in the field of water policy, amending and subsequently repealing Council Directives 82/176/EEC, 83/513/EEC, 84/156/EEC, 84/491/EEC.

European Commission, 2011. Proposal for a DIRECTIVE OF THE EUROPEAN PARLIAMENT AND OF THE COUNCIL amending Directives 2000/60/EC and 2008/105/EC as regards priority substances in the field of water policy.

Ferrando-Climent, L., Collado, N., Buttiglieri, G., Gros, M., Rodriguez-Roda, I., Rodriguez-Mozaz, S., Barceló, D., 2012. Comprehensive study of ibuprofen and its metabolites in activated sludge batch experiments and aquatic environment. Sci. Total Environ. 438, 404–413.

Ferrari, B., Paxéus, N., Giudice, R. Lo, Pollio, A., Garric, J., 2003. Ecotoxicological impact of pharmaceuticals found in treated wastewaters: study of carbamazepine, clofibric acid, and diclofenac. Ecotoxicol. Environ. Saf. 55, 359–370.

Flores, X., Rodríguez-Roda, I., Poch, M., Jiménez, L., Bañares-Alcántara, R., 2007. Systematic procedure to handle critical decisions during the conceptual design of activated sludge plants. Ind. Eng. Chem. Res. 46, 5600–5613.

Flores-Alsina, X., Rodríguez-Roda, I., Sin, G., Gernaey, K.V., 2008. Multi-criteria evaluation of wastewater treatment plant control strategies under uncertainty. Water Res. 42 (17), 4485–4497.

Flores-Alsina, X., Corominas, L., Snip, L., Vanrolleghem, P.A., 2011. Including greenhouse gas emissions during benchmarking of wastewater treatment plant control strategies. Water Res. 45 (16), 4700–4710.

Flores-Alsina, X., Gernaey, K.V., Jeppsson, U., 2012. Benchmarking biological nutrient removal in wastewater treatment plants: influence of mathematical model assumptions. Water Sci. Technol. 65 (8), 1496–1505.

Flores-Alsina, X., Arnell, M., Amerlinck, Y., Corominas, L., Gernaey, K.V., Guo, L., Lindblom, E., Nopens, I., Porro, J., Shaw, A., Snip, L., Vanrolleghem, P.A., Jeppsson, U., 2014a. Balancing effluent quality, economic cost and greenhouse gas emissions during the evaluation of (plant-wide) control/operational strategies in WWTPs. Sci. Total Environ. 466-467, 616–624.

Flores-Alsina, X., Saagi, R., Lindblom, E., Thirsing, C., Thornberg, D., Gernaey, K.V., Jeppsson, U., 2014b. Calibration and validation of a phenomenological influent pollutant disturbance scenario generator using full-scale data. Water Res. 51, 172–185.

Flores-Alsina, X., Mbamba, C.K., Solon, K., Vrecko, D., Tait, S., Batstone, D.J., Jeppsson, U., Gernaey, K.V., 2015. A plant-wide aqueous phase chemistry module describing pH variations and ion speciation/pairing in wastewater treatment process models. Water Res. 85, 255-265.

Foley, J., de Haas, D., Hartley, K., Lant, P., 2010a. Comprehensive life cycle inventories of alternative wastewater treatment systems. Water Res. 44 (5), 1654–1666.

Foley, J., de Haas, D., Yuan, Z., Lant, P., 2010b. Nitrous oxide generation in full-scale biological nutrient removal wastewater treatment plants. Water Res. 44 (3), 831–844.

Gan, Z., Sun, H., Wang, R., Feng, B., 2013. A novel solid-phase extraction for the concentration of sweeteners in water and analysis by ion-pair liquid chromatography-triple quadrupole mass spectrometry. J. Chromatogr. A 1274, 87–96.

García-Galán, M.J., Rodriguez-Mozaz, S., Barceló, D., Petrović, M., Rodríguez-Mozaz, S., Petrovic, M., Barceló, D., 2015. Multiresidue trace analysis of 14 pharmaceuticals, their human metabolites and transformation products by fully automated on-line solid-phase extraction-liquid chromatography-tandem mass spectrometry. In prep.

Gernaey, K.V., Jørgensen, S.B., 2004. Benchmarking combined biological phosphorus and nitrogen removal wastewater treatment processes. Control Eng. Pract. 12, 357–373.

Gernaey, K.V., Flores-Alsina, X., Rosen, C., Benedetti, L., Jeppsson, U., 2011. Dynamic influent pollutant disturbance scenario generation using a phenomenological modelling approach. Environ. Model. Softw. 26, 1255–1267.

Gernaey, K.V., Jeppsson, U., Vanrolleghem, P.A., Copp, J.B., 2014. Benchmarking of control strategies for wastewater treatment plants. IWA Scientific and Technical Report No. 23. IWA Publishing, London, UK.

Gevaert, V., 2010. Integrated dynamic modelling of the fate of organic priority pollutants in the urban wastewater system. Ph.D Thesis, Department of Applied Mathematics, Biometrics and Process Control, Ghent University, Ghent, Belgium.

Göbel, A., Thomsen, A., McArdell, C.S., Joss, A., Giger, W., 2005. Occurrence and sorption behavior of sulfonamides, macrolides, and trimethoprim in activated sludge treatment. Environ. Sci. Technol. 39, 3981–3989.

Grady, C.P.L., 1998. Factors influencing biodegradation of synthetic organic chemicals in natural and engineered aquatic environments. Pure Appl. Chem. 70, 1363–1373.

Gros, M., Petrović, M., Ginebreda, A., Barceló, D., 2010. Removal of pharmaceuticals during wastewater treatment and environmental risk assessment using hazard indexes. Environ. Int. 36, 15–26.

Guisasola, A., Petzet, S., Baeza, J.A., Carrera, J., Lafuente, J., 2007. Inorganic carbon limitations on nitrification: Experimental assessment and modelling. Water Res. 41 (2), 277–286.

Guo, L., Vanrolleghem, P.A., 2014. Calibration and validation of an activated sludge model for greenhouse gases no. 1 (ASMG1): Prediction of temperature-dependent N2O emission dynamics. Bioprocess Biosyst. Eng. 37, 151–163.

Harding, T., Ikumi, D., Ekama, G., 2011. Incorporating phosphorus into plant wide wastewater treatment plant modelling–anaerobic digestion. 8th IWA Symp. Syst. Anal. Integr. Assess. (Watermatex), June 20-22, 2011, San Sebastian, Spain.

Hastings, W., 1970. Monte-Carlo sampling methods using Markov Chains and their applications. Biometrika 57, 97–109.

Hauduc, H., Rieger, L., Takács, I., Héduit, A., Vanrolleghem, P.A., Gillot, S., 2010. A systematic approach for model verification: Application on seven published activated sludge models. Water Sci. Technol. 61 (4), 825–839.

Hauduc, H., Takács, I., Smith, S., Szabo, A., Murthy, S., Daigger, G.T., Spérandio, M., 2015a. A dynamic physicochemical model for chemical phosphorus removal. Water Res. 73, 157–70.

Hauduc, H., Neumann, M.B., Muschalla, D., Gamerith, V., Gillot, S., Vanrolleghem, P.A., 2015b. Efficiency criteria for environmental model quality assessment: A review and its application to wastewater treatment. Environ. Model. Softw. 68, 196–204.

Heberer, T., Feldmann, D., 2005. Contribution of effluents from hospitals and private households to the total loads of diclofenac and carbamazepine in municipal sewage effluents - Modeling versus measurements. J. Hazard. Mater. 122, 211–218.

Helbling, D.E., Johnson, D.R., Honti, M., Fenner, K., 2012. Micropollutant biotransformation kinetics associate with WWTP process parameters and microbial community characteristics. Environ. Sci. Technol. 46, 10579–10588.

Henze, M., Grady, C.P.L., Gujer, W., Marais, G. v. R., Matsuo, T., 1987. A general model for single-sludge wastewater treatment systems. Water Res. 21 (5), 505–515.

Henze, M., Gujer, W., Mino, T., van Loosdrecht, M.C.M., 2000. Activated Sludge Models ASM1, ASM2, ASM2d and ASM2. IWA Scientific and Technical Report No. 9. IWA Publishing, London, UK.

Hiatt, W.C., Grady, C.P.L., 2008. An updated process model for carbon oxidation, nitrification, and denitrification. Water Environ. Res. 80, 2145–2156.

Holbrook, R.D., Love, N.G., Novak, J.T., 2004. Investigation of sorption behavior between pyrene and colloidal organic carbon from activated sludge processes. Environ. Sci. Technol. 38, 4987–4994.

Hollender, J., Zimmermann, S.G., Koepke, S., Krauss, M., McArdell, C.S., Ort, C., Singer, H., von Gunten, U., Siegrist, H., 2009. Elimination of organic micropollutants in a municipal wastewater treatment plant upgraded with a full-scale post-ozonation followed by sand filtration. Environ. Sci. Technol. 43, 7862–7869.

Hug, T., Benedetti, L., Hall, E.R., Johnson, B.R., Morgenroth, E., Nopens, I., Rieger, L., Shaw, A., Vanrolleghem, P.A., 2009. Wastewater treatment models in teaching and training: The mismatch between education and requirements for jobs. Water Sci. Technol. 59 (4), 745–753.

Huisman, J.L., Gujer, W., 2002. Modelling wastewater transformation in sewers based on ASM3. Water Sci. Technol. 45 (6), 51–60.

Hvitved-Jacobsen, T., Vollertsen, J., Nielsen, P.H.H., 1998. A process and model concept for microbial wastewater transformations in gravity sewers. Water Sci. Technol. 37 (1), 233–241.

Hyland, K.C., Dickenson, E.R.V., Drewes, J.E., Higgins, C.P., 2012. Sorption of ionized and neutral emerging trace organic compounds onto activated sludge from different wastewater treatment configurations. Water Res. 46 (6), 1958–1968.

Ikumi, D., Brouckaert, C., Ekama, G., 2011. Modelling of struvite precipitation in anaerobic digestion. 8th IWA Symp. Syst. Anal. Integr. Assess. (Watermatex), June 20-22, 2011, San Sebastian, Spain.

IPCC, 2006. 2006 IPCC Guidelines for national greenhouse gas inventories, Prepared by the National Greenhouse Gas Inventories Programme, Eggleston H.S., Buendia L., Miwa K., Ngara T. and Tanabe K. (eds), IGES, Japan.

IPCC, 2013. Climate change 2013: The physical science basis. Contribution of Working Group I to the Fifth Assessment Report of the Intergovernmental Panel on Climate Change. Stocker, T.F. Qin, D. Plattner, G.-K. Tignor, M. Allen, S.K. Boschung, J. Nauels, A. Xia, Y. Bex, V. Midgley, P.M. (eds) Cambridge University Press, Cambridge, United Kingdom and New York, NY, USA.

Itokawa, H., Hanaki, K., Matsuo, T., 2001. Nitrous oxide production in high-loading biological nitrogen removal process under low COD/N ratio condition. Water Res. 35 (3), 657–664.

Jelic, A., Cruz-Morató, C., Marco-Urrea, E., Sarrà, M., Perez, S., Vicent, T., Petrović, M., Barceló, D., 2012. Degradation of carbamazepine by Trametes versicolor in an air pulsed fluidized bed bioreactor and identification of intermediates. Water Res. 46 (4), 955–964.

Jelic, A., Rodriguez-Mozaz, S., Barceló, D., Gutierrez, O., 2015. Impact of in-sewer transformation on 43 pharmaceuticals in a pressurized sewer under anaerobic conditions. Water Res. 8, 98–108.

Jeppsson, U., Pons, M.-N., Nopens, I., Alex, J., Copp, J.B., Gernaey, K.V., Rosen, C., Steyer, J.-P., Vanrolleghem, P.A., 2007. Benchmark simulation model no 2: general protocol and exploratory case studies. Water Sci. Technol. 56 (8), 67–78.

Johnson, A.C., Ternes, T.A., Williams, R.J., Sumpter, J.P., 2008. Assessing the concentrations of polar organic microcontaminants from point sources in the aquatic environment: Measure or model? Environ. Sci. Technol. 42, 5390–5399.

Johnson, D.R., Helbling, D.E., Lee, T.K., Park, J., Fenner, K., Kohler, H.-P.E., Ackermann, M., 2015. Association of biodiversity with the rates of micropollutant biotransformations among full-scale wastewater treatment plant communities. Appl. Environ. Microbiol. 81, 666–675.

Joshi, M., Seidel-Morgenstern, A., Kremling, A., 2006. Exploiting the bootstrap method for quantifying parameter confidence intervals in dynamical systems. Metab. Eng. 8, 447–455.

Joss, A., Keller, E., Alder, A.C., Göbel, A., McArdell, C.S., Ternes, T., Siegrist, H., 2005. Removal of pharmaceuticals and fragrances in biological wastewater treatment. Water Res. 39 (14), 3139–3152.

Joss, A., Zabczynski, S., Göbel, A., Hoffmann, B., Löffler, D., McArdell, C.S., Ternes, T.A., Thomsen, A., Siegrist, H., 2006. Biological degradation of pharmaceuticals in municipal wastewater treatment: Proposing a classification scheme. Water Res. 40 (8), 1686–1696.

Joss, A., Siegrist, H., Ternes, T.A., 2008. Are we about to upgrade wastewater treatment for removing organic micropollutants? Water Sci. Technol. 57 (2), 251–255.

Kampschreur, M.J., Tan, N.C.G., Kleerebezem, R., Picioreanu, C., Jetten, M.S.M., van Loosdrecht, M.C.M., 2008. Effect of dynamic process conditions on nitrogen oxides emission from a nitrifying culture. Environ. Sci. Technol. 42, 429–435.

Kampschreur, M.J., Temmink, H., Kleerebezem, R., Jetten, M.S.M., van Loosdrecht, M.C.M., 2009. Nitrous oxide emission during wastewater treatment. Water Res. 43 (17), 4093–4103.

Karvelas, M., Katsoyiannis, A., Samara, C., 2003. Occurrence and fate of heavy metals in the wastewater treatment process. Chemosphere 53, 1201–1210.

Katsoyiannis, I.A., Canonica, S., von Gunten, U., 2011. Efficiency and energy requirements for the transformation of organic micropollutants by ozone, O3/H2O2 and UV/H2O2. Water Res. 45 (13), 3811–3822.

Keller, J., Hartley, K., 2003. Greenhouse gas production in wastewater treatment: Process selection is the major factor. Water Sci. Technol. 47 (12), 43–48.

Lai, F.Y., Ort, C., Gartner, C., Carter, S., Prichard, J., Kirkbride, P., Bruno, R., Hall, W., Eaglesham, G., Mueller, J.F., 2011. Refining the estimation of illicit drug consumptions from wastewater analysis: Co-analysis of prescription pharmaceuticals and uncertainty assessment. Water Res. 45 (15), 4437–4448.

Lange, A., Paull, G.C., Coe, T.S., Katsu, Y., Urushitani, H., Iguchi, T., Tyler, C.R., 2009. Sexual reprogramming and estrogenic sensitization in wild fish exposed to ethinylestradiol. Environ. Sci. Technol. 43, 1219–1225.

Law, Y., Lant, P., Yuan, Z., 2011. The effect of pH on N2O production under aerobic conditions in a partial nitritation system. Water Res. 45 (18), 5934–5944.

Law, Y., Ni, B.J., Lant, P., Yuan, Z., 2012a. N2O production rate of an enriched ammonia-oxidising bacteria culture exponentially correlates to its ammonia oxidation rate. Water Res. 46 (10), 3409–3419.

Law, Y., Ye, L., Pan, Y., Yuan, Z., 2012b. Nitrous oxide emissions from wastewater treatment processes. Philos. Trans. R. Soc. B Biol. Sci. 367, 1265–1277.

Leclercq, M., Mathieu, O., Gomez, E., Casellas, C., Fenet, H., Hillaire-Buys, D., 2009. Presence and fate of carbamazepine, oxcarbazepine, and seven of their metabolites at wastewater treatment plants. Arch. Environ. Contam. Toxicol. 56, 408–415.

Lee, K.-C., Rittmann, B.E., Shi, J., McAvoy, D., Lee, A.K., 1998. Advanced steady-state model for the fate of hydrophobic and volatile compounds in activated sludge. Water Environ. Res. 70, 1118–1131.

Lee, Y., von Gunten, U., 2012. Quantitative structure-activity relationships (QSARs) for the transformation of organic micropollutants during oxidative water treatment. Water Res. 46 (19), 6177–6195.

Lee, Y., Gerrity, D., Lee, M., Bogeat, A.E., Salhi, E., Gamage, S., Trenholm, R.A., Wert, E.C., Snyder, S.A., von Gunten, U., 2013. Prediction of micropollutant elimination during ozonation of municipal wastewater effluents: Use of kinetic and water specific information. Environ. Sci. Technol. 47, 5872–5881.

Leu, S., Chan, L., Stenstrom, M.K., 2012. Toward long solids retention time of activated sludge processes: benefits in energy saving, effluent quality, and stability. Water Environ. Res. 84, 42–53.

Lindblom, E., Gernaey, K.V., Henze, M., Mikkelsen, P.S., 2006. Integrated modelling of two xenobiotic organic compounds. Water Sci. Technol. 54 (6-7), 213–221.

Lindblom, E., Press-Kristensen, K., Vanrolleghem, P.A., Mikkelsen, P.S., Henze, M., 2009. Dynamic experiments with high bisphenol-A concentrations modelled with an ASM model extended to include a separate XOC degrading microorganism. Water Res. 43 (13), 3169–3176.

Lindblom, E., Ahlman, S., Mikkelsen, P.S., 2011. Uncertainty-based calibration and prediction with a stormwater surface accumulation-washoff model based on coverage of sampled Zn, Cu, Pb and Cd field data. Water Res. 45 (13), 3823–3835.

Lindblom, E., Arnell, M., Flores-Alsina, X., Stenström, F., Gustavsson, D.J.I., Yang, J., Jeppsson, U., 2015. Dynamic modelling of nitrous oxide emissions from three Swedish sludge liquor treatment systems. Water Sci. Technol. Submitted.

Loos, R., Carvalho, R., António, D.C., Comero, S., Locoro, G., Tavazzi, S., Paracchini, B., Ghiani, M., Lettieri, T., Blaha, L., Jarosova, B., Voorspoels, S., Servaes, K., Haglund, P., Fick, J., Lindberg, R.H., Schwesig, D., Gawlik, B.M., 2013. EU-wide monitoring survey on emerging polar organic contaminants in wastewater treatment plant effluents. Water Res. 47 (17), 6475–6487.

Lu, H., Chandran, K., Stensel, D., 2014. Microbial ecology of denitrification in biological wastewater treatment. Water Res. 64, 237–254.

Lust, M., Makinia, J., Stensel, H.D., 2012. A mechanistic model for fate and removal of estrogens in biological nutrient removal activated sludge systems. Water Sci. Technol. 65 (6), 1130–1136.

Ma, Y., Sundar, S., Park, H., Chandran, K., 2015. The effect of inorganic carbon on microbial interactions in a biofilm nitritation–anammox process. Water Res. 70, 246–254.

Mackay, D., Shiu, W.Y., Ma, K.-C., Lee, S.C., 2006. Handbook of physical-chemical properties and environmental fate for organic chemicals. Taylor & Francis Group, Boca Raton, USA.

Madsen, H., Spliid, H., Thyregod, P., 1985. Markov models in discrete and continuous time for hourly observations of cloud cover. J. Clim. Appl. Meteorol. 24, 629–639.

Magdeburg, A., Stalter, D., Schlüsener, M., Ternes, T., Oehlmann, J., 2014. Evaluating the efficiency of advanced wastewater treatment: Target analysis of organic contaminants and (geno-)toxicity assessment tell a different story. Water Res. 50, 35–47.

Mampaey, K.E., Beuckels, B., Kampschreur, M.J., Kleerebezem, R., van Loosdrecht, M.C.M., Volcke, E.I.P., 2013. Modelling nitrous and nitric oxide emissions by autotrophic ammonia-oxidizing bacteria. Environ. Technol. 34, 1555–1566.

Mansouri, K., Ringsted, T., Ballabio, D., Todeschini, R., Consonni, V., 2013. Quantitative structure-activity relationship models for ready biodegradability of chemicals. J. Chem. Inf. Model. 53, 867–878.

Martin, C., Vanrolleghem, P.A., 2014. Analysing, completing, and generating influent data for WWTP modelling: A critical review. Environ. Model. Softw. 60, 188–201.

Mathieu, C., Rieckermann, J., Berset, J.-D., Schürch, S., Brenneisen, R., 2011. Assessment of total uncertainty in cocaine and benzoylecgonine wastewater load measurements. Water Res. 45 (20), 6650–6660.

McArdell, C.S., Molnar, E., Suter, M.J.F., Giger, W., 2003. Occurrence and fate of macrolide antibiotics in wastewater treatment plants and in the Glatt valley watershed, Switzerland. Environ. Sci. Technol. 37, 5479–5486.

Meinel, F., Ruhl, A.S., Sperlich, A., Zietzschmann, F., Jekel, M., 2014. Pilot-Scale Investigation of Micropollutant Removal with Granular and Powdered Activated Carbon. Water, Air, Soil Pollut. 226, 1.

Melcer, H., Bell, J.P., Thompson, D.J., Yendt, C.M., Kemp, J., Steel, P., 1994. Modeling Volatile Organic Contaminants' Fate in Wastewater Treatment Plants. J. Environ. Eng. 120, 588–609.

Mikola, A., Heinonen, M., Kosonen, H., Leppänen, M., Rantanen, P., Vahala, R., 2014. N2O emissions from secondary clarifiers and their contribution to the total emissions of the WWTP. Water Sci. Technol. 70 (4), 720–728.

Morel, F.M.M., Hering, J.G., 1993. Principles and applications of aquatic chemistry. John Wiley & Sons, New York, USA.

Musolff, A., Leschik, S., Reinstorf, F., Strauch, G., Schirmer, M., 2010. Micropollutant loads in the urban water cycle. Environ. Sci. Technol. 44, 4877–4883.

Musvoto, E.V., Wentzel, M.C., Ekama, G.A., 2000. Integrated chemical-physical processes modelling - II. Simulating aeration treatment of anaerobic digester supernatants. Water Res. 34 (6), 1868–1880.

Nelson, E.D., Do, H., Lewis, R.S., Carr, S.A., 2011. Diurnal variability of pharmaceutical, personal care product, estrogen and alkylphenol concentrations in effluent from a tertiary wastewater treatment facility. Environ. Sci. Technol. 45, 1228–1234.

Neumann, M.B., von Gunten, U., Gujer, W., 2007. Sources of parameter uncertainty in predicting treatment performance: The case of preozonation in drinking water engineering. Environ. Sci. Technol. 41, 3991–3996.

Neumann, M.B., Gujer, W., 2008. Underestimation of uncertainty in statistical regression of environmental models: Influence of model structure uncertainty. Environ. Sci. Technol. 42, 4037–4043.

Ni, B.J., Yuan, Z., Chandran, K., Vanrolleghem, P.A., Murthy, S., 2013. Evaluating four mathematical models for nitrous oxide production by autotrophic ammonia-oxidizing bacteria. Biotechnol. Bioeng. 110, 153–163.

Ni, B.J., Peng, L., Law, Y., Guo, J., Yuan, Z., 2014. Modeling of nitrous oxide production by autotrophic ammonia-oxidizing bacteria with multiple production pathways. Environ. Sci. Technol. 48, 3916–3924.

Nopens, I., Benedetti, L., Jeppsson, U., Pons, M.-N., Alex, J., Copp, J.B., Gernaey, K.V., Rosen, C., Steyer, J.-P., Vanrolleghem, P.A., 2010. Benchmark Simulation Model No 2: finalisation of plant layout and default control strategy. Water Sci. Technol. 62 (9), 1967–1974.

Oliveira, T.M.B.F., Pessoa, G. de P., dos Santos, A.B., de Lima-Neto, P., Correia, A.N., 2015. Simultaneous electrochemical sensing of emerging organic contaminants in full-scale sewage treatment plants. Chem. Eng. J. 267, 347–354.

Olsson, G., 2012. ICA and me - A subjective review. Water Res. 46 (6), 1585–1624.

Omlin, M., Reichert, P., 1999. A comparison of techniques for the estimation of model prediction uncertainty. Ecol. Modell. 115, 45–59.

Ort, C., Schaffner, C., Giger, W., Gujer, W., 2005. Modelling stochastic load variations in sewer systems. Water Sci. Technol. 52 (5), 113–122.

Ort, C., Gujer, W., 2006. Sampling for representative micropollutant loads in sewer systems. Water Sci. Technol. 54 (6-7), 169–176.

Ort, C., Lawrence, M.G., Rieckermann, J., Joss, A., 2010. Sampling for pharmaceuticals and personal care products (PPCPs) and illicit drugs in wastewater systems: Are your conclusions valid? A critical review. Environ. Sci. Technol. 44, 6024–6035.

Otterpohl, R., Freund, M., 1992. Dynamic models for clarifiers of activated sludge plants with dry and wet weather flows. Water Sci. Technol. 26 (5-6), 1391–1400.

Pan, Y., Ni, B.-J.-J., Bond, P.L., Ye, L., Yuan, Z., 2013. Electron competition among nitrogen oxides reduction during methanol-utilizing denitrification in wastewater treatment. Water Res. 47 (10), 3273–3281.

Pan, Y., Ni, B.-J., Lu, H., Chandran, K., Richardson, D., Yuan, Z., 2014. Evaluating two concepts for the modelling of intermediates accumulation during biological denitrification in wastewater treatment. Water Res. 71, 21–31.

Parker, W.J., Monteith, H.D., Bell, J.P., Melcer, H., Berthouex, P.M., 1994. Comprehensive fate model for metals in municipal wastewater treatment. J. Environ. Eng. 120, 1266–1283.

Payraudeau, S., Gregoire, C., 2012. Modelling pesticides transfer to surface water at the catchment scale: A multi-criteria analysis. Agron. Sustain. Dev. 32, 479–500.

Peng, L., Ni, B.-J., Ye, L., Yuan, Z., 2015. N2O production by ammonia oxidizing bacteria in an enriched nitrifying sludge linearly depends on inorganic carbon concentration. Water Res. 74, 58–66.

Petrie, B., McAdam, E.J., Hassard, F., Stephenson, T., Lester, J.N., Cartmell, E., 2014. Diagnostic investigation of steroid estrogen removal by activated sludge at varying solids retention time. Chemosphere 113, 101–108.

Plósz, B.G., Leknes, H., Liltved, H., Thomas, K.V., 2010a. Diurnal variations in the occurrence and the fate of hormones and antibiotics in activated sludge wastewater treatment in Oslo, Norway. Sci. Total Environ. 408, 1915–1924.

Plósz, B.G., Leknes, H., Thomas, K.V., 2010b. Impacts of competitive inhibition, parent compound formation and partitioning behavior on the removal of antibiotics in municipal wastewater treatment. Environ. Sci. Technol. 44, 734–742.

Plósz, B.G., Langford, K.H., Thomas, K.V., 2012. An activated sludge modeling framework for xenobiotic trace chemicals (ASM-X): Assessment of diclofenac and carbamazepine. Biotechnol. Bioeng. 109, 2757–2769.

Plósz, B.G., Reid, M.J., Borup, M., Langford, K.H., Thomas, K.V., 2013a. Biotransformation kinetics and sorption of cocaine and its metabolites and the factors influencing their estimation in wastewater. Water Res. 47 (7), 2129–2140.

Plósz, B.G., Benedetti, L., Daigger, G.T., Langford, K.H., Larsen, H.F., Monteith, H., Ort, C., Seth, R., Steyer, J.-P., Vanrolleghem, P.A., 2013b. Modelling micro-pollutant fate in wastewater collection and treatment systems: Status and challenges. Water Sci. Technol. 67 (1), 1–15.

Polesel, F., Lehnberg, K., Dott, W., Trapp, S., Thomas, K.V., Plósz, B.G., 2014. Factors influencing sorption of ciprofloxacin onto activated sludge: Experimental assessment and modelling implications. Chemosphere 119, 105–111.

Pomiès, M., Choubert, J.M., Wisniewski, C., Coquery, M., 2013. Modelling of micropollutant removal in biological wastewater treatments: A review. Sci. Total Environ. 443, 733–748.

Popa, C., Favier, L., Dinica, R., Semrany, S., Djelal, H., Amrane, A., Bahrim, G., 2014. Potential of newly isolated wild Streptomyces strains as agents for the biodegradation of a recalcitrant pharmaceutical, carbamazepine. Environ. Technol. 35, 3082–3091.

Porro, J., Milleri, C., Comas, J., Rodriguez-roda, I., Pijuan, M., Corominas, L., Guo, L., Daelman, M.R.J., Volcke, E.I.P., van Loosdrecht, M.C.M., Vanrolleghem, P.A., Nopens, I., 2014. Risk assessment modelling of N2O production in activated sludge systems : Quality not Quantity. 4th IWA/WEF Wastewater Treat. Model. Semin. (WWTmod), March 30 - April 2 2014, Spa, Belgium.

Radjenović, J., Petrović, M., Barceló, D., 2009. Fate and distribution of pharmaceuticals in wastewater and sewage sludge of the conventional activated sludge (CAS) and advanced membrane bioreactor (MBR) treatment. Water Res. 43 (3), 831–841.

Ráduly, B., Gernaey, K.V., Capodaglio, A.G., Mikkelsen, P.S., Henze, M., 2007. Artificial neural networks for rapid WWTP performance evaluation: Methodology and case study. Environ. Model. Softw. 22, 1208–1216.

Ratola, N., Cincinelli, A., Alves, A., Katsoyiannis, A., 2012. Occurrence of organic microcontaminants in the wastewater treatment process. A mini review. J. Hazard. Mater. 239-240, 1–18.

Ravishankara, A.R., Daniel, J.S., Portmann, R.W., 2009. Nitrous oxide (N2O): the dominant ozone-depleting substance emitted in the 21st century. Science 326, 123–125.

Reichert, P., Borchardt, D., Henze, M., Rauch, W., Shanahan, P., Somlyódy, L., Vanrolleghem, P.A., 2001. River water quality model no. 1 (RWQM1): II. Biochemical process equations. Water Sci. Technol. 43 (5), 11–30.

Richardson, S.D., 2012. Environmental mass spectrometry: Emerging contaminants and current issues. Anal. Chem. 84, 747–778.

Rieckermann, J., Anta, J., Scheidegger, A., Ort, C., 2011. Assessing wastewater micropollutant loads with approximate bayesian computations. Environ. Sci. Technol. 45, 4399–4406.

Rieger, L., Gillot, S., Langergraber, G., Ohtsuki, T., Shaw, A., Takács, I., Winkler, S., 2012. Guidelines for using Activated Sludge Models. IWA Scientific and Technical Report No. 22. IWA Publishing, London, UK.

Rivas, A., Irizar, I., Ayesa, E., 2008. Model-based optimisation of wastewater treatment plants design. Environ. Model. Softw. 23, 435–450.

Rodriguez-Roda, I.R., Sànchez-Marrè, M., Comas, J., Baeza, J., Colprim, J., Lafuente, J., Cortes, U., Poch, M., 2002. A hybrid supervisory system to support WWTP operation: Implementation and validation. Water Sci. Technol. 45 (4-5), 289–297.

Rosen, C., Jeppsson, U., Vanrolleghem, P.A., 2004. Towards a common benchmark for long-term process control and monitoring performance evaluation. Water Sci. Technol. 50 (11), 41–49.

Rosen, C., Vrecko, D., Gernaey, K.V., Pons, M.-N., Jeppsson, U., 2006. Implementing ADM1 for plant-wide benchmark simulations in Matlab/Simulink. Water Sci. Technol. 54 (4), 11–19.

Rosen, C., Rieger, L., Jeppsson, U., Vanrolleghem, P.A., 2008. Adding realism to simulated sensors and actuators. Water Sci. Technol. 57 (3), 337–344.

Saagi, R., Flores-Alsina, X., Fu, G., Benedetti, L., Gernaey, K.V., Jeppsson, U., Butler, D., 2014. Benchmarking integrated control strategies using an extended BSM2 platform. 13th Int. Conf. Urban Drainage, 7-14 Sept. 2014, Kuching, Malaysia.

Sathyamoorthy, S., Ramsburg, C.A., 2013. Assessment of quantitative structural property relationships for prediction of pharmaceutical sorption during biological wastewater treatment. Chemosphere 92, 639–646.

Schütze, M., Butler, D., Beck, B., 2002. Modelling, simulation and control of urban wastewater systems. Springer, London, UK.

Schwartz, T., Kohnen, W., Jansen, B., Obst, U., 2003. Detection of antibiotic-resistant bacteria and their resistance genes in wastewater, surface water, and drinking water biofilms. FEMS Microbiol. Ecol. 43, 325–335.

Sharma, K.R., Yuan, Z., de Haas, D., Hamilton, G., Corrie, S., Keller, J., 2008. Dynamics and dynamic modelling of H2S production in sewer systems. Water Res. 42 (10-11), 2527–2538.

Sin, G., van Hulle, S.W.H., De Pauw, D.J.W., van Griensven, A., Vanrolleghem, P.A., 2005. A critical comparison of systematic calibration protocols for activated sludge models: A SWOT analysis. Water Res. 39 (12), 2459–2474.

Sin, G., Kaelin, D., Kampschreur, M.J., Takács, I., Wett, B., Gernaey, K.V., Rieger, L., Siegrist, H., van Loosdrecht, M.C.M., 2008a. Modelling nitrite in wastewater treatment systems: A discussion of different modelling concepts. Water Sci. Technol. 58 (6), 1155–1171.

Sin, G., De Pauw, D.J.W., Weijers, S., Vanrolleghem, P.A., 2008b. An efficient approach to automate the manual trial and error calibration of activated sludge models. Biotechnol. Bioeng. 100, 516–528.

Snip, L., Flores-Alsina, X., Plósz, B.G., Jeppsson, U., Gernaey, K.V., 2014. Modelling the occurrence, transport and fate of pharmaceuticals in wastewater systems. Environ. Model. Softw. 62, 112–127.

Solon, K., Flores-Alsina, X., Mbamba, C.K., Volcke, E.I.P., Tait, S., Batstone, D., Gernaey, K.V., Jeppsson, U., 2015. Effects of ionic strength and ion pairing on (plant-wide) modelling of anaerobic digestion. Water Res. 70, 235–245.

Spongberg, A.L., Witter, J.D., 2008. Pharmaceutical compounds in the wastewater process stream in Northwest Ohio. Sci. Total Environ. 397, 148–157.

Stasinakis, A.S., Kordoutis, C.I., Tsiouma, V.C., Gatidou, G., Thomaidis, N.S., 2010. Removal of selected endocrine disrupters in activated sludge systems: Effect of sludge retention time on their sorption and biodegradation. Bioresour. Technol. 101, 2090–2095.

Stenström, F., Tjus, K., la Cour Jansen, J., 2014. Oxygen-induced dynamics of nitrous oxide in water and off-gas during the treatment of digester supernatant. Water Sci. Technol. 69 (1), 84–91.

Stumm, W., Morgan, J.J., 1996. Aquatic Chemistry: Chemical Equilibria and Rates in Natural Waters. John Wiley & Sons, New York, USA.

Suarez, S., Lema, J.M., Omil, F., 2010. Removal of Pharmaceutical and Personal Care Products (PPCPs) under nitrifying and denitrifying conditions. Water Res. 44 (10), 3214–3224.

Takács, I., Patry, G.G., Nolasco, D., 1991. A dynamic model of the clarification-thickening process. Water Res. 25 (10), 1263–1271.

Taylor, D., Senac, T., 2014. Human pharmaceutical products in the environment - The “problem” in perspective. Chemosphere 115, 95–99.

Teerlink, J., Hering, A.S., Higgins, C.P., Drewes, J.E., 2012. Variability of trace organic chemical concentrations in raw wastewater at three distinct sewershed scales. Water Res. 46 (10), 3261–3271.

Ternes, T.A., 1998. Occurrence of drugs in German sewage treatment plants and rivers. Water Res. 32 (11), 3245–3260.

Ternes, T.A., Herrmann, N., Bonerz, M., Knacker, T., Siegrist, H., Joss, A., 2004a. A rapid method to measure the solid-water distribution coefficient (Kd) for pharmaceuticals and musk fragrances in sewage sludge. Water Res. 38 (19), 4075–4084.

Ternes, T.A., Joss, A., Siegrist, H., 2004b. Scrutinizing pharmaceuticals and personal care products in wastewater treatment. Environ. Sci. Technol. 38, 392A–399A.

Ternes, T.A., Joss, A., 2006. Human pharmaceuticals, hormones and fragrances. IWA Publishing, London, UK.

Torà, J.A., Lafuente, J., Baeza, J.A., Carrera, J., 2010. Combined effect of inorganic carbon limitation and inhibition by free ammonia and free nitrous acid on ammonia oxidizing bacteria. Bioresour. Technol. 101, 6051–6058.

Upadhyay, N., Sun, Q., Allen, J.O., Westerhoff, P., Herckes, P., 2011. Synthetic musk emissions from wastewater aeration basins. Water Res. 45 (3), 1071–1078.

Van Nuijs, A.L.N., Castiglioni, S., Tarcomnicu, I., Postigo, C., de Alda, M.L., Neels, H., Zuccato, E., Barceló, D., Covaci, A., 2011. Illicit drug consumption estimations derived from wastewater analysis: A critical review. Sci. Total Environ. 409, 3564–3577.

Van Nuijs, A.L.N., Abdellati, K., Bervoets, L., Blust, R., Jorens, P.G., Neels, H., Covaci, A., 2012. The stability of illicit drugs and metabolites in wastewater, an important issue for sewage epidemiology? J. Hazard. Mater. 239-240, 19–23.

Vanrolleghem, P.A., Keesman, K.J., 1996. Identification of biodegradation models under model and data uncertainty. Water Sci. Technol. 33 (2), 91–105.

Vanrolleghem, P.A., Petersen, B., De Pauw, D.J.W., Dovermann, H., Weijers, S., Gernaey, K.V., 2003. A comprehensive model calibration procedure for activated sludge models. Environ. Eng. 1–28.

Vanrolleghem, P.A., Borsányi, P., Benedetti, L., Dirckx, G., De Keyser, W., Muschalla, D., Solvi, A., Vandenberghe, V., Weyand, M., 2008. Modelling real-time control options on virtual sewer systems. J. Environ. Eng. Sci. 7, 395–410.

Vasquez, M.I., Lambrianides, A., Schneider, M., Kümmerer, K., Fatta-Kassinos, D., 2014. Environmental side effects of pharmaceutical cocktails: What we know and what we should know. J. Hazard. Mater. 279, 169–189.

Verlicchi, P., Al Aukidy, M., Zambello, E., 2012. Occurrence of pharmaceutical compounds in urban wastewater: Removal, mass load and environmental risk after a secondary treatment-A review. Sci. Total Environ. 429, 123–155.

Verstraete, W., Van de Caveye, P., Diamantis, V., 2009. Maximum use of resources present in domestic "used water." Bioresour. Technol. 100, 5537–5545.

Vezzaro, L., Eriksson, E., Ledin, A., Mikkelsen, P.S., 2012. Quantification of uncertainty in modelled partitioning and removal of heavy metals (Cu, Zn) in a stormwater retention pond and a biofilter. Water Res. 46 (20), 6891–6903.

Vezzaro, L., Benedetti, L., Gevaert, V., De Keyser, W., Verdonck, F., De Baets, B., Nopens, I., Cloutier, F., Vanrolleghem, P.A., Mikkelsen, P.S., 2014. A model library for dynamic transport and fate of micropollutants in integrated urban wastewater and stormwater systems. Environ. Model. Softw. 53, 98–111.

Vieno, N., Tuhkanen, T., Kronberg, L., 2007. Elimination of pharmaceuticals in sewage treatment plants in Finland. Water Res. 41 (5), 1001–1012.

Vrecko, D., Gernaey, K.V., Rosen, C., Jeppsson, U., 2006. Benchmark Simulation Model No 2 in Matlab-Simulink: Towards plant-wide WWTP control strategy evaluation. Water Sci. Technol. 54 (8), 65–72.

Vree, T.B., van der Ven, A.J.A.M., Koopmans, P.P., van Ewijk-Beneken Kolmer, E.W.J., Verwey-van Wissen, C.P.W.G.M., 1995. Pharmacokinetics of sulfamethoxazole with its hydroxy metabolites and N4-acetyl-, N1-glucuronide conjugates in healthy human volunteers. Clin. Drug Investig. 9, 43–53.

Wang, J., Zhang, J., Xie, H., Qi, P., Ren, Y., Hu, Z., 2011. Methane emissions from a full-scale A/A/O wastewater treatment plant. Bioresour. Technol. 102, 5479–5485.

Wang, J.M., Huang, C.P., Allen, H.E., Poesponegoro, I., Poesponegoro, H., Takiyama, L.R., 1999. Effects of dissolved organic matter and pH on heavy metal uptake by sludge particulates exemplified by copper(II) and nickel(II): Three-variable model. Water Environ. Res. 71, 139–147.

Wang, X., Grady Jr., C.P.L., 1995. Effects of biosorption and dissolution on the biodegradation of di-n-butyl phthalate. Water Environ. Res. 67, 863–871.

Warren, N., Allan, I.J., Carter, J.E., House, W.A., Parker, A., 2003. Pesticides and other micro-organic contaminants in freshwater sedimentary environments—A review. Appl. Geochemistry 18, 159–194.

Weigel, S., Berger, U., Jensen, E., Kallenborn, R., Thoresen, H., Hühnerfuss, H., 2004. Determination of selected pharmaceuticals and caffeine in sewage and seawater from Tromsø/Norway with emphasis on ibuprofen and its metabolites. Chemosphere 56, 583–592.

Wett, B., Rauch, W., 2003. The role of inorganic carbon limitation in biological nitrogen removal of extremely ammonia concentrated wastewater. Water Res. 37 (5), 1100–1110.

Wunderlin, P., Mohn, J., Joss, A., Emmenegger, L., Siegrist, H., 2012. Mechanisms of N_2O production in biological wastewater treatment under nitrifying and denitrifying conditions. Water Res. 46 (4), 1027–1037.

Wunderlin, P., Lehmann, M.F., Siegrist, H., Tuzson, B., Joss, A., Emmenegger, L., Mohn, J., 2013. Isotope signatures of N2O in a mixed microbial population system: Constraints on N2O producing pathways in wastewater treatment. Environ. Sci. Technol. 47, 1339–1348.

Yamamoto, H., Liljestrand, H.M., Shimizu, Y., Morita, M., 2003. Effects of physical-chemical characteristics on the sorption of selected endocrine disruptors by dissolved organic matter surrogates. Environ. Sci. Technol. 37, 2646–2657.

Yang, Q., Liu, X., Peng, C., Wang, S., Sun, H., Peng, Y., 2009. N2O production during nitrogen removal via nitrite from domestic wastewater: Main sources and control method. Environ. Sci. Technol. 43, 9400–9406.

Yu, Y., Wu, L., Chang, A.C., 2013. Seasonal variation of endocrine disrupting compounds, pharmaceuticals and personal care products in wastewater treatment plants. Sci. Total Environ. 442, 310–316.

Zenker, A., Cicero, M.R., Prestinaci, F., Bottoni, P., Carere, M., 2014. Bioaccumulation and biomagnification potential of pharmaceuticals with a focus to the aquatic environment. J. Environ. Manage. 133, 378–387.

Zhang, Y., Geißen, S.U., Gal, C., 2008. Carbamazepine and diclofenac: Removal in wastewater treatment plants and occurrence in water bodies. Chemosphere 73, 1151–1161.

Zimmermann, S.G., Wittenwiler, M., Hollender, J., Krauss, M., Ort, C., Siegrist, H., von Gunten, U., 2011. Kinetic assessment and modeling of an ozonation step for full-scale municipal wastewater treatment: Micropollutant oxidation, by-product formation and disinfection. Water Res. 45 (2), 605–617.

Zuccato, E., Chiabrando, C., Castiglioni, S., Calamari, D., Bagnati, R., Schiarea, S., Fanelli, R., 2005. Cocaine in surface waters: a new evidence-based tool to monitor community drug abuse. Environ. Health 4.

Zuccato, E., Chiabrando, C., Castiglioni, S., Bagnati, R., Fanelli, R., 2008. Estimating community drug abuse by wastewater analysis. Environ. Health Perspect. 116, 1027–1032.

Zumft, W.G., 1997. Cell biology and molecular basis of denitrification? Microbiol. Mol. Biol. Rev. 61, 533–616.

Appendix A.1

Corrected process matrices for models B and D, and list of parameter values used in the simulations.

Table A.1.1 Corrected process matrix for model B

Process	S_{O2}	S_{NH4}	S_{NO2}	S_{NO}	S_{N2O}	X_{AOB}	S_{ALK}	*rate*
B-1	$-\frac{3.43-Y_{AOB}}{Y_{AOB}}$	$-\frac{1}{Y_{AOB}}-i_{N_{AOB}}$	$\frac{1}{Y_{AOB}}$			*1*	$-\frac{1}{Y_{AOB}}-i_{N_{AOB}}$ $*\, i_{Charge,NH4}+\frac{1}{Y_{AOB}}$ $*\, i_{Charge,NO2}$	$\mu_{AOB}\frac{S_{O2}}{K_{O2\_AOB}+S_{O2}}\frac{S_{NH4}}{K_{NH4,AOB}+S_{NH4}}X_{AOB}$
B-2	$-\frac{2.29-Y_{AOB}}{Y_{AOB}}$	$-\frac{1}{Y_{AOB}}-i_{N_{AOB}}$	$-\frac{1}{Y_{AOB}}$	$\frac{2}{Y_{AOB}}$		*1*	$-\frac{1}{Y_{AOB}}-i_{N_{AOB}}$ $*\, i_{Charge,NH4}-\frac{1}{Y_{AOB}}$ $*\, i_{Charge,NO2}$	$\mu_{AOB}*\eta_{\mu AOB,Ax}$ $\frac{S_{O2}}{K_{O2\_AOB}+S_{O2}}\frac{S_{NH4}}{K_{NH4,AOB}+S_{NH4}}\frac{S_{NO2}}{K_{NO2,AOB}+S_{NO2}}\frac{S_{NH4}}{K_{NH4}+S_{NH4}}X_{AOB}$
B-3	$-\frac{2.29-Y_{AOB}}{Y_{AOB}}$	$-\frac{1}{Y_{AOB}}-i_{N_{AOB}}$	$\frac{1}{Y_{AOB}}$	$-\frac{2}{Y_{AOB}}$	$\frac{2}{Y_{AOB}}$	*1*	$-\frac{1}{Y_{AOB}}-i_{N_{AOB}}$ $*\, i_{Charge,NH4}+\frac{1}{Y_{AOB}}$ $*\, i_{Charge,NO2}$	$\mu_{AOB,HAO}\eta_{\mu,AOB,Ax}$ $\frac{S_{O2}}{K_{O2\_AOB}+S_{O2}}\frac{S_{NH4}}{K_{NH4,AOB}+S_{NH4}}\frac{S_{NO}}{K_{NO,AOB}+S_{NO}}\frac{S_{NH4}}{K_{NH4}+S_{NH4}}X_{AOB}$
ASMN-12						***-1***		$\boldsymbol{b_{AOB}X_{AOB}}$

Table A.1.2 Corrected process matrix for model D

Process	S_{O2}	S_{NH4}	S_{NH2OH}	S_{NO2}	S_{NO}	S_{N2O}	X_{AOB}	S_{ALK}	*rate*
D-1	-1.14	*-1*	*1*					$-1 * i_{Charge,NH4}$	$\mu_{AOB,AMO}\frac{S_{O2}}{K_{S1,O2\_AOB}+S_{O2}}\frac{S_{NH4}}{K_{NH4,AOB}+S_{NH4}}X_{AOB}$
D-2	$-\frac{1.71-Y_{AOB}}{Y_{AOB}}$	$\boxed{-i_{N_{AOB}}}$	$-\frac{1}{Y_{AOB}}$		$\frac{1}{Y_{AOB}}$		*1*	$-i_{N_{AOB}} * i_{Charge,NH4}$	$\mu_{AOB,HAO}\frac{S_{O2}}{K_{S2,O2\_AOB}+S_{O2}}\frac{S_{NH2OH}}{K_{NH2OH,AOB}+S_{NH2OH}}\frac{S_{NH4}}{K_{NH4}+S_{NH4}}X_{AOB}$
D-3	$\underline{-0.57}$			$\underline{1}$	$\underline{-1}$			$1 * i_{Charge,NO2}$	$\frac{\mu_{AOB,HAO}}{Y_{AOB}}\frac{S_{O2}}{K_{S2,O2\_AOB}+S_{O2}}\frac{S_{NO}}{K_{NO,AOB}+S_{NO}}X_{AOB}$
D-4			*-1*	*1*	*-4*	*4*		$1 * i_{Charge,NO2}$	$\mu_{AOB,HAO}\eta_{\mu,AOB,Ax}\frac{S_{NO}}{K_{NO,AOB}+S_{NO}}\frac{S_{NH2OH}}{K_{NH2OH,AOB}+S_{NH2OH}}X_{AOB}$
ASMN-12							***-1***		$\boldsymbol{b_{AOB}X_{AOB}}$

Table A.1.3 Parameter values of the different models used in the simulations.
Other parameter values are taken from Hiatt and Grady (2008) and Corominas *et al.* (2012).

Parameter	*Value*	*Unit*
	All models	
$i_{Charge,NH4}$	$+\frac{1}{14}$	charge/g N
$i_{Charge,NO2}$	$-\frac{1}{14}$	charge/g N
$i_{N_{AOB}}$	0.07	g N/g COD
Y_{AOB}	0.150	g COD/g N
K_{NH4}	0.05	g N/m^3
	Model A	
$\mu_{AOB,AMO}$	2.928	1/d
$\mu_{AOB,HAO}$	2.208	1/d
$K_{S1,O2_{AOB}}$	0.043	g COD/m^3
$K_{S2,O2_{AOB}}$	0.6	g COD/m^3
$K_{I,O2_{AOB}}$	0.112	g COD/m^3
$\eta_{\mu,AOB,Ax}$	0.074	-
$K_{NH4,AOB}$	2.4	g N/m^3
$K_{NH2OH,AOB}$	2.4	g N/m^3
$K_{NO2,AOB}$	0.14	g N/m^3
$K_{NO,AOB}$	0.0084	g N/m^3
	Model B	
μ_{AOB}	1.824	1/d
$\eta_{\mu,AOB,Ax}$	0.72	-
$K_{NH4,AOB}$	1.0	g N/m^3
$K_{NO2,AOB}$	8.0	g N/m^3
$K_{NO,AOB}$	3.91	g N/m^3
$K_{O2_{AOB}}$	0.13	g COD/m^3
	Model C	
$q_{AOB,1,max}$	3.48	g COD/m^3
$q_{AOB,2,max}$	3.54	g COD/m^3
$q_{AOB,3,max}$	1.04	g COD/m^3
$q_{AOB,4,max}$	14.88	g COD/m^3
$K_{NH4,AOB}$	2.38	g N/m^3
$K_{NH2OH,AOB}$	0.7	g N/m^3
$K_{NOH,AOB}$	0.7	g N/m^3
K_{NOH}	0.05	
$K_{S1,O2_{AOB}}$	0.608	g COD/m^3
$K_{S2,O2_{AOB}}$	0.0608	g COD/m^3
$K_{S3,O2_{AOB}}$	0.0608	g COD/m^3
	Model D	
$\mu_{AOB,AMO}$	3.48	1/d
$\mu_{AOB,HAO}$	1.8	1/d
$K_{S1,O2_{AOB}}$	0.043	g COD/m^3
$K_{S2,O2_{AOB}}$	0.6	g COD/m^3
$\eta_{\mu,AOB,Ax}$	0.45	-
$K_{NH4,AOB}$	2.4	g N/m^3
$K_{NH2OH,AOB}$	2.4	g N/m^3
$K_{NO,AOB}$	0.0084	g N/m^3

Appendix A.2

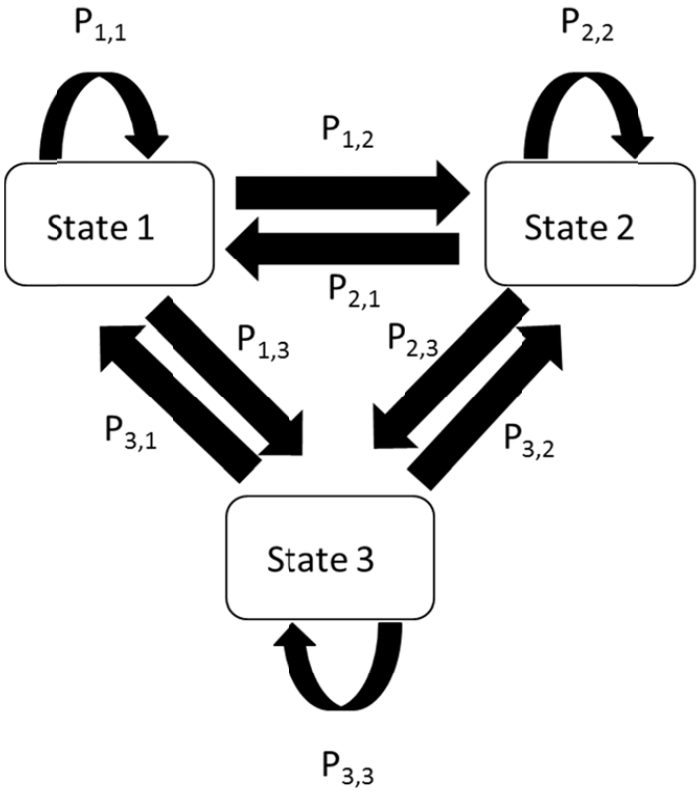

Figure A.2.1. Schematic representation of the transition probability matrix with three different states and their transition probabilities.

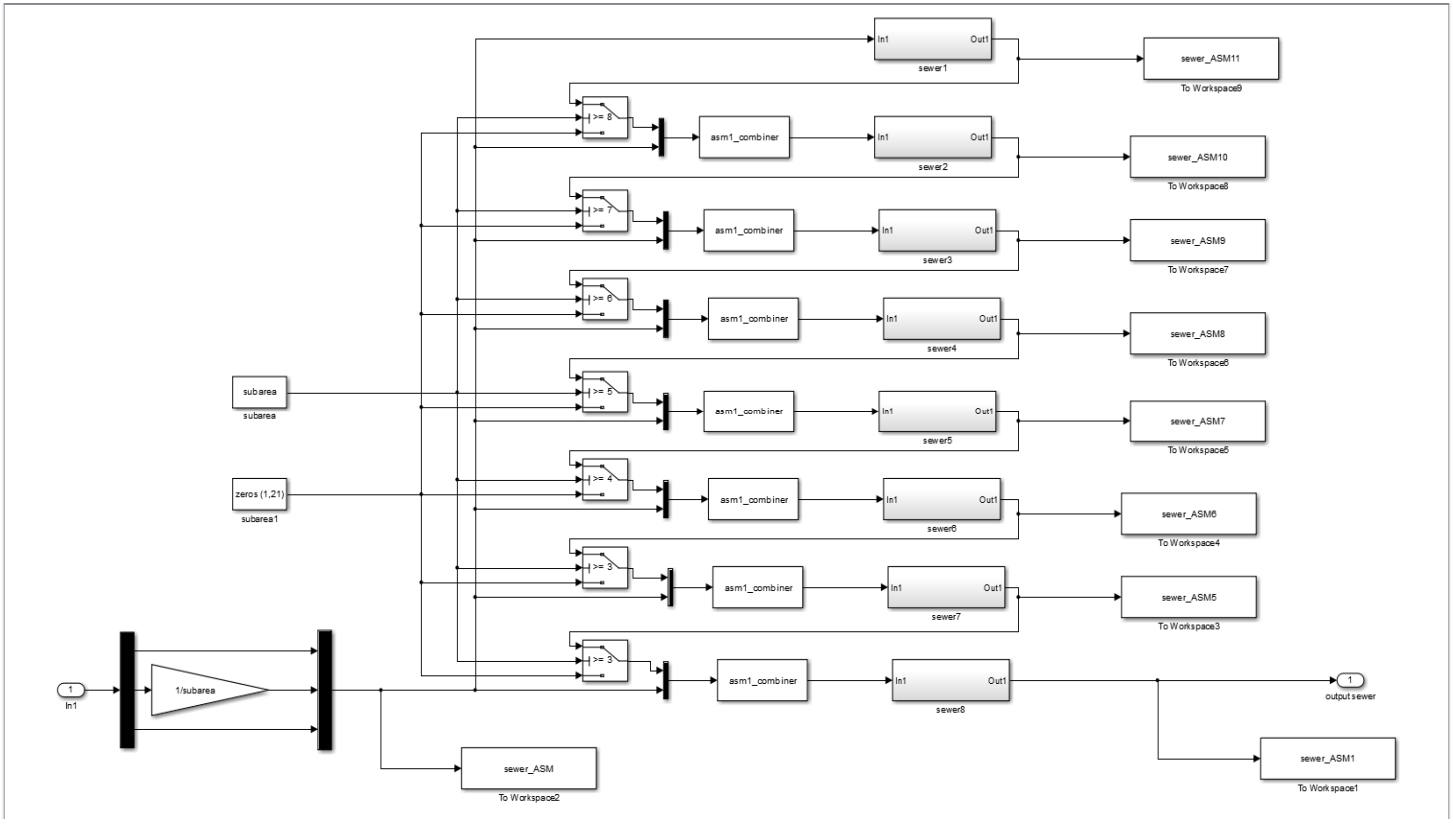

Figure A.2.2. The sewer system blocks in Simulink with deterministic variable volume tank models in series.

The mass balance that describes the first flush effect:

$$\frac{dM}{dt} = Q_{in} * TSS_{in} * (1 - \frac{M}{M_{\max}}) - \frac{(Q_{in})^n}{(Q_{\lim})^n + (Q_{in})^n} * M * FF \qquad \textbf{Eq. A.2.1.}$$

The mass balance describes the accumulation of solids in the sewer as a function of the flux of solids that is entering and leaving the system. M is the total mass of solids accumulated in the sewer (kg), Q_{in} is the influent flow rate (m^3/d), TSS_{in} is the S_S concentration (kg/m^3), M_{max} is the maximum amount of solids that can be stored in the sewer system (kg), Q_{lim} is the flow rate limit triggering the first flush effect (m^3/d), and FF and n are dimensionless tunable parameters to adjust the desired strength of the first flush effect (Gernaey et al., 2011).

Appendix A.3

Table A.3.1. Calculation of different criteria, Q_i is the observed value, $\hat{Q}_i$ is the predicted value and $\bar{Q}$ is the mean of the observed values (Dawson et al., 2007; Hauduc et al., 2015b).

Peak evaluation Optimum = 0	Peak difference (*PDIFF*)	$max(Q_i) - \max(\hat{Q}_i)$
	Percentage error in peak (*PEP*)	$\frac{max(Q_i) - \max(\hat{Q}_i)}{max(Q_i)} x\ 100\%$
	Mean square derivative error (*MSDE*)	$\frac{1}{n-1}\sum_{i=1}^{n}\left((Q_i - Q_{i-1}) - (\hat{Q}_i - \hat{Q}_{i-1})\right)^2$
Absolute criteria Optimum = 0	Mean error (*ME*)	$\frac{1}{n}\sum_{i=1}^{n}(Q_i - \hat{Q}_i)$
	Mean square error (*MSE*)	$\frac{1}{n}\sum_{i=1}^{n}(Q_i - \hat{Q}_i)^2$
	Root mean square error (*RMSE*)	$\sqrt{\frac{\sum_{i=1}^{n}(Q_i - \hat{Q}_i)^2}{n}}$
Index of agreement (*IoAd*) Optimum = 1		$1 - \frac{\sum_{i=1}^{n}(Q_i - \hat{Q}_i)^2}{\sum_{i=1}^{n}(\lvert\hat{Q}_i - \bar{Q}\rvert + \lvert Q_i - \bar{Q}\rvert)^2}$

Appendix A.4

Table A.4.1. Calculation of relative criteria, Q_i is the observed value, $\hat{Q}_i$ is the predicted value and $\bar{Q}$ is the mean of the observed values (Dawson et al., 2007; Hauduc et al., 2015b).

Relative criteria Optimum = 0	Mean percentage error (*MPE*)	$\frac{100}{n}\sum_{i=1}^{n}\frac{(Q_i - \hat{Q}_i)}{Q_i}$
	Mean absolute relative error (*MARE*)	$\frac{1}{n}\sum_{i=1}^{n}\frac{(\lvert Q_i - \hat{Q}_i \rvert)}{Q_i}$
	Mean square relative error (*MSRE*)	$\frac{1}{n}\sum_{i=1}^{n}\left(\frac{Q_i - \hat{Q}_i}{Q_i}\right)^2$

CAPEC-PROCESS Research Center

Copyright: Laura Snip
Print: GraphicCo - www.graphicco.dk

CAPEC-PROCESS Research Center
Department of Chemical and Biochemical Engineering

Technical University of Denmark (DTU)
Søltofts Plads, Building 229
DK-2800 Kgs. Lyngby
Tel. +45 4525 2800

www.capec-process.kt.dtu.dk
ISBN 13: 978-87-93054-77-6
ISSN